Durham E-Theses

A seismic study of crustal structure in the region of the western isles of Scotland

Summers, T. P.

A SEISMIC STUDY OF CRUSTAL STRUCTURE

IN THE REGION OF THE WESTERN ISLES OF SCOTLAND

by

T.P. SUMMERS

A thesis submitted for the degree of

Doctor of Philosophy at the University of Durham

Grey College   September, 1982

ABSTRACT

In November 1979, the Department of Geological Sciences, University of Durham, in conjunction with the Department of Geology, University of Glasgow, carried out a marine seismic refraction survey between Barra in the Outer Hebrides and Girvan on the Ayrshire coast. In August/September 1981, a shorter profile, between Mull and Kintyre, was undertaken. Temporary recording stations were set up on land and explosives and airguns used as sources at sea. In addition, data were obtained from the permanent recording networks in Scotland. The application of digital filtering techniques to the airgun lines is presented and reviewed. The explosive shot data were interpreted using time-term analysis, the plus-minus method and ray-tracing. Gravity and magnetic studies were used as a control on the interpretation.

The depth to the basin has been examined, indicating sedimentary cover of between 1 and 3 km along the line. The variation in basement velocity has been determined. A velocity model for the upper crust has been developed indicating large lateral changes. A steep gradient is thought to exist between Colonsay and Jura and a more gentle gradient beneath Mull. There does not seem to be evidence for a mid-crustal refractor with a sharp velocity transition across the boundary. Large changes in Pn time-terms across the Minch and Inner Hebrides basin are thought to be largely due to the varying velocity structure of the basement.

The basin formation and deformation of the lower crust are thought to involve movement within the mantle.

ACKNOWLEDGEMENTS

CONTENTS

LIST OF FIGURES

LIST OF TABLES

CHAPTER 1

INTRODUCTION AND GEOLOGY OF THE REGION

1.1 The Western Isles Seismic Experiment.

In November 1979 and August/September 1981 seismic refraction surveys were carried out in the region of the Western Isles of Scotland. The area and line of survey is shown in Fig. 1.1. The first phase of the Western Isles Seismic Experiment (WISE) involved shooting at sea into recording stations on land situated on the islands and peninsulas between Girvan on the Ayrshire coast and Barra in the Outer Hebrides. For the second phase of the experiment stations were only situated on the section of the line between Mull and Kintyre. The aim of the experiment was to map the surface of the Lewisian basement and define the major north-easterly trending structural blocks of the area, and also to determine the velocity structure of the Lewisian. They are considered important in the development of the Mesozoic sedimentary basins of the region.

The line of the profile crossed all the major sedimentary basins, the Sea of the Hebrides Basin, Inner Hebrides Basin, Islay Basin and Arran Basin and also the major faults, Minch Fault, Camasunary-Skerryvore Fault, Great Glen Fault and the Highland Boundary Fault. Knowledge of the changes in basement structure and sedimentary sequences across the faults would provide important information on the tectonic development of the area.

An airgun source with a shot separation between two and three hundred metres was used for upper crustal studies, the close separation enabling examination of lateral changes in structure by tracing phases across records. Explosive shots were used for studies of the deeper

1

WESTERN ISLES SEISMIC EXPERIMENT
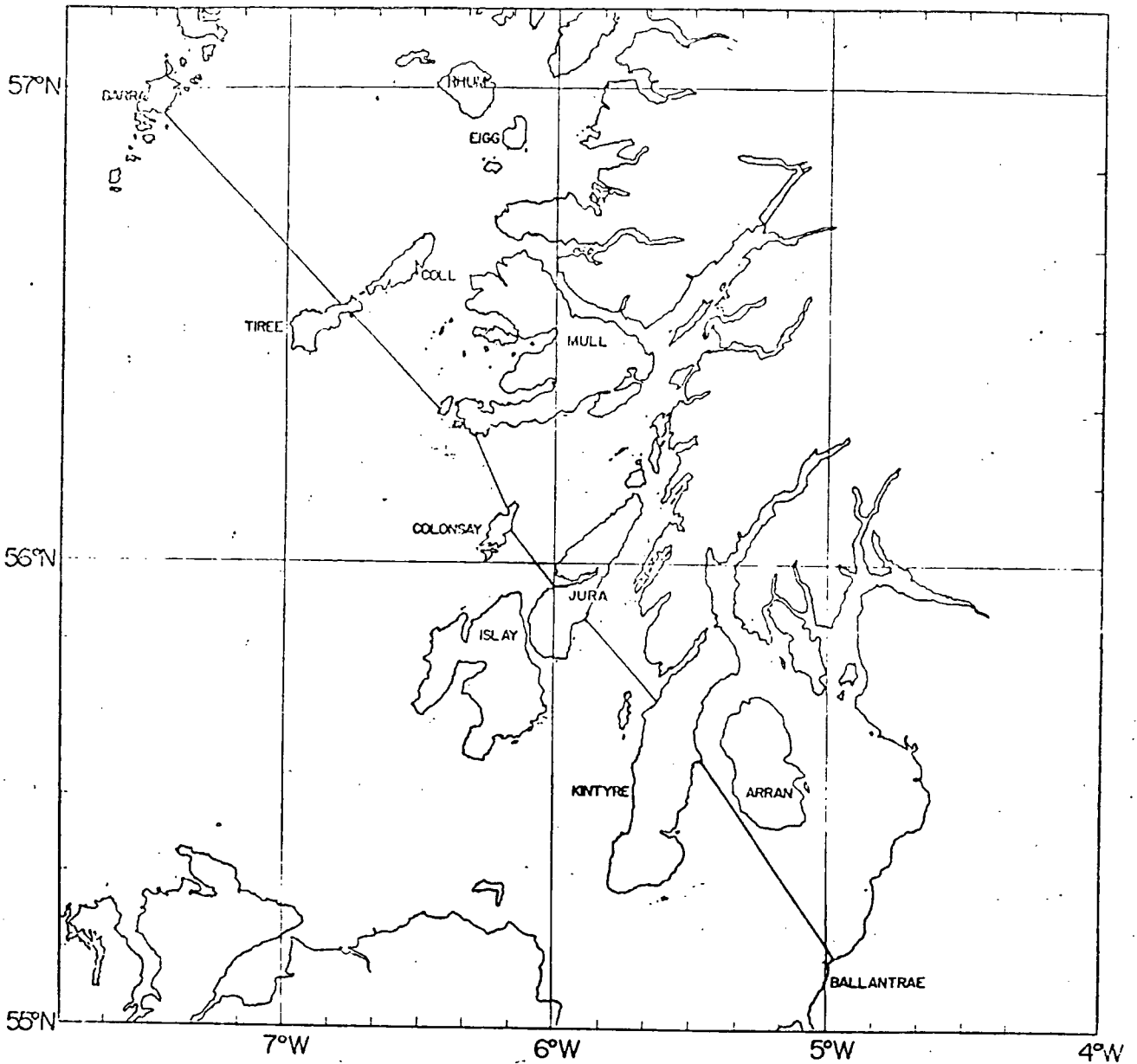
Fig.1.1:   Map of the region of study showing the line of the profile from the mainland to Barra.

crustal structure, primarily of the middle crust but also to provide estimates of depth and structure to the Moho. Comparisons were to be made between the crustal structure of the Hebridean Shelf determined from WISE and those of previous experiments in surrounding areas such as NASP, LISPB and HMSP, and the results of the study integrated with previous gravity and magnetic investigations to provide a coordinated analysis of the geophysical data.

1.2 General Geological Regime.

The geology of the shelf area can be divided into two distinct regions of differing structure separated by the Moine Thrust belt. To the east lies a series of metamorphosed and folded Precambrian and Palaeozoic rocks that were deformed during the Caledonian Orogeny whereas· in the region west of the zone the rocks of the same age formed a stable region during Caledonian times and retain evidence of earlier tectonic events. The Moine Thrust zone itself is a series of south-eastwardly dipping thrusts, the major thrust being traced from the west coast of Scotland to the west of the Shetlands (Watts, 1971). In post Caledonian times, the region acted as a single tectonic unit with widespread Mesozoic basin and graben formation along previous lines of weakness that were reactivated probably by the tensional regime responsible for the opening of the Atlantic.

The different phases of tectonic activity have resulted in large variation in structure and rock type. To the north, at Barra and stretching to the Moine Thrust, the basement is of Lewisian rocks overlain by Mesozoic and older sediments in half grabens. To the south, the basement is overlain by Dalradian metasediments, while south of Kintyre another

2

complex sedimentary basin occupies the Firth of Clyde.

1.3 Basement Structure and Development North-West of the Moine Thrust.

The presently proposed geological structure of this area is given in Fig. 1.2. The outcropping basement of the area is Lewisian gneiss. a highly metamorphosed rock type which is one of the oldest rocks exposed on the eastern side of the Atlantic. Two phases of metamorphism are generally recognised, separated by phases of uplift, erosion and dyke injection (Sutton and Watson, 1957; Park, 1970). The two units, known as Scourian and Laxfordian have respective ages of 2600 myrs and 1600 myrs. A detailed definition and descripion of the Laxfordian and Scourian and their formation is given by Watson (1975). Evans (1965) however, has recognised a third phase, Inverian, occuring between 2200 and 1950 myrs ago. Rocks outcropping on Tiree, Coll and Iona are generally recognised to be Laxordian in age (Bowes, 1968), these being of amphibolite facies, whereas ˙ the Scourian rocks are granulite facies. Westbrook (1972) and Drury (1972), however, provide structural evidence for the age of the gneiss on Tiree and Coll and find evidence for both granulite and amphibolite facies metamorphism. Scourian gneisses are seen on the east coast of the Outer Hebrides above the Outer Isles Thrust, an overthrust to the west of probable Caledonian age. Different periods of deformation are observed on Barra along with a supra-structure of acid amphibolite gniess within an infra structure of orthopyroxene bearing gneiss (Francis, 1973).

Comparisons have been made between the Lewisian of the islands with that of the Scottish mainland in attempts to distinguish movements along the major faults. Dearnley (1962) suggests there are similarities between the two with three zones evident, and that there are a
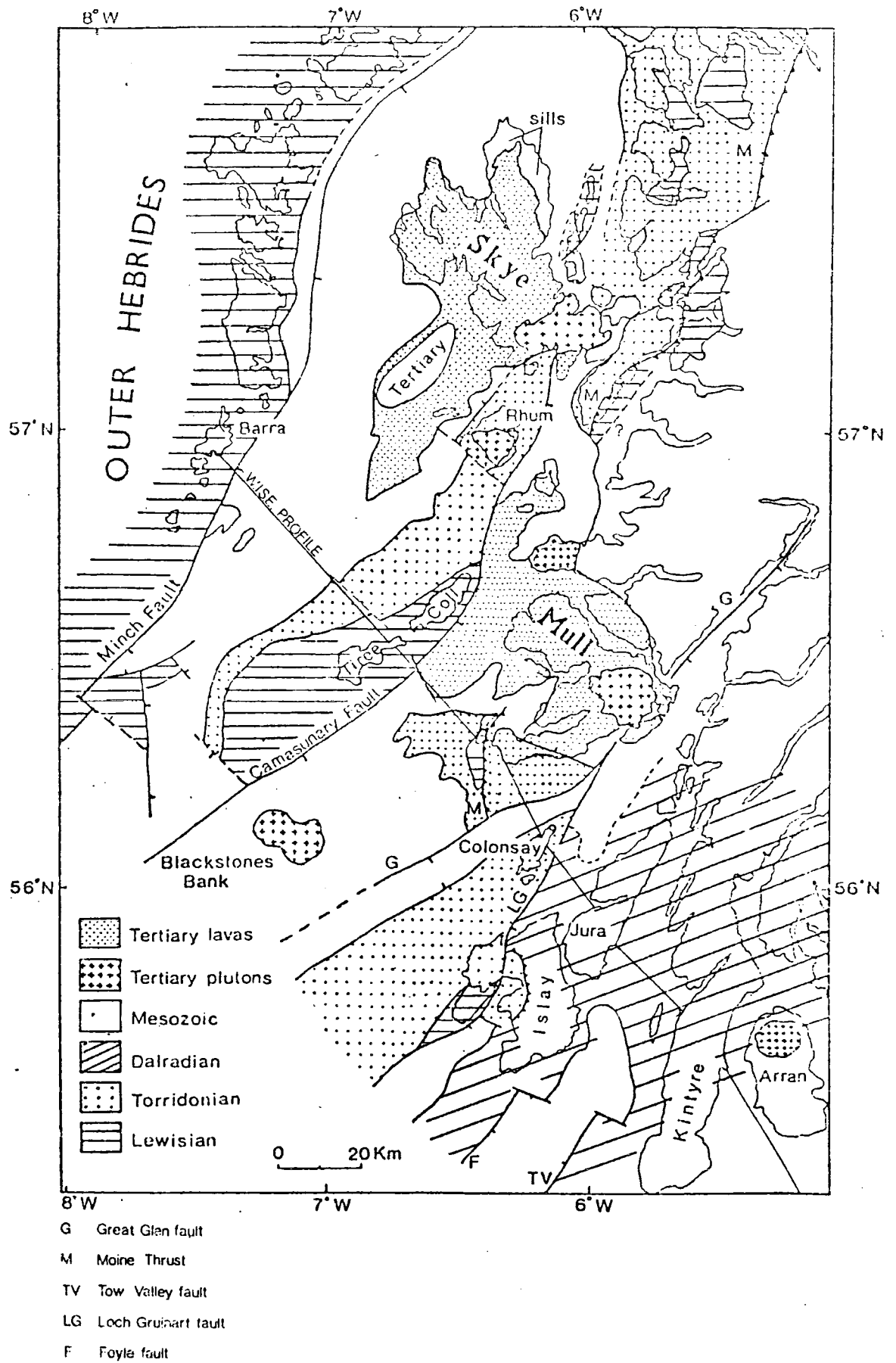
Fig.1.2: Geology of the Sea of the Hebrides and Minches. Redrawn from Binns et al. (1975).

Legend (map):

- Tertiary lavas
- Tertiary plutons
- Mesozoic
- Dalradian
- Torridonian
- Lewisian

0 — 20 Km

G   Great Glen fault

M   Moine Thrust

TV   Tow Valley fault

LG   Loch Gruinart fault

F   Foyle fault

large number of faults present in the Minch with associated sinistral movement. This would then explain why the boundary lines btween the three zones do not line up when they are projected NW or SE. On the mainland in Sutherland, Bott et al. (1972) have suggested that the Ben Stack Line defines the boundary between the two distinct metamorphic assemblages, a fact previously suggested by Peach et al. (1907).

The two facies types have different geophysical properties, the Scourian having higher density and velocity. Smith and Bott (1975) suggest from gravity and seismic studies, that in the North Scottish shelf area a two layered crust exists, which represents the change of facies type with Scourian representing the lower crustal rocks. Jones (1981) has shown that the two different rock types have markedly different velocities and densities west of the Outer Hebrides, those of the Scourian being appreciably higher. The velocity of the Lewisian on the mainland has also been shown to vary with depth and laterally (Hall, 1978a).

Resting on the Lewisian are Torridonian sediments, which may be of the order of 2-3 km thick in some areas, upon a basement surface showing considerable relief. Two groups are recognised (Stewart, 1966; Moorbath, 1969; Stewart and Irving, 1974). The lower, the Stoer group, a red sandstone conglomerate and shale series dated at 980 myrs old, and above this, a similar facies aged 750 myrs, comprising the main Torridonian Group. Above these, there may be lower Palaeozoic rocks. However, these are difficult to define in the offshore regions by geophysical methods, although their presence is inferred from a study of onshore sections.

1.4 Basement Structure and Development South-East of the Moine Thrust.

East of the suggested path of the Moine thrust between Mull and Iona lies the Ross of Mull granite and to the east and south, Moine schists. The composition of the granite and Moinian rocks is given by Richey et al. (1961). On Colonsay, there is thought to be up to 4 km of Torridonian rocks with Lewisian confined to a limited area at the northern tip of the island (Stewart, 1962). To the south-east the Lewisian basement is overlain by Dalradian and Moinian metasediments, the former outcropping on Islay. The Loch Skerrols Thrust has carried the Islay anticline over the Bowmore sandstones of Torridonian age. Gravity studies by Durrance (1976) and gravity and magnetic studies by Westbrook and Borradaile (1978), have improved structural sections to provide evidence of faulting associated with the Great Glen Fault in the area, and determined the shape of the Lewisian/Dalradian interface. The Moinian, Dalradian and lower Palaeozoics were deformed and metamorphosed during the Caledonian orogeny. The orogeny is thought to have lasted approximately 150 myrs, interpreted as being the time of collision between the North American-Greenland continent and the Britain-Baltic continent (Dewey and Pankhurst, 1970). After the main metamorphic episode there was a phase of granitic intrusion and it was during this period that the development of the Moine Thrusts, overthrusting to the west, occured.

In the Firth of Clyde, Dalradian rocks form the basement with pre-Dalradian basement rocks present locally under the upper Palaeozoic succession of the Midland Valley Graben. In addition, pyroxene granulites are probably also present at shallow depth in the northern Sound of Jura. Palaeozoic rocks rest on the Dalradian series but it is difficult to distinguish between the two geophysically (McLean and Deegan, 1978).

5

1.5 Sedimentary Basins of the Sea of the Hebrides.

The considerable amount of relief on the basement in the area is associated with the development of sedimentary basins in which thick Mesozoic and earlier sediments accumulated. The basins are generally fault controlled on their north-west margin, with the sediments dipping north-westerly and forming north-easterly trending half grabens. Structural highs in the basement are found at most of the islands, where Lewisian basement outcrops. To the south of the Moine Thrust zone, the Dalradian metasediments forming the basement, crop out. The development of the basins is thought to be the result of the tensional regime that existed prior to the opening of the Atlantic, which reactivated previous lines of weakness.

After the Caledonian orogeny, northern Britain was at the centre of a large continental mass situated in mountainous areas, resulting in the accumulation of Old Red Sandstone and conglomerates in inter-montane basins. Similar conditions persisted up until the Permian, when a broad tensional regime resulted in the deposition of fluviatile deposits in the fault bounded basins. By Mesozoic times, the large basins had developed over much of western Britain and particularly on the shallow shelf off Western Scotland.

1.5.1 The Sea of the Hebrides Basin (South Minch Basin)

The basin is controlled on its western margin by the Minch Fault which throws down Mesozoic sediments to the east against amphibolite and granulite facies Lewisian gneiss. The northern margin is a structural high of Torridonian rocks which separates the basin from the North Minch basin and the boundary to the south-east is the structural high to the west of the Camasunary-Skerryvore fault. The basin has a synclinal structure, defined North-West of Tiree and Coll by a basal reflector which has been

6

interpreted as the top of the Torridonian (Binns et al., 1975). There is no absolute evidence, however, that the reflector is of this age and may be lower Palaeozoic, perhaps as young as Carboniferous. The maximum thickness of sediments has been quoted by Binns et al. (1975) as being of the order of 2.5 km. They also suggest that the possibility of large amounts of Tertiary sediments being present is eliminated by the capping of Eocene lavas and the presence of Mesozoic rocks in cores. It has been suggested that either a substantial thickness of Permo-Triassic exists with up to 2.5 km of New Red Sandstone around northern Skye (Smythe et al., 1972), or that Devonian and Carboniferous sediments lie above the basal reflector. The existence of some Carboniferous is supported by the the presence of erratics in the Outer Hebrides (Jehu & Craig, 1925). The presence of Jurassic and Cretaceous sediments is unlikely from the lack of variation in the thin sequences of the onshore sediments, although Whitbread (1975) states that on Skye and Raasay Jurassic sediments total 1000m.

Smythe and Kenolty (1975), however, have suggested, from seismic velocities obtained in the Sea of the Hebrides, the presence of a significant thickness of Tertiary sediments. They propose the ending of igneous activity throughout the Eocene, followed by erosion, downwarping and deposition in the Oligocene. This is supported by cores obtained north-west of Canna which contained sediments of Oligocene age (Evans et al., 1975).

The southern margin of the basin is poorly understood and although the convergence of the Minch and Camasunary faults explain to some extent the narrowing of the basin, north-westerly faulting and the intersection of the Minch Fault with the south-easterly limb of the syncline are proposed as the main cause of the wedging out of the Mesozoic

outcrop (Binns _et al.,_ 1975). Palaeozoic and Permo-Triassic sediments can however be traced to the east of the Stanton banks.

The North Minch basin lies to the north of the Torridonian structural high, bounded once again on the west by the Minch Fault and to the east by the outcrop of Precambrian rocks on the mainland. The suggested maximum fill of the basin is 4.0 km with up to 0.7 km of Middle Jurassic sediments underlying the Quaternary (Binns et al., 1975). With a lack of hard evidence, the basin fill is thought from reflection sections to have a lowermost layer of Permo-Triassic and upper sediments of possibly Cretaceous or Tertiary age.

1.5.2 The Inner Hebrides Basin.

This basin is narrower than the Sea of the Hebrides Basin but is similar in its structural trend. It also has a strong asymetric attitude, its sediments dipping to the north-west where they are bounded by the Camasunary-Skerryvore Fault which can be traced down from Skye. The basin extends from Skye to south of Blackstones Bank and is floored by Palaeozoic sediments upon which rest a wedge of Mesozoic rocks varying in thickness and width. The onshore sections of the basin show Permo-Triassic continental red beds up to 90m thick passing conformably into Jurassic sediments (Binns et al., 1975). On Skye, Jurassic sediments are seen to be thrown down at least 650m to the east against the Precambrian. The deeper structure of the basin is unknown because of overlying Tertiary lavas (McQuillin & Binns, 1975).

Recent studies ,have suggested alluvial fan and floodplain environments for the Permo-Triassic sediments (Bruck et al 1967; Steel, 1971; Steel, 1974), the direction suggesting contemporaneous movement on

8

the Camasunary Fault.

1.5.3 Small Basins In the Region of the Great Glen Fault.

A small Mesozoic basin lies to the north of Colonsay in the area of the Great Glen Fault and Its splays. South of the fault, the basement plunges beneath a thick layer of Quaternary sediments, reappearing as the Torridonian of Colonsay. The east coast of Colonsay is also fault controlled, with possibly a splay from the Great Glen responsible for downfaulting Permo-Triassic sandstones. No complem*e*ntary fault is found to the west coast of Jura. An unconformity of sandstone on Dalradian metamorphosed rocks is seen at the entrance to the Firth of Lorne. Rast et al. (1968) have suggested that approximately 2 km of New Red Sandstone lie west of the fault on southeastern Mull.

1.5.4 Structural Development of the Basins of the Sea of the Hebrides and History of Fault Movement.

The geology is controlled by the three major faults, Minch Fault, Camasunary-Skerryvore Fault and Great Glen Fault, bounding the basins and having origins that pre-date the basin structures themselves. They have however, been reactivated and syndepositional movements along them has influenced the process of sedimentation. Onshore sections show the presence of Devonian and Carboniferous sediments in the bottom of the basins (Stephenson, 1972; Lee & Bailey, 1925; Jehu & Craig, 1925), but the extent to which the movements along the faults controlled accumulation is uncertain. The variation in thickness of New Red Sandstone, however, can be explained by the influence of fault movement. A major phase of faulting and uplift In the late Jurassic and early Cretaceous is thought to be responsible for the present configuration of the basin structures (Binns et al., 1975).

9

The nature of the movement along each of the faults is still a matter of contention, with evidence proposed for both transcurrent and vertical movement. The faults are thought to have been initiated as Caledonian structures which responded to Hercynian stresses and developed into major north-easterly trending wrench faults. Finally, they reacted to Mesozoic and Tertiary tension with large vertical movements (Smythe et al., 1972). Dearnley (1962) also proposed such a situation for the Minch fault and Whitbread (1975) has suggested it might have been a wrench fault in the pre-Mesozoic but has been predominately vertical from the Permian. Bott and Watts (1970) propose vertical movement in the region north of Scotland near the Shetlands, downthrown to the south-east, thus explaining the development of thick sedimentary piles in the basins. Although Steel (1971) originally thought that the vertical movement in the region of Lewis was a downthrow to the north-west in order to explain the thickness of the Stornaway Beds, he later stated this to be incorrect and it was more likely to be an area of complex faulting (Steel & Wilson, 1975). It has been suggested (Pitcher, 1969; Whitbread, 1975) that the Minch fault is primarily a wrench fault with a significant amount of vertical movement associated with it. Extensive erosion is thought to have occured at several periods of its evolution, with Mesozoic rocks more widespread originally.

The history of the Great Glen Fault has undergone considerable examination in regard to its movement and path from the Scottish mainland to the offshore regions. Kennedy (1946), proposed sinistral movement of 65 km along the fault, based on evidence from the Strontian and Foyers granites which he thought to be the same body originally, and also from the displacement of metamorphic zones. The major movement was thought to have occured between lower and middle Old Red

10

Sandstone times. Ahmed (1967), however, using magnetic evidence, suggests that the bodies are different and thus throws doubt on the strike slip proposals and Shand (1951) states that no evidence of slickensides can be found in the region, these being characteristic of strike slip faults. Marston (1967), though, states that the possibility of the granites being connected should not be excluded on structural and geochemical grounds and proposes sinistral movement accompanied by a dip slip component downthrowing to the south-east.

Dextral movements have also been suggested for the fault. Holgate (1963) suggests an eighteen mile dextral shift, shown by the displacement of dykes. This he dated at 52 myrs, which is the minimum age of the dykes. Garson and Plant (1972) propose that all the motion is dextral with shifts of a much earlier age having occured. Pitcher (1969) however, cites evidence against Holgate's proposals and agrees with Kennedy in that there was little transcurrent movement after the Carboniferous, although he suggests there might be evidence of a powerful dip slip component from comparison of grades of metamorphism either side of the fault.

McQuillin and Binns (1975) suggest a downthrow to the east occured in the Late Jurassic and early Cretaceous with upper Cretaceous sediments overstepping from Middle to Lower Jurassic. Bacon and Chesher (1974) state that in the Moray Firth, all Mesozoic movement has been entirely normal and that no transcurrent movement occured after this time. There was a final phase of movement at least post lower Cretaceous. Although this is contrary to Holgate's hypothesis of Tertiary transcurrent movement, it does not damage the theories of Garson and Plant (1972). Westbrook (1973b) disagrees with Garson and Plant, stating that the theory

of dextral movement ^ is unfounded on the basis of the metasediment type on Coll and Tiree being no more similar to South Harris as to other localities in the Outer Hebrides. Storetvedt (1974) also suggests that palaeomagnetic evidence from Scotland and Norway indicates large scale sinistral movement of Devonian age. This is supported by Winchester (1973) who suggests strongly, from the regional metamorphism pattern of the Moine assemblages, that the only possible shift was a sinistral displacement of up to 160 km.

The development of the fault system and therefore, the sedimentary basins is thought to have occured by extensive normal faulting during a pronounced tensional phase probably in the Permo-Triass (Dobson and Evans, 1974). Binns et al. (1975) believe that the process of formation may be considered in the context of continental drift in the North Atlantic (Bullard, 1965) and the reconstruction of the Caledonian-Appalachian orogenic belt (Dewey, 1969) of which the Hebridean shelf is a part. Whitbread (1975), however, states that no single system of rifting accounts for the disposition of basins west of Britain.

Hallam (1972) suggests that the early Mesozoic graben subsidence relates to the separation of north-west Africa from north America 180 myrs ago, followed by widespread subsidence prior to the opening of the Atlantic. He states, however, that the relationship between the major tectonic events in the British area to the opening phases of the Atlantic proposed by Pitman and Talwani (1972) are only tenuous. Suggestions are made that the phase of northwesterly faults and dyke intrusion mark a change in the regime of NW-SE tension to one of NE-SW or a combination of both. Regional extension is thought to have commenced in the Permo-Trias with the major phase occuring during the late Jurassic or early Cretaceous, possibly coinciding with the opening of the Rockall

Trough in the Mesozoic resulting in major block faulting. The separation of Greenland from northwest Europe in the Tertiary resulted in much igneous activity and accompanied by NW-SE cross faulting and further block faulting (McQuillin and Binns, 1973).

Hall and Smythe (1973) propose that the Rockall Trough was more relevant to the development of the sedimentary basins than the formation of the Reykjanes Ridge as suggested by Hallam (1972). They indicate that the trend of the Tertiary dyke swarm show crustal extension parallel and not perpendicular to the Ridge. Bott (1975) states that the basins are related to the formation and development of the continental margins either side of the Faroe-Shetland channel and the Rockall-Faroe microcontinent. This is supported by Roberts (1975).

1.6 Basins South-East of the Moine Thrust Zone.

South-east of the Great Glen fault zone are basins of considerable thickness resting on a basement of Dalradian metasediments. A larger basin than that just north of Colonsay runs from the south-east of Islay, south-westwards towards Antrim bounded by the Foyle and Tow Valley Faults. Further south lies a large basin in the Firth of Clyde of complex structure and varying sedimentary thickness. These basins may have similar structural histories to those north of the Moine Thrust zone but differ in their geology.

Dobson and Evans (1974) have shown that faults form the margins of the Mesozoic troughs in the Malin Sea which are floored by downthrown Palaeozoic and Precambrian rocks. They probably developed during the Permo-Trias by extensive normal faulting during a phase of tensional stresses. The Firth of Clyde basins are controlled primarily by the

13

Highland Boundary Fault and Southern Uplands Fault, and as such represent an extension of the Midland Valley graben.

1.6.1 Region Between Colonsay and Kintyre.

This area is controlled by four faults, the Great Glen, Loch Gruniart, Lough Foyle and Tow Valley. The geology is shown in Fig. 1.2. The faults downthrow Mesozoic sediments against the Dalradian metasediments of Islay and Jura. There is evidence of syndepositional movement along marginal faults (Dobson & Evans, 1974).

Considerable amount of uncertainty exists concerning the nature of the faults, their strike in the submarine areas and the relationship they have with the Great Glen fault. Of fundamental importance to the area is the Loch Gruniart fault which has been proposed as being a continuation of the Great Glen fault across Islay (Bailey, 1916). Westbrook and Borradaile (1978), however, find no evidence to support this hypothesis from magnetic studies, because the sharp deflection to the south that would be required disagrees with the proposals concerning the continuation of the fault into fault zones in Ireland (Pitcher, 1969).

Bailey (1916) first conceived the Loch Gruniart fault to be a normal fault although more recently Garson and Plant (1972) considered it to be a transcurrent fault with large dextral movement associated with some vertical displacement. No evidence has been brought forward in support of the suggestion that the fault passes through Loch Gruniart and Loch Indaal with 105 km sinistral displacement (Bailey, 1960). It now appears likely that the Loch Gruniart fault and other faults of the area are second order faults associated with the Great Glen fault (Durrance, 1976; Westbrook & Borradaile, 1978). The vertical component of the movement seems to be displayed by the Mesozoic and Lewisian rocks on either side of the fault at

14

Rhinns, where there is a downthrow of 1 km to the south-east. Offshore, the line of the fault extends between Islay and Colonsay, reaching at least the north of Colonsay and very possibly meeting the Great Glen fault (Dobson et al., 1975).

The initiation of the four major faults probably occured in the late Devonian although an earlier date is quite possible. Syndepositional movement along the faults followed the Permo-Trias with gentler deposition occuring later in the Mesozoic, most notably during the Lias and Upper Cretaceous (Dobson and Evans, 1974). In the early Tertiary, extensive igneous activity began, as in the area further north and associated structural adjustments occured. The Permo-Triassic basins are thought possibly to be related to the early movements of the opening of the Atlantic and the late Cretaceous and Tertiary faulting and vulcanicity representing the opening and formation of the Reykjanes Ridge 60 myrs ago (Dobson et al., 1975).

1.6.2 Geology of the Firth of Clyde Region.

The Firth of Clyde region is the seaward extension of the Midland Valley of Scotland occupying the area between Kintyre and the Scottish mainland, where it forms a graben structure with sedimentary infill. Fig. 1.3 gives a summary of the geology of the region. A detailed map of the area is presented by McLean and Deegan, (1978). The area is bounded by the Highland Boundary fault to the north and the Southern Uplands fault to the south, creating a downthrown crustal block covered by upper Palaeozoic strata. Correlations along the strike of the Highland Boundary fault suggest that its direction changes to $N38^{o}$ compared to $N57^{o}$ on the mainland, but no change is noted in strike of the Southern Uplands

15
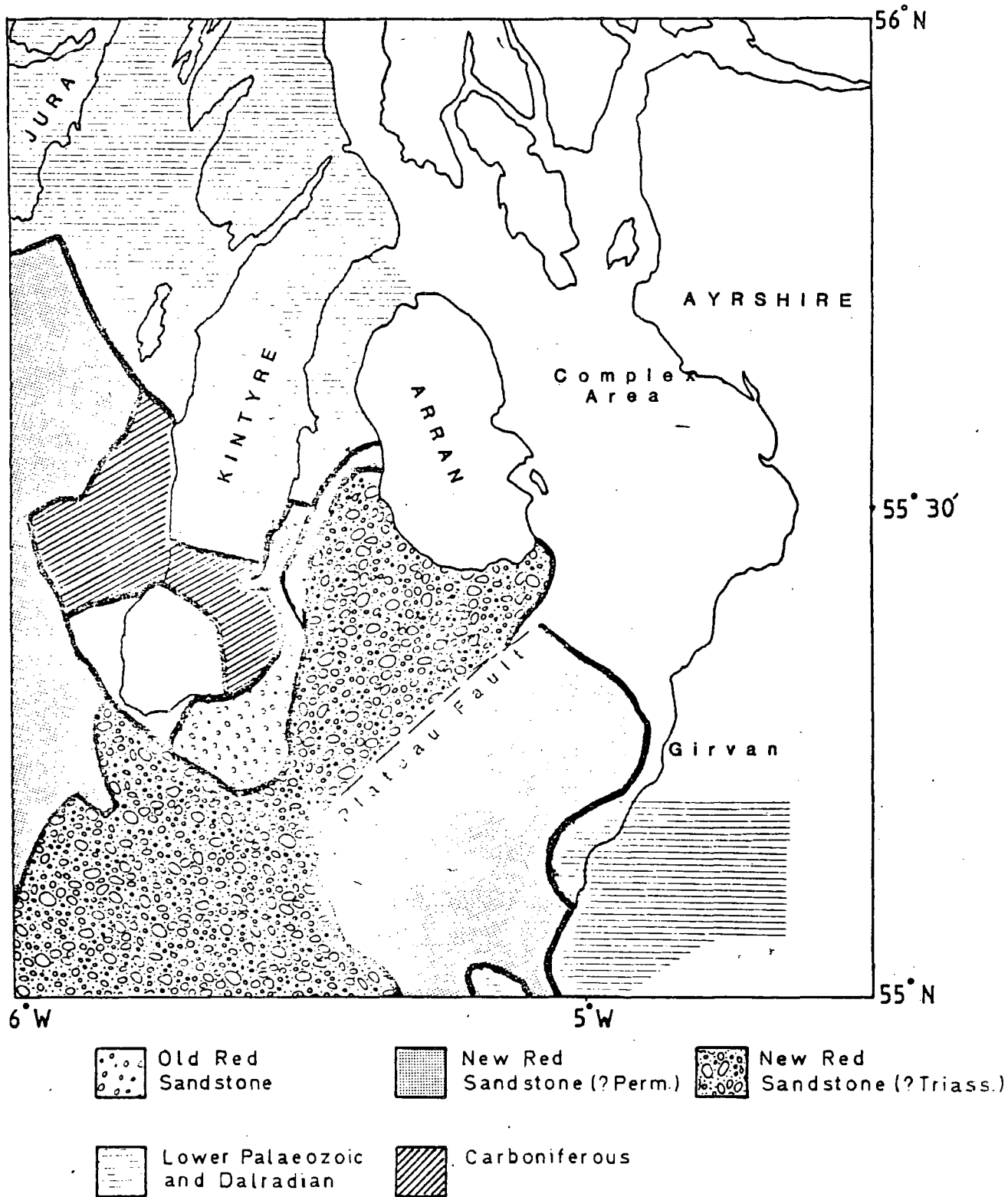
Fig.1.3:   Summary of the geology of the Firth of Clyde and surrounding areas showing main units between Jura and Girvan.

fault (Anderson, 1947; Friend & MacDonald, 1968). This results in a narrowing of the graben from 80 km on the mainland to 50 km in the Clyde. The graben itself is floored by Dalradian low grade metamorphic rocks. In some places there may be pre-Dalradian basement rocks locally present beneath the upper Palaeozoic succession of the Midland Valley graben with Lewisian pyroxene granulites present at shallow depth in the northern sound of Jura (McLean & Deegan, 1978).

Resting upon the Dalradian basement are lower and upper Old Red Sandstone deposits, the upper everywhere unconformable with the lower due to the lack of middle Old Red Sandstone. The unconformity is shown to be greater towards the margin of the graben. Thick lavas are found within the lower Old Red Sandstone but few igneous rocks are known to exist in the upper succession. During Old Red Sandstone times, there was considerable tectonic activity with movement along several of the major north-east trending faults, accompanied by widespread erosion. A decrease in thickness is noted along the northern margin on going towards the south-west (Friend & MacDonald, 1968) and large local variations in the upper Old Red Sandstone are seen where it spreads across eroded structures in the lower Old Red Sandstone and across the Highland Boundary fault. (Richey et al., 1930) have proposed that the lower Old Red Sandstone may be thinner near the central axis of the Midland Valley, quoting thicknesses of 1800m at Arran and Loch Lomond and 1200m on Kintyre. In addition, McLean and Deegan (1978) have suggested that if Dalradian rocks between Arran and Kintyre are unfaulted, 1800m exist south of the presumed extension of the Highland Boundary fault with only 40m to the north.

Resting on the Devonian sequence is a succession of Carboniferous rocks of varying thickness, the most notable variations being

16

where the lower Carboniferous straddles the north-easterly trending faults. The changes are related to contemporaneous movement along the faults resulting in differential subsidence. Significant thicknesses may be preserved locally but in general the Carboniferous sequence is attenuated or absent towards the south-west, mainly due to breaks in sedimentation and lateral changes, combined with westerly overstep of New Red Sandstone (McClean & Deegan, 1978). Hall(1978b) has suggested, from seismic refraction studies, a thickness of about 1.1 km overlying the Clyde Plateau lavas in the north-east Arran trough. Across the Highland Boundary fault the Carboniferous, and in some regions, Old Red Sandstone, oversteps onto the Dalradian schists. The late Carboniferous was marked by the intrusion of thick dolerite sills and east-west dykes in Ayrshire and Arran, a pattern thought to be repeated offshore.

New Red Sandstone crops out over most of Arran and has a south-westerly dip towards the North Channel covering most of the plateau areas of the Firth of Clyde. In the eastern half it oversteps the upper Palaeozoic strata to rest on the lower Palaeozoic. The greatest thickness is preserved in the south-west Arran trough with possibly up to 1.0 km on the downthrown side of the Plateau fault.

Gunn (1903) inferred a stratigraphy for the Clyde by comparing the Rhaetic, Lower Liassic and Cretaceous strata of Northern Ireland with fragments found in the central complex of Arran. McLean & Deegan (1978) propose that chalk would rest unconformably on Lower Lias, consistent with the samples found in the Central Complex. Lower Lias sediments are found but there is no evidence of Upper Jurassic and lower Cretaceous existing in Ireland. Their existence can therefore only be postulated upon. There is evidence of upper Cretaceous deposition and it is

17

possible that the chalk extended at least as far as Arran and Mull.

Although layered rocks of Tertiary age crop out to the west, there is no evidence of these plateau basalts being preserved from erosion in the Firth of Clyde. There are also no sediments of Tertiary age found in the area. Intrusive Tertiary rocks are widespread, with dykes of the Mull swarm cutting rocks near the Upper Firth along with dykes of the Arran centre seen along the Ayrshire coast and Kintyre. It is inferred from this that many dykes probably outcrop in the sea areas and are particularly abundant in the upper Firth south-west of Arran.

The southerly course of the Highland Boundary fault defining the basin appears at first to suggest that this area is structurally anomalous with respect to surrounding parts. Here the faults follow the uniform NE-SW paths distinctive of Caledonian structures. However, gravity and magnetics indicate that the Highland Boundary Fault is broken into distinct segments by sinistral faults causing it to step to the south, resulting in the individual trends being similar in trend to that of the main faults in Scotland. Considering such circumstances, George (1960) suggests that a miscorrelation between the major faults is more likely than a southerly trend for the Highland Boundary Fault. In another respect however, the Firth of Clyde is an anomalous region as it has important structures trending north-south modifying the graben, the line of Tertiary igneous centres being of this form, whereas all other dominant features in the area trend NE-SW.

18

CHAPTER 2

DATA ACQUISITION

2.1 Introduction.

The data for WISE were collected on two cruises, the first in November 1979 and the second in late August/early September 1981. On both occasions, recording stations were positioned on land and explosives and airguns were used as sources at sea. The recording stations were set up on the islands and peninsulas between Barra and Girvan for the first phase of the experiment and on those between Mull and Kintyre for the second phase. In addition, records were obtained from the permanent LOWNET array set up by I.G.S. and from the Eskdalemuir array of the U.K.A.E.A..

The continuous airgun profile was intended to provide details over the entire line of the upper sedimentary cover and lateral changes in velocity of the Lewisian basement. The furthest range that the airguns were expected to reach was the distance between two consecutive stations, this generally being between 20 and 30 km. The explosive shots were required to provide information on the deeper crustal structure, mainly that of the middle crust but also some estimate of the depth to the Moho. It was also hoped that phases other than first arrivals, such as wide-angle reflections and S-waves would provide valuable information on properties of the rocks, such as Poisson's ratio and sedimentary velocities.

The layout of explosive shots was designed to give optimum coverage and penetration along the line and therefore, charge sizes were varied accordingly (Sections 2.2 & 2.3). The recording stations were manned by research students and staff from Durham and Glasgow Universities. The

work at sea was carried out by personnel from Durham and R.V.S. Barry, South Glamorgan under the supervision of Dr. G.K. Westbrook using R.R.S. John Murray in 1979 and M.T. Farnella in 1981.

2.2 WISE Phase 1.

This phase of the experiment was completed between 12th and 27th of November 1979. Initially it was the only period of fieldwork planned for the experiment, but because of poor data quality in the central section of the line, another period of data acquisition was undertaken (Section 2.3). It was this first phase of the experiment though, that provided the majority of the data that was used for the study.

Most of the stations operated with three orthogonal component seismometer sets, the horizontal seismometers placed parallel and perpendicular to the line. This was to enable all components of ground motion to be measured. The seismometer and recorder sets used were of two types. Either Willmore Mk.3 seismometers operating with a Geostore recorder on loan from the N.E.R.C. equipment pool at I.G.S. Edinburgh, or Willmore Mk.2 seismometers operating with the Mk.3 Seismic Recorder developed at Durham by R.E. Long. Some outstations at Jura and Girvan operated with vertical seismometers only and the data were transmitted to the main recording station by radio telemetry links, where they were recorded on a Geostore. A three component set at Iona was recorded at Mull by the same method. This enabled the siting of stations in areas where a recorder could not be placed due to the lack of suitable cover. A map of the area of study indicating site locations and recorder type is given in Fig. 2.1. All tapes from each of the recording sites are accompanied by a set of log sheets giving details about the site, such as rock type, gain changes and breakdowns.
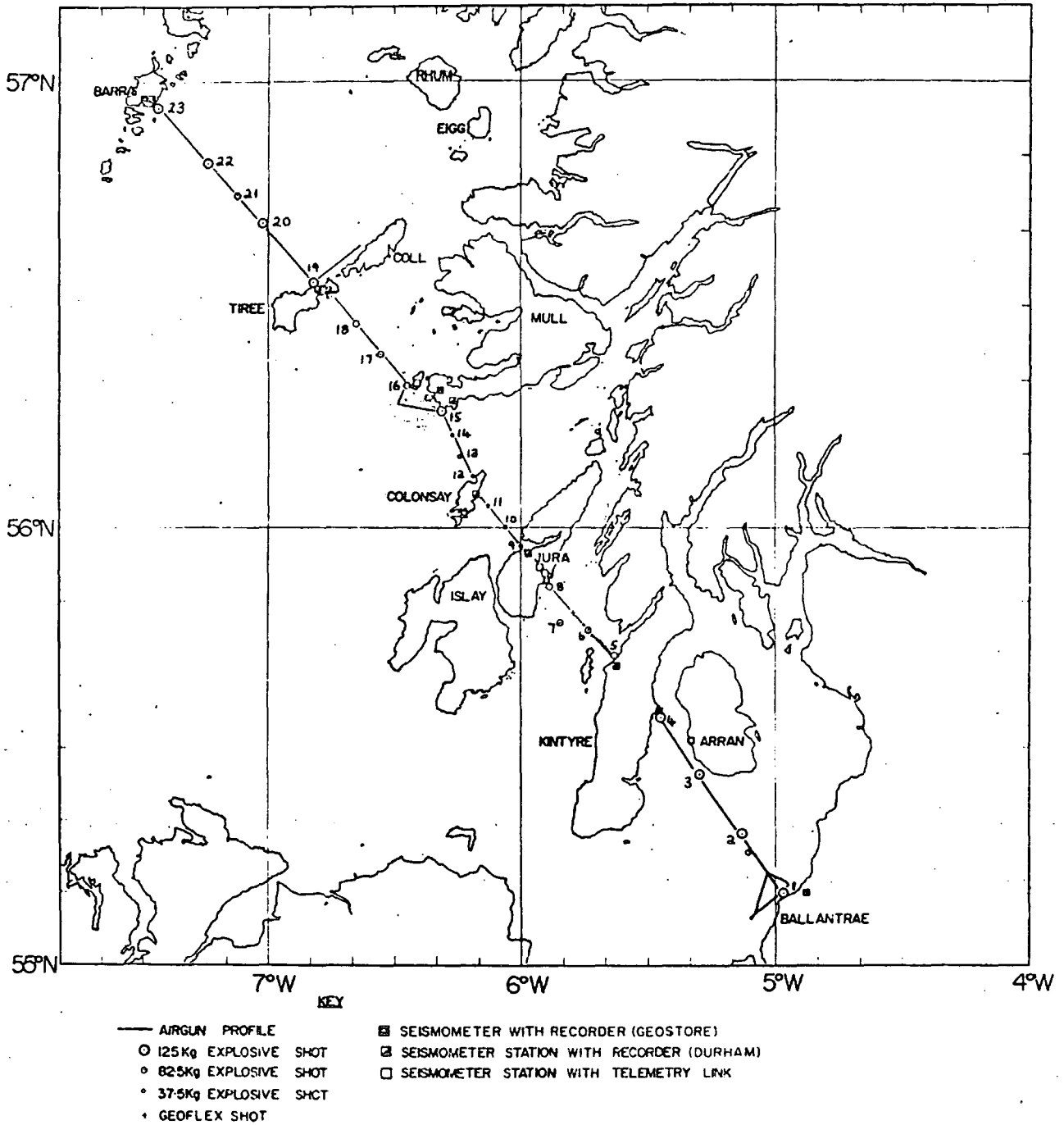
Fig.2.1: Station locations, shot locations and line of airgun profile for phase one of WISE. The type of recorder used at each station and size of shot charge are shown.

Twenty-three explosive shots were fired during this phase of the experiment, their locations and charge size also shown in Fig. 2.1. Full details of the explosive shots, including size, detonation time and depth of water are provided in Table 2.1. The airgun source had a capacity of 1000 cu.in., firing once every three minutes, providing a shot separation of approximately three hundred metres. The dates of each leg of the airgun profile along the line are given in Table 2.2. As some sections of the line were notably longer than others, for example that between Tiree and Barra, they were not expected to be reversed by using just the recording stations at both ends. In these cases it had been planned to use a moored sonobouy to provide the extra coverage required. However, the very poor performance of the sonobouy transmitter when the buoy was in the water meant that it could not be used. As a consequence of this, the short lines that were to be shot along the strike of the major structures also had to be cancelled.

2.3 WISE Phase 2.

With the availability of ship time at the start of a seismic reflection cruise, it was decided that the section of the line between Mull and Kintyre should be re-shot as the data obtained from this area during the first phase were poor because of wind noise at many of the stations. The degree of noise depended on the station, but was particularly noticeable at stations between Tiree and Colonsay. This second phase of the experiment had a very much reduced shot/station coverage. Two different types of recording equipment were used. Mull, Iona and Colonsay operated with Willmore Mk.3 seismometers and Durham Mk.3 recorders, and the station at North Jura used Willmore MK.2 seismometers with this recorder type. On

Table 2.1

WESTERN ISLES SEISMIC EXPERIMENT

Positions and times of detonation of large explosive shots

No	Weight	Latitude	Longitude	Water Depth	Date	Time ± .03s
1	125 Kg	55°10.0'	04°58.4'	20.1 m	12.11.79	1532 05.79
2	125	55°18.1'	05°08.0'	46.6 m	12.11.79	1332 20.33
3	125	55°26.45'	05°18.1'	18.3 m	12.11.79	1132 01.39
4	125	55°34.08'	05°27.25'	38.4 m	12.11.79	0939 40.57
5	87.5	55°42.54'	05°38.21'	11.9 m	13.11.79	0818 12.40
6	87.5	55°46.05'	05°43.79'	73.2 m	13.11.79	0911 29.47
7	87.5	55°47.04'	05°50.75'	181.1 m	18.11.79	1142 48.86
8	87.5	55°51.84'	05°53.54'	31.1 m	18.11.79	1047 10.14
9	37.5	55°57.5'	06°00.00'	21.0 m	13.11.79	1316 47.90
10	37.5	56°00.0'	06°03.5'	17.4 m	13.11.79	1346 56.62
11	37.5	56°02.9'	06°07.9'	36.6 m	13.11.79	1416 35.19
12	37.5	56°06.9'	06°11.7'	30.2 m	13.11.79	1531 40.83
13	37.5	56°09.6'	06°14.95'	81.4 m	13.11.79	1611 49.85
14	37.5	56°12.5'	06°16.35'	73.2 m	13.11.79	1641 51.46
15	125	56°15.7'	06°18.5'	29.3 m	19.11.79	0948 51.02
16	87.5	56°19.2'	06°27.7'	25.6 m	19.11.79	1117 08.26
17	87.5	56°23.38'	06°32.96'	100.6 m	19.11.79	1211 49.27
18	87.5	56°27.48'	06°39.02'	82.3 m	19.11.79	1311 52.48
19	125	56°32.9'	06°49.3'	230 m	15.11.79	0911 51.16
2C	125	56°41.15'	07°01.55'	157.3 m	15.11.79	1048 43.38
21	50	56°44.77'	07°07.38'	197.5 m	15.11.79	1126 50.81
22	125	56°49.09'	07°14.10'	155.4 m	15.11.79	1216 59.26
23	125	56°56.65'	07°26.25'	21.0 m	15.11.79	1347 16.37

Table 2.2

1000 cu.in.   AIRGUN PROFILE – PHASE 1

Station Pair	Start		End	
Colonsay–Mull	11.06	14.11.79	18.39	14.11.79
Mull–Tiree	18.42	14.11.79	23.03	14.11.79
Barra–Tiree	22.18	15.11.79	01.44	16.11.79
Barra–Tiree (2)	21.15	16.11.79	08.48	17.11.79
Jura–Kintyre	13.21	18.11.79	16.54	18.11.79
Kintyre–Girvan	21.24	20.11.79	11.21	21.11.79
Kintyre–Jura (2)	09.21	23.11.79	12.54	23.11.79
Jura–Colonsay	15.30	23.11.79	18.00	23.11.79
Shot 21 – Tiree	17.39	26.11.79	22.06	26.11.79
	Shot Firing – 3 minute intervals			

the southern section, that is on Kintyre and South Jura, the cassette recorder, developed at Glasgow University was used. The station locations and type are given in Fig. 2.2. Log sheets were made for all stations.

Ten 50 kg explosive shots were fired in total, this being thought sufficient to provide good coverage over the extent of the line. One of the shots was located as closely as possible to that of the previous phase to provide a link between the two sections of the experiment in addition to the reoccupation of the same recording stations. All the relevant information concerning the explosive shots is provided by Table 2.3. The airgun profile was run along the line between Mull and Kintyre, but in this case, using experience gained from the first phase, two 1000 cu.in. airguns were fired simultaneously. Thus it was hoped to ensure that the shots would be received along the entire extent of the line, providing complete reversal, whereas attempts had to be made to filter the earlier airgun records to locate the signal where it was obscured by noise (Chapters 3 & 4). The firing interval was every two minutes, giving a shot separation of approximately two hundred metres.

The completion of the second phase of the experiment took only two days, the explosive shots being fired on August 31st, and the airgun profile taking twelve hours on September 1st. Table 2.4 gives the time of each leg of the profile. Although problems in data quality still existed, especially concerning the airgun data (Chapters 3 & 6), the data quality for this section of the line was superior to that obtained in 1979.

2.4 Shot Details

As the majority of the information concerning the explosive shots has already been provided in Tables 2.1 and 2.3, only their type and timing procedure needs to be presented here. I.C.I. Geophex explosive was

WESTERN ISLES SEISMIC EXPERIMENT - 2
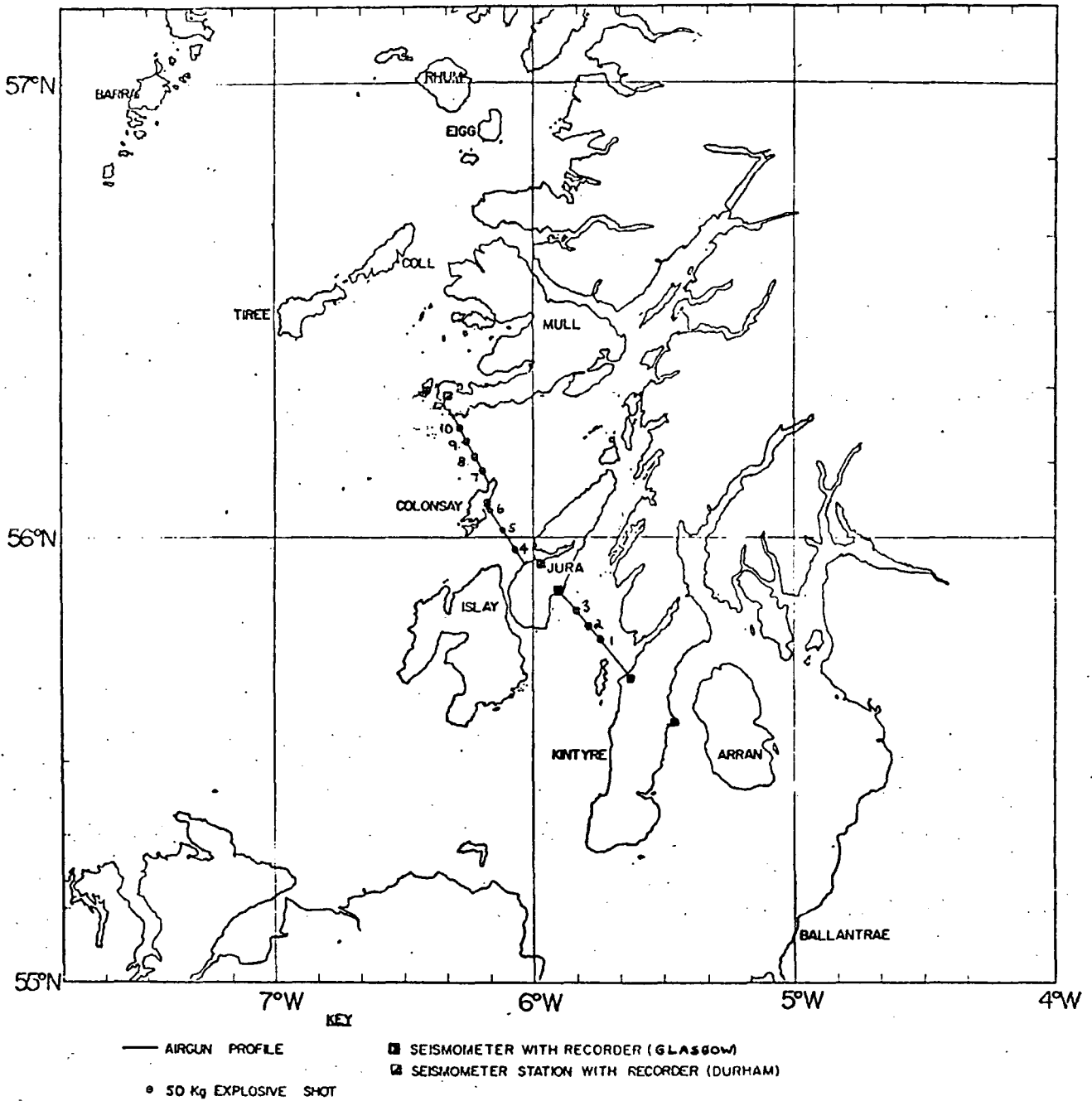
Fig.2.2: Station locations, shot locations and line of airgun profile for phase two of WISE. The type of recorder used at each station is shown. All shots were 50 kg.

Table 2.3

WESTERN ISLES SEISMIC EXPERIMENT   -   PHASE 2

Positions and detonation times of explosive shots - 31.8.81

No.	LATITUDE	LONGITUDE	WATER DEPTH	TIME $\pm$0.03
10	56° 14.16'	6° 17.55'	49.5 m	0915 22.03
9	56° 11.32'	6° 15.25'	75.8 m	0948 10.35
8	56° 9.80'	6° 13.94'	75.9 m	1018 17.02
7	56° 7.65'	6° 12.27'	31.1 m	1043 40.89
6	56° 4.42'	6° 9.35'	20.1 m	1138 51.42
5	56° 1.45'	6° 5.23'	31.3 m	1220 00.59
4	55° 58.37'	6° 1.38'	22.5 m	1245 45.64
3	55° 50.52'	5° 50.22'	56.4 m	1515 48.83
2	55° 49.00'	5° 48.31'	180.8 m	1544 10.80
1	55° 47.56'	5° 46.04'	69.6 m	1616 43.09

All shots 50 kg weight

Table 2.4

2 x 1000 cu.in. AIRGUN PROFILE - PHASE 2

(1.9.81)

Station Pair	Start	End
Kintyre-Jura	10.00	11.36
Juran-Colonsay	15.12	17.54
Colonsay-Mull	19.30	20.06
Shot Firing - 2 minute intervals		

used. made up to the required charge size by strapping together the necessary number of 12.5 kg sticks. They were released with a fuse long enough to ensure that they did not detonate until they were resting on the sea floor. This firing procedure was used in preference to that described by Jacob (1976) and is often implemented in marine studies. The method used is quicker and safer, and in the region of WISE, the depths are too shallow for detonation of the charges at a depth of one quarter of a wavelength beneath the sea surface. Detonation at the sea bed is also efficient with no reflective losses because the source is at the media boundary.

The shots, received at a hull geophone and a hydrophone towed behind the ship, were recorded on eight track analog magnetic tape together with MSF time code and internal clock code. The tape was then played out onto paper records using a jet pen oscillograph and the arrival time measured. During the second phase of the experiment, such records were made at the same time as recording on tape and the arrival time of the water wave could be picked directly from these. Correction was then made for the time delay due to the distance between the shot drop point and the ship's location on receiving the arrival to derive the shot instant. The timing of the shots using this method was accurate to 0.03 seconds.

2.5 Recorder Details.

2.5.1 Durham Mk.3 Recorders.

The Mk.2 seismic recorders developed at the department of Geological Sciences, Durham have been well described by Long (1974). The Mk.3 recorders are a development of the Mk.2 system and have been given a thorough description by Savage (1979). In the light of this therefore, it is not necessary to provide a full description of the recorder but only

outline its major features.

The recorder operates from either an external or internal battery source providing 24 volts. Facilities exist to change the batteries whilst continuing recording and operation of the clock. The tape drive uses standard triple or double play, eight track, quarter inch tapes running at a speed of 15/160 i.p.s.. This allows either seven or four and a half days continuous recording. Build up of oxide on the the tape heads occurs often though, making it inadvisable to leave a significant length of time between inspections of the recorder, as this seriously degrades the quality of the recording. For WISE, checks were made twice a day. Although eight tracks can be recorded, only six are used, their allocation given in the equipment manual. Tracks 1 to 5 record in frequency modulated mode, using a 30% deviation of a carrier frequency of 71 Hz centre frequency. Track 6 records a 100 Hz signal at saturation which is used for flutter compensation. Tracks 7 and 8 record time pulses represented in switches of carriers between 50 and 100 Hz.

Two time codes are recorded, the internally generated code, and either time pips from B.B.C. radio or a continuous recording of MSF, the latter being used for WISE. Three seismic channels can be recorded, which are amplified after being sent down the cable from the seismometer and frequency modulated before being recorded on tape. The gains on the seismometers can be changed by means of a thumbwheel, and are stepped up by factors of two. At gains greater than seven, a high cut filter is used to reduce the noise at the station (Section 2.8). Extensive checkout facilities are incorporated in the recorder, enabling a monitoring of any of the channels before and after recording. This is done by both audio and visual means. Three meters are used to indicate whether sufficient voltage

24

is present across both the recording and playback heads to allow good quality recording, and an earphone can be used to check the quality of the recording as the tape passes the playback head.

For an extensive description of the recorder's character- istics and its operation, a manual by Long (1975) is available at Durham University. A detailed appraisal of the difficulties and breakdowns encountered with the use of the recorder in the field is provided by Savage (1979) and should be consulted before the recorder is used.

2.5.2 Geostore Recorders.

For the work carried out in 1979, six Geostore recorders were obtained on loan from the N.E.R.C. equipment pool. Much information on the recorder is readily available and a comprehensive technical handbook is provided by the manufacturers (Racal Thermionics, 1979). This describes all the recorders operational features and provides circuit diagrams and' layout. Therefore, as in the case of the Durham Mk.3 recorder, only a brief description is given here in order to outline the recorder's main features.

The Geostore is operated by three 12 volt external batteries, two of which are used for the recorder and one for the outstation. As only 12 volts are required to supply the recorder, the other battery is used when changeover takes place, ensuring that there is continuous recording and that the clock does not stop. Fourteen tracks are recorded on half inch width, seven inch diameter magnetic tape running at a speed of 15/160 i.p.s., although this can be varied depending on the frequency of the data that is being recorded. This recording speed, which is the fastest available provides a bandwidth of 0-32 Hz .

Two operational modes exist enabling either six or three

days continuous recording. The first mode is unidirectional, allowing an internal time code, an external time code (MSF in this case), two flutter tracks and ten seismic channels to be recorded. Alternatively, the recorder can be used in a bi-directional mode, using an auto-reverse mechanism. This enables seven tracks to be recorded in one direction and seven in the other. Using this type of operation, two time codes, a flutter track, and four seismic tracks are recorded on each complete cycle of the tape. The channel allocation on tape for seismic and flutter tracks and time codes is given in the manual quoted above.

With three component seismometer sets the auto-reverse mechanism was used, but with the additional vertical seismometers telemetered into the main station on Jura and at Girvan, and with the extra three component set on Iona recorded at Mull, the Geostores were used in uni-directional mode.

Unlike the Durham Mk.3 recorder there is no built-in modulator for the seismic tracks but instead the signal is modulated when it is received at the seismometer by an amplifier modulator, before it is passed down the cable. The external time channel has this built-in and therefore must always be used for this purpose. The internal time code is frequency modulated before recording. All tracks use a carrier frequency of 676 Hz with a maximum 40% deviation. The gains on the seismic channels can be adjusted individually using a setting on the modulator. A gain of 1 requires 250 mV to produce a 40% deviation of the carrier frequency, which then decreases in steps of 2 or 2.5 until the maximum gain of 10 which requires only 0.25 mV input voltage to produce the same deviation.

No built-in test and monitor facilities are provided but a field test box is available to carry out the important tests in the field

to ensure good quality recording. This enables a monitoring of the frequency modulated signal and the amplifier modulator output. Unfortunately not all the station operators were equipped with a field test box with complete facilities but each had an audio monitor to check that signals were being recorded on each channel.

2.6 North Sea Shots.

In July 1980, as part of a crustal seismic refraction project in the North Sea, Cambridge University fired a line of large explosive shots between the Moray Firth on the east of Scotland and the west coast of Norway. As several of these shots were large (1000 kg and 500 kg) and relatively close to Scotland, three of the recording stations of WISE were reoccupied to record the shots. It was hoped that these data would provide extra control on the crustal delays because all the stations were at sufficient distance from the shots to receive first arrivals from sub-Moho travelling waves, whereas in WISE no single shot gave sub-Moho arrivals at all stations along the line. Durham Mk.3 recorders were used with Willmore Mk.2 seismometers at Barra and Girvan and a Geostore operating with Mk.3 seismometers was used on Mull. Two shots were recorded, F2 (1000 kg) and F7 (500 kg).

2.7 Navigation and Bathymetry.

2.7.1 Decca.

For both phases of the experiment Decca Main Chain was used for navigation and shot positioning, although for the second phase it was used as a secondary method to the Trisponder system. The Decca Main Chain is normally used only for navigation and not for surveying. The system uses a master and three slave transmitters. It is a phase comparison system with

the master and each of the slaves providing a hyperbolic pattern, the intersection of which defines the position before correction. A fuller description is given by McQuillin and Ardus (1977). The system has been used in all marine refraction projects so far undertaken in British waters, and providing the data are processed correctly, by taking into account the fixed and variable errors, results to an accuracy of 100m can be obtained. This figure being quoted by Decca for the Hebridean and North-West Britain area. Considering the range of the shots for WISE and the accuracy in timing of the shot, this introduces a relatively small amount of error into velocity and delay time measurements.

2.7.2 Trisponder System.

This system is far more accurate for obtaining absolute positions, quoted as having an accuracy of one metre providing the position of the receiver can be so determined. It was used wherever possible on the second phase of WISE, resorting to Decca Main Chain only when breakdowns occured. The system functions by transmitting a continuous known frequency from the ship to the receiver on land which, when identified, is returned. The travel time is then converted to distance knowing the velocity of the wave. The distance between the two is given directly in metres. It is always advisable to have three Trisponder receivers in line of sight as the intersection between the arcs from each receiver will give the position. The error involved is shown by the amount of non-intersection that exists between the three. However, for WISE only two were available in any area and so the intersection of the two arcs from the receiver locations had to be taken as the position of the ship.

2.7.3 Bathymetry.

The depth to the sea floor was monitored along the line using Echosounder records. The records are given in fathoms which can be converted to time delays through the water by converting to kilometres and then using a velocity of 1.5 km/sec.

2.8 Criticisms Concerning Data Acquisition.

In order to appreciate the problems in the processing and interpretation of the data, it is necessary to give details of difficulties during data acquisition. Many of the problems identified by Savage (1979) were apparent on WISE especially during the first phase, with recorder malfunctions resulting in poor data quality at several of the stations. The reduced sections of the explosive shots shown in Chapter 6 and the airgun data presented in Chapters 3 and 4 provides evidence of this. A summary of data quality at each station for the first phase is given in Appendix 1.

Although it is felt that the equipment might not be as reliable as has often been suggested, and that reasons such as dirty heads were responsible for much poor quality data, certain steps could have been taken to ensure that it was in a better condition prior to the experiment. A state of bad preparation existed in the case of the Durham Mk.3 recorders, which were found not to be working a week before the project was due to commence, resulting in the amount of time station operators had to familiarize themselves with the equipment being insufficient. This was also the situation with the Geostore recorders. Several of the station operators indicated that the training course they attended at I.G.S. was insufficient and the lack of time before installation meant that a thorough examination and familiarization of the equipment in the laboratory could

not take place.

The characteristics of the Mk.3 recorders also appear to be unsuitable for the aquisition of airgun data, as there was a poor return of data for both phases. Although this may be attributed to tape flutter in many cases, it is also felt that the bandwidth is insufficient. Long (1974) has quoted the bandwidth of the Mk.2 recorders as being 0-20 Hz up to gains 7, cutting off sharply at the higher gains with a decrease in relative gain of 50% between 1 and 10Hz. At 20 Hz, the roll-off is complete. Therefore at large range, where the signal frequency would be low, high frequency noise at the station should be cut out. The Mk.3 recorders, were designed as an extension to this system, and were primarily to be used for studying teleseismic earthquakes. As such, the bandwidth was reduced and they also have a high-cut filter at high gains. The characteristics have not been fully documented, but investigation by G. Ruth has shown that there is a step in the response at 5 Hz for all gains. For gains 1-4 the filter rolls off slowly giving a bandwidth of 17 Hz. The rate of the roll-off increases significantly at a gain of 6 reducing the bandwidth to 12 Hz. At higher gains the bandwidth is even further reduced to no more than 8 Hz. It must be stated that the response curves are strange in character and do not follow the simple trend of the Mk.2 recorders shown by Long (1974).

Noise proved to be a major difficulty in the processing and interpretation of the data (Chapters 3, 4 and 6). As previously stated, this can be attributed to tape flutter for some of the airgun data of the second phase. However, even though the pits for WISE were positioned on bedrock, covered,and located in areas that were hoped to be free of wind noise, it still had an effect on the quality of the recording. For HMSP and

the station set up by the U.K.A.E.A. for NASP, a concrete base was placed on solid bedrock and the pit was lined with P.V.C. tubing to lower noise levels and keep the pit free of water. This was not done for WISE and even though the sites had been selected earlier, it is thought that some of the data, especially from the first phase, indicates high levels of wind noise at the station. In addition, as the first phase was carried out in November, several pits had to be dug at the stations as water seepage into the pit proved a problem. For the second phase, carried out in late summer, the pit preparation was adequate as the weather was more favourable and as the duration of the experiment was far shorter, less difficulties could be expected.

The author feels that from the experience gained from WISE, more care should be taken in the preparation of data acquisition to ensure that the quality of the data reaches the highest possible standard with the equipment used. Obviously breakdowns must be expected, but their occurence can be greatly limited through careful checking of equipment and more thorough training and familiarization being given to the station operators. It is clear that they have a limited time available for this process but some did state their wish to know more about the equipment and their unease in going into the field with insufficient knowledge of its operation.

CHAPTER 3

DATA PROCESSING

3.1 Introduction.

In order to handle and interpret large amounts of seismic data efficiently, they must be in a form that is easy to display. For WISE all the data were digitized from the analog magnetic tapes and then processed, displayed and interpreted with the aid of a computer. Prior to digitizing, the analog tapes were replayed onto paper records using a jet pen oscillograph to learn exactly which shots had been recorded at each station, and to pick arrival times initially.

Replaying and digitizing was carried out both at Durham and at I.G.S. in Edinburgh. At Durham, those tapes recorded on the Durham Mk.3 seismic recorders were played back on the quarter inch processing system, and at Edinburgh a permanent system is available in the Global Seismology Unit for the rapid replay and digitizing of tapes recorded on Geostore recorders. After completion of digitizing, a library of FORTRAN computer programs and subroutines was written to process the data on the NUMAC IBM 370/168 computer. Programs for handling the data on tape and disk and for graphical display to aid analysis were developed (Appendix 2).

The processing of the airgun data was carried out along different lines to that of the explosive shots. As there were a large number of airgun records and the arrivals could not always be seen throughout the entire section, attempts at their detection by automatic methods were made. This work was initiated by Birtles (1980) and much developed by Warren (1981). A summary is provided in section 3.5.

3.2 Replay and Digitizing.

3.2.1 Durham Mk.3 Recordings.

Processing of these data was delayed considerably due to a changeover in the processing system from use of a Modular 1 computer to one operating with LSI 11 computers. The complete system, with tape drives to enable transfer of data to the NUMAC computer was not fully operational until April 1981, leading to an eighteen month delay before any of this data could be processed. The main processing was carried out on the IBM 370/168 because programs were written for use on that machine and not on the computer of the seismology laboratory. It is only recently that full processing facilities have been implemented on the system.

The set up of the system is shown in Fig. 3.1. By controlling the analog replay deck with the computer, the tape can be scanned for events, viewing any of the six channels on a Tectronix graphics terminal. Three hours can be displayed at one time. When an event is found, either by direct identification or by reading the time code, it is digitized by placing cursors at the beginning and end of the required section. Playback onto a paper record can be made at the same time as digitizing. The data is then stored on a hard disk in multiplexed format in blocks of 512 bytes. Direct transfer can then be made between the disk and 9-track magnetic tape.

Tapes from Tiree and Colonsay for the first phase were digitized and those of Mull, North Jura and Colonsay for the second phase. The sampling rate was 50 samples/second, each sample being two byte integers. Digitizing using this system proved efficient providing that data quality was good. Often dirty heads on the recorder or poor or non-existent
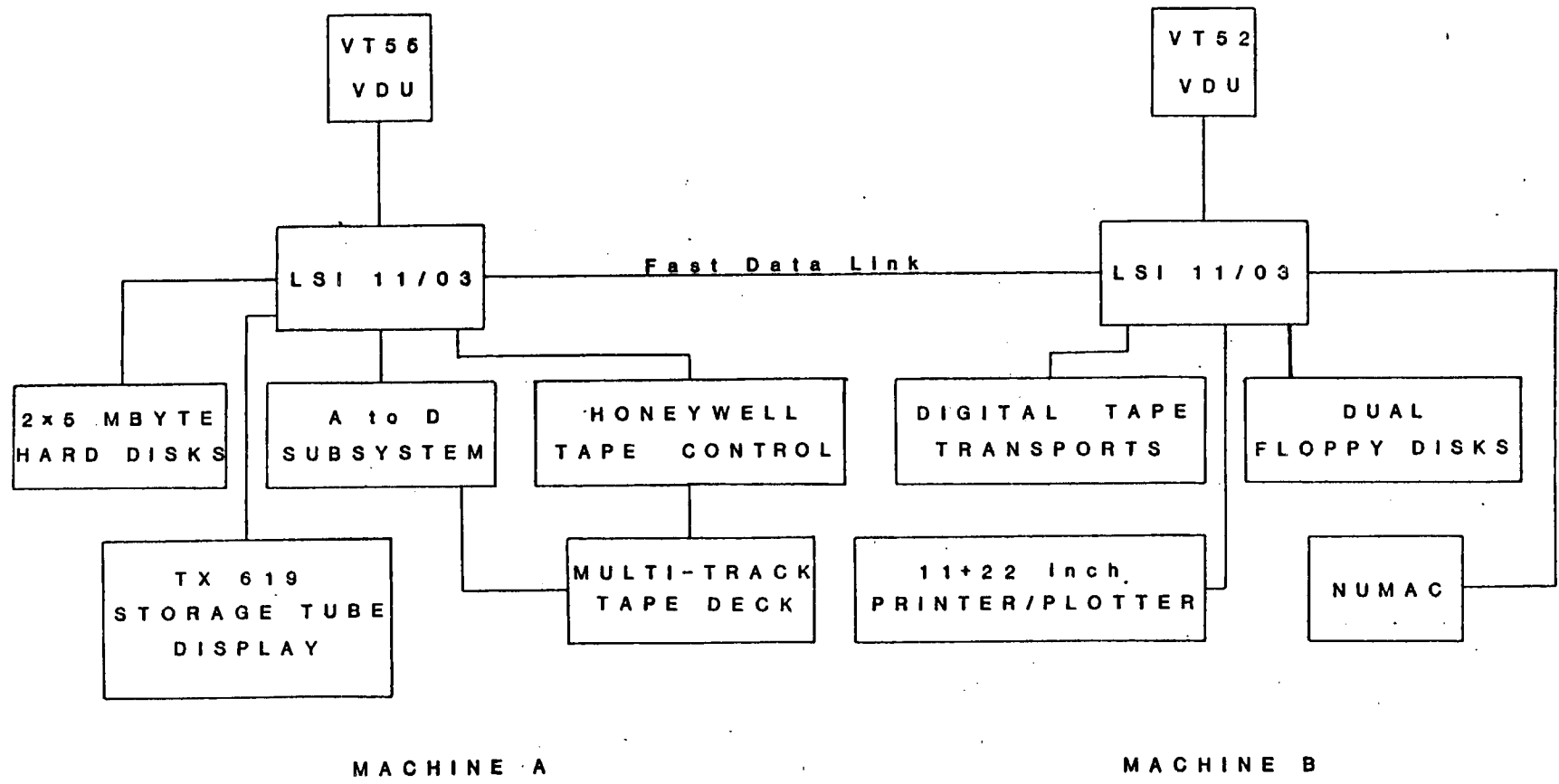
Fig.3.1:   Block diagram of the seismic data processing system
used at Durham.

time code meant that events were sometimes difficult or impossible to locate.

The main criticism about the system which has an important bearing on the subsequent use of the records is that complete flutter compensation is not achieved. Although some attempt is made to remove the effects of variation in tape speed not all has been removed and the sampling rate for each second is not constant. Details of the errors involved are given in section 3.4.

3.2.2 Geostore Replay and Digitizing.

The tapes from all the stations that used Geostore recorders were replayed at Durham using a Store-14 replay unit acquired from the N.E.R.C equipment pool. This required the use of different playback speeds and bandpass filters to bring out the signals to the optimum extent. This procedure was made more difficult by incorrect settings of the internal clock and poor MSF reception.

Analog records were made of all the explosive shots received at Barra, Jura, Mull, Iona and Girvan. At North and South Kintyre, however, and hence the Arran station which was recorded at South Kintyre by a telemetry link, incorrect setting up of the station resulted in no MSF being recorded.

The explosive shots were played back at two speeds with the time code played out both sides of the seismic events to ensure correct picking of shot times. Before playing out on the jet pen oscillograph, a calibration marker was placed simultaneously on each of the traces to ensure that there was no horizontal displacement between the pens. This was necessary for the correct timing of the arrivals. The two speeds used were 25 cm/sec. and 100 cm/sec. enabling quick location of the events on tape

and providing records that could be easily picked.

Most of the airgun data were played out at a far slower speed as it was thought that the amount of data to be examined required the use of a computer. The slower speed of playback merely provided records that gave an indication of the amplitude of the arrivals and of the maximum range from the station that they could be expected. The airgun data recorded on Mull and Iona were played back at the faster speed as from the first set of records these looked to be of good quality and could be examined without resorting to too much filtering.

When the events had been recognised, they were digitized at I.G.S. in Edinburgh. A diagram showing the steps in the operation is given in Fig. 3.2. The number of channels to digitize can be varied, although it was always kept at eight to aid the later processing. The sampling rate used was 64 samples/second as this was the maximum possible for the recording speed used for WISE. The number of seconds to digitize and gain can be varied and the starting time for digitizing once fed into the computer, is located and each channel is recorded on magnetic tape from that instant. The number of seconds to digitize is also given along with the gain, thus preventing the clipping of large arrivals. The digitized tape can be replayed to ensure all events have been recorded correctly.

In general, the system has more options than that at Durham, which is largely due to it being set up for this type of processing with varying tape speeds. Problems do occur though when bad patches of time code are found on tape as the computer program that controls the digitizing relies on being able to read the time code. This can be overcome by using a manual digitizing operation and starting and stopping the tape at the points about the region to be digitized. One important feature of the
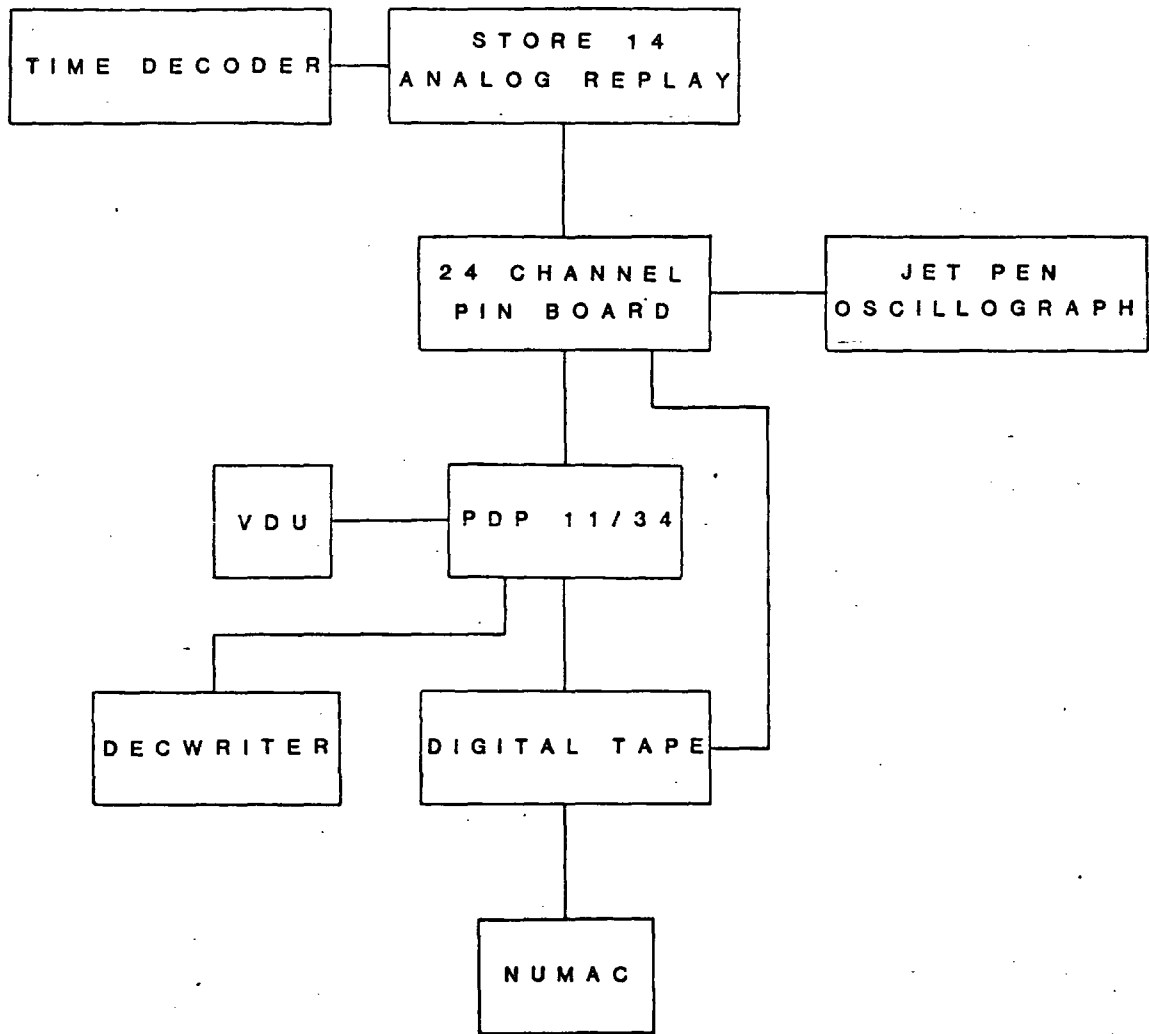
Fig.3.2:   Block diagram of the processing system used for digitizing seismic data at I.G.S. in Edinburgh.

system is that flutter compensation is very efficient, and as the sampling is controlled by the flutter track, the number of samples in each second always remains constant.

All shots and airgun data recorded at Barra, Jura, Mull, Iona and Girvan were digitized. Channel relationships between analog and digital data on tape for each station are provided in the tape log book. The files on tape are unlabelled but the location on tape where each shot can be found is also provided in the log book.

3.3 Programs Developed For Data Processing.

Although seismic refraction experiments are well established techniques, and the processing of the data carried out along standard lines, no one set of programs existed for use on the IBM 370/168 computer to process the WISE data. The reason for this is that most programs that have been developed are very specific and are generally not well enough stored or documented for anyone other than their author to use them. A suite of programs was written to handle the data from WISE rather than a modification of pre-existing programs. These programs are presented in Appendix 2, and are commented to indicate where they have to be altered if data different in form to the WISE data are available. Such modification would hopefully only have to be small though if the data is digitized on the systems at Durham and I.G.S. and processed on the NUMAC computer.

Fig. 3.3 is a diagram indicating the various stages of the processing and the options available from the point when the data is on digital tape. The following give brief descriptions of the operation of each of the stages. The comments in the programs provide details on the operation of each one. All programs are used interactively and the user is

DIGITAL TAPE

TPTODSC.G
TPTODSC.D Demultiplex and Transfer to Disk

Check Sampling Rate **TIMESAMP** **PUBLIC DISK** **CHPLOT.G**
CHPLOT.D Plot File

TCPLOTS Plot Time Codes

Dump Trace **CHDUMP.G**
CHDUMP.D **TIME DECODING SUBROUTINES**

GEOSECT
DURHSECT Plot Reduced Section

Plot Power Spectrum **FREQPLOT**

BANDPASSING SUBROUTINES **GEOPLOT**
DURHPLOT Plot Event
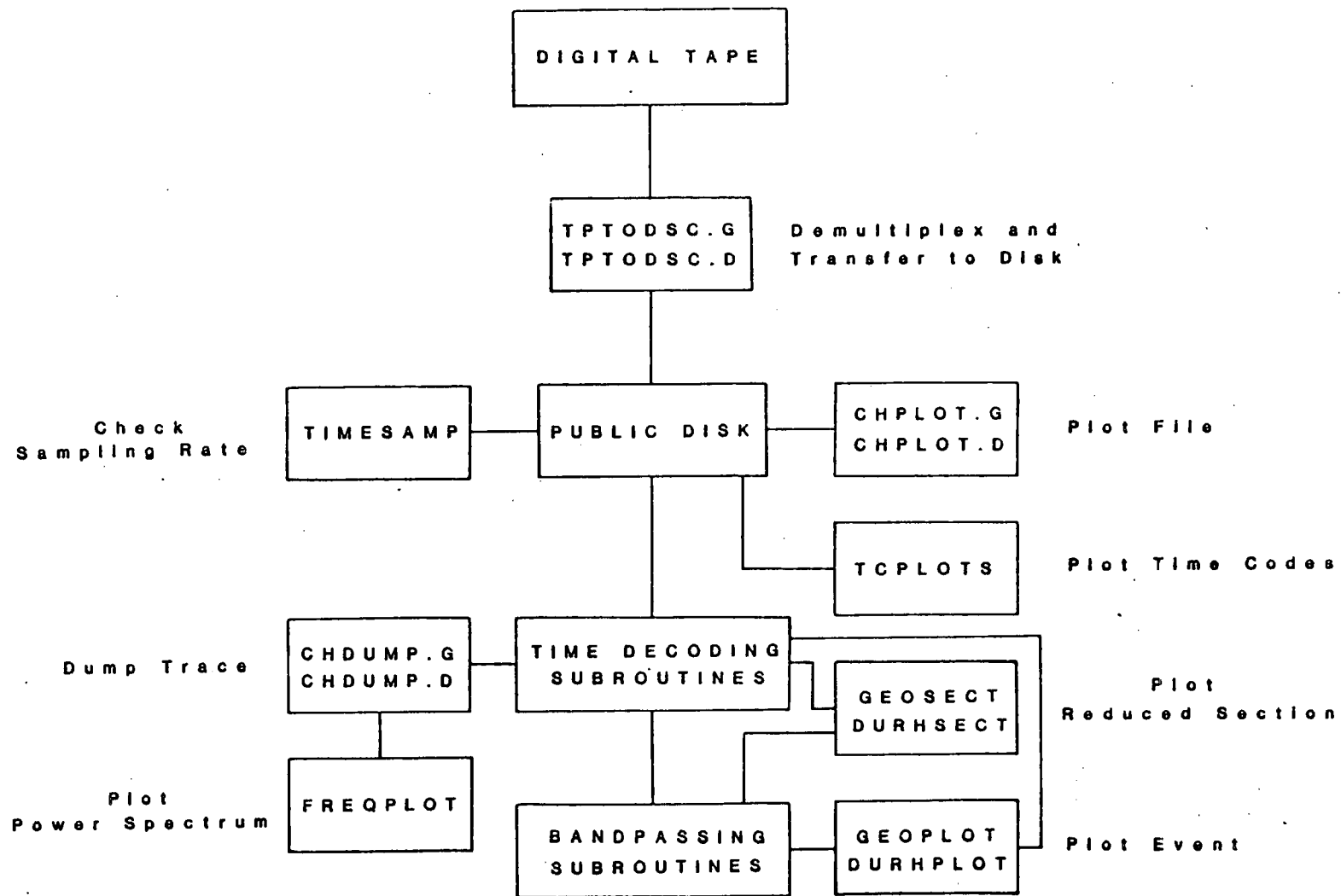
Fig.3.3:   Block diagram showing the different processing stages that can be carried out on seismic data using NUMAC, and the programs that carry out each operation. Those beginning with GEO and with the suffix .G are for use on data recorded on Geostores and digitized at I.G.S. in Edinburgh. Those beginning with DUR and with the suffix .D are for use on data recorded on Mk.3 recorders and digitized at Durham.

prompted for any parameters about the data that are required, eg. sampling rate, channel number.

3.3.1 Transfer Programs.

These were written to transfer data from magnetic tape to a permanent disk file. Two versions are available, one for tapes produced at Durham (TPTODSC.D) and the other for those produced at Edinburgh (TPTODSC.G). The programs are used interactively and the user is prompted for parameters on the data, such as the number of channels on tape and the number of blocks to transfer. The output is to a line file with one channel per line.

3.3.2 Time Decoding Subroutines.

Three time decoding subroutines were written to enable the location of events on the disk. These are GDCODE, DDCODE and MDCODE. They are used for decoding the Geostore clock, the internal time code of the Durham Mk.3 recorders and the MSF recorded on the Mk.3 recorders respectively.

3.3.3 Plotting Programs.

A number of plotting programs have been developed to display the data in different forms for specific purposes. The main method of display of seismic refraction data is in the form of a reduced travel time section. Such plots make the identification of different phases and velocity changes easier and delays at stations are brought out more clearly. Plots are made of travel time reduced by shot range/velocity against range. Any reducing velocity can therefore be used. The programs were written to allow either normalization of the traces (GEOSECT.N, DURHSECT.N), or give plots at true amplitude with allowances made for

recorder and digitizer gain and shot distance from the station (GEOSECT.T).
Two versions are present depending on whether the data were recorded on a
Geostore or the Durham recorders.

In addition programs are available to plot the three seismic
traces straddled by the time code (GEOPLOT, DURHPLOT). Fifteen or thirty
seconds of data can be plotted from a time specified by the user. The two
time codes can be plotted side by side in order to determine time
differences in samples (TCPLOTS), and a section of a file of demultiplexed
data showing all channels to check on the digitizing (CHPLOT.G, CHPLOT.D).
These programs enable the accurate location and timing of phases of the
seismogram.

3.3.4 Bandpass Filtering Subroutines and Analysis Programs.

Bandpassing of the seismic data can be carried out when
using all the plotting subroutines if required. This is provided as an
option when running the programs. The subroutines require data in the
frequency domain, transforming the data using a subroutine of Nunns (1980)
modified from Claerbout (1976). The bandpassing takes account of the
problems encountered when multiplying spectra shown by Bergland (1969).
Care must be taken not to use too narrow band a filter as ringing about the
onset results.

To obtain data in the form required for the application of
the airgun processing programs, 700 samples can be dumped from any time
specified (CHDUMP.G, CHDUMP.D). The spectra of the data can also be studied
(FREQPLOT), these providing important information especially on the airgun
data and prior to the application of bandpass filters. A program is also
available to examine the variation in sampling rate of the records produced

at Durham (TIMESAMP). A list of the subroutines used for bandpassing and in conjunction with the programs, along with comments on each one's operation, is presented in Appendix 2.

3.3.5 Programs for Filtering Airgun Data.

Two M.Sc. projects brought about the development of a set of programs and subroutines for the enhancement and detection of airgun shots in noise (Section 3.5). The names and listings of these programs and the subroutines called are provided in the two theses. The problem with the programs and subroutines is that they were developed using only one data set and as a result, were rather specific. They have therefore been altered in order to allow options on entering different numbers of traces and to change certain operational parameters depending on sampling rate, trace spacing and data quality. Their names are as given by Warren (1981) but with the suffix (.2).

3.4 Picking Arrival Times, Accuracy and Corrections.

In refraction seismology, accurate identification and timing of events must be obtained. For WISE, several methods of display were used in order to achieve this. As has been previously stated, paper records direct from the analog tapes were only made for the Geostore recordings. For both data types, records were made from the digitized data using the plotting subroutines. These records retained all the character of the signal as seen from direct comparison with the jet pen records and were quite adequate for picking arrival times. When it was possible to identify the first arrival clearly, the subsequent arrival time was accurate to one sample, this being 0.016 sec for the Geostore recordings and 0.02 sec for the Durham Mk.3 recordings. The timing of the shots was only accurate to

0.03 sec and so this timing of the arrivals was considered sufficient. Throughout the picking, use was made of the reduced sections. Arrivals could be seen on these records more clearly and once identified, the same point was found on the larger scale records and timed accurately.

Wherever possible the MSF was used for timing as no correction then had to be made. This was not always possible though with poor MSF recorded at some stations. In such situations drift curves were drawn for each station for the duration of each phase of the experiment. The difference in samples between both time codes could be found by plotting them alongside each other using the computer. This could then be converted to seconds and the approriate correction made to the travel times.

It was initially thought that incomplete flutter compensation on the playback of the Durham Mk.3 tapes might prove troublesome when picking arrival times. An analysis of the sampling rate, however, showed that the variation about the mean was not large, being normally no more than one sample, this being 0.02 sec. The method of display used for the explosive shots (Fig. 3.4) did not introduce sizeable errors into the timing of the shots. The small variation meant that large errors were not introduced into the bandpassing of the traces. If the variation from the mean had been large then the transforming of the data into the frequency domain would have introduced significant inaccuracies.

3.5 Filtering Techniques Used on the Airgun Data.

The airgun profiles that were shot during the two phases of WISE provided only a limited amount of data that could be picked by eye. Figs. 3.5 and 3.6 give an example of this. This amounted to little more than 50% of the data on most lines and no section of the profile was
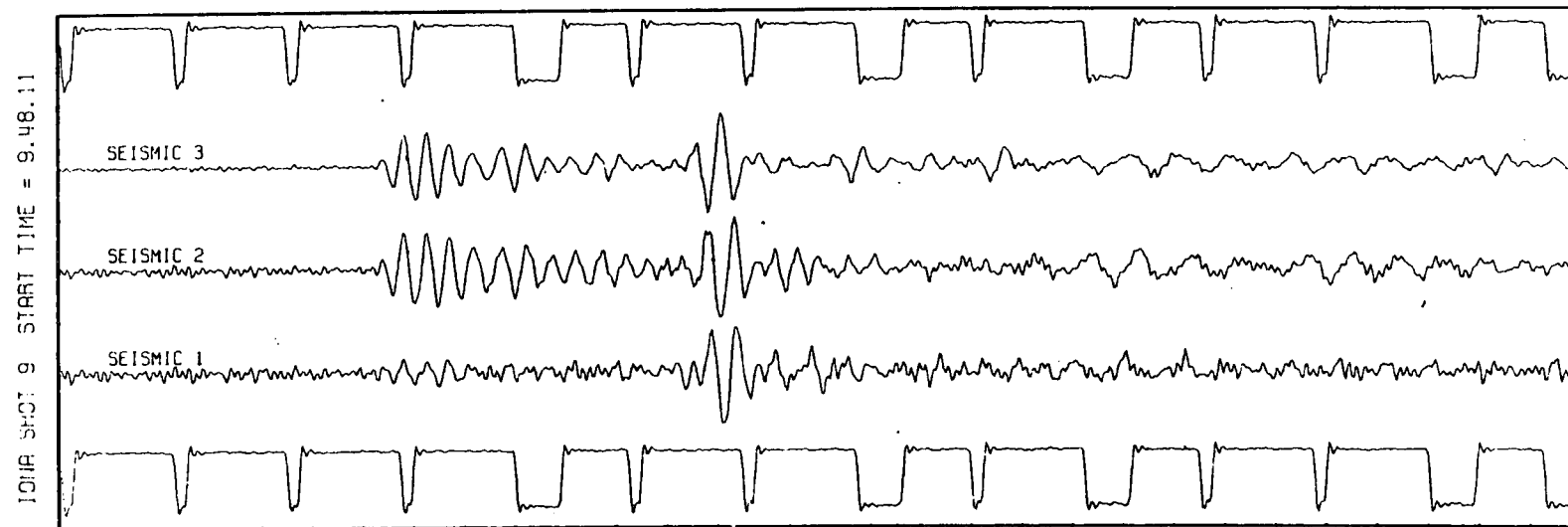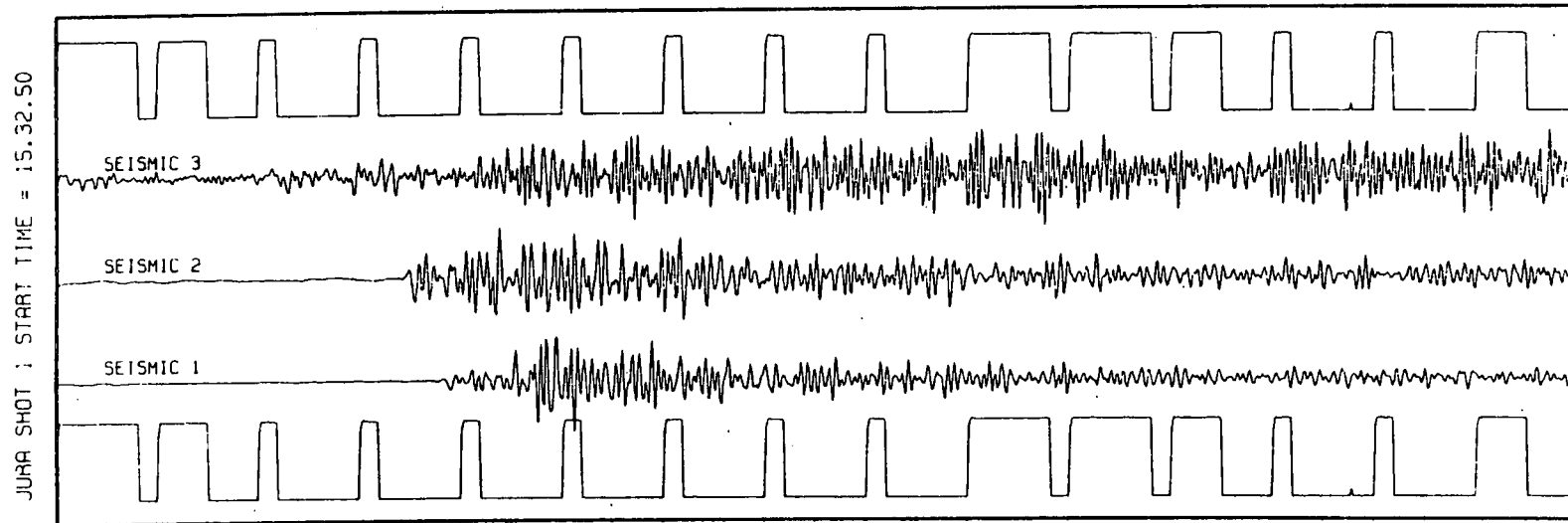
Fig.3.4: Example of explosive shot records from both phases of WISE showing the method of display used to time the arrivals once identified on the reduced sections.
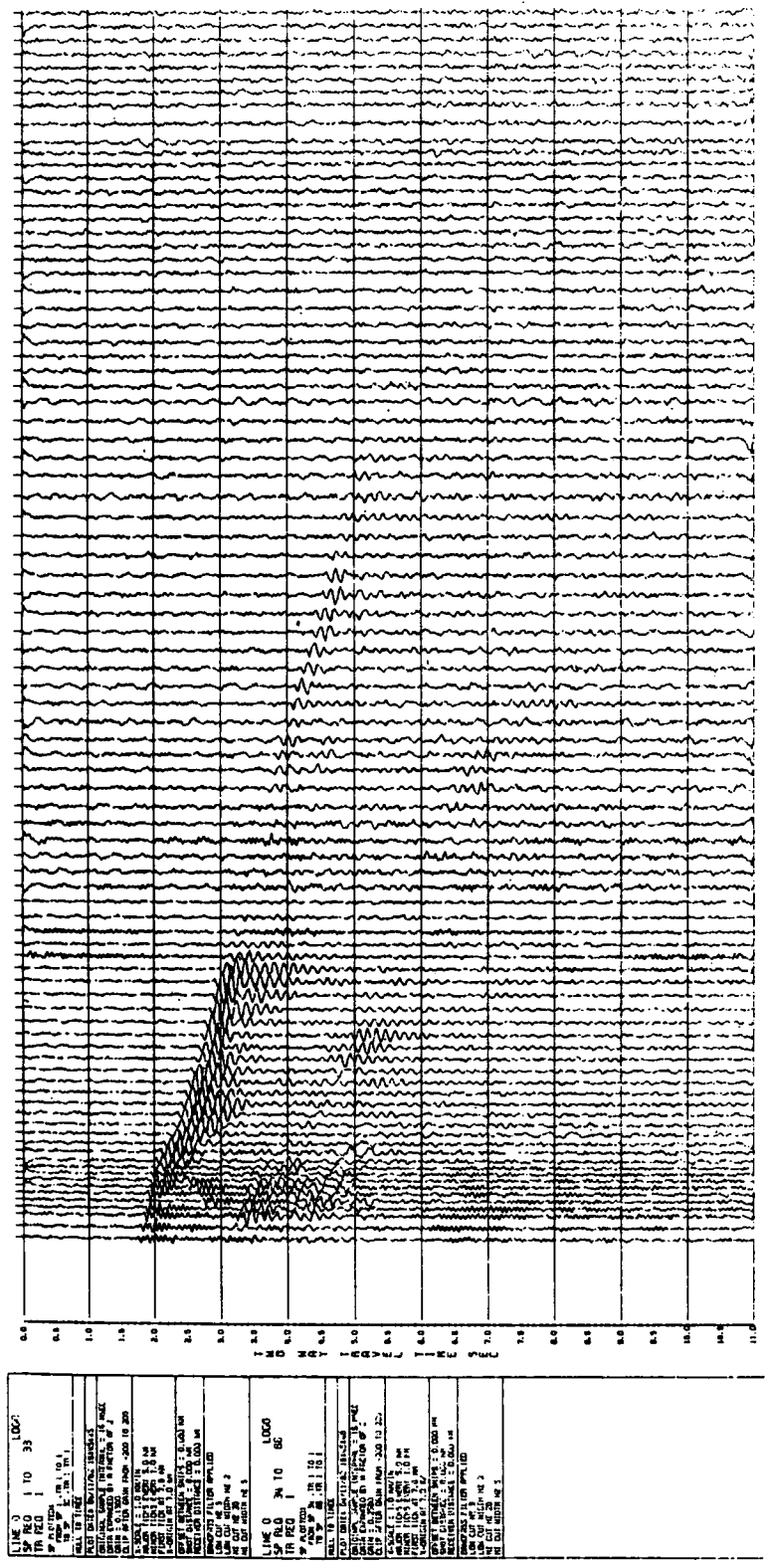
Fig.3.5:   Bandpassed airgun data for the   Inner   Hebrides   Basin   recorded
at the Mull Geostore station.

Fig.3.6:   Bandpassed airgun data for the Inner Hebrides Basin received
            at the Iona station and recorded by telemetry link at
            the Mull Geostore station.

reversed. Any interpretation of this data would be extremely limited as the only information that could be extracted would be the apparent velocities close to the station. No reversals of the lines were achieved and therefore no depths and lateral velocity variations could be examined. In attempts to extract the arrivals where they could not be seen in noise, filtering techniques normally used in reflection seismology were adapted for use on the WISE data. The work was initiated by Birtles (1980) and much furthered by Warren (1981).

The work of Birtles involved investigating the possibilities of using predictive deconvolution in an attempt to increase the signal above the noise where it could not be seen by eye. Numerous different lags were used for predictive filtering, including a zero gap in order to find the optimum filter. On close examination though, errors were found in the bandpassing and Levinson recursion subroutines making the results inconclusive. Another technique used was the cross-correlation across traces using an estimate of the signal to detect arrivals where they could not be seen. An estimate of the waveform was made up of a window of data about the arrival on the first five traces. These were stacked at their position of maximum cross-correlation and averaged. This was then cross-correlated with the next trace and its onset deemed to be at the position of maximum correlation. Updating of the waveform was carried out by dropping off the earliest trace and adding the next at this position to take account of changing signal shape. Although the method appeared to work to some extent there was no detailed review of results. The data was reworked and given a much more thorough examination by Warren (1981). This account is summarized here.

3.5.1 Signal Enhancement.

The basis for the study was an extension of the cross-correlation technique but bandpassing and predictive deconvolution were first applied in an attempt to enhance the arrivals prior to the matched filter's use. The deconvolution was to serve to make the signal on each of the traces appear as similar as possible so that the application of the matched filter would be successful. If there is not sufficient similarity between the signal shape on separate traces and distinction from the noise then correlation techniques cannot work. Modification of the techniques had to be carried out before application to the refraction data as many of their properties are different to reflection data on which they are normally used.

A typical trace with good signal to noise ratio recorded at Mull is shown in Fig. 3.7. The low frequency component on the seismic records had to be removed as it is apparent that cross-correlation would not be successful on such data (Warren, 1981). The filter used by Warren was a bandpass filter between 4 and 32 Hz. As 32 Hz represented the Nyquist frequency for the sampling rate used, this essentially meant that there was no high cut filter applied. The reason for this was that the predictive deconvolution introduced high frequency noise and therefore a high cut filter would be applied after the process, prior to applying the matched filter.

Although noise was damaging to the success of the detection process, a more serious problem was the variation in the shape of the signal on adjacent traces. It was felt that this led to poor results in Birtles work. The number of cycles of the wavetrain varied from trace to trace and if correlation was attempted in such a situation, then an

42
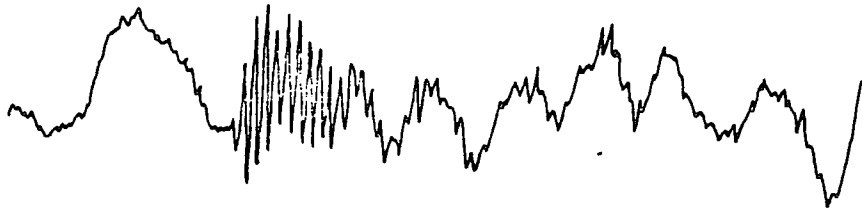
Fig.3.7:   A typical airgun trace recorded at Mull from a shot within close range of the station. Reproduced from Warren (1981).
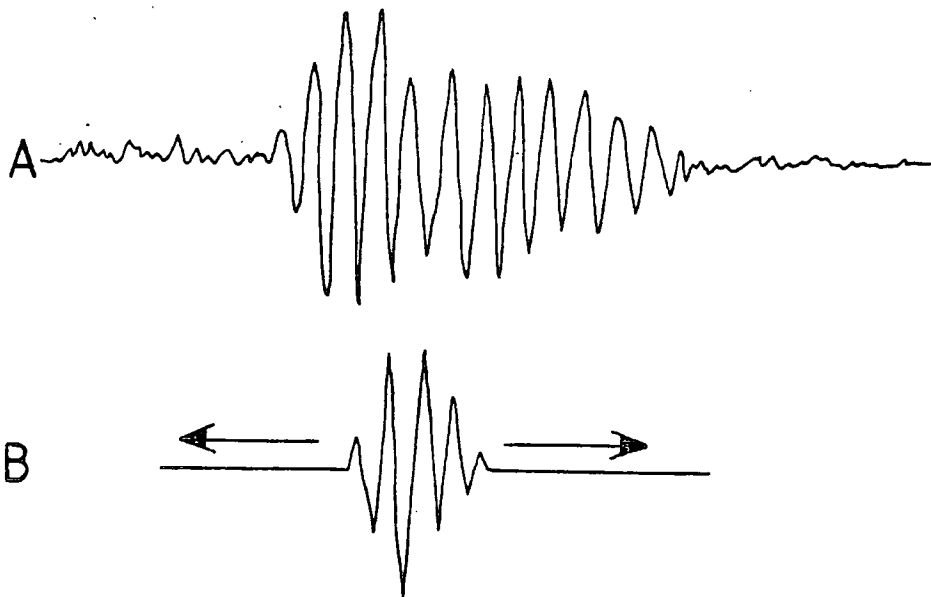
Fig.3.8:   An example of the error in cross-correlating signals with different numbers of cycles to find the onset time. If signal B is the estimate of the arrival and is cross-correlated with trace A, larger correlation values may be obtained for positions other than the onset time. Reproduced from Warren (1981).

Incorrect position for the onset of the signal may have resulted (Fig. 3.8). Warren suggested that predictive deconvolution could be used to truncate the signal and leave the same number of cycles on each trace to give a distinctive character to the signal for its detection by matched filtering.

To design a prediction error filter, the autocorrelation of the signal is substituted into the normal equations (Robinson, 1967). The filter coefficients are then calculated and the prediction error filter is constructed using the required gap. Convolution of this filter with the time series should remove the energy of the later cycles of the signal. The success of the method relies on certain assumptions being made about the data. As the autocorrelation of the whole time series would not give a good estimate of that of the signal, a window of data was taken about the arrival of interest, in this case the first arrival, and the autocorrelation function was designed from this. It was proposed that provided the window of interest did not include much noise, the autocorrelation function would be a good estimate of that of the signal. Due to the changing shape of the signal from trace to trace, it was thought necessary to redesign the filter on each trace as the previous filter would not be effective.

The gap used with the prediction error filter was small and often resulted in the filter approaching a spiking filter. As a result, the amount of noise in that part of the spectrum where it was weak was increased, that is , in the high frequency range. The reason for this can be seen by examining the action of the filter in the frequency domain. The filter is the approximate inverse of the signal and as such will have high coefficients where those of the signal are weak. When the filter is

convolved with the seismogram the noise is increased at these frequencies (Ziolkowski, 1980). In many cases the amplitude of the noise was unacceptably high and as the bandpass filter used to remove them was very narrow, some ringing about the onset resulted. This problem is overcome by adding a small amount of white noise to the spectrum of the signal prior to the calculation of the filter coefficients. This raises all the values in the spectrum and does not allow the filter coefficients to approach infinity at frequencies where there are near zero values of the signal. White noise only contributes to the zero lag value of the autocorrelation function and therefore the addition of white noise only requires a boosting of the value of the zero lag coefficient of the signal's autocorrelation function. The addition of white noise does however result in poorer signal truncation due to the altering of the signal coefficients. Warren proposed that the addition of 40% white noise provided the best trade off between signal truncation and decrease in noise. It must be stressed that all the tests were made on traces with a very good signal to noise ratio where the onset could be picked adequately.

An extension to the deconvolution process was the application of the algorithm of Burg (1976) for the calculation of the autocorrelation function. A subroutine to perform the operation was obtained from Wright (1980) and adapted for use on the WISE data. It is designed for use on short data sets and therefore, it was thought that it might be applicable to the 120 samples used in the calculation of the autocorrelation function of the airgun data. It did not provide better results, however, although this is thought to be due to the inapplicability of predictive deconvolution to this data described in the next chapter, rather than the role of the algorithm itself.

3.5.2 Signal Detection.

Signal detection techniques using matched filtering are widely used in reflection seismology but have not been studied in detail for application in refraction seismology. With little knowledge on the performance of matched filters on such data, the optimum choice of parameters had to be investigated. This was carried out to some extent by Warren, but due to the method only being tested on one data set, problems arose when it was applied to other data. The technique was developed on the best quality data from WISE, that is the data from the Inner Hebrides Basin recorded at Mull and Iona, and appeared successful. An outline of the method is presented here.

After the initial processing it was hoped that the onset might be picked reliably on an increased number of records, but more importantly, that there would be a greater similarity between the signals on each of the traces. Using an estimate of the signal shape and the known onset, it was hoped that the arrival could then be found on the poorer traces by use of cross-correlation. The estimate of the signal was obtained in the same manner as before, that is by adding the windowed first arrivals from the first five traces together and finding the average. The position of addition was determined by finding the position of maximum cross-correlation between the traces. The average waveform was then correlated with the next trace and the position of maximum correlation was deemed to be that of the onset of the signal. Due to limits on velocity and delay between the shots, it was reasonable to expect that the arrival on one trace would lie within a certain range of that of the previous one. For this reason the search for the onset was confined to a limited window so

that later arrivals could not be correlated with. The window taken for the search for the local maximum was set at positions of up to ten samples from the previous onset for the Mull and Iona data but changed to seven with the data from the second phase of WISE. This was thought practical as the shots were more closely spaced and the sampling rate was less than the airgun data from Mull and Iona of phase one. These search windows allowed for realistic refractor velocities in the area. A 'decision function', which is a statistical expression relating the correlation between two data sets, eg. cross-correlation and semblance, was used when attempting to locate the onset. For the WISE data, the correlation coefficient was found to be the most effective as it was found not to be too sensitive to amplitude variations and provided the best results in data with a low signal to noise ratio. An examination of the performance of each is given in Warren's thesis.

The shape of refraction arrivals continuously changes on moving greater distances away from the station stretching out the separate phases at further distances. It is unlikely therefore, that the waveform that gives the best correlation at the beginning of the line will give the best correlation at the end. To take account of the changing waveform shape, updating of the waveform was carried out. This was done by replacing the oldest trace of the five used in the average by the one that had just been correlated at the position of maximum correlation. Updating in this way was only performed if the value of the decision function exceeded the threshold value. This value was set by Warren at 0.7 as this was felt high enough not to be corrupted by noise and not too high to never allow detection to occur. The threshold level was changed for different data sets however depending on similarity between signal and noise and the signal to

46

noise ratio. Any value below this was thought to suggest that the true onset of the signal was not found and addition to the average waveform would only result in contamination by noise.

The final stage of the processing of the airgun data was the stacking of the traces to improve the signal to noise ratio. Each trace was taken in turn from trace three and along with the two adjacent traces on both sides, shifted and stacked according to the onset times obtained from the matched filtering. This was suggested to give an indication of whether the process had been successful as the signals should enhance when stacked whereas the noise, being random, should not. The result of each stage of processing on the data from Mull is shown in Figs. 3.9 to 3.11. This was the first data set upon which the techniques had been tried and although the results seemed impressive, further examination and thorough testing showed severe limitations in the method when applied to other data of WISE (Chapter 4).

3.6 Shot-Station Distances.

The distances between shot and station pairs were calculated after the processing of the Decca and Trisponder fixes had given locations of the shots. The Decca fixes first had to be corrected for fixed and variable errors that are always introduced before plotting on navigation charts. The fixed errors for the region were available in a manual provided by Decca and can alter the position by between 50 and 100 metres. The variable errors are smaller than this but cannot be easily determined.

The location of the explosive shots did not provide too much of a problem as they were few in number and the fixes could be plotted on a Decca lattice and found. Due to the large number of shots involved, however, this could not be done for the airgun data and an automatic method

47

TIREE TO MULL UNFILTERED SECTION
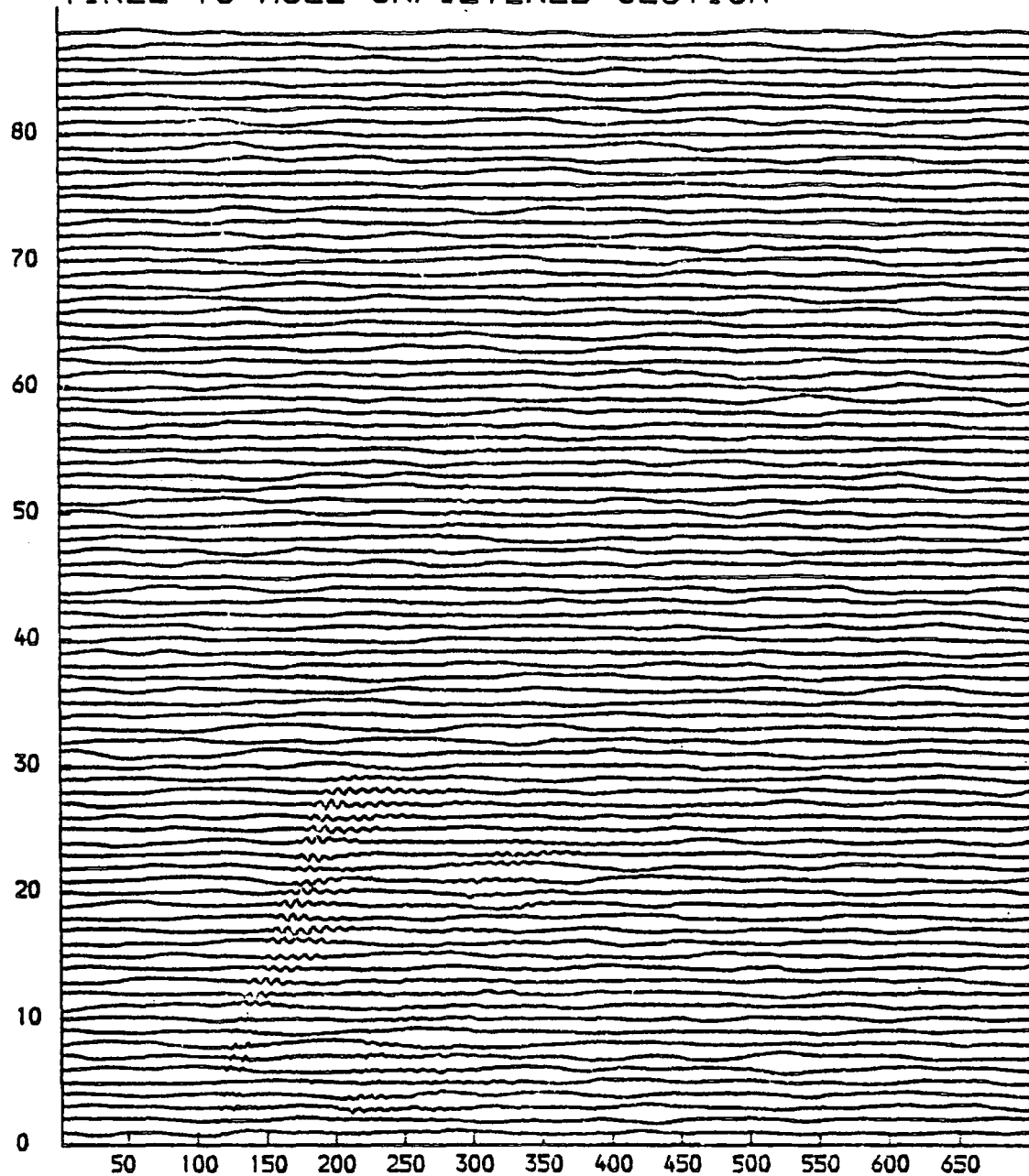
Fig.3.9:   Raw data for Mull to Tiree airgun line recorded at Mull. Reproduced from Warren (1981).

TIREE TO MULL,BANDPASSING AND PREDICTIVE DECONVOLUTION APPLIED.,
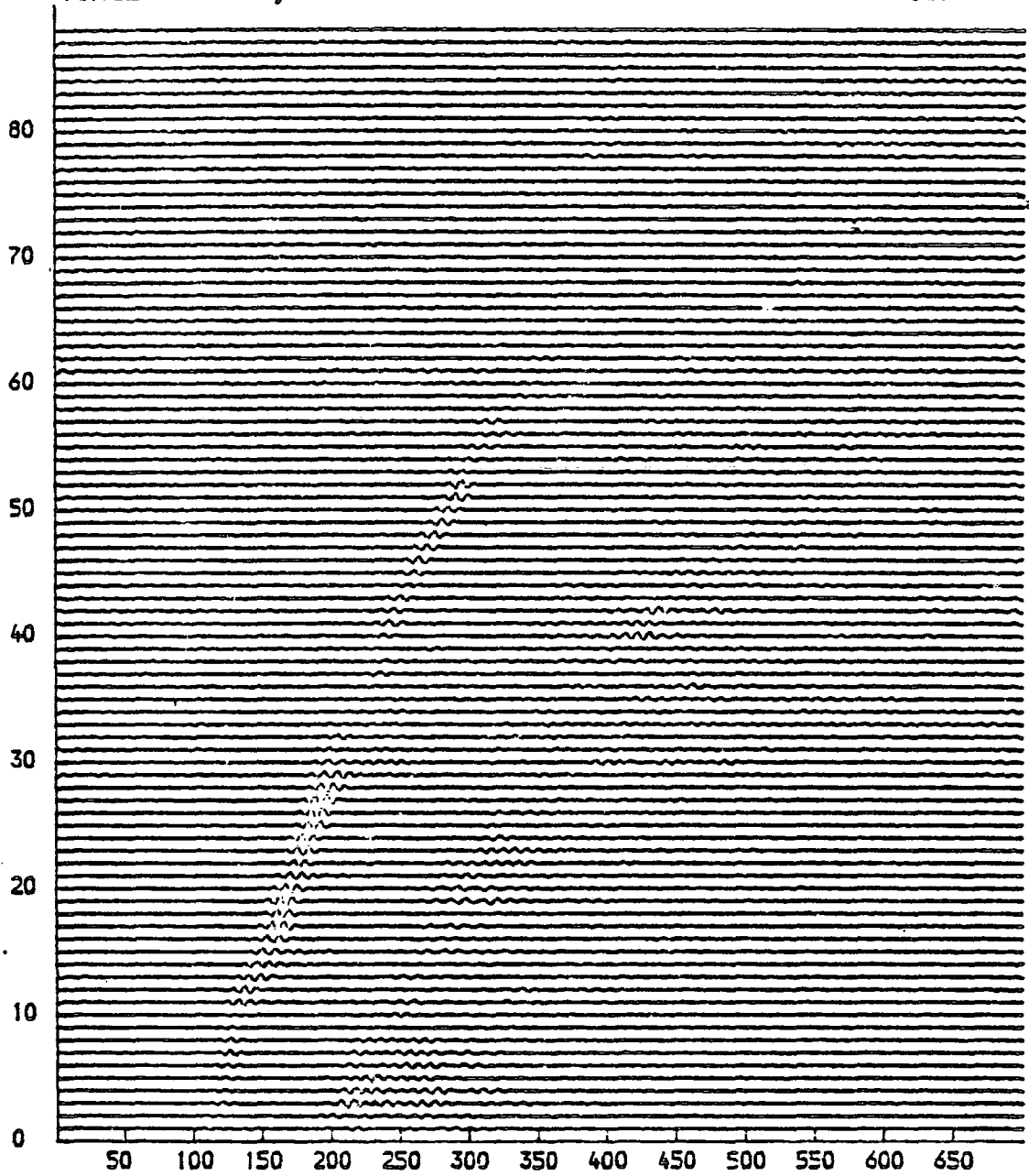
Fig.3.10:   Data   from   Mull   after   the   application   of   predictive
deconvolution. Reproduced from Warren (1981).

MULL, STACKED AND AVERAGED SECTION, NORMALISED PLOTTING.
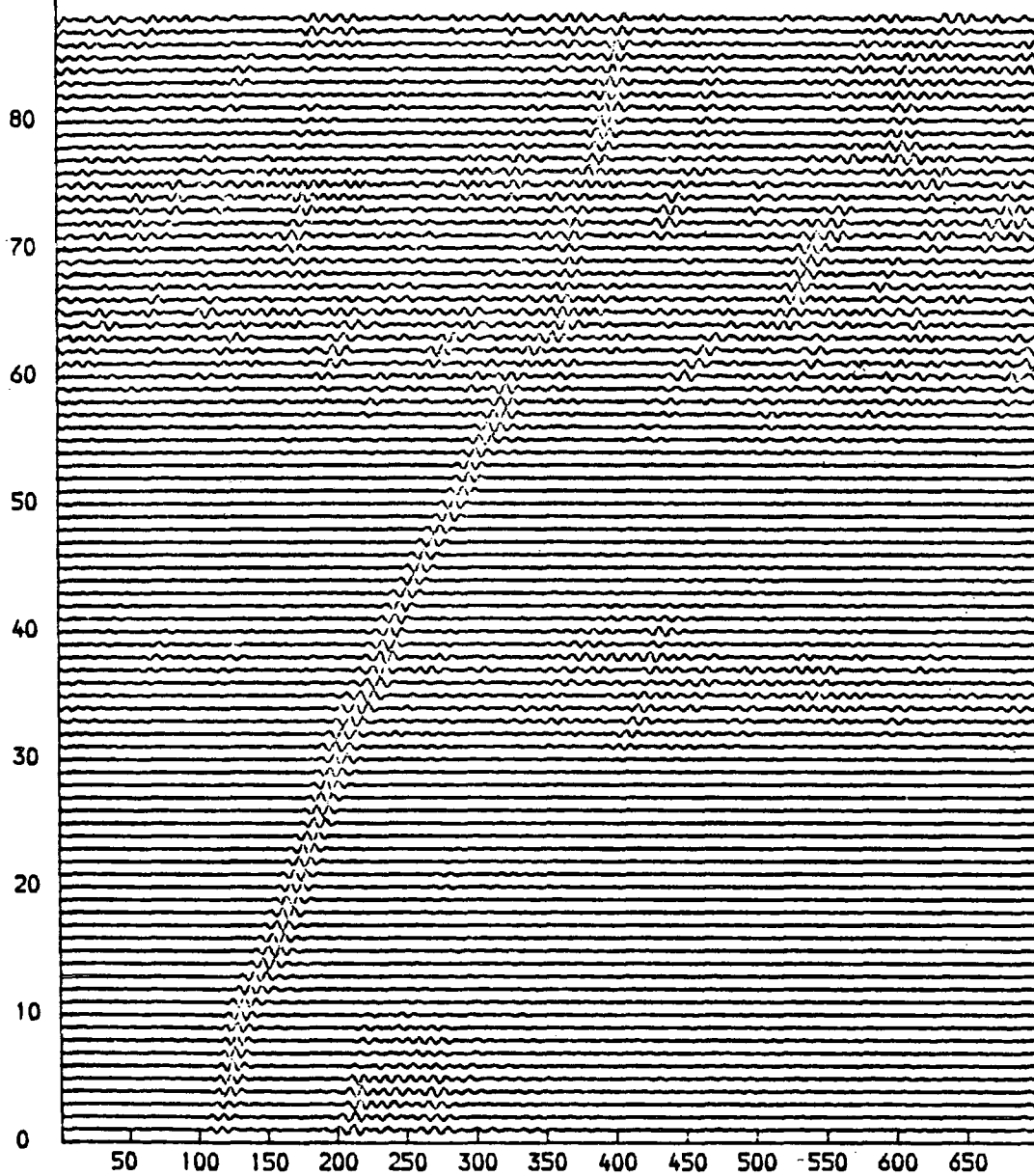
Fig.3.11:   Data from Mull after application of the matched filter and with every five adjacent traces stacked at their position of maximum cross-correlation throughout the section. Reproduced from Warren (1981).

of processing was preferable. Attempts were made to use a program written at the Department of Geology of Cardiff University. This required some alteration, and when eventually successful gave far from accurate results. A program used by R.V.S. Barry also did not provide reliable locations when the raw data were processed. Several fixes from each section of the line were then sent to Racal Thermionics, who operate the network and accurate positions obtained. Using these positions, the results from the program could be corrected and the postions found to an accuracy of 100m. This was checked by plotting several of the fixes on a lattice after applying the fixed error corrections.

Positioning of the recorder sites was an easy process as each of the station operators provided the grid reference of the location used. The calculation of shot-station distances was then carried out using the departmental program DISTAZ (Westbrook, 1973a), which gives the distance and azimuth between points of known latitude and longitude. A table of shot-station distances is provided in Appendix 1.

CHAPTER 4

REVIEW OF THE PROCESSING TECHNIQUES USED ON
THE AIRGUN DATA

4.1 Introduction.

The methods of processing used on the airgun data of WISE were developed using only two data sets, those from stations at Mull and Iona for the line in the Inner Hebrides Basin, recorded on the same Geostore recorder. On first examination the results of the processing seemed likely to provide correct detection of onset times where they could not be identified by eye. When the processes were used on different data sets, however, they were shown to lack robustness and the arrival times they returned were unreliable (Attree, 1982; Casson, 1982). A more detailed examination of the results from the Mull and Iona stations, involving a comparison of arrival times returned with those of adjacent explosive shots, revealed that onsets that were previously thought to be correct were not so. The poor performance of the techniques implied that something incorrect existed in the way in which they were being adapted and applied to airgun refraction data.

The following sections are aimed at giving a review of the assumptions involved in the development and operation of the techniques, and how they apply to seismic refraction data. The properties of the data must approach the requirements of these assumptions for signal enhancement and detection to be successful. The examination has led to certain criticisms of the application of predictive deconvolution for signal enhancement, and matched filtering for signal detection, to the data of WISE. The criticism might also apply to refraction data in general. As the techniques were originally developed for use on seismic reflection data,

49

comparisons are made between the properties of refraction data and reflection data, and their effect on the design and implementation of the filters.

4.2 The Use of Predictive Deconvolution.

Predictive deconvolution is a standard technique used in reflection seismology for the removal of multiple reverberations from the seismogram where they overlap with later primaries. With a knowledge of the shape of the autocorrelation function of the wavelet it is possible to design a filter to predict the position of the multiples in the seismogram and remove them, leaving only the first occurrence of the waveform. By applying the technique to the airgun data of WISE it was thought that the later cycles of a multi-cycled waveform could be removed to leave only the initial cycle, or at worst, the first few cycles. It was hoped that the processing of each trace in such a way would enhance the signal and increase the similarity of its shape along the record section, allowing the application of a matched filter to locate the arrivals where they could not be seen by eye. The initial justification for this is provided by Warren (1981), and summarized in the previous chapter.

Predictive deconvolution, however, requires a reliable estimate of the autocorrelation function of the signal to develop a filter that will perform the operation successfully. In reflection seismology, a reasonable estimate of this autocorrelation function can be obtained providing some assumptions are made about the data. For the purposes of Wiener filtering, a reflection seismogram is considered to be a close approximation to the convolution of a seismic source wavelet with the impulse response of the earth, which is assumed to be white, random and

50

stationary. When dealing with real data this is generally not the case but by massaging the data it is possible to approach the above situation (Ziolkowski, 1980). If the convolutional model is taken as being valid, then the autocorrelation of the seismogram is the same as that of the source wavelet except for an unimportant scaling factor (Robinson & Treitel, 1967). By using this autocorrelation function, therefore, an effective prediction error filter can be designed from the normal equations providing the impulse response is a spike series and the source wavelet is minimum delay. If the multiple shape is the same as that of the primary then no alteration to the seismogram except suppression of the multiple occurs. Due to the impulse response not generally being a spike series, however, incomplete suppression takes place. If short period multiples are being removed, then the contraction of the wavelet is accompanied by an increase in high frequency noise (Peacock and Treitel, 1969). This is due to the use of a small predictive gap which results in the filter approaching a spiking filter, whose overall effect is to whiten the spectrum by increasing those frequencies that are weak (Section 3.5).

An examination of the airgun data indicates that the time series does not represent the convolution of a minimum delay wavelet with a white, random and stationary impulse response series but instead, the addition of several different signals to coloured noise. The data from all the stations are very band limited, with a bandwidth of between 10 and 15 Hz (Casson, 1982; Smith, 1982), non-random, and non-stationary. The use of an autocorrelation function based on the entire trace would not provide a good estimate of that of any one particular phase of the signal. Warren (1981) proposed the use of a window of data about the arrival of interest upon which the filter could be designed. Although this may at first appear

51

feasible, serious limitations exist, resulting in badly designed filters that make the successful truncation of the signal and increased similarity between successive traces unattainable, when the signal to noise ratio is low.

A consideration of those traces close to the station, which have a high signal to noise ratio, seems to indicate that there may be some justification in the windowing of the data. Here the signal would not seem to be too corrupted by noise and a reasonable estimation of the autocorrelation function might be made. Even in this situation however, limitations are being placed upon the action of the filter by using a non-minimum delay wavelet. In reflection seismology, even though the source wavelet may not be minimum delay, the multiple series always is, as successive multiples have suffered more reflections and therefore contain less energy. This enables the predictive deconvolution to be successful on removing multiples from reflection data.

The property of minimum delay is important to the successful operation of the filter. For any autocorrelation function of length $2n-1$ there are 2^n possible wavelets, only one of which is minimum delay. The result of applying the prediction error filter obtained from this autocorrelation function will have a different effect on each of the unknown mixed delay wavelets. This effect cannot easily be determined. In the case of the Mull airgun data, only those traces close to the station, displaying good signal to noise ratio, show some minimum delay characteristics, although the the second or third peak of the waveform is generally the largest. On the later traces, for which the processes are most required, the largest peak, used in the window for filter design, is not near the onset. This is shown by comparison of the explosive shot and

airgun records. An efficient prediction error filter cannot be designed with such a wavelet.

The discussion above is only concerned with the form of the signal that is being filtered. No account has been taken of the noise along the seismogram. The presence of noise is important, however, when considering the extent of signal enhancement that can be expected when the WISE airgun data undergo predictive deconvolution. This becomes evident when the action of the prediction error filter is examined.

The seismogram can be considered as,

$x(t) = s(t) + n(t)$

where $s(t)$ = source wavelet, $n(t)$ = noise

After deconvolution, the seismogram becomes, .

$y(t) = z(t) + n(t)*p(t)$

where,

$p(t)$ = prediction error filter,

$z(t)$ = deconvolved source wavelet shown by Fig. 4.1

The filter $p(t)$ has the form $(1,0,0,...,-p0,-p1,-p2,...-pN)$,

therefore its energy must be > 1

If the noise is white,

the energy of $n(t)*p(t)$ > the energy of $n(t)$

B e f o r e   D e c o n v o l u t i o n
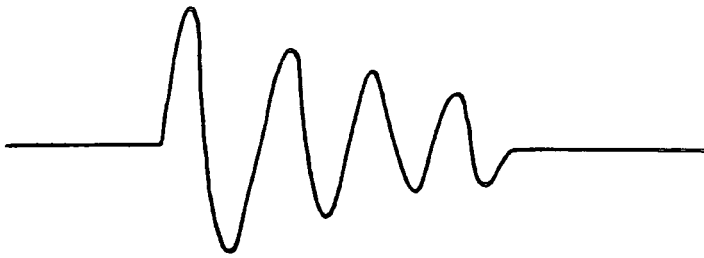
A f t e r   D e c o n v o l u t i o n
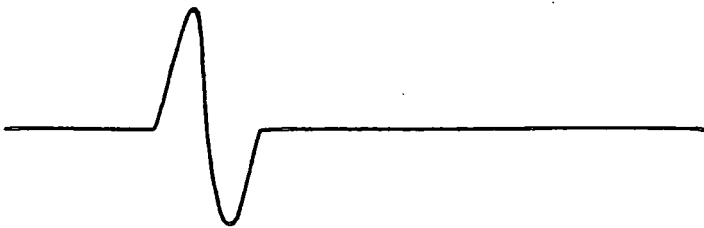
Fig.4.1:   Diagram   indicating   the   effect   of   applying   predictive
            deconvolution   to   a   reverberant   trace   in   the   ideal
            case of complete removal of the reverberations.

Therefore, if the noise is white, the signal to noise ratio must be reduced as a result of predictive deconvolution, even if there is successful truncation. Although the noise of the WISE data is not white and the effect of the filter cannot be easily defined, it is quite possible that an increase in the noise will result. It can be seen, then, that even when the signal to noise ratio is high, enhancement of the signal cannot be expected due to it being non-minimum delay and because of the action of the filter on signal and noise.

The most serious problem, however, is found to arise when an examination is made of the implementation of the technique on those traces with a poor signal to noise ratio. This condition worsens on the traces with increasing offset from the station. It must be remembered that it is in this case that the processing has to be most successful. The first arrival can be quite adequately picked from the early traces, the processing only being applied to increase the similarity of the signal along the line for use with a matched filter. It can clearly be seen from the records that on most of the traces the signal to noise ratio is very low and on many the signal cannot be seen at all (Figs. 4.2 and 4.3). In such a situation, the filter is bound to be designed on data considerably contaminated by noise. In the predictive deconvolution process it is an extremely important requirement that the only contributions to the autocorrelation function come from the signal. The introduction of noise leads to an erroneous autocorrelation function and results in poor filter design. Furthermore, even though some of the noise might be predicted out by its contribution to the autocorrelation function, high frequency noise will also be introduced due to the small gap used with the prediction error

Fig.4.2: Raw airgun data for the Mull to Colonsay line recorded at Mull.

Fig.4.3: Raw airgun data for the Colonsay to Jura line recorded at Colonsay.

filter on this data (Section 3.5). Also, in many instances, for example along two thirds of the Tiree-Mull line and one third of the Mull-Colonsay line, the filter is designed using a window within which the signal cannot be seen but is expected to lie. Such a procedure could never result in successful enhancement of the signal as the filter has been designed almost entirely on noise.

From this discussion of the application of predictive deconvolution to the WISE refraction data, it is apparent that the main assumptions about the properties of the data upon wich the method is based, are violated. Although the use of predictive deconvolution on a non-minimum delay wavelet is strongly discouraged, the application of the process with an unchanging filter designed on a good representation of the signal, such as an average of those traces close to the station, would have been less likely to be corrupted by noise and might have been more effective, even on the later traces. The method of predictive deconvolution, however, was not designed to enhance a signal where it cannot be seen but to remove reverberations where they interfere with primary reflections. As such the technique is not suited for the enhancement of signals that are present in traces with extremely poor signal to noise ratios, such as the WISE airgun data.

The amplitude spectra of the signal only, and of an entire trace with a good signal to noise ratio recorded at Mull for the Mull to Tiree line is shown in Fig. 4.4. It is clear that the data are very band limited. When using such data, wavelet shaping may be a more appropriate way of enhancing the signal on the traces. It must, however, be stressed that such a use is only applicable where the signal is evident, and not on data with a very poor signal to noise ratio. In addition, the use of this
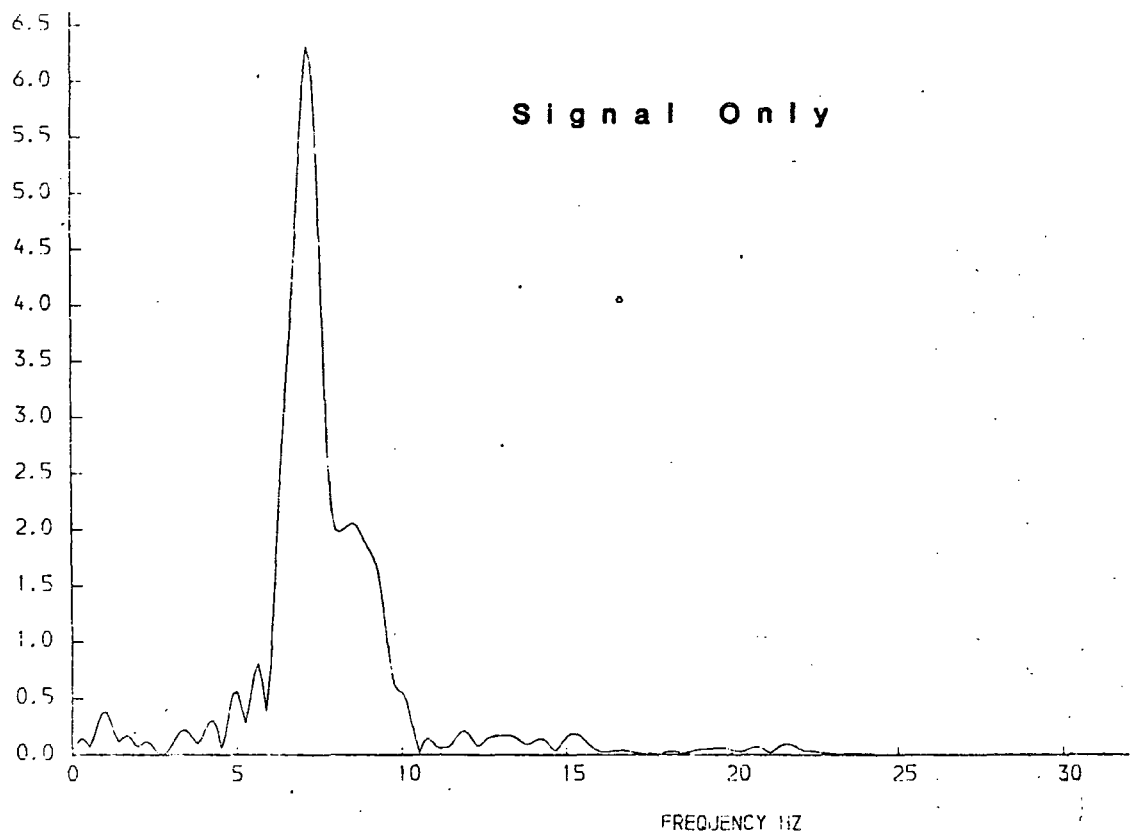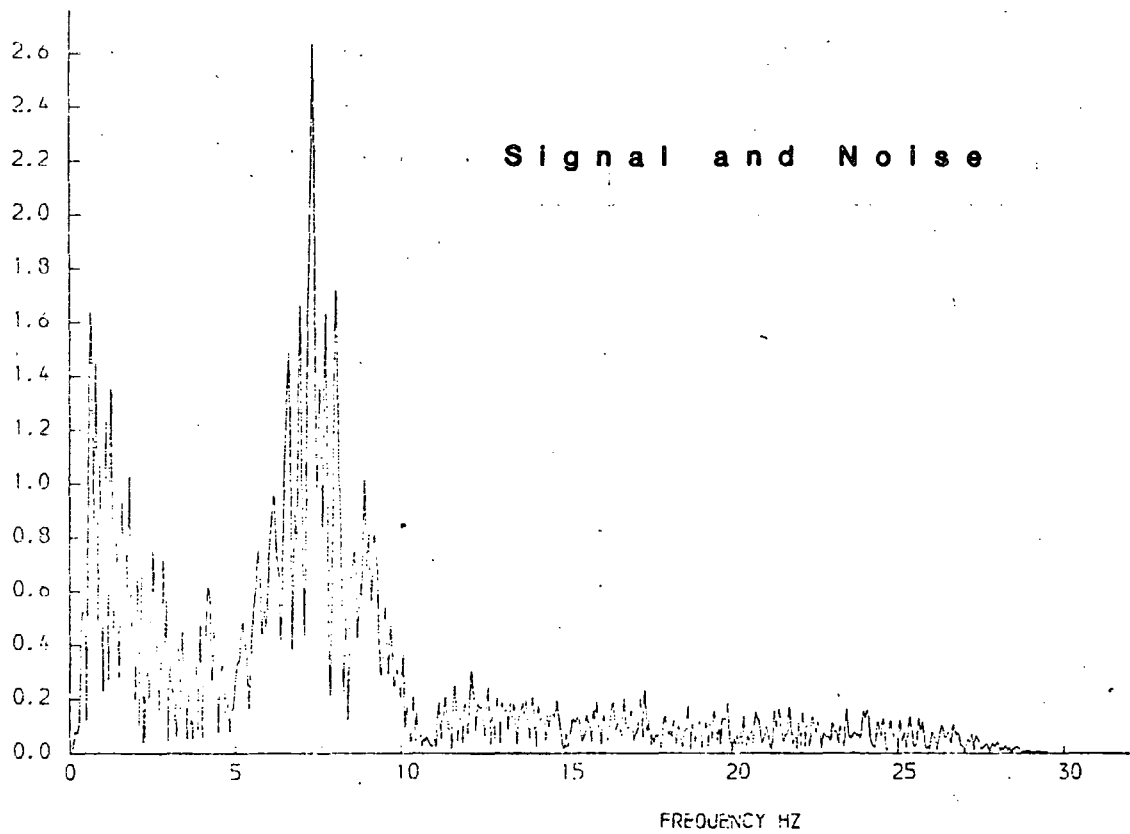
Fig.4.4: Amplitude spectra for signal and noise of trace 19 of the airgun line between Mull and Tiree recorded at Mull, and an average of the signal(first arrival) only over the first eight traces.

method requires an accurate knowledge of the wavelet so that it can be shaped into its zero phase equivalent.

i.e. $s(t) * fo(t) = so(t)$

where,

$s(t) =$ wavelet

$so(t) =$ zero phase wavelet

$fo(t) =$ filter

The zero phase wavelet is a symmetrical wavelet centred about t=0. The autocorrelation function of $s(t)$ is the same as $so(t)$ and therefore so are their amplitude spectra. In applying the operation, the signal to noise ratio remains unaltered as the amplitude spectrum of $fo(t)$ is equal to one at all frequencies. The zero phase wavelet, however, is often not very sharp and some additional spiking has to be carried out. This results in some increase of the noise, but providing the contraction of the wavelet is not too severe, the signal to noise ratio is not greatly altered.

The filter coefficients are obtained by having the cross-correlation of the zero phase wavelet and the input on the right hand side of the normal equations (Robinson, 1967). Although $s(t)$ is realizable, $so(t)$ is not and therefore $fo(t)$ will not be causal. In this case, only a time delayed version of the filter can be designed, $fo(t-n)$, resulting in a time delayed version of the zero phase wavelet, $so(t-n)$, along the seismogram. By designing the filter with various delays applied to the desired output, and finding the one that gives the minimum error energy between the actual and desired output, the optimum filter can be determined. The appropriate time shift can then be applied to the seismogram using that delay. This process is an extension of that attempted

56

by Warren (1981) where he attempted to find the optimum delayed spiking filter. The process, however, seems to be more applicable to data with a narrow bandwidth as it does not alter the spectrum whereas spiking attempts to flatten it. Therefore, the signal to noise ratio is not changed. To use the technique on the WISE refraction records, a good estimate of the signal would have to be made from those traces close to the station and should not be altered throughout the process. Although some alteration of the signal takes place due to moving away from the station, it is felt that the poor signal to noise ratio on many of the traces would lead to significant corruption of the filter resulting in far poorer operation than an unchanging filter.

The method described has recently been tested by Smith (1982) on the same Mull data processed by Warren (1981). A summary of the results is given in Section 4.3.

4.3 The Use of Matched Filtering.

The use of a matched filter to detect arrivals along a seismogram is a well established technique in reflection seismology using a Vibroseis source. This involves the passing into the ground of a very distinctive source signature of several seconds duration, with frequencies increasing from 6 to 50 Hz. Whenever a reflection occurs, the same signal is received at the surface although some modification takes place, such as attenuation of the high frequencies, during its passage through the earth. The seismic records are then cross-correlated with the source signature to identify reflections, these being at positions of maximum cross-correlation. The success of the technique relies on the fact that the signal has a very distinctive character, therefore correlating very poorly with the noise. The high values of correlation can then be positively

Identified as reflections.

In the filtering of the airgun traces, the matched filter was used in a form that was expected to locate first arrivals where they could not be detected by eye. As previously stated, the deconvolution process was used in an attempt to increase the similarity of the signal between traces. A representative waveform was then calculated from an average of the early deconvolved traces and used as the matched filter, continuously updating it on moving away from the station to take account of the changing signal shape (Section 3.5).

Even ignoring the suspect nature of the predictive deconvolution process, a number of difficulties exist that make matched filtering of the WISE data difficult to perform. Of utmost importance to the success of the process is the bandwidth of the data, in order to provide a signal with a distinct character. This is especially important when the traces have poor signal to noise ratios. Due to the narrow bandwidth of the raw data, the signal does not have a character that is unique compared to the noise. When filtering the data, the final step after the predictive deconvolution was the application of a narrow bandpass filter, between 4 and 13 Hz, to remove the unwanted frequencies that had been introduced during the process. This immediately limits the frequency range and hence the possibility of the signal being distinct compared to the noise. Furthermore, the Mull-Colonsay, Jura-Colonsay and Tiree-Mull sections show a rapid drop in the signal to noise ratio with increasing offset and after deconvolution, the signal no longer looks different from bursts of noise along the seismogram. This is also noticed on the Mull-Tiree data where the signal to noise level is low (Fig.4.5). Further away from the station no signal is seen to exist, nor can it be enhanced, for

58
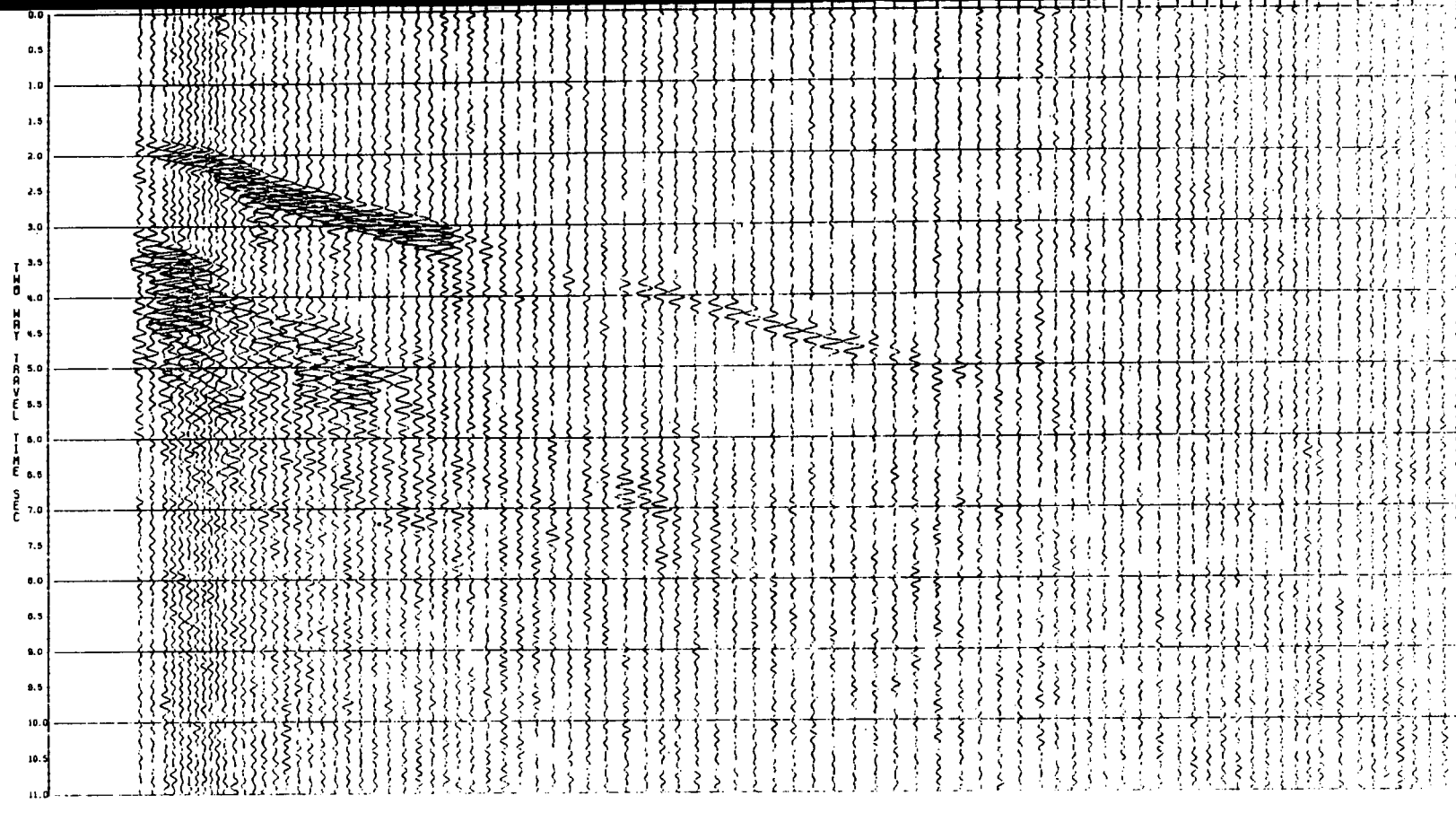
Fig.4.5: Airgun data recorded at the Mull station for the Mull to Tiree line after the application of predictive deconvolution.

the reasons presented in Section 4.2. These factors immediately indicate the limited success that can be expected from the application of a matched filter.

In order to ensure correct detection, the search for the maximum in the correlation coefficient function along each trace was confined to a certain range, initially set between the onset of the previous trace and ten samples later. This value was varied depending on shot separation and the sampling rate of the data. It would appear that if the waveform was reasonably distinctive, then over this range the maximum correlation found should indicate the position of the signal with some degree of confidence. It was noticed, however, that even when the correlation coefficient was quite high, it was by no means indicative of a successful detection (Attree,1982; Casson, 1982). Due to the very narrow bandwidth of the data and similarity between the shape of the signal and noise, correlation between the two can often be quite high. The continuous updating of the waveform was thought to allow for its changing shape along the line and was only used if an arrival could be positively identified. Warren (1981), suggested that this would be the case if the correlation coefficient was greater than a threshold value of 0.7, inhibiting the corruption of the filter by the noise. Examination shows though, that the correlation between noise and signal was often above the threshold value, the noise then contributing to the filter coefficients and damaging the detection process. The threshold value was then raised, but this only resulted in the correlation coefficient never exceeding it, which suggests that no identifiable arrivals are present. Investigation into using different threshold values indicated a trade-off had to be made between corruption by noise and no detection at all. Neither case is satisfactory

59

for confident location of arrivals. For data with very poor signal to noise ratios and coherent noise, such as that beyond trace 30 received at Tiree (Fig. 4.6), very low values for the maximum correlation coefficient were obtained for several traces followed by a high value, often above 0.8. An examination of the raw data shows that this could not possibly be an arrival as the traces are seen to be very similar in frequency content and amplitude, and a high correlation with the filter would be expected on all traces if the signal is present and not just on one. The high correlation in these cases reflects an alignment between two noise trains. Such a pattern is repeated all along the section.

The stacking of the records at their position of maximum correlation was suggested by Warren to illustrate correct detection by the filter, in that the signals should be enhanced when stacked whereas the noise, being random, should not. It can be seen from Figs. 4.7 and 4.8 however, that it can be made to appear as if coherent events exist all the way along the line from Tiree to Iona at different places by using different search windows for the local maximum with a constant filter length. Only the first four values for the first arrival remained unchanged on changing the window length. This is an indication of the similarity between signal and noise and that noise has corrupted the filter very early on in the process, rather than that of the method's success. Similar results were obtained using the data from the second phase of WISE (Attree, 1982; Casson, 1982). Tables 4.1 and 4.2 show how the location of the first arrivals returned for the Tiree-Mull and Mull-Colonsay lines varied, depending on the search window used. Even where the first arrival could be detected by eye the matched filter failed to function properly, returning different postions of maximum correlation on the same trace for different
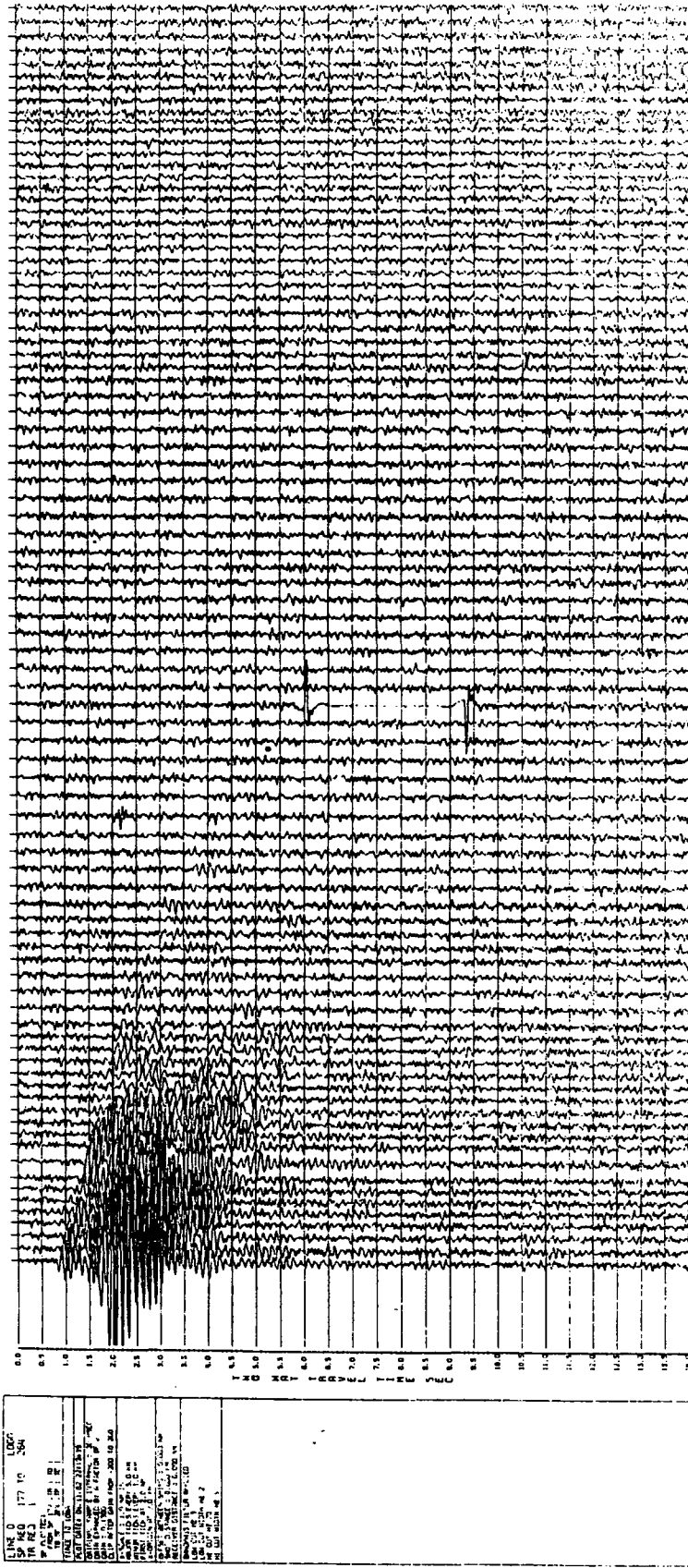
Fig.4.6:   Raw   airgun   data   for   the   Mull   to   Tiree   line   recorded   at
the Tiree station.

TIREE TO IONA   SEARCH WINDOW = 7
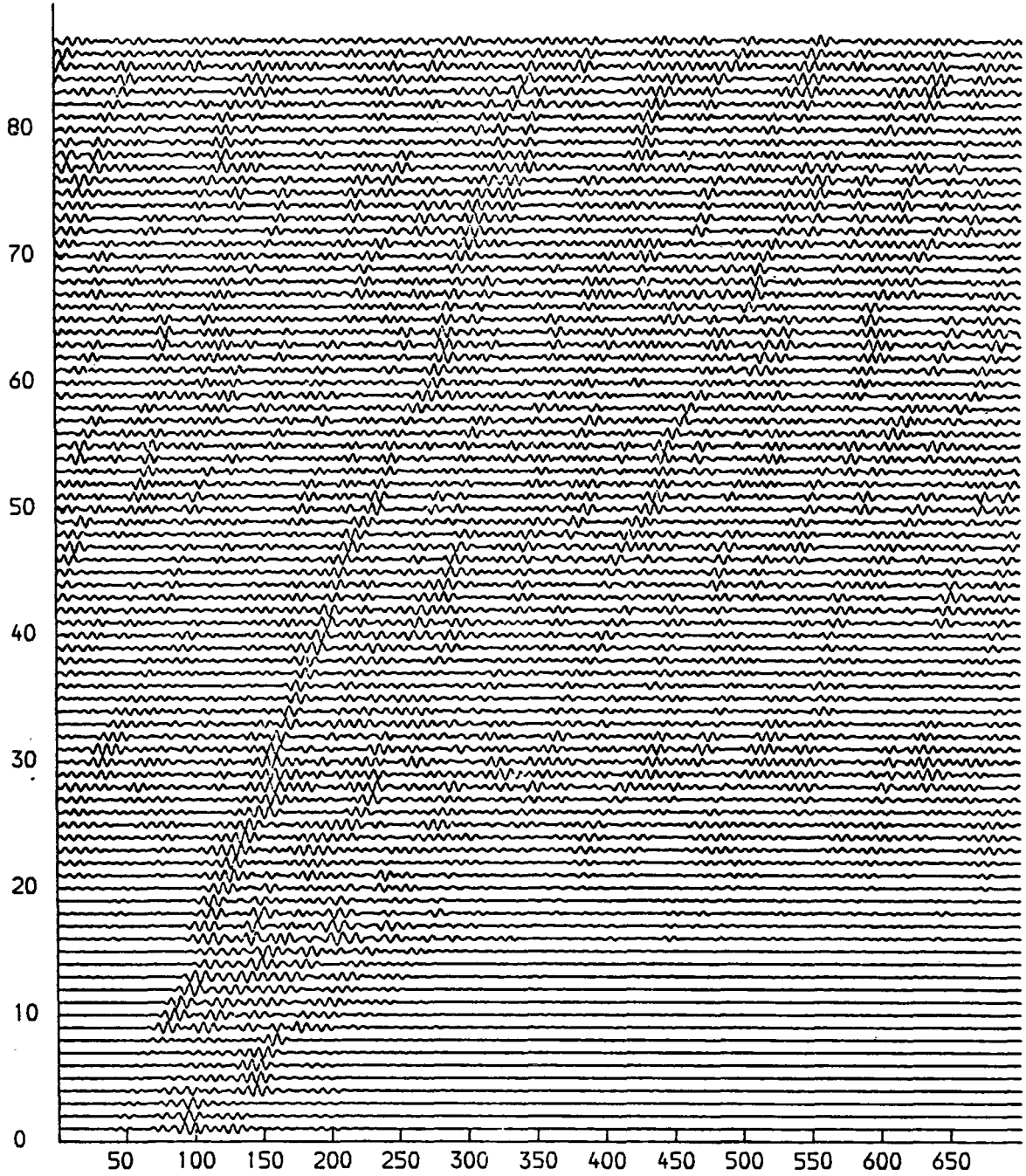
Fig.4.7:   Final output from processing techniques applied to data recorded at Tiree.

TIREE TO IONA   SEARCH WINDOW = 10
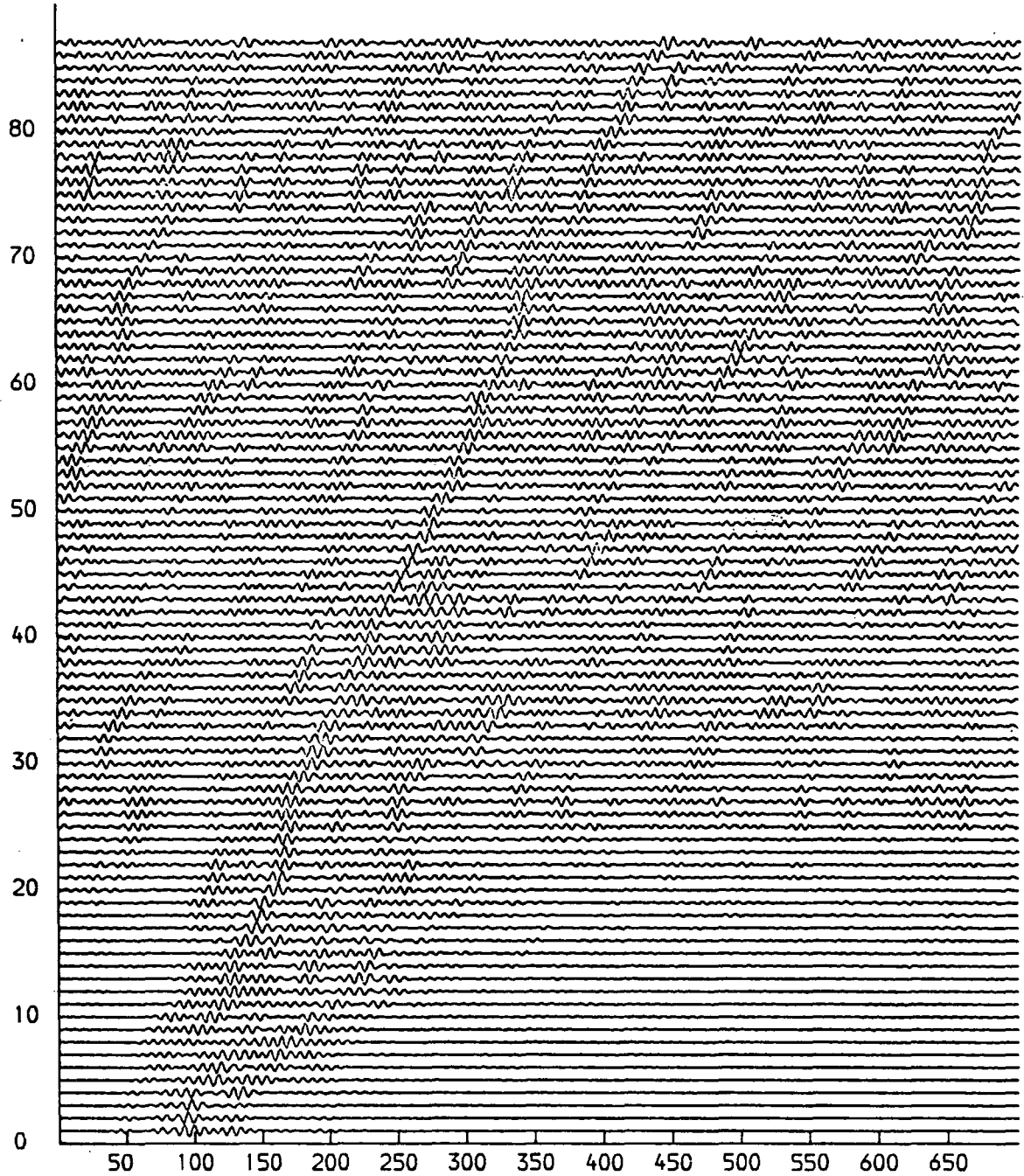
Fig.4.8:   Final output from processing techniques applied to data recorded at Tiree.

Table 4.1

<u>TIREE - MULL</u>

Selected onsets in samples for different search windows

Shot	WINDOW = 7		WINDOW = 10	
	Onset	Corrn.Coeff.	Onset	Corrn.Coeff.
202	37	1.000	37	1.000
201	40	0.987	40	0.987
200	43	0.976	43	0.976
199	46	0.982	46	0.982
198	49	0.859	55	0.935
197	49	0.285	65	0.888
196	54	0.742	66	0.881
195	61	0.845	74	0.938
190	85	0.873	108	0.688
185	104	0.582	135	0.710
180	119	0.708	152	0.541
175	140	0.938	161	0.496
170	159	0.824	181	0.576
165	174	0.805	206	0.846
160	188	0.600	226	0.920
155	202	0.907	250	0.789
150	224	0.725	279	0.818
145	245	0.753	301	0.921
140	269	0.979	321	0.761
135	284	0.505	336	0.875
130	303	0.889	368	0.763
125	320	0.554	383	0.833
120	330	0.460	408	0.859
115	351	0.424	435	0.875

Table 4.2

MULL — COLONSAY

Selected onsets in samples for different search windows

Shot	WINDOW = 10 Onset	Corrn.Coeff.	WINDOW = 7 Onset	Corrn.Coeff.
67	79	1.000	79	1.000
66	82	0.824	81	0.882
65	85	0.952	84	0.981
64	87	0.699	86	0.798
63	89	0.886	88	0.926
62	98	0.822	90	0.856
61	101	0.874	93	0.983
60	104	0.534	96	0.924
55	116	0.769	108	0.849
50	132	0.699	118	0.304
45	145	0.922	127	0.897
40	153	0.543	136	0.981
35	174	0.572	148	0.961
30	185	0.772	155	0.707
25	213	0.544	169	0.667
20	223	0.543	177	0.851
15	236	0.877	177	0.847
10	272	0.899	172	0.898

search windows.For the Mull-Colonsay data, the search window of 7 samples was allowed to scan 3 samples back from the onset of the previous trace to determine the maximum cross-correlation position. The fact that it found onsets prior to that of the previous trace highlights the problems in the method. As the process was unsuccessful where a good estimate of the signal was available, confidence should not be placed in results returned further along the section where the signal to noise ratio is very much lower. It becomes evident therefore, that employing such techniques is not worthwhile if confidence cannot be placed in the results obtained.

As a comparison of the application of the techniques of Warren (1981) and the shaping filter of Smith (1982), the travel time of explosive shot 17, fired close to airgun trace 36 from Mull was used. The onset time from the predictive deconvolution and matched filtering was found to be 3.36 sec and with the shaping filter, 3.14 sec. The explosive shot time was found to be 3.04 +/- 0.05 sec. The travel time of other explosive shot along the line, shot 18, was poorly defined but thought to be 5.00 +/- 0.05 sec. The application of the shaping filter to the corresponding airgun trace, number 63, could not shape the arrival enough to allow the onset time to be identified confidently. The former techniques gave an arrival time of 5.38 sec.

There appears therefore, to be a discrepancy of 0.35 +/- 0.03 sec along this section of the line between the explosive shot travel time and the results of Warren. It is thought that this is due to the windowing of the data about a later part of the arrival train showing higher amplitudes in the trace when designing the deconvolution filter, and when the matched filter was applied, correlation took place along this trajectory. Although there is consistency between the difference in times

of the airgun arrivals and explosive shots. It does not help in detecting the true onset times any more than constraining the raw or bandpassed data with the explosive shots and picking by eye. The shaping filter does, however, go some way towards placing the peak about the onset although this peak is difficult to discern on many of the traces due to the band limited data used (Smith, 1982).

4.4 Conclusions.

The processing techniques described above were not developed in their original form for determining the precise position of the onset of band limited signals where they are immersed in high amplitude, narrow band noise. In this respect their adaption for use on the WISE airgun data represents misconceived ideas about their application, as illustrated in the previous sections. Section 4.2 has shown that the use of predictive deconvolution is inappropriate in that the data do not conform to the assumptions upon which the technique is based. It was not developed for use on non-minimum delay wavelets, or for enhancing signals immersed in noise of equal or greater amplitude. The matched filter should only be employed if the filter can be adequately designed on a good estimate of the signal shape. The essential prerequisite is that the autocorrelation function of the signal has a large central peak that can be recognised above the level of the correlation between signal and noise. This means that the filter will have a high resolution. This is difficult to achieve with severely band-limited data.

It is proposed that if any method of automatic detection is to be used, then the filter should be designed on those traces where a good estimate of the signal can be obtained and a Wiener shaping filter used.

Although it may be necessary to make some modification due to the changing shape of the signal with distance, extreme care must be taken not to corrupt the filter by noise. This cannot be achieved when using data where cross-correlation of the noise and the signal is as high as the autocorrelation of the signal. The basic premise for operations involving digital filtering requires that data of good quality and wide bandwidth are present. As the WISE airgun data that were required to be enhanced do not display these properties it cannot be expected that the application of these processing techniques should be successful.

CHAPTER 5

INTERPRETATION METHODS

5.1 Introduction.

The interpretation of the data involved the correct identification of phases, the determination of their arrival times and their use in a number of techniques of analysis. The first step in the interpretation of the explosive shots was the construction of reduced record sections and travel time graphs for the first arrivals. These provided first estimates of the P-wave velocity of the layers, their dip and estimates of the crustal layering. Subsequently, more elaborate methods were used to give detailed information on the crustal structure. The plus-minus method of Hagedoorn (1959) was used to delineate lateral changes in velocity, although this was only possible where reversed coverage existed along profiles. When such a situation did not exist, time term analysis was used to provide delay times to a single refractor and determine the velocity of that refractor.

Later arrivals on the records, such as S-waves and surface waves are important in providing details of the crustal structure, and wide-angle reflections are useful in obtaining values of the velocity of the rocks overlying the refractor. For the identification of these phases, reduced travel time sections were used.

The interpretation of the airgun data was carried out differently to that of the explosive shots. Travel time graphs and reduced sections were constructed in the same way but much interpretation was restricted by thedata quality. Evaluation of the velocities along the airgun sections was made at Lamont-Doherty Geological Observatory using a

program RAYSCAN. With this, analysis of semblance along linear time-distance trajectories after moveout by different ray parameters is made. In addition, a program was developed to iteratively determine the depth to the refractor and any lateral velocity variations. It could not be used on the unreversed lines however.

5.2 Interpretation of the Explosive Shot Data.

All the explosive shots were displayed on reduced travel time sections to aid in the picking of arrivals and the identification of phases. Using first arrival times, the standard refraction interpretation methods were applied. These are well described by Dobrin (1976), Telford et al (1976) and in previous theses (Swinburn, 1974; Smith, 1974; Armour, 1977).

5.2.1 Time-Term Analysis.

The time-term analysis technique is presented in various papers, Willmore and Bancroft (1960), Berry and West (1966), and Bamford (1976). As these are readily available, no mathematical theory is presented here. In addition, a very useful account is given by Båth (1976), highlighting the approximations of the method and the pitfalls involved in its use.

A computer program written by Swinburn (1974) for use on the IBM 370/168 was used for time-term analysis. Data input for this program was clumsy as all the sites had to be numbered and entered in order. Problems arose if new data were introduced as all the sites then had to be renumbered. Changes were made to the program to make data input easier. Numbering is carried out automatically by providing a list of the stations in the order required at the beginning of the input. New data can then be

introduced at any point of the data set providing the new site name is placed at the correct position in the site list. Renumbering of each site is then effectively carried out. In addition, the matrix inversion operation was carried out using a subroutine from the outdated SSP subroutine library which is no longer supported by NUMAC and can often give unreliable results. The program was altered to use the more efficient NAG subroutine library.

5.2.2 Minus-Time Analysis.

The recording stations and shot points of WISE, as can be expected from the logistics of the experiment did not lie along one straight line but were offset from the line from Barra to the mainland by varying amounts. The normal method of applying a minus-time analysis to the data could not therefore be employed as the difference in travel times for the shots along a section of the profile, when projected onto a straight line, would result in erroneous velocities being evaluated. Under such circumstances, a different method of interpretation had to be used. Two approaches were employed. The first method was that described by Armour (1977) where a theoretical reduced minus-time curve is plotted for the ranges of shots to a station pair using a reducing velocity close to the true velocity expected for the refractor. The minus-times from this theoretical curve are then compared with the observed, and the square of the residuals between the two, summed. The process is carried out for several reducing velocities and the one giving the minimum sum of residuals squared is deemed the best velocity to fit that station pair. This was done for all possible station combinations to determine the velocity between the two and thus, give an indication of change in velocity along the line.

The second method took account of the relative travel times

between two shots in relation to a receiver pair. The details are given below.

Travel time of shot 1 to station A:-

$$T1A = DA + D1 + XA/V$$

Travel time of shot 2 to station B:-

$$T1B = DB + D1 + XB/V$$

where DA, DB = Delay time at stations A & B

$D1$ = delay time at shot 1

XA, XB = Distances between shot 1 and stations A & B

V = Velocity of refractor between the two shots

Similarly for shot 2 to stations A & B:-

$$T2A = DA + D2 + YA/V$$

$$T2B = DB + D2 + YB/V$$

Subtracting:-

$$T1A - T1B = DA - DB + (XA - XB)/V \quad ----- 1$$

$$T2A - T2B = DA - DB + (YA - YB)/V \quad ----- 2$$

Subtracting 2 from 1 :-

$$(XA - YA + YB - XB)/V = Z/V = T1A - T1B - T2A + T2B$$

where Z = difference in range between shots and receivers

Therefore, by using the difference in minus times and ranges of the shots, the velocity can be determined.

Providing that the shot points are sufficiently close enough together that no velocity change occurs between them and that deviation of the shots and stations from a straight line are not too large, the method gives a good estimate of the velocity over the small range. It is possible

67

using this method to map the velocities along the line and determine lateral changes within the refractor and the dependence of velocity on range.

5.2.3 Ray Tracing.

After interpretation by the above techniques, a velocty/-depth model was obtained. This estimate of crustal structure along the line was then modelled using the ray tracing method based on the algorithm of Červený et al. (1974). The model was entered into the program by way of a grid defining the velocity structure. Linear interpolation is used to define the velocity variation over the line. Any interface can be modelled by defining the coordinates in the grid. For the WISE data, the top of the basement was entered as an interface and variations in structure and velocity within the crust, by way of changes in the velocity values of the grid. This enabled both lateral and vertical velocity variations to be modelled. The grid line spacing was varied so that both rapid and slow variations could be modelled.

5.3 Interpretation of the Airgun Data.

The interpretation of the airgun data was limited because of their quality and only values of apparent velocity close to the station could be obtained with any confidence. Reduced and unreduced sections were obtained at Lamont-Doherty Geological Observatory and the program, RAYSCAN, was also applied to the data to estimate velocities. As the expected depth to the refractor was thought to be large compared to the shot separation, significant overlap would exist between raypaths either side of each adjacent shot. As such, the plus-minus method would not be accurate enough in determining the true structure and therefore, an iterativemethod of

68

determining the topography of the interface was developed. The application of the technique could not be used on the unreversed lines of WISE as reversal is essential for the technique's implementation. The method is included however, as future refraction lines with closely spaced shot points may be able to use it.

5.3.1 Analysis of Airgun Lines at Lamont-Doherty Geological Obsevatory.

The seismic processing system at Lamont-Doherty operates with two Data General NOVA 830 and 840 computers and one ECLIPSE S/250, sharing eight tape drives allowing rapid transfer and processing of data. Unreduced sections of the airgun data and sections reduced to a velocity of 6.0 km/sec were made on the system.

A method of determining the velocities has been developed by Stoffa et al. (1981) involving the direct mapping onto the Tau-p plane of reflected and refracted arrivals. The method, employed in RAYSCAN, is described below.

The data set is divided into overlapping arrays, the size of which is determined by the number of traces required to give good semblance. Care was taken not to make these too large, which would introduce arrivals with a differing velocity, or too small, which may not provide enough data to calculate the semblance effectively and allows high correlation between the backround noise on each trace. Linear trajectories are chosen for equally spaced horizontal slowness parameters. The semblance is then calculated along them using the equation,

$$S = \frac{\sum\limits_{w} \left(\sum\limits_{k=1}^{N} y_k \right)^2}{N \sum\limits_{w} \sum\limits_{k=1}^{N} y_k^2}$$

Where y is the sample of the k th trace lying along the trajectory in

the X-T plane and W is the time window centred about the trajectory. In the program, RAYSCAN, W is set to one sample.

Semblance maxima indicate the value of the velocity at the mid point of the array at that particular travel time. Starting with the first airgun trace and a pre-defined initial array size, overlapping groups of traces are analysed until plots of semblance at all ray parameters are made for all arrays along the line and a measure of the change in apparent velocity with offset is obtained. The size of array that is used can be kept constant or can be increased along the section to take in more traces.

It is common to plot the semblance values as a function of Tau, the intercept time, and p, the horizontal slowness. If the layers being examined are not planar, however, and lateral velocity variations exist, then negative intercept times are possible. Such a sitution was expected for WISE and therefore, semblance was plotted as a function of ray parameter and travel-time. An example of the output from RAYSCAN is presented and discussed in the following chapter.

at the centre of each array

5.3.2 Airgun interpretation program.

For this method to be successful there must be a significant amount of overlap of arrivals from one refractor recorded at stations at both ends of a seismic line. The program uses the geometry of the raypaths, and the travel time equation of a refracted wave which is separated into its components of delays at each end of the line and travel time along the refractor. An iterative procedure is then used to converge on a velocity/depth profile consistent for arrivals at both ends of the line. The theory of the method is presented below.

The ray diagram for a refracted wave is.
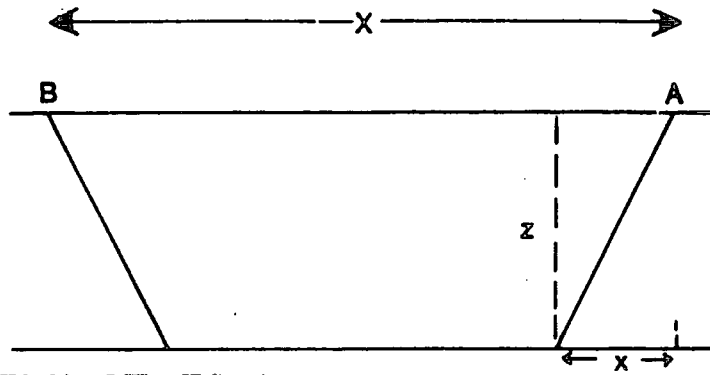
The angle of incidence can be related to the velocities of layers using the relationships:-

$$\sin (I) = \frac{V1}{Va} \, , \quad \cos (I) = \sqrt{1 - \left(\frac{V1}{Va}\right)^2}$$

where, $V1$ = vel. of overburden

Va = apparent vel. of refractor

The travel time from A to B is:-

$$T = \frac{(X-x)}{Vr} + DB + \frac{z}{(V1 \times \cos (I))} \quad ---------------1$$

where, Vr = refractor velocity

$$x = z \times \tan (I)$$

substituting for z in 1,

$$T = \frac{(X-x)}{Vr} + DB + \frac{x}{(V1 \times \sin (I))}$$

$$= \frac{(X-x)}{Vr} + DB + \frac{(x \cdot Va)}{V1^2}$$

$$= \frac{X}{Vr} + DB + x \cdot \left(\frac{Va}{V1^2} - \frac{1}{Vr}\right)$$

$$x = (T - \frac{X}{V_r} - DB) \Big/ \left(\frac{V_a}{V1^2} - \frac{1}{V_r}\right)$$

$$= \frac{(T - DB) \, V1^2.V_r - (X.V1^2)}{(V_a.V_r - V1^2)}$$

substituting for x in 1,

$$T = \frac{X - z \tan (i)}{V_r} + DB + \frac{z}{V1 \cos (i)}$$

$$= \frac{X}{V_r} + DB - \frac{z.\sin (i)}{V_r.\cos (i)} + \frac{z}{V1.\cos (i)}$$

$$= \frac{X}{V_r} + DB + z \left(\frac{1}{\sqrt{1-\left(\frac{V1^2}{V_a^2}\right)}.V1} - \frac{V1}{V_a.V_r.\left(\sqrt{1 - \frac{V1^2}{V_a^2}}\right)}\right)$$

$$z = T - \frac{X}{V_r} - DB \Big/ \left(\frac{1}{V1\sqrt{1 -\left(\frac{V1^2}{V_a^2}\right)}} - \frac{V1}{V_r \, (\sqrt{V_a^2 - V1^2})}\right)$$

equivalent expressions can be derived for a raytravelling in the opposite direction.

The travel times, apparent velocities and ranges to both stations for all the shot points are known. The velocity of the overlying rocks is either known or estimated along with the delays at each station. By providing an estimate of the refractor velocity, a first solution can be obtained by solving the equations for each shot point. Figs. 5.1. and 5.2 show the type of output that will be obtained from this operation, which involves an estimate of depth and velocity in relation to the distance travelled along the refractor. The true velocity and depth will lie somewhere within the shaded region. Using the average of the apparent

72
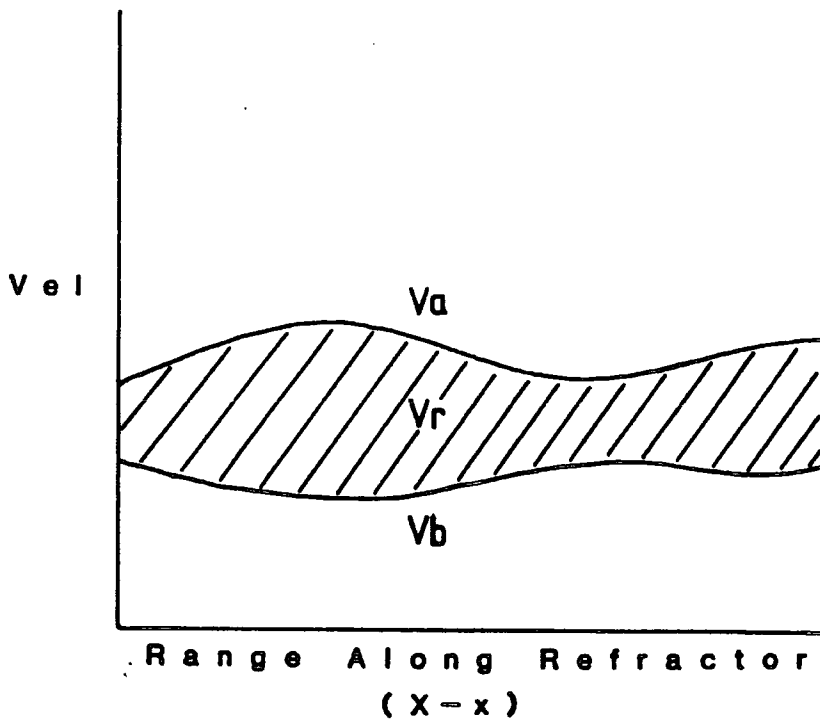
Fig.5.1:   Type of function derived by AGINTER.   The variation in
apparent velocity of rays observed at both ends of the
line, plotted against distance travelled along the
refractor.
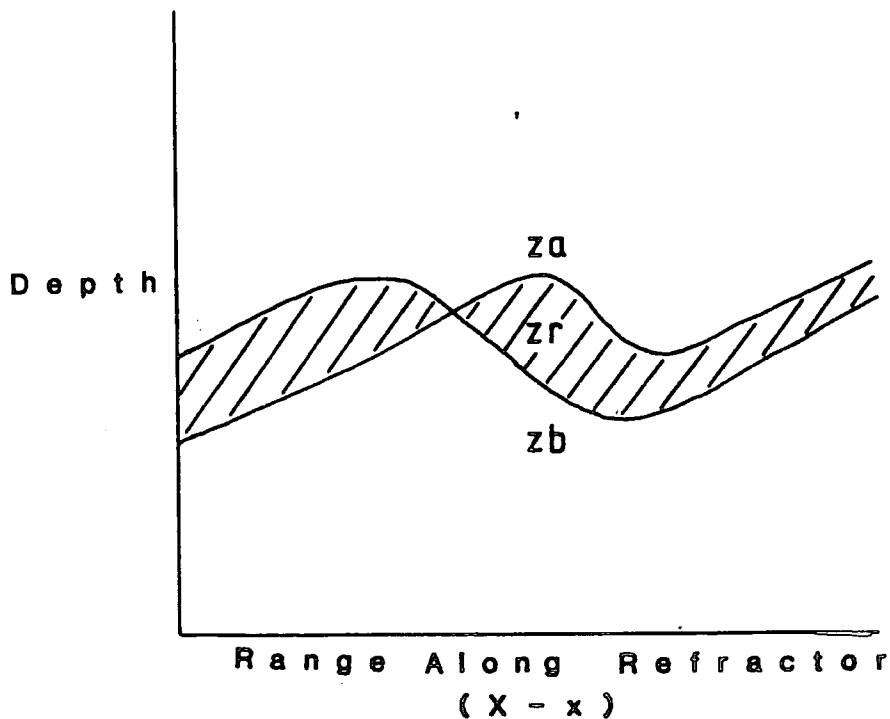
Fig.5.2:   Second type of function derived by AGINTER. The
variation in depth derived from rays travelling in
opposite directions plotted against distance travelled
along the refractor.

velocities from both ends of the line, a new estimate of refractor velocity can be obtained up to the point where each ray leaves the interface. This can then be used to calculate a new solution of the type shown. By an iterative procedure, the velocity and depth variation can be mapped out along the line. This method takes account of any significant overlap of rays between adjacent shots.

The program, AGINTER, presented in Appendix 2, was written to carry out this procedure but was not fully tested due to the lack of suitable data. The new velocity function defined from the apparent velocities along the refractor undergoes interpolation to provide the velocity at 1 km intervals along the line. This spacing may need to be refined if it is found to give unsatisfactory results. Although full testing has not been carried out, the program can act as a basis for further development of an interpretational technique to apply to closely spaced refraction data along a reversed profile using airguns or other sources.

CHAPTER 6

PRESENTATION AND INTERPRETATION OF RESULTS

6.1 Introduction.

The interpretation of the data was carried out initially in two phases. The airgun data were examined before and after the application of the processing techniques to determine the velocity structure of the sedimentary basins, obtain an estimation of their depth and delineate any lateral velocity variation within the basement. The explosive shots were used to examine the changes in velocity and structure of the Pre-Cambrian basement along the line and provide time and depth estimates to the interface. In addition, although the ranges of the shots along the WISE profile were not sufficient to provide many arrivals from the Moho, data from the LOWNET and Eskdalemuir stations were included in an examination of crustal delay times and sub-Moho velocity.

Reduced travel time sections, constructed for all the explosive shots provided details of phases recorded, velocities along the line and relative delay times at each shot and station point. Travel time graphs were also constructed for each station to obtain initial velocity estimates and to determine whether particular arrivals were from the basement refractor or deep sediments in the basins. The latter was possible where shot separation was smallest, such as the region between Colonsay and Kintyre for phase two. Reduced travel time graphs were also made of the airgun records to aid in identifying variations in apparent velocity along the line.

Both sets of data were then used to develop a velocity model of the crust down to the Moho. Delay times to the basement and Moho were obtained from time-term analysis. Velocity variations within the basement

were determined using minus- time analysis and applying Wiechert inversion to the velocity/distance distributions obtained. Ray-tracing was then carried out on the model to investigate further the crustal structure. The ray-traced models presented are only preliminary attempts to define the structure and test the results from the time-term and minus-time analyses. They are not the product of a full iterative modelling procedure.

6.2 Interpretation of the Airgun Data.

The poor quality of most of the sections of the airgun profile prohibited detailed interpretation $_\wedge$ depth and velocity structure of the basins. Travel time sections, both unreduced and reduced were made for each part of the profile between Tiree and Jura. The processing techniques were applied to all the data but due to the lack of confidence that could be placed in the results, and the fact that justification of the methods' application to the data is not satisfactory (Chapter 4), the results were not used. The airgun sections that were examined have been presented in the previous chapters. These are the data from the middle section of the line that could realistically be expected to be reversed. However, even along these sections, reversal was not achieved. The only information that could be extracted from the data were the apparent velocities of refractors close to the receiver station. A limit was placed on the range over which arrivals from a particular refractor could be expected and a limiting depth estimate evaluated.

The apparent velocity of each refractor was first determined by picking the arrivals and plotting travel time graphs (Attree, 1982; Casson, 1982). By applying RAYSCAN (Chapter 5), more detailed information and changes in the apparent velocity were determined. Fig. 6.1 provides the

75
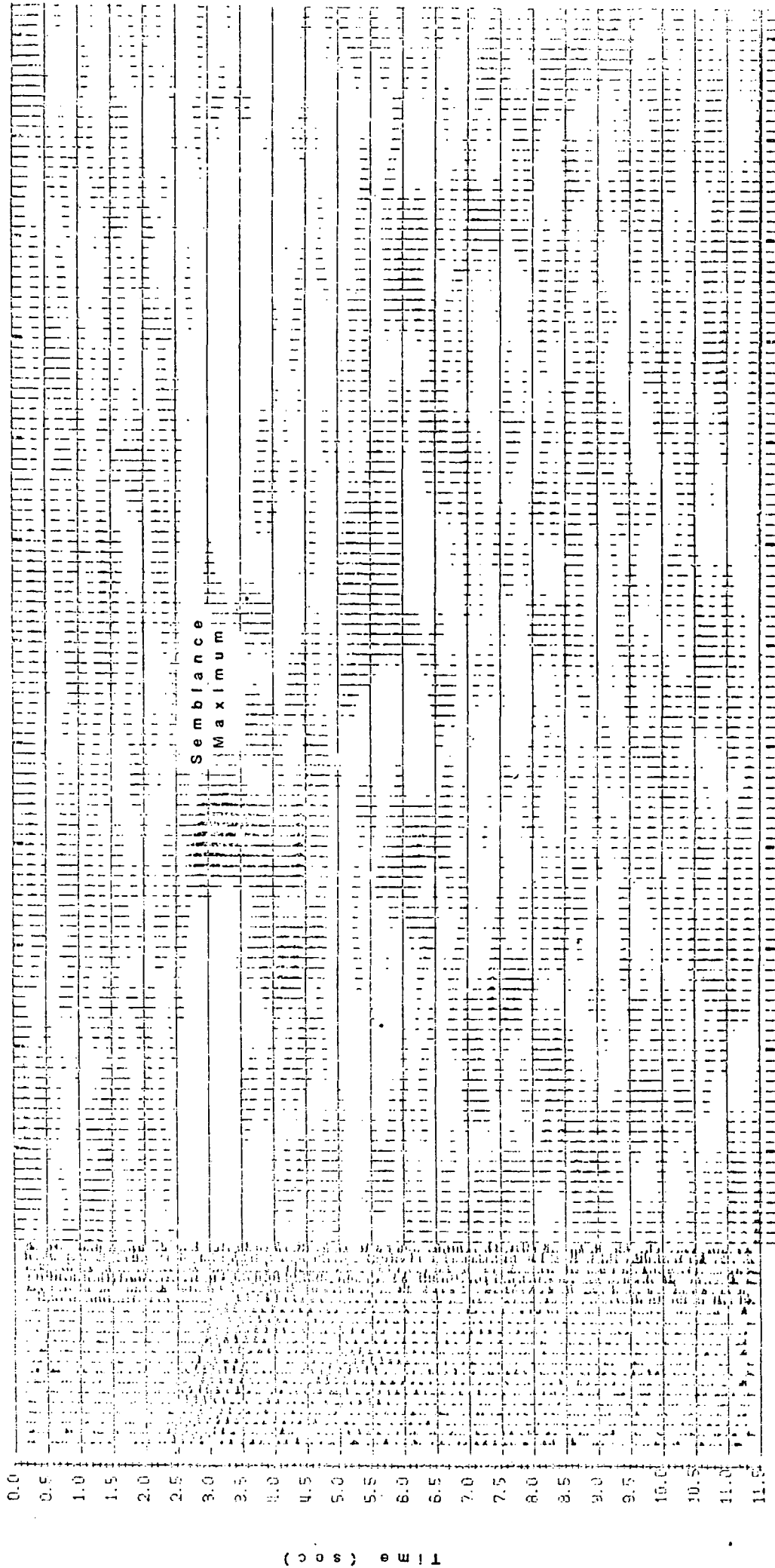
Fig.6.1: Example of the output from RAYSCAN for the airgun line between Mull and Tiree for the Mull station with features of the plot indicated.

output from the program for the Mull to Tiree section of the line for the receiving station at Mull for one array of traces along the line. The left hand side of the plot shows the array used with the first trace number and range of the mid-point. The right hand side indicates the value of semblance at particular travel times after moveout by different ray parameters, these values shown at the base of the plot. The semblance maximum is indicated. Semblance maxima can be identified and traced across plots of cosecutive arrays of traces indicating the changes in velocity along the line. The number of traces included in the array upon which the semblance was calculated was increased along the profile. The size by which the arrays were increased depended on the range between shots: a function involving a linear increase in range was used to increase the number of traces. Although the velocity was determined for the mid-point of each array, and a discrete value obtained, the variation could be plotted against this mid-point to give a continuous function along the line. Fig. 6.2 is an example of such a function for the Mull station. Similar analyses were made for each of the other sections of the line where the data allowed it. However, the noise on many of the Mk.3 recordings limited the success of the method as it correlated very well at numerous moveouts and hence aliased at multiples of a particular ray parameter. Output from RAYSCAN for the line between Mull and Colonsay, recorded at Mull is given in Fig. 6.3. The mid-point of the array is only 20 traces from the beginning of the line but noise in the semblance can be clearly seen. Although a strong peak can be seen at travel time 2.4 sec corresponding to a ray parameter of 0.200, interpretation of the data becomes more difficult beyond this point, due to the increase in noise.

Table 6.1 provides the values of the velocity for different
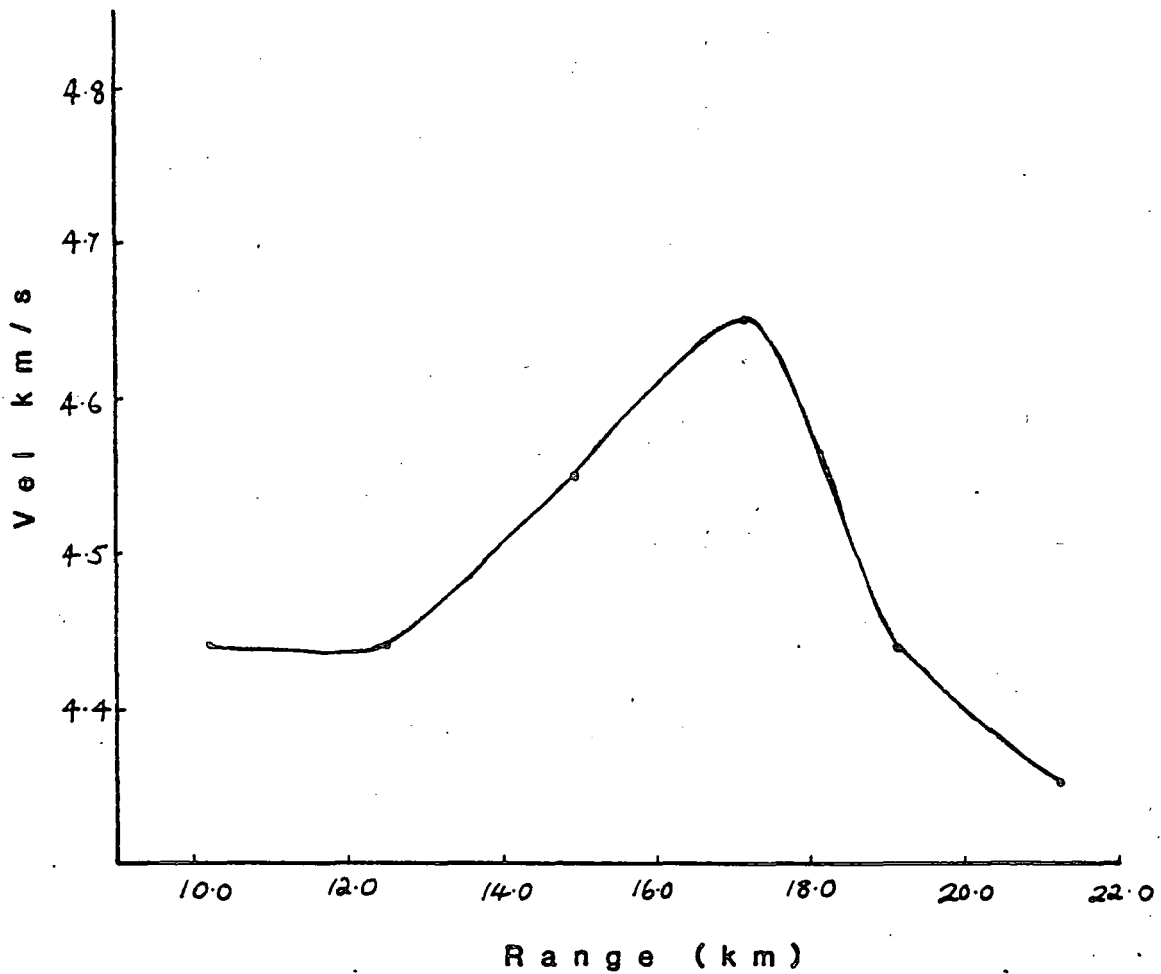
Fig.6.2:   Plot constructed from the ten consecutive RAYSCAN semblance determinations used to calculate the apparent velocity along the Mull to Tiree line as recorded at the Mull station. The discrete points are the velocities obtained for the mid-points of each array at the ranges shown.

RANGE (KM)
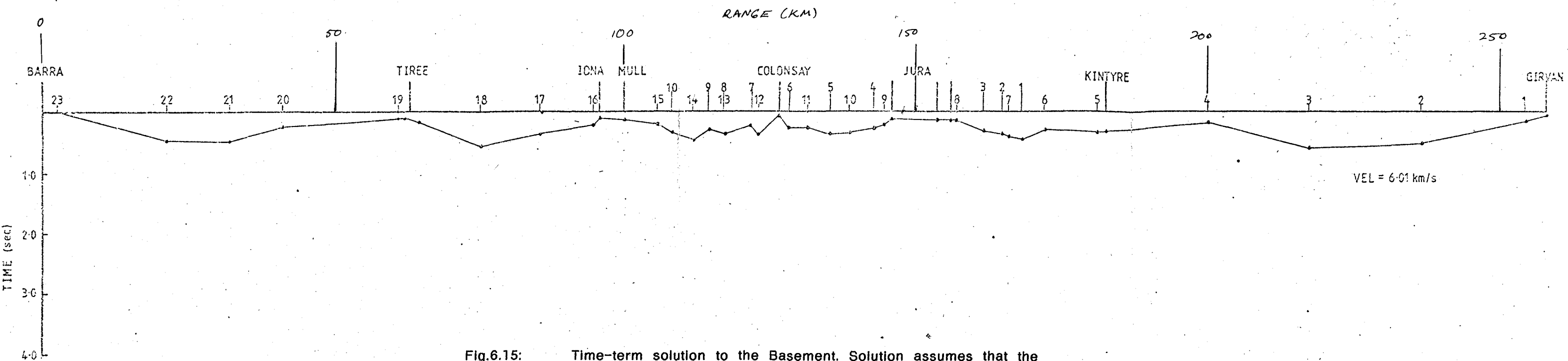
Fig.6.15:   Time-term solution to the Basement. Solution assumes that the time-term is independent of the shot location relative to the station. Rock type given in text.

VEL = 6·01 km/s

VEL.= 5·95 km/s
— — S. TIME TERM
——— N. TIME TERM
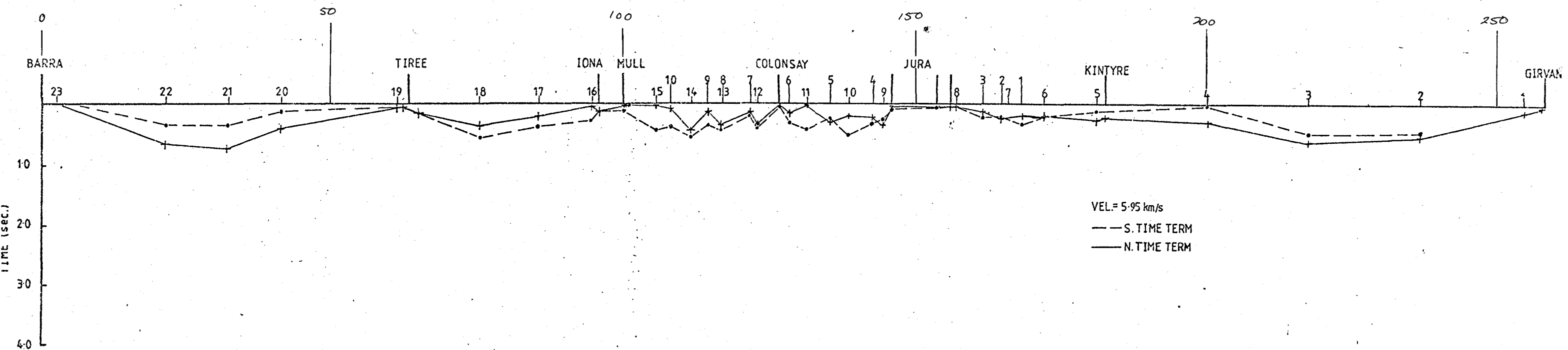
Fig.6.16:   Time-term solution to the Basement. Solution assumes that there is a dependence on the location of shot relative to the station. The solid line indicates time-terms to the north of the stations and shots, the broken line, those to the south.
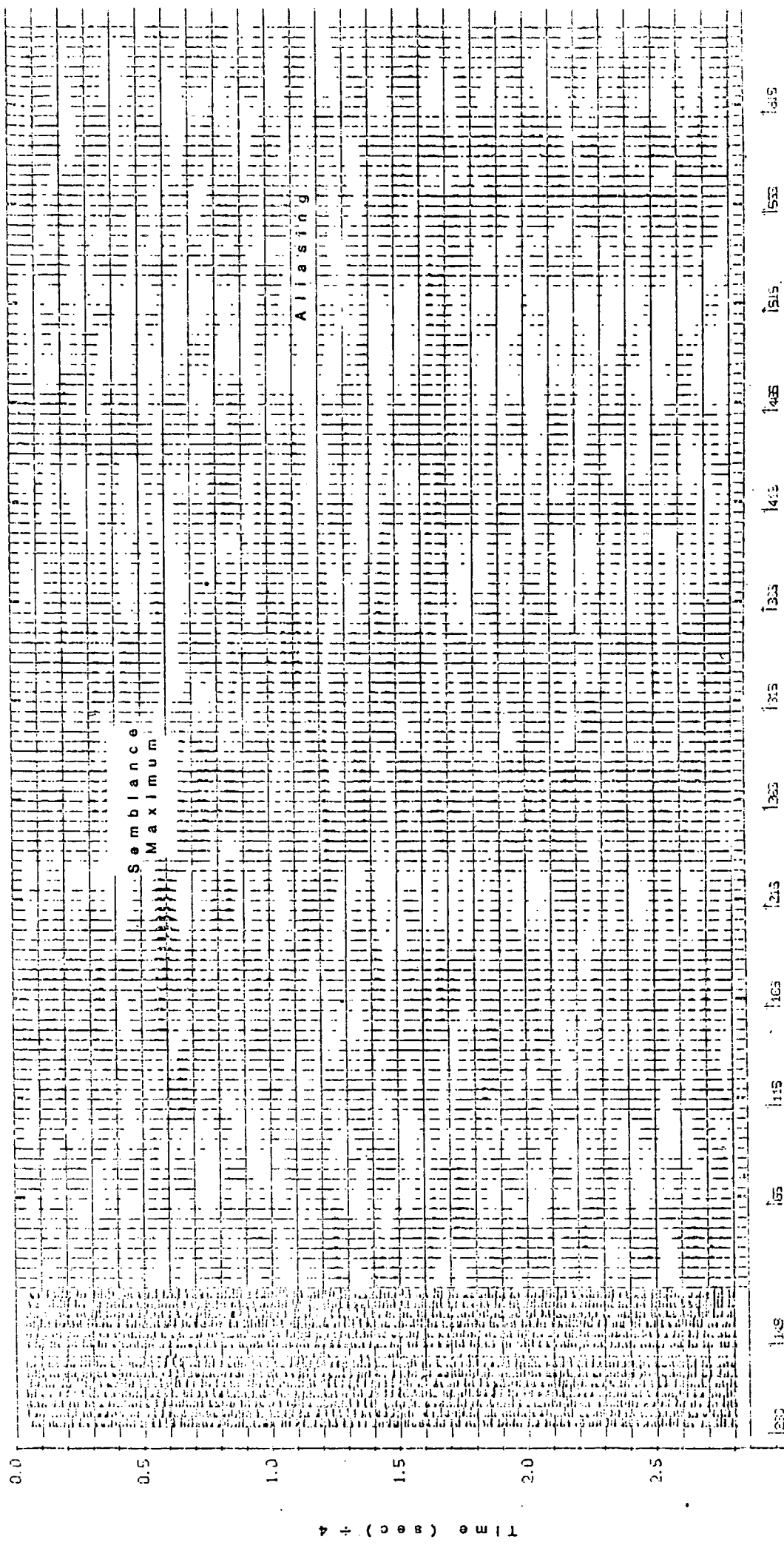
Fig.6.3: Output from RAYSCAN for the Mull station for the Mull to Colonsay airgun line.

RANGE (KM)

0   50   100   150   200   250

BARRA   TIREE   IONA MULL   COLONSAY   JURA   KINTYRE   GIRVAN

23   22   21   20   19   18   17   16   15 10 14 9 8 13 7 12 6 11 5 10 4 9   8 3 2 7 6 5   4   3   2   1

VEL = 6·01 km/s

VEL = 7·99 km/s

TIME (sec.)

1·0

2·0

3·0

4·0
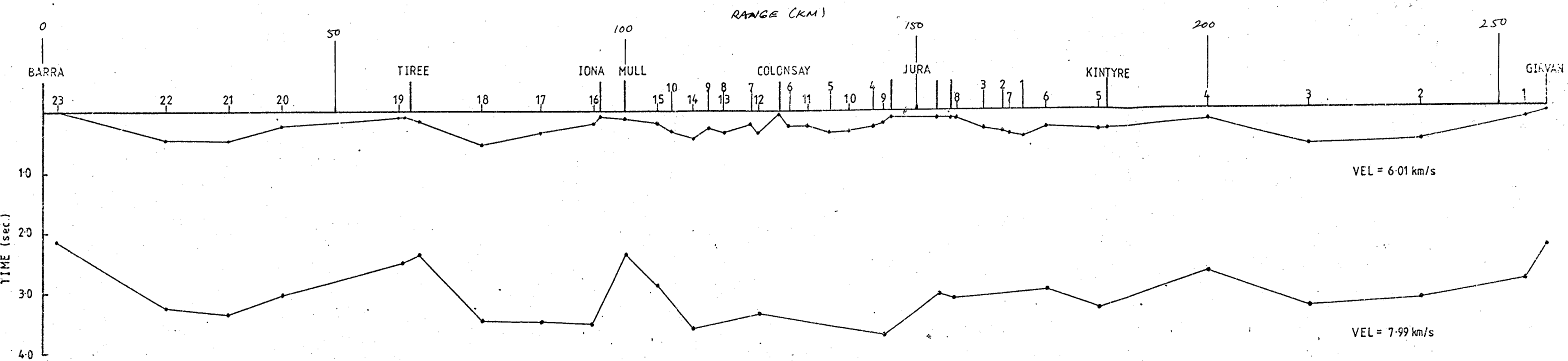
Fig.6.20:   Time-term solution determined from the Pn arrivals.

RANGE (KM)

0   50   100   150   200   250

BARRA   TIREE   IONA MULL   COLONSAY   JURA   KINTYRE   GIRVAN

23   22   21   20   19   18   17   16   15 10 14 9 8 13 7 12 6 11 5 10 4 9   8 3 2 7 6 5   4   3   2   1

4·0 km/s

6·0 km/s

8·0 km/s

10·0

20·0

30·0

40·0
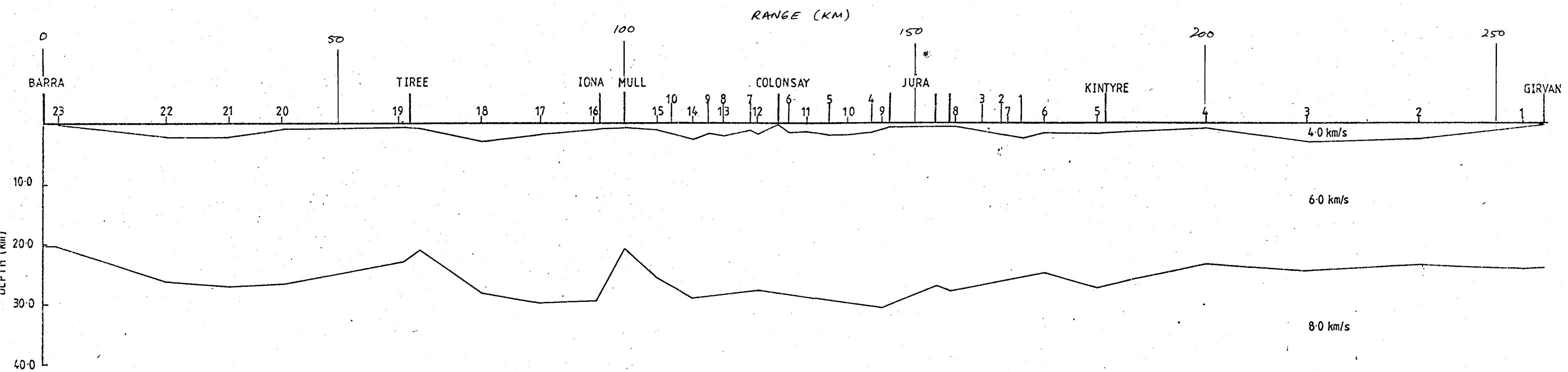
Fig.6.21:   Depth section to the Basement and Moho determined from the
              time-term solution. Constant average velocities were used as
              shown.

Table 6.1

VELOCITIES DETERMINED FROM RAYSCAN

Trace No.	Range(Km)	Vel.(Km/sec)
Mull-Tiree		
1	8.54	5.88
3	9.27	4.44
15	13.96	4.44
24	19.46	4.55
31	24.55	4.65
37	28.06	4.44
43	31.19	4.35
Iona-Tiree		
1	4.37	4.65
8	4.99	4.26
19	6.70	4.44
28	8.88	4.65
34	10.20	4.65
39	12.11	4.35
45	14.13	4.35
Tiree-Iona		
1	3.77	4.55
4	4.81	4.65
10	6.22	3.92
18	8.25	5.26
Mull-Colonsay		
1	8.81	3.85
6	7.86	4.08
12	8.92	4.88
19	10.48	6.06
25	11.81	4.88
31	13.23	4.26
Colonsay-Jura		
1	5.13	4.0
16	8.80	5.13
26	11.19	4.65
31	12.42	5.56

arrays along each section of the line where they could be calculated. The trace number quoted is the first one for that array. Each section of the profile is discussed separately below.

6.2.1 Mull-Tiree.

The velocities found for the Mull to Tiree line, recorded at Mull, are close to, but fluctuate about 4.5 km/sec, which can be reasonably attributed to the spread about the maximum peak of the semblance function and incorrect picking of this peak. The velocity is thought to represent Torridonian strata at the bottom of the Inner Hebrides Basin as it is too high to be that of the overlying Mesozoic or younger rocks and not great enough for basement. The initial high value of 5.88 km/sec found in the first scan can be attributed to the Lewisian basement, which according to sampling and sparker records, extends some 6 km offshore from the Mull station (Uruski, pers. comm.). This change in rock type in the region is supported by the velocity change. A velocity between 4.35 and 4.65 km/sec was found for the same stretch of line recorded at Iona which is also within reasonable bounds for Torridonian velocities. The difference between the Mull and Iona velocities is thought to be due to incorrect picking of the semblance peaks.

The data at the opposite end of the line was disappointing in that quality was very poor and the velocity could only be determined for 22 traces from the station. The velocity is difficult to determine, but close to the station, the velocity of 4.75 km/sec once again lies within limits expected of Torridonian rocks and the higher values may indicate that the strata dip towards Tiree. The velocity found at both ends of the line is however less than the value further north of 4.80 km/sec for Torridonian quoted by Armour (1977).

Using the apparent velocity for the proposed Torridonian layer in the basin, a limiting value of its depth was calculated assuming that the point where arrivals could no longer be clearly identified was the minimum point where they could be overtaken by arrivals from a refractor with a greater velocity. A velocity of 6.0 km/sec was used for the underlying basement with crossover values of 24.4 km and 18 km depending on the interpretation of the extent of the arrivals along the section. These values gave thicknesses of 3.31 km and 2.21 km for the Torridonian respectively. This does not take into account any younger sediments above. From the evidence proposed by Binns et al. (1975) of thicknesses of strata in the Inner Hebrides Basin obtained from reflection records, the second estimate should be taken as being the most realistic.

6.2.2 Mull-Colonsay.

The Mull to Colonsay line has been interpreted by Atree (1982). The results presented should be treated with caution as the velocities were obtained, either in full or in part, from the output of the predictive deconvolution and matched filtering programs. The velocities along the line for the Mull station, obtained from RAYSCAN have already been presented in Table 6.1. These differ in some respect from those determined by Attree (Table 6.2) but the general pattern along the line is the same. The discrepancies are probably a result of incorrect picking, erroneous results from the processing programs, and inaccurate determination of the position of the semblance maxima.

As the only data obtained were from the Mull station, a detailed examination could not be carried out and therefore the interpretation was very limited. The section of the line interpreted by

Table 6.2

<u>VELOCITY ALONG MULL-COLONSAY LINE</u>

<u>DETERMINED BY ATTREE (1982)</u>

Range (km)	App. Vel. (km/s) $\pm$ 0.03
8 - 10	3.83
10 - 11	3.20
11 - 12	5.20
12 - 15	5.50
15 - 17.5	3.80
17.5 - 20	7.10
20 - 22	5.20

<u>VELOCITY ALONG COLONSAY-JURA LINE</u>

<u>DETERMINED BY CASSON (1982)</u>
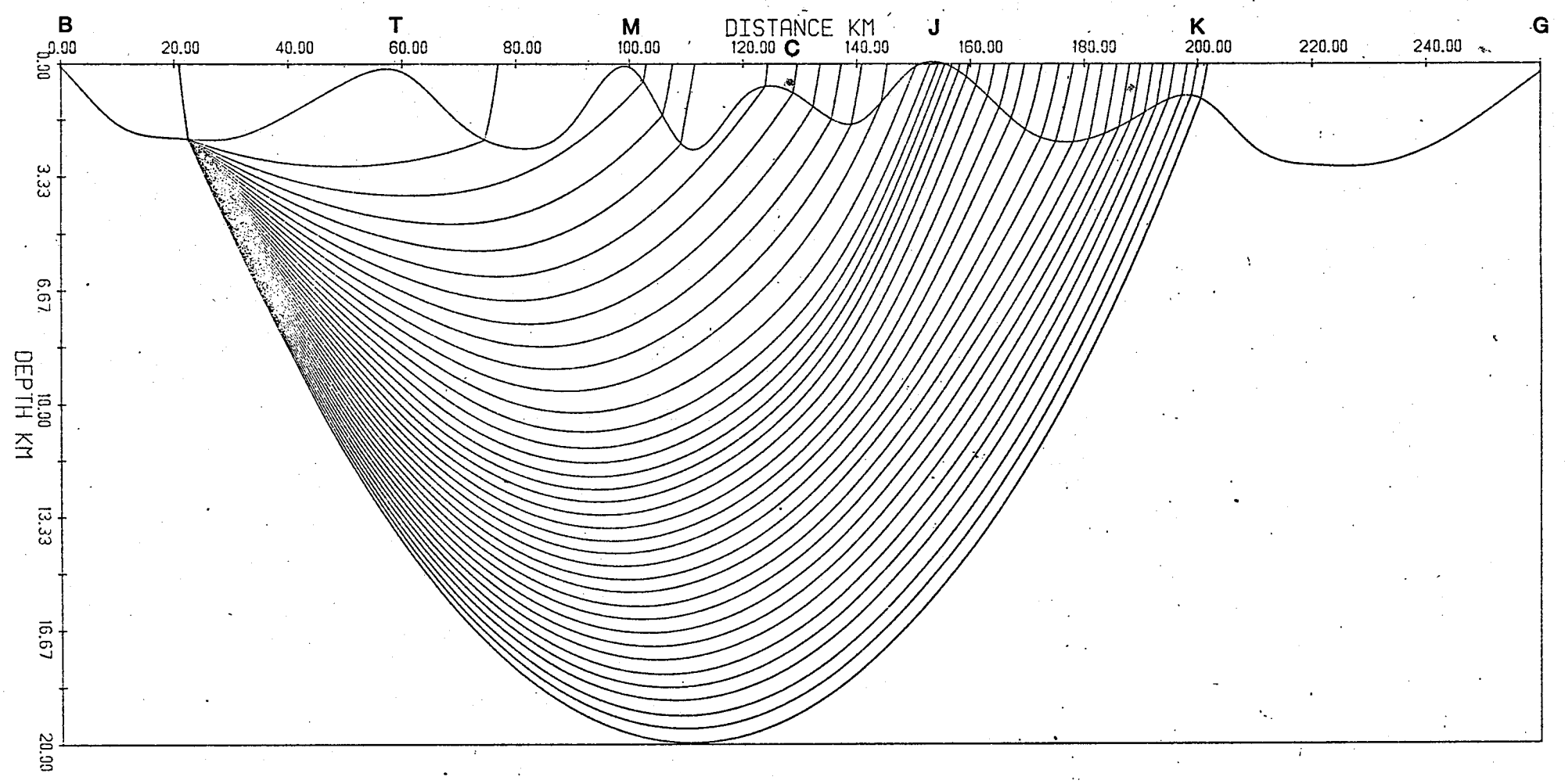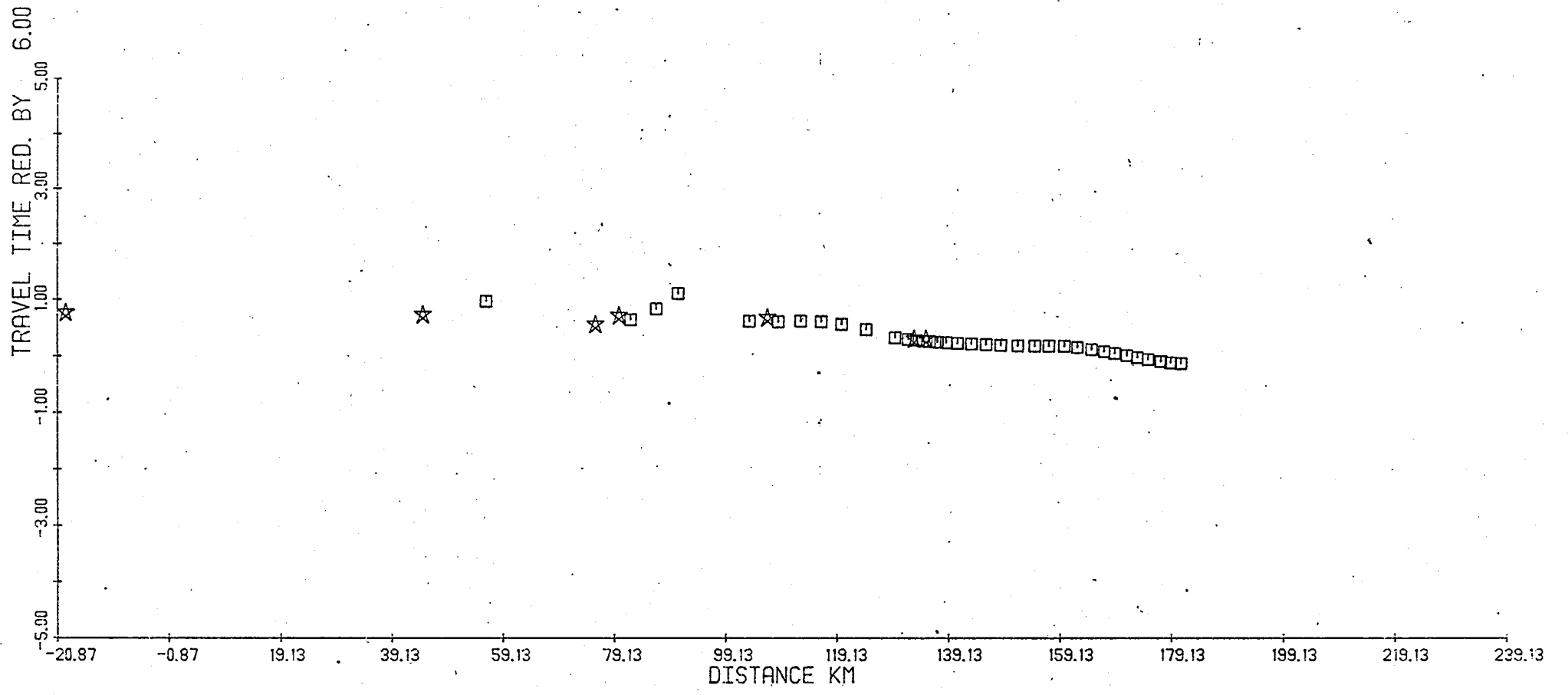
Range (km)	App. Vel. (km/s) $\pm$ 0.03
0 - 3	4.03
3 - 4.20	6.69
4.20 - 6.90	variable
6.90 - 9.65	5.47
9.65 - 10.90	variable
10.90 - 14.60	6.65
14.60 - 15.70	4.63

Atree is given in Fig. 6.4. It has been suggested that the Great Glen Fault forms a significant boundary between Torridonian and Moinian strata and that the Mesozoic sediments thicken greatly to the south of the fault. The dips on the Moine and Torridonian are estimates obtained from the apparent velocities and quoted values for Mesozoic sediment velocities. The interface dipping from Colonsay might not necessarily be real but rather, the low velocities found 15 to 18 km from Mull may reflect a thick pile of sediments in a downfaulted block.

The low velocity found close to Mull is interpreted as being a weathered' surface of the Ross of Mull granite. This is proposed in the absence of sediments with such a low velocity in the region south of Mull. The higher velocities on going further south were thought to be possibly a southward extension of the granite. However, examination of the Bouger anomaly map of Barber et al. (1979) does not show a significant feature and hence does not confirm this proposal. The velocity of 5.5 km/sec is therefore thought to represent Moinian strata dipping away from Mull.
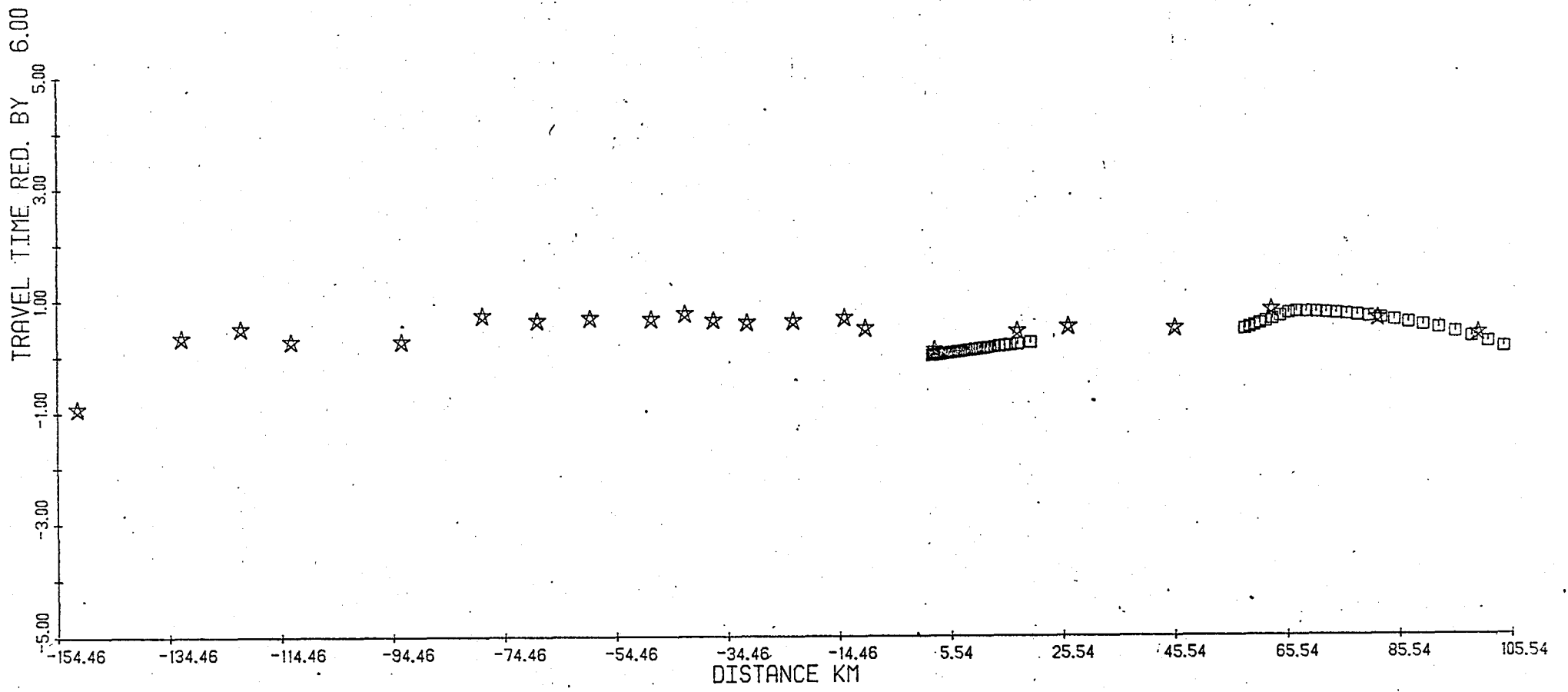
6.2.3 Colonsay to Jura.

The line between Colonsay and Jura was interpreted by Casson (1982) as a reversed refraction line, the data from the Jura station being obtained entirely from the processing output. It is felt that because of this, the interpretation, although thoroughly carried out after the determination of travel times, is very suspect. Examination of the original section from Jura shows a great deal of coherent noise and little signal but after processing it appears as if the signal can be retrieved. However, velocities as high as 9.0 km/sec were found in the central section of the line, complemented by 5.47 km/sec in the opposite direction. This interpretation is not presented therefore.
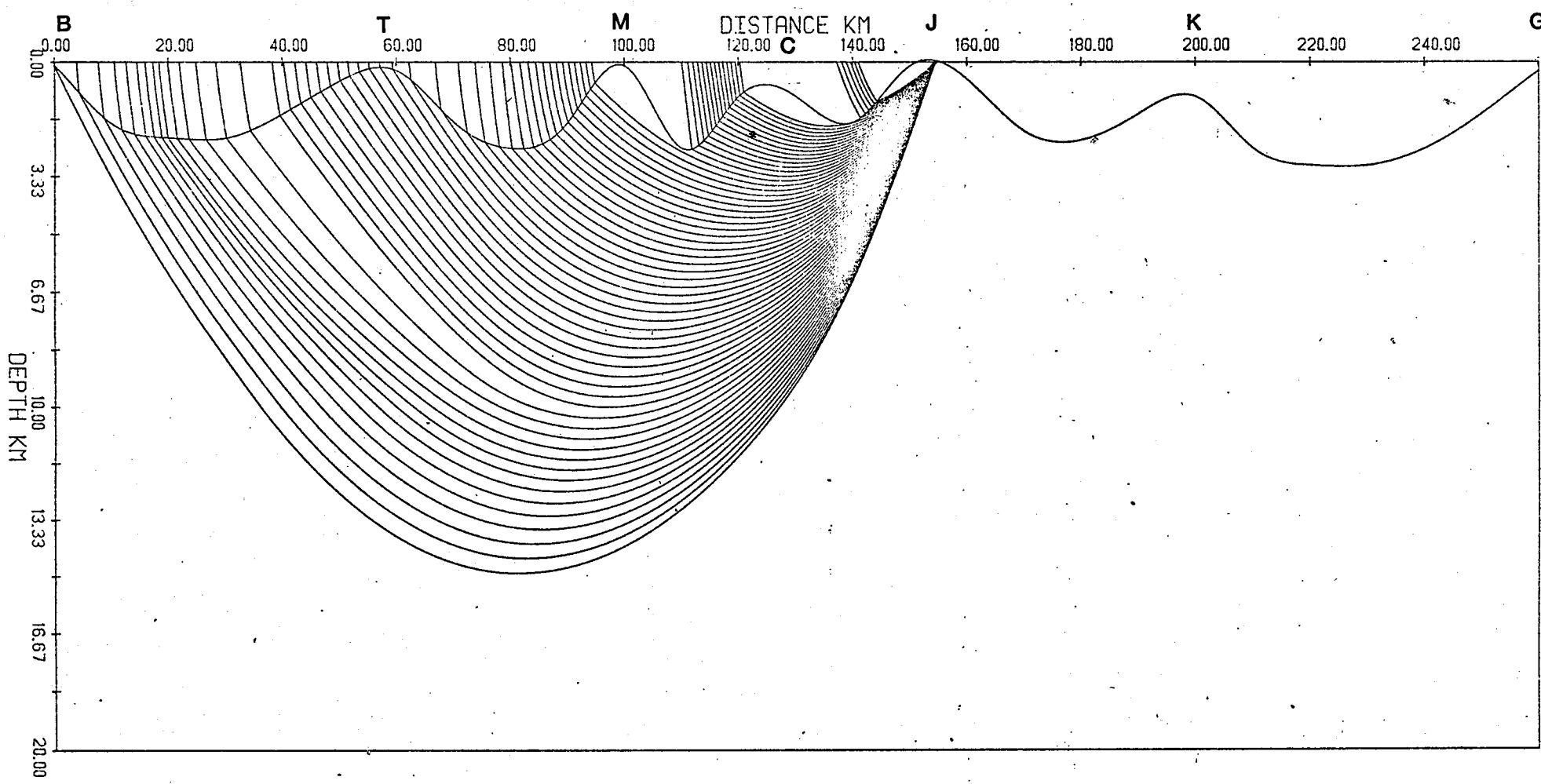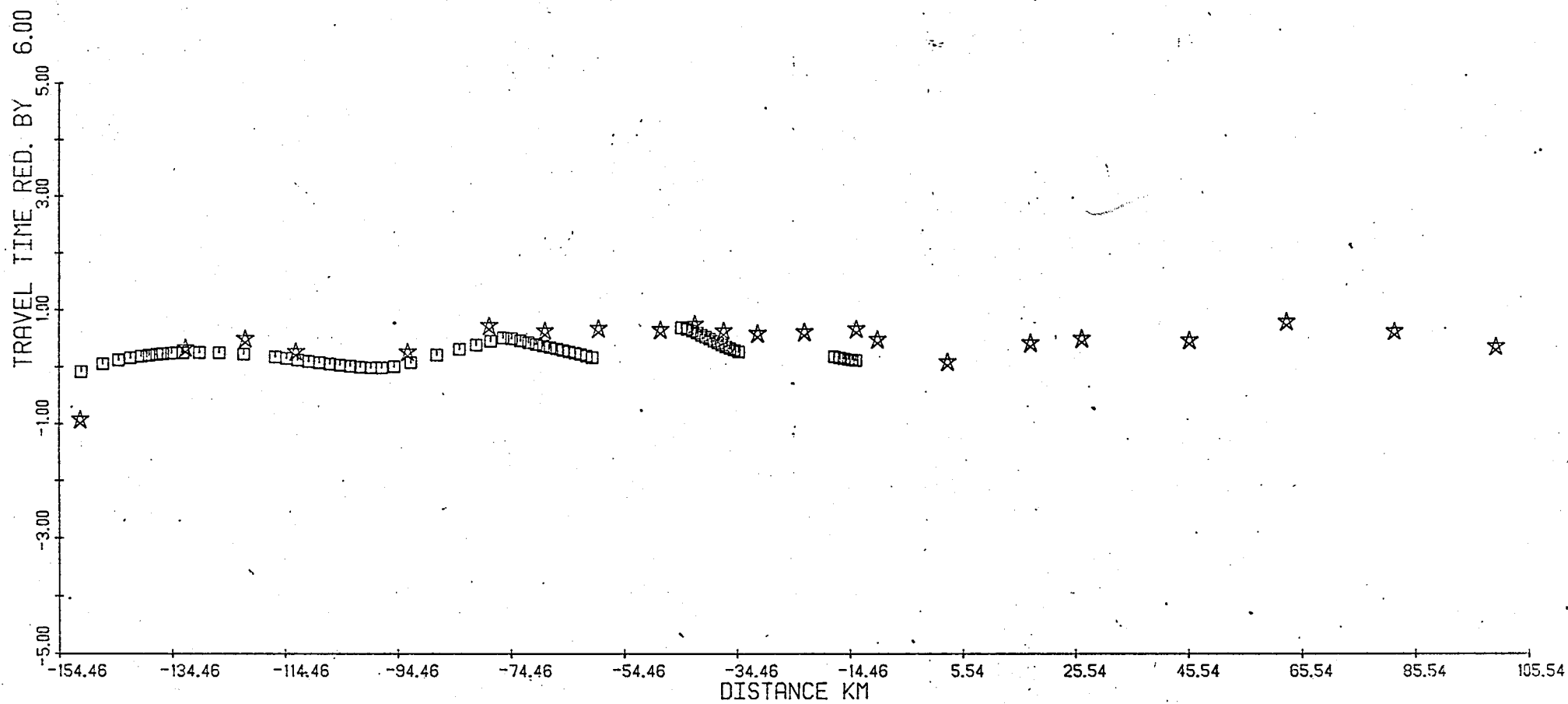
79

Fig.6.35:   Ray traced diagram and reduced travel time section
obtained from upper crustal model for shot 22.
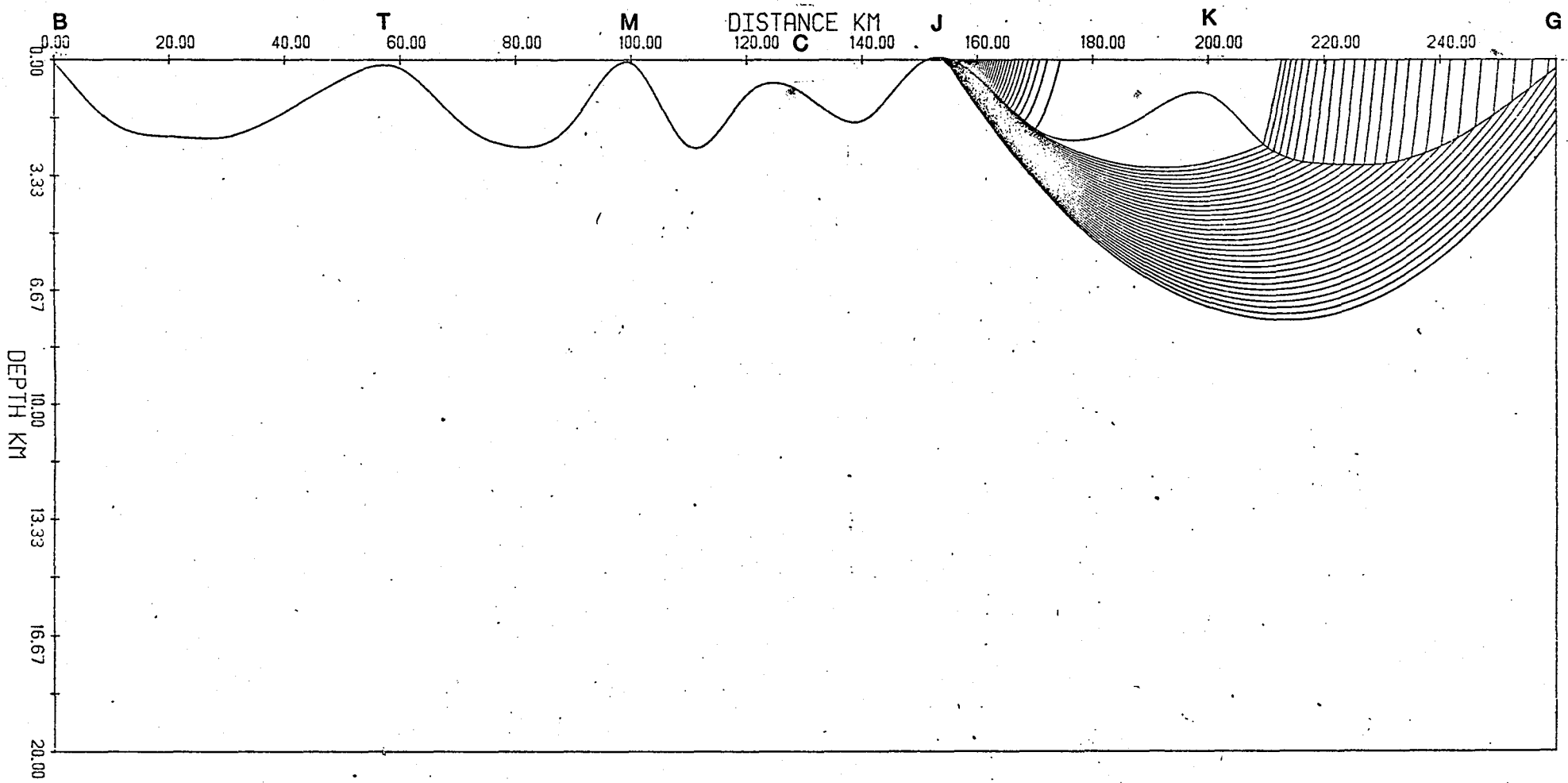
Fig.6.34: Ray traced diagram and reduced travel time section obtained from upper crustal model for the South Jura station using all shots. Southern shots.

Fig.6.33: Ray traced diagram and reduced travel time section obtained from upper crustal model for the South Jura station using all shots. Northern shots.

Fig.6.31: Recalculated crustal depth section derived from time-terms taking account of the velocity structure derived from the minus time analysis and subsequent Wiechert inversion.
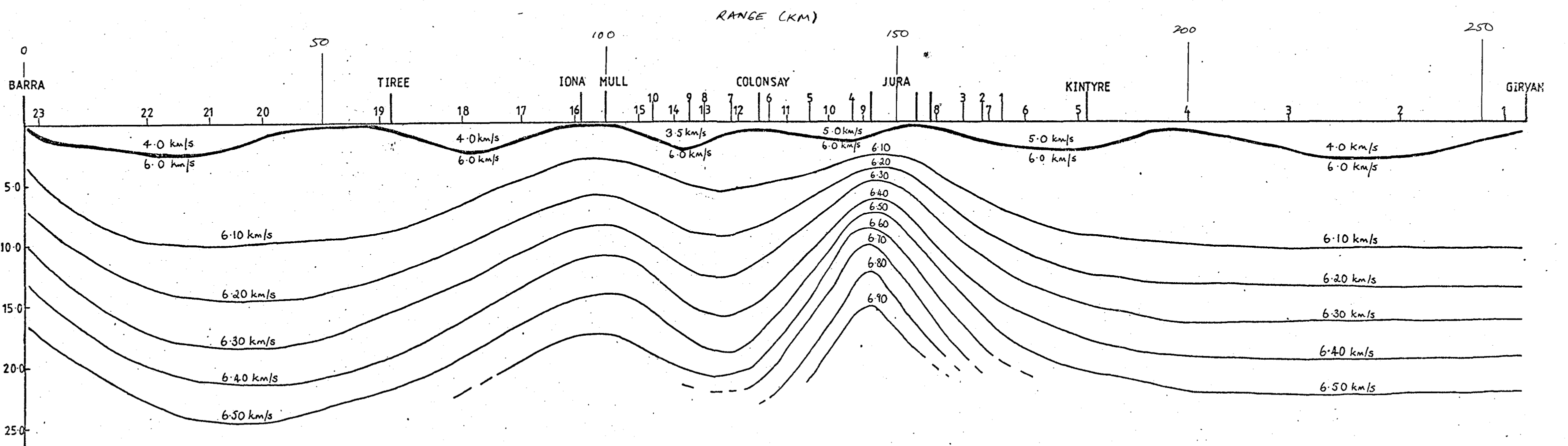
Fig.6.32: Upper crustal velocity model used in the application of the ray tracing method. The model shows modifications made to that derived using the minus times after ray tracing.
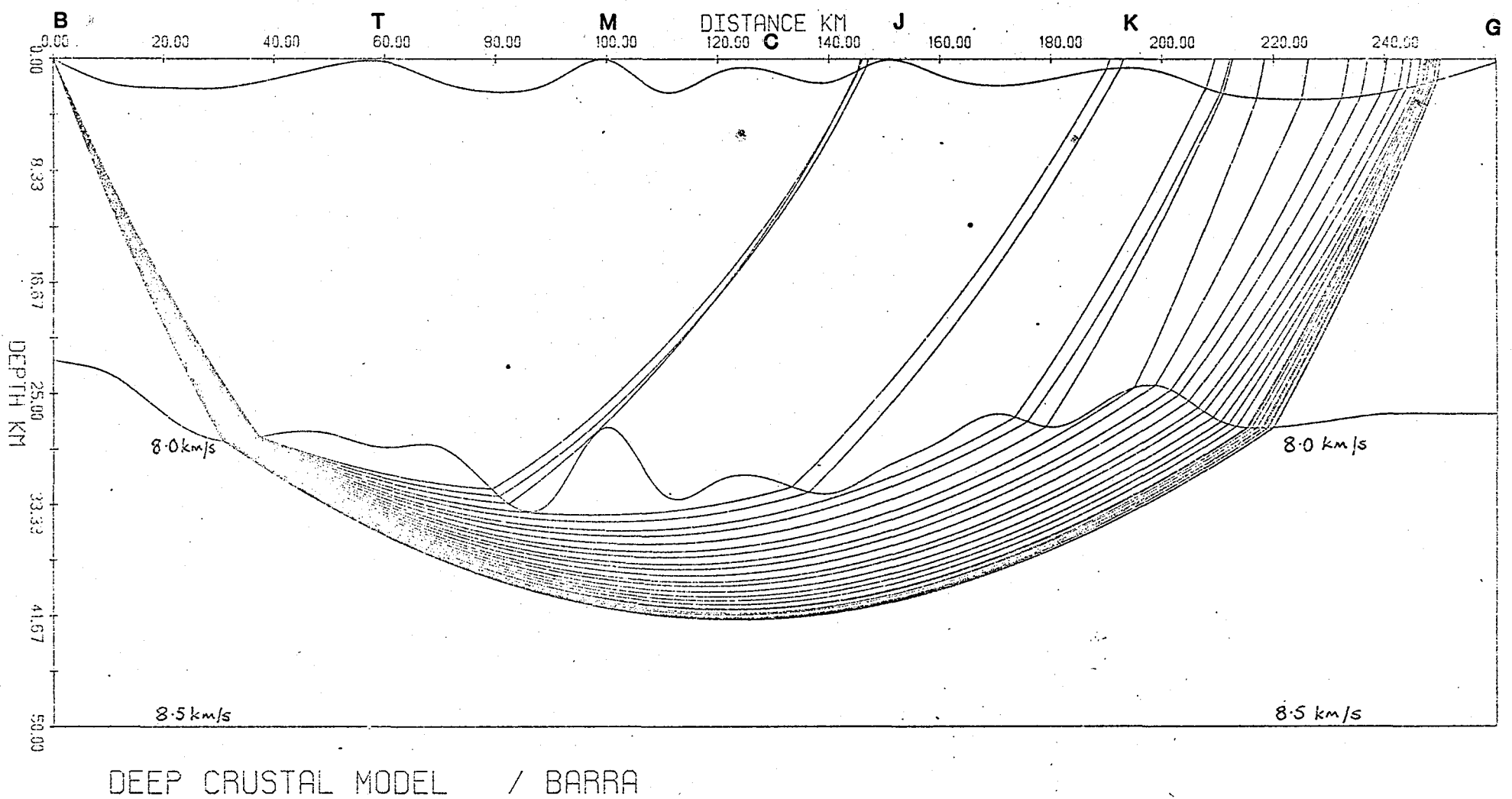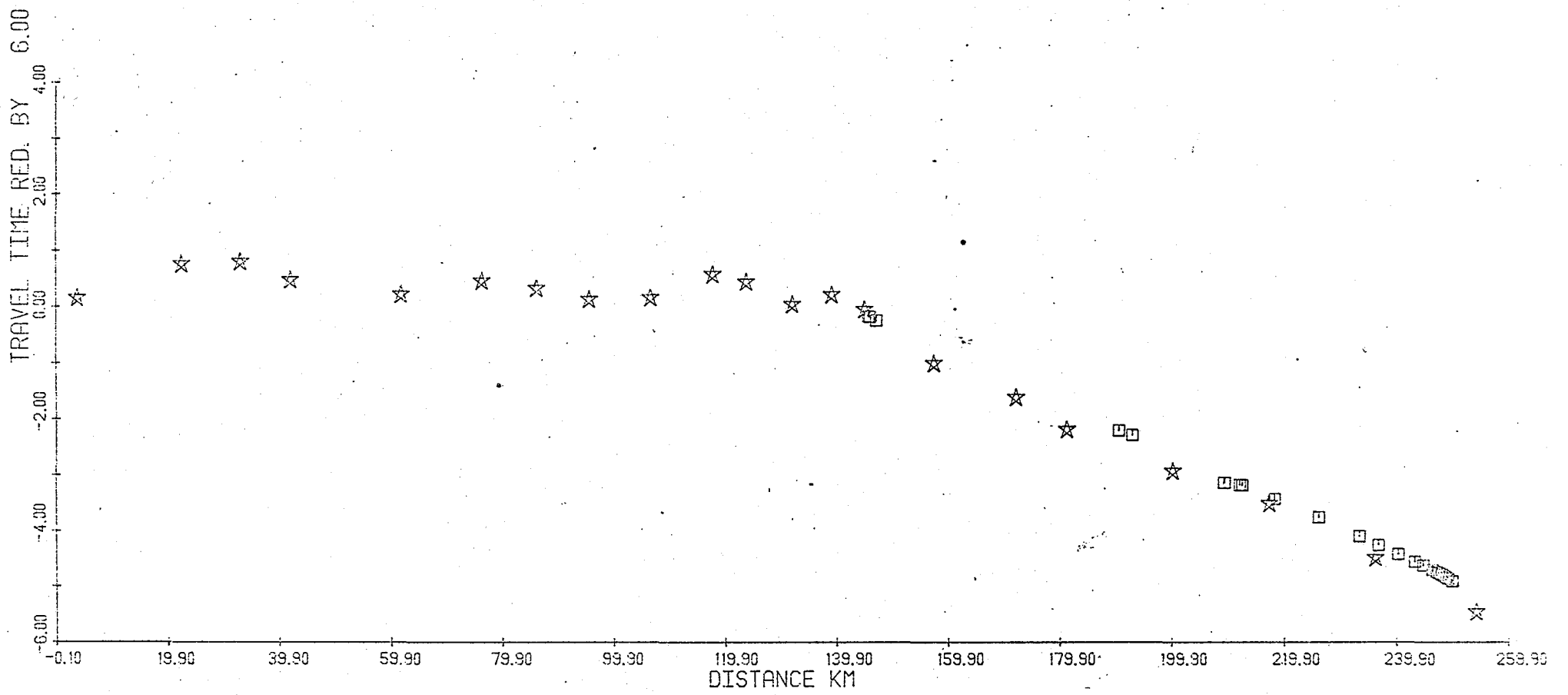
Fig.6.39: Ray traced diagram and reduced travel time section obtained from deep crustal model for the Barra station and Moho arrivals. The velocity structure down to the Moho was derived by extending the gradients of the upper crustal model down to the interface.
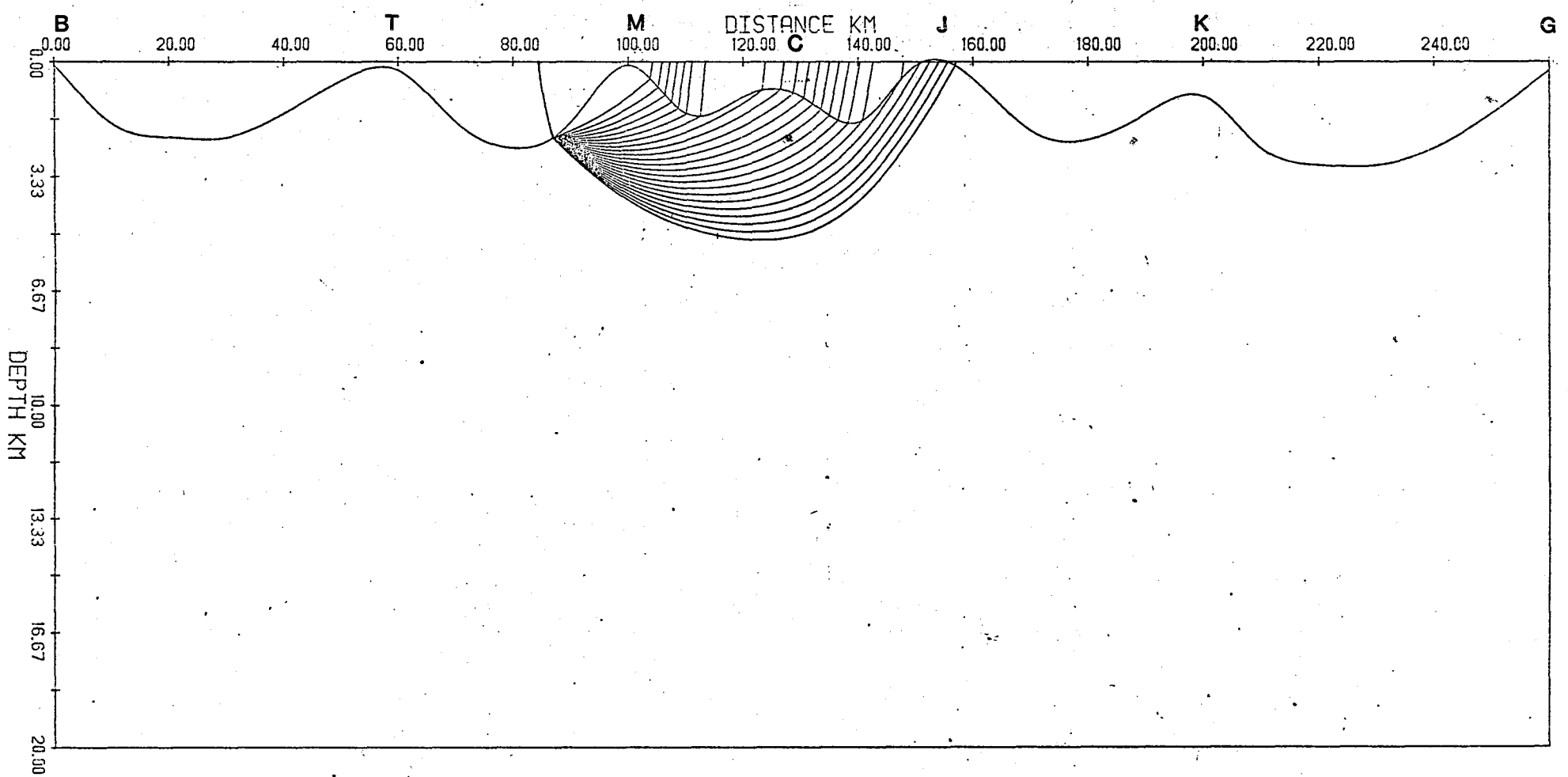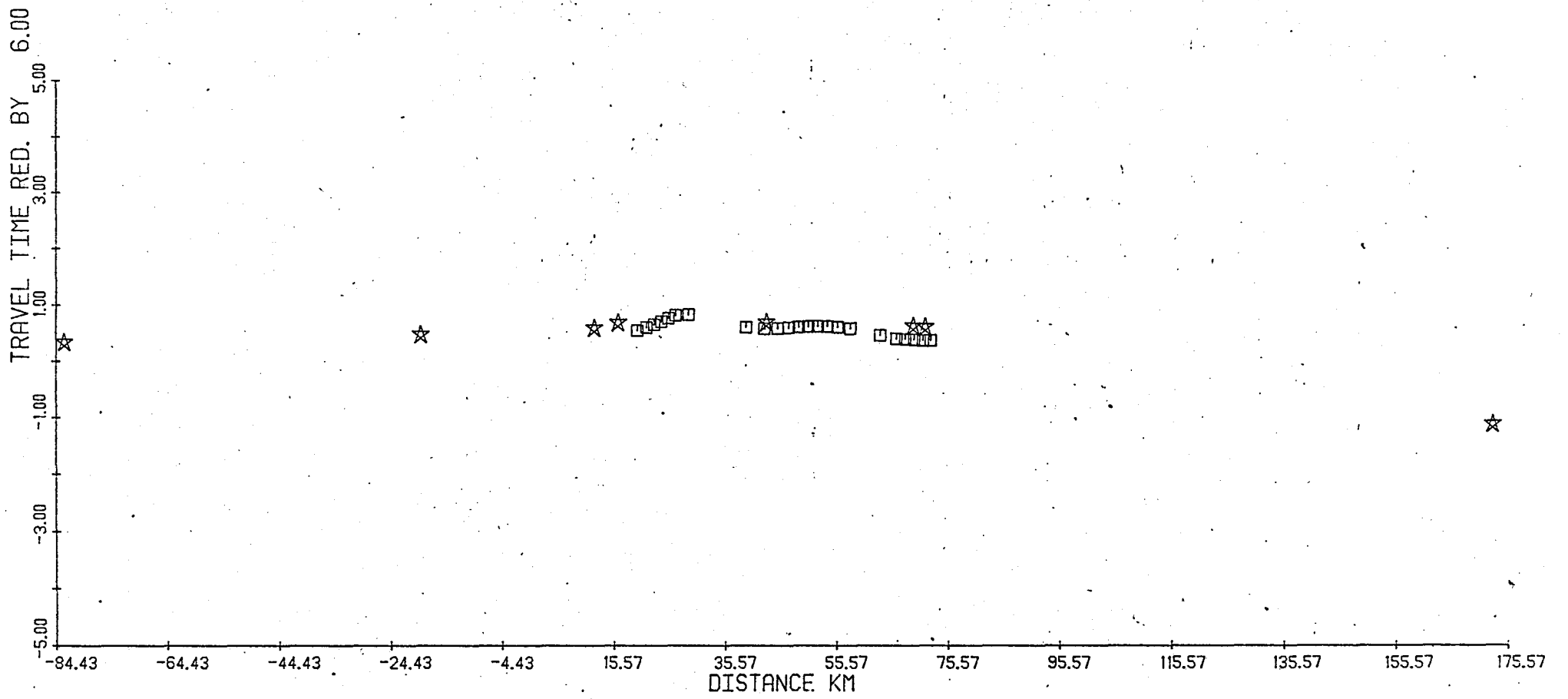
UPPER CRUSTAL MODEL   / SHOT 17

Fig.6.38:   Ray traced diagram and reduced travel time section obtained
             from upper crustal model for shot 17, phase 1. The depth of
             the basin between Colonsay and Mull has been reduced by 1 km
             compared to the previous model.
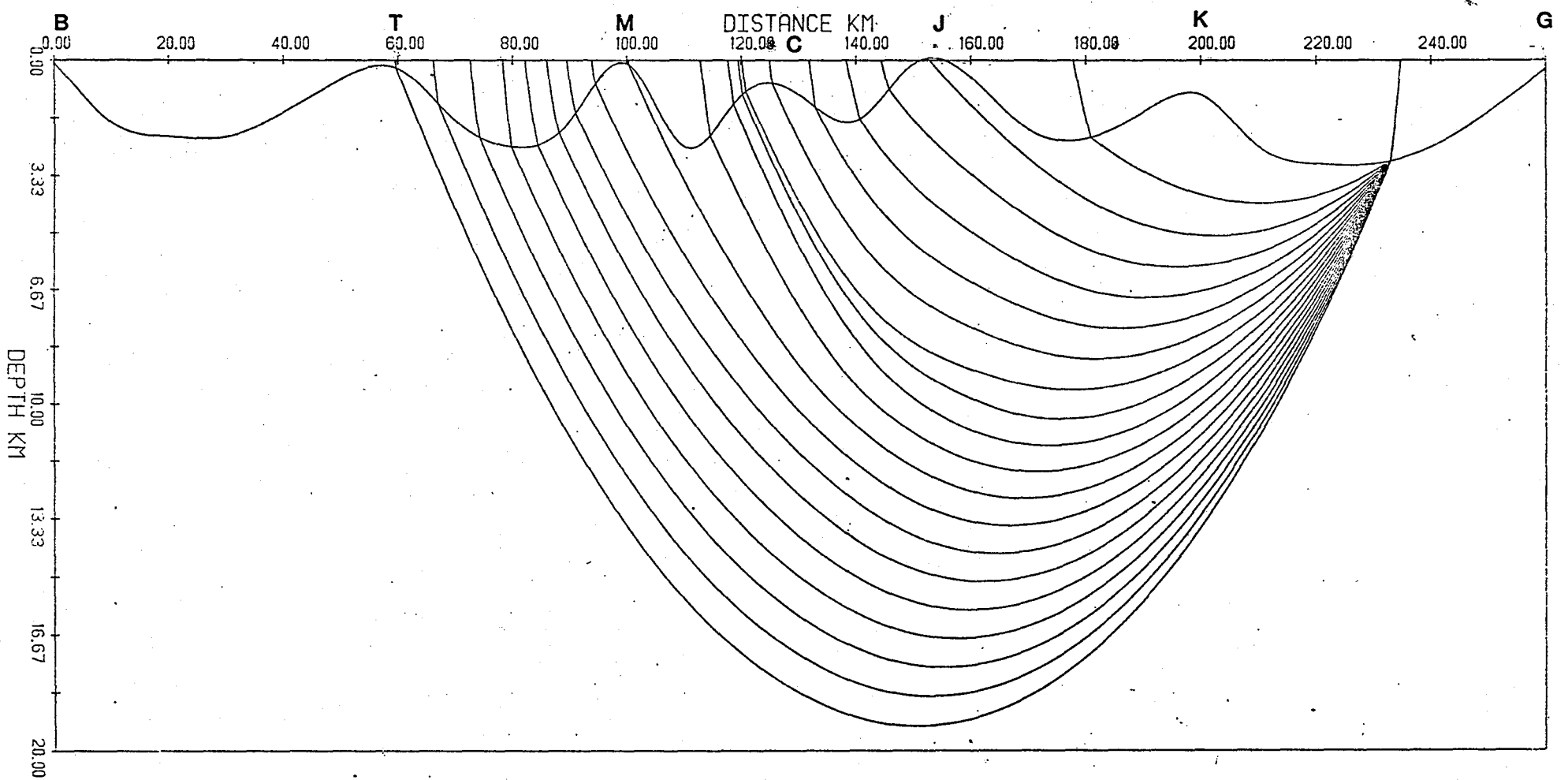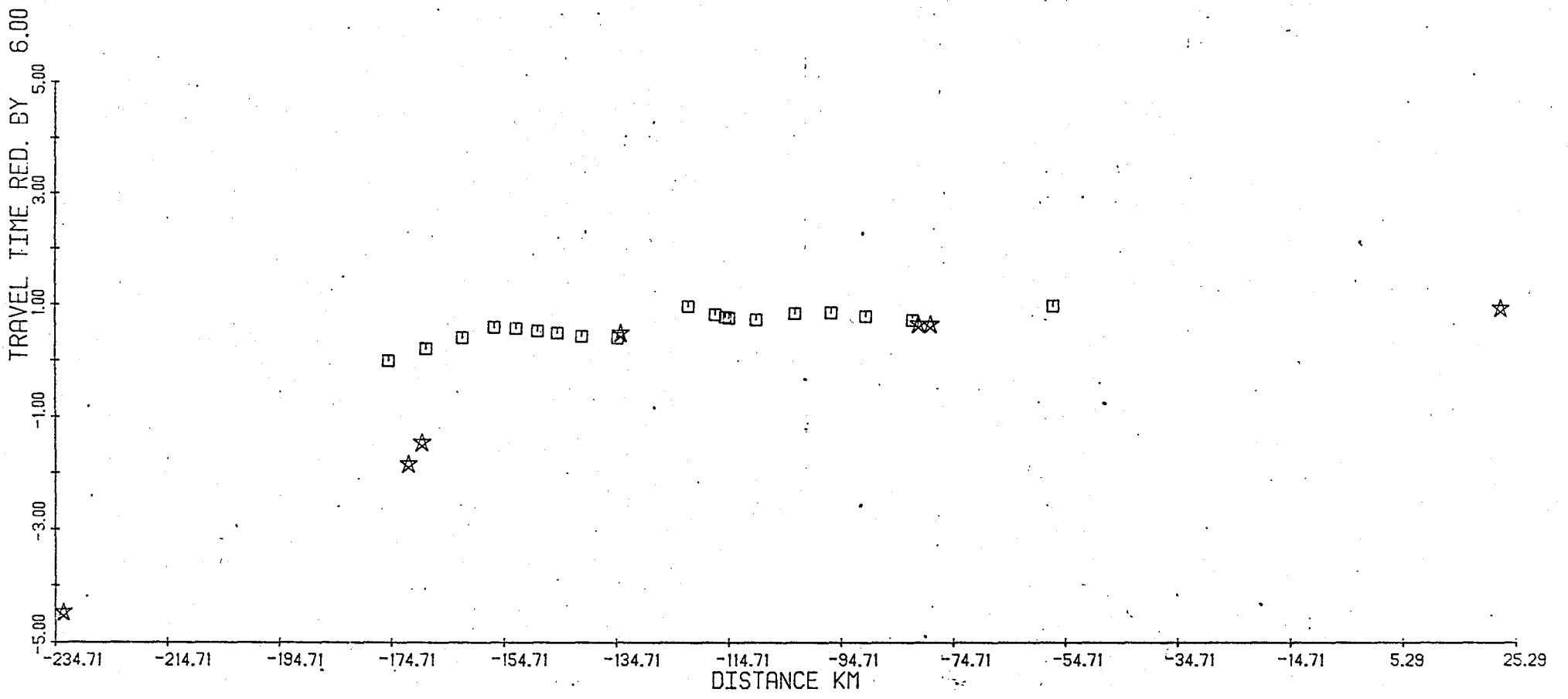
Fig.6.37:   Ray traced diagram and reduced travel time section
obtained from upper crustal model for shot 2, phase 1.
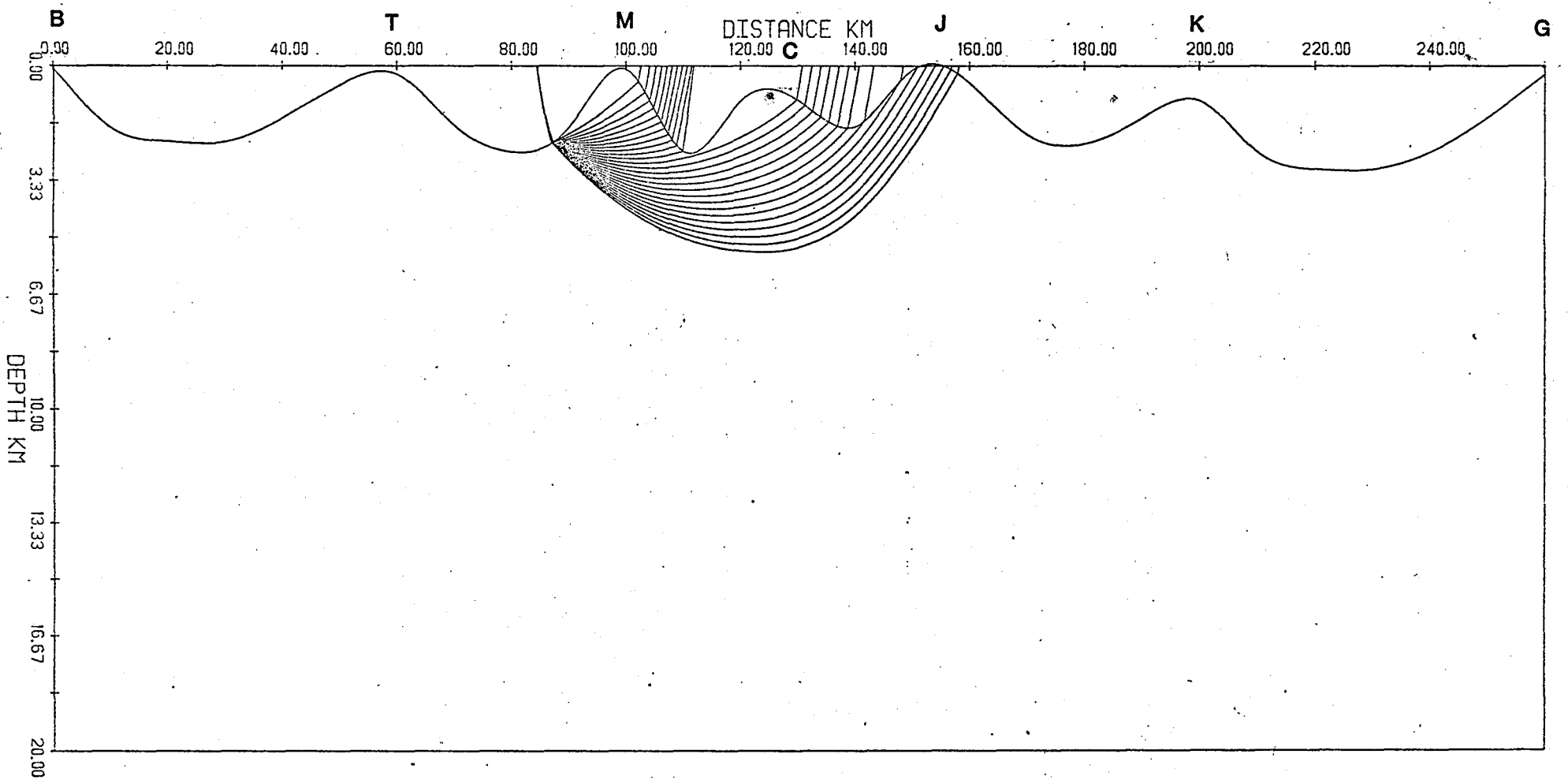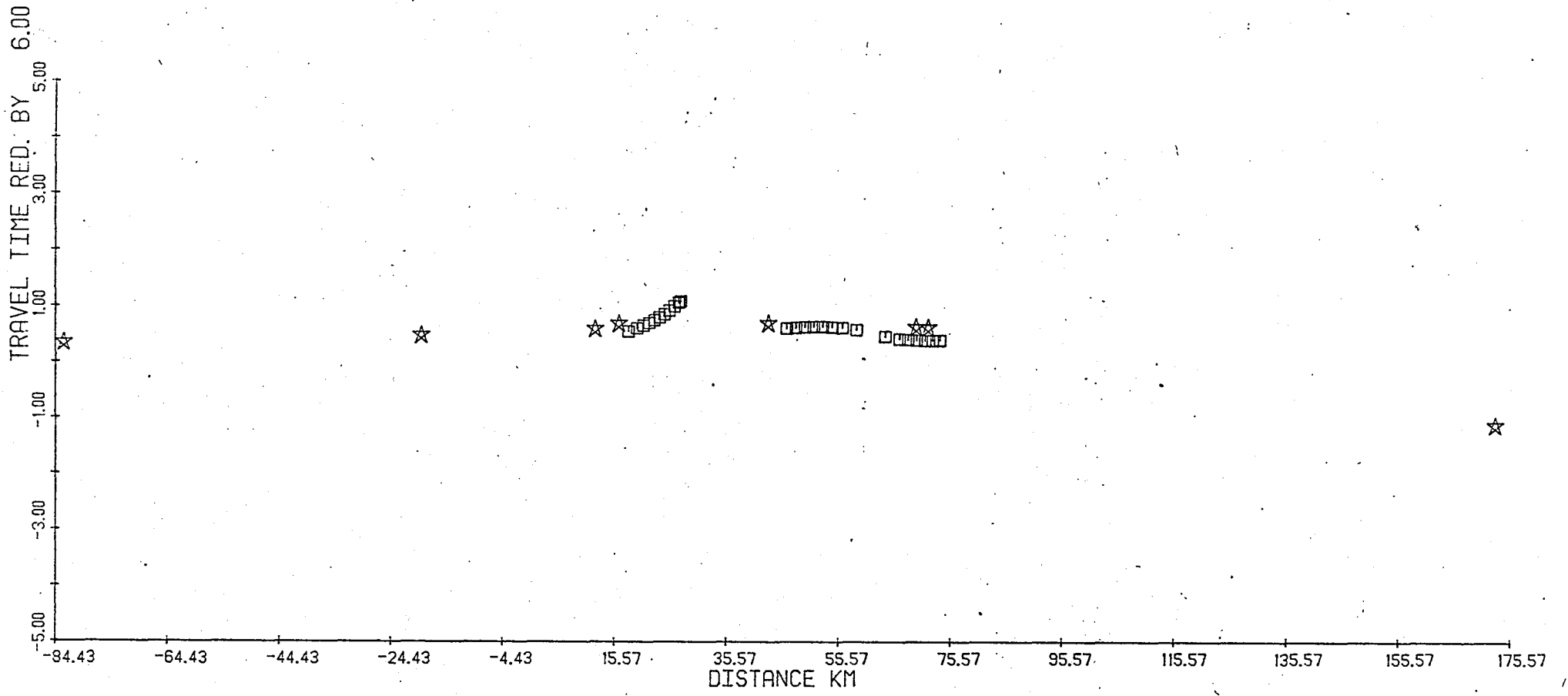
Fig.6.36: Ray traced diagram and reduced travel time section obtained from upper crustal model for shot 17.

Fig.6.35:   Ray   traced   diagram   and   reduced   travel   time   section
obtained from upper crustal model for shot 22.

Fig.6.34: Ray traced diagram and reduced travel time section obtained from upper crustal model for the South Jura station using all shots. Southern shots.

Fig.6.33: Ray traced diagram and reduced travel time section obtained from upper crustal model for the South Jura station using all shots. Northern shots.

RANGE (KM)

Fig.6.31:   Recalculated crustal depth section derived from time-terms taking account of the velocity structure derived from the minus time analysis and subsequent Wiechert inversion.

RANGE (KM)

Fig.6.32:   Upper crustal velocity model used in the application of the ray tracing method. The model shows modifications made to that derived using the minus times after ray tracing.

Fig.6.4:   Interpretation of the structure between Mull and Colonsay as obtained from airgun data. Reproduced from Attree (1982).

The apparent velocities along the line for the Colonsay station obtained from RAYSCAN are shown in Table 6.1, and from the output of the matched filter and picking by eye in Table 6.2. The low velocities near Colonsay are thought to represent Torridonian sediments dipping away from the station. The high velocities reflect a transition into the metasediments of the region. However, the low velocities at the far end are poorly determined and are not reliable. The geology of this area and relationship between units within the metasediments is complex. As only one unreversed line was obtained and the velocities can be seen to be scattered about values expected of many of the Islay an Jura quartzites, little can be quantitatively stated about the structure of the area.

6.3 Discussion on the Reduced Record Sections of the Explosive Shots.

The representative record sections of arrivals along the line are presented in Figs. 6.5 to 6.14. Sections are not available for the Kintyre stations for the first phase due to the reasons given in Chapter 2 on problems in the field. Most stations in 1979 had two recorders placed at the same site or close together to cover breakdowns. The sections presented represent the best data recorded at each particular island or peninsula .

All the sections produced are those constructed from data recorded on the Durham Mk.3 recorders or on Geostores as these could be digitized. Paper records were made of the South Jura and north Kintyre stations of the second phase that operated with the Glasgow cassette recorders. These could be picked quite adequately but due to saturation and gain of playback, the records did not always retain the shape of separate phases without clipping and were not made into reduced sections.
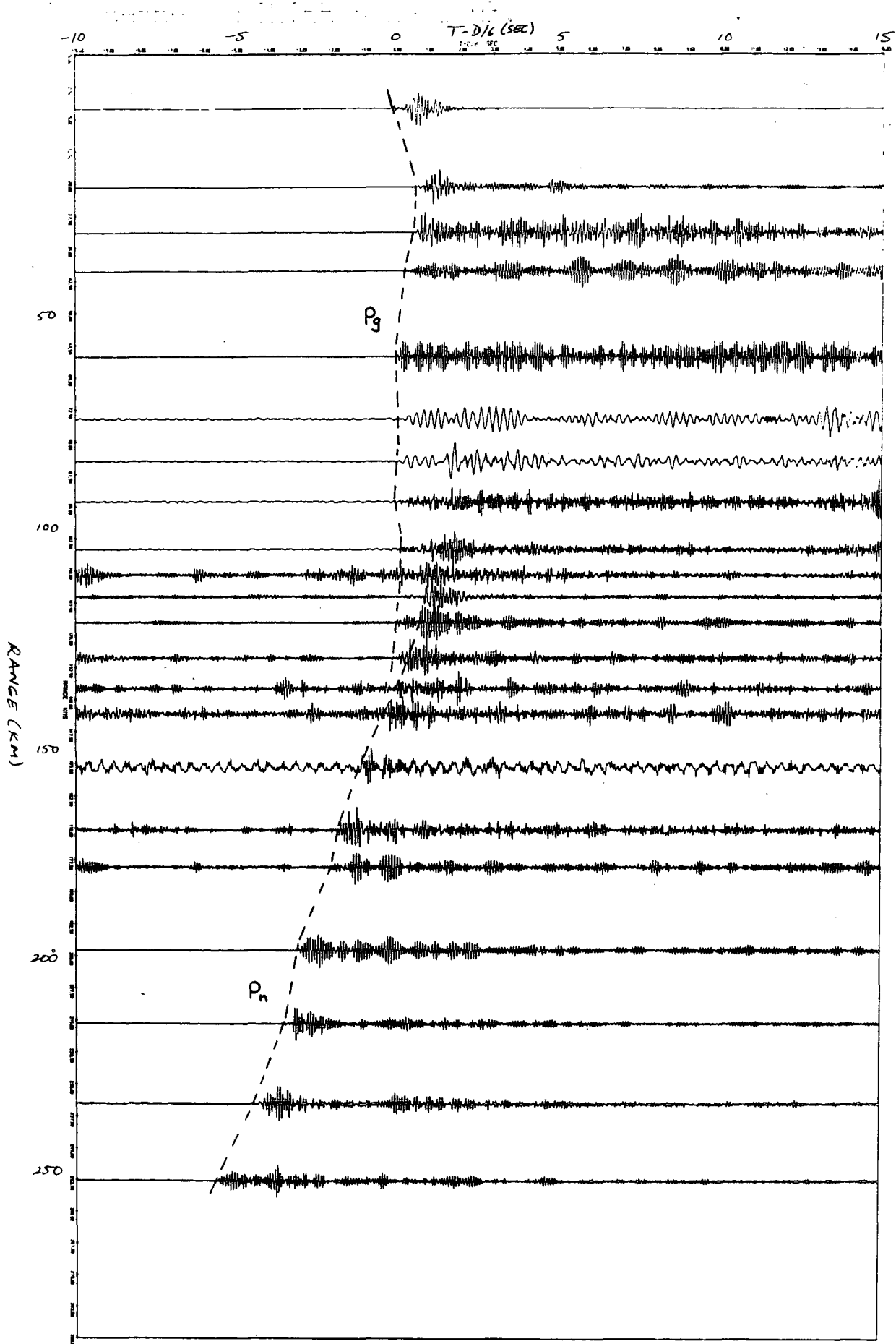
Fig.6.5: Reduced record section for Barra station.
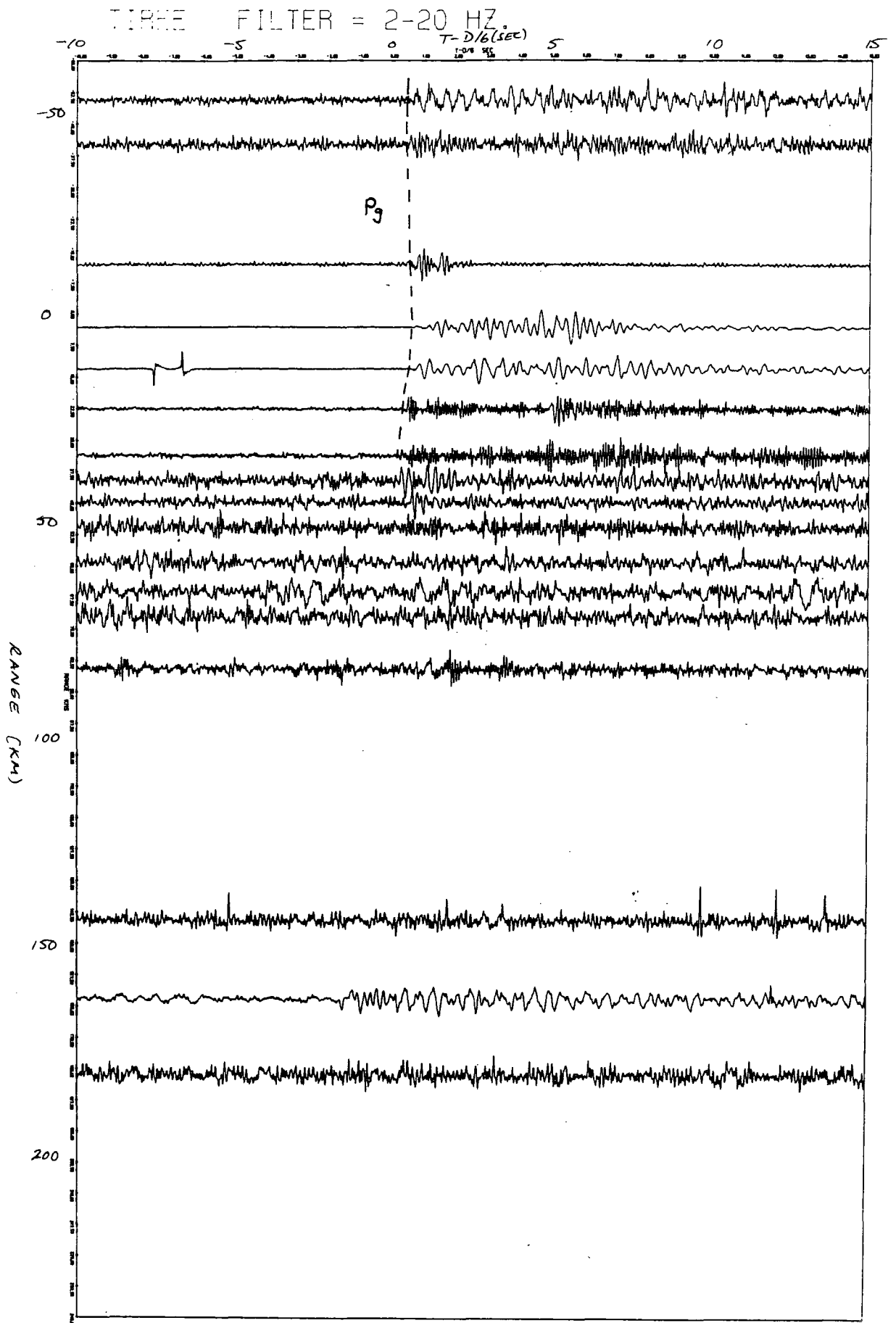
Fig.6.6:   Reduced record section for Tiree station (Ruaig).
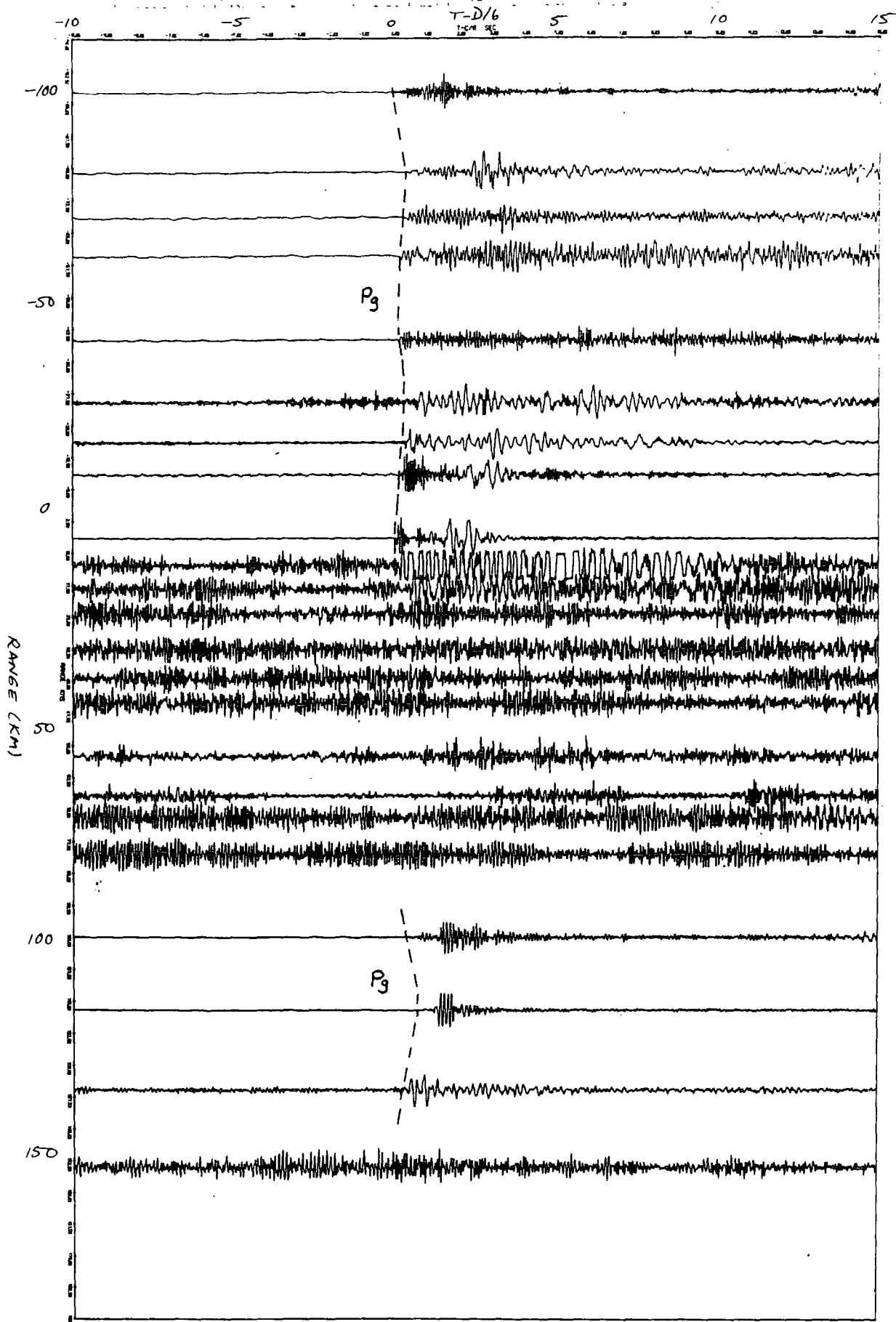
Fig.6.7:   Reduced record section for Mull Geostore station. Phase 1.

MID JURA   FILTER = 2-20 HZ.

T-D/6 (SEC)

-10   -5   0   5   10   15

P_n

-150

P_3

-100

-50

RANGE (KM)

0

P_g

50

100
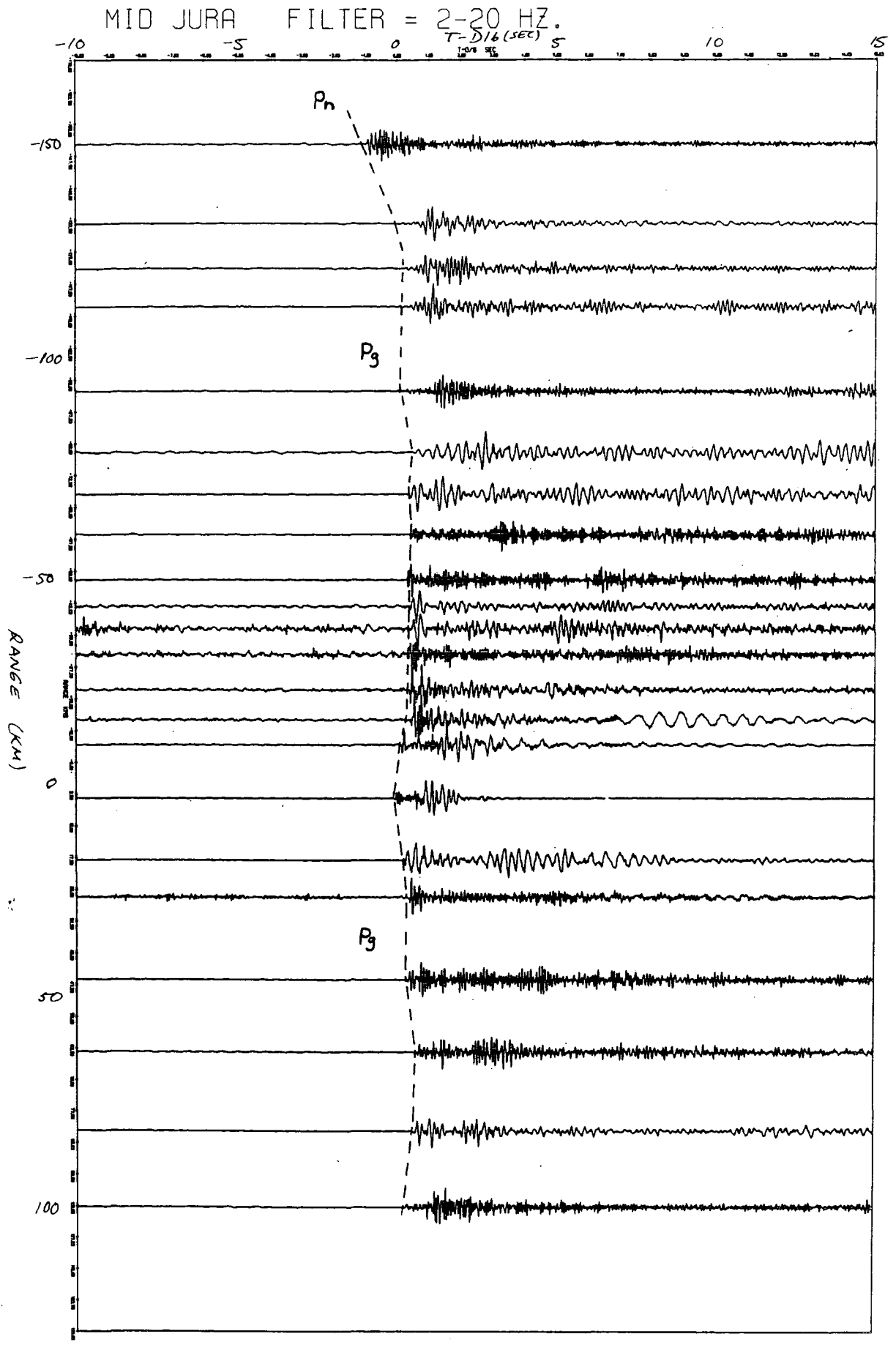
Fig.6.8:   Reduced record section for Mid Jura (2) station.
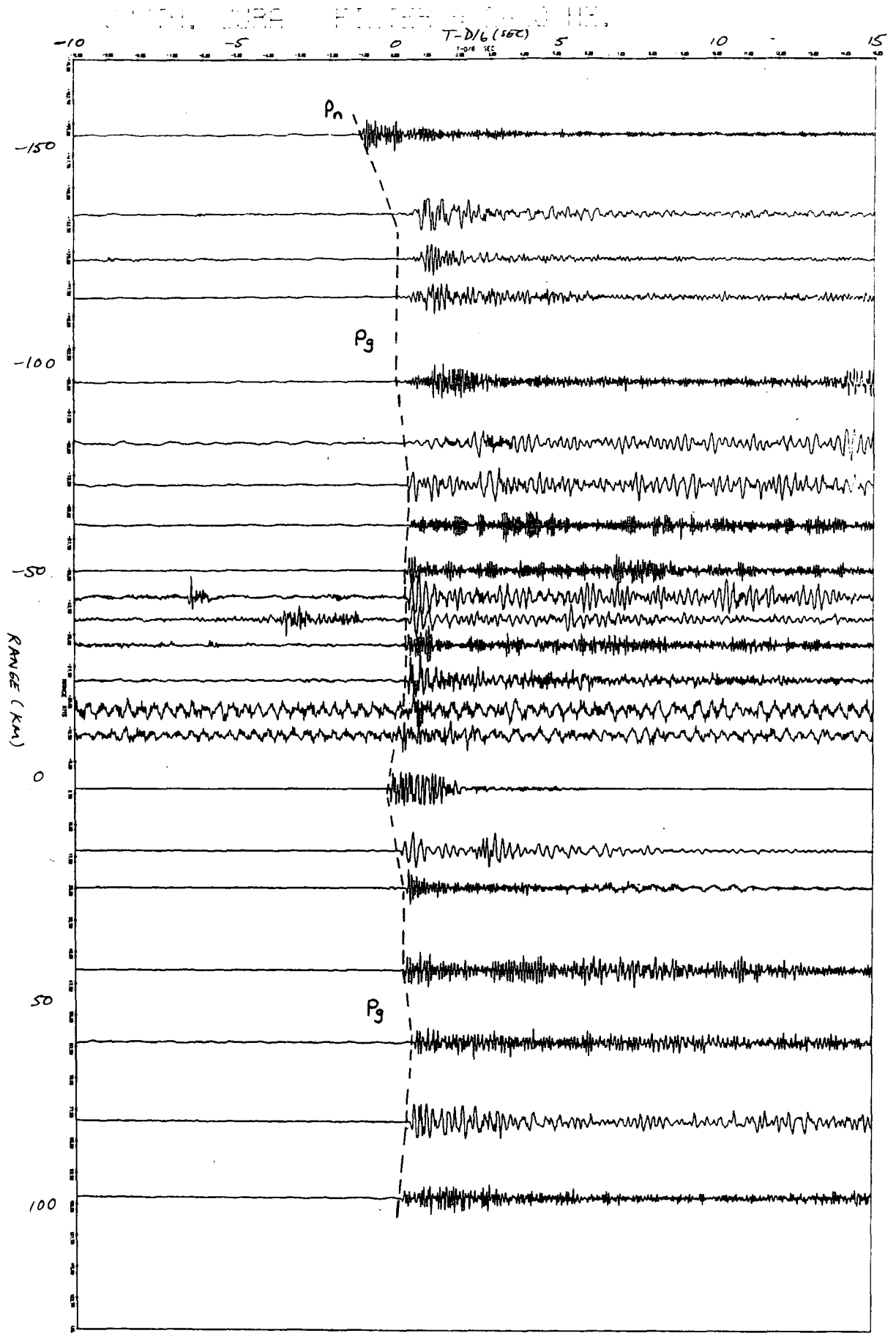
Fig.6.9:   Reduced record section for South Jura station. Phase 1
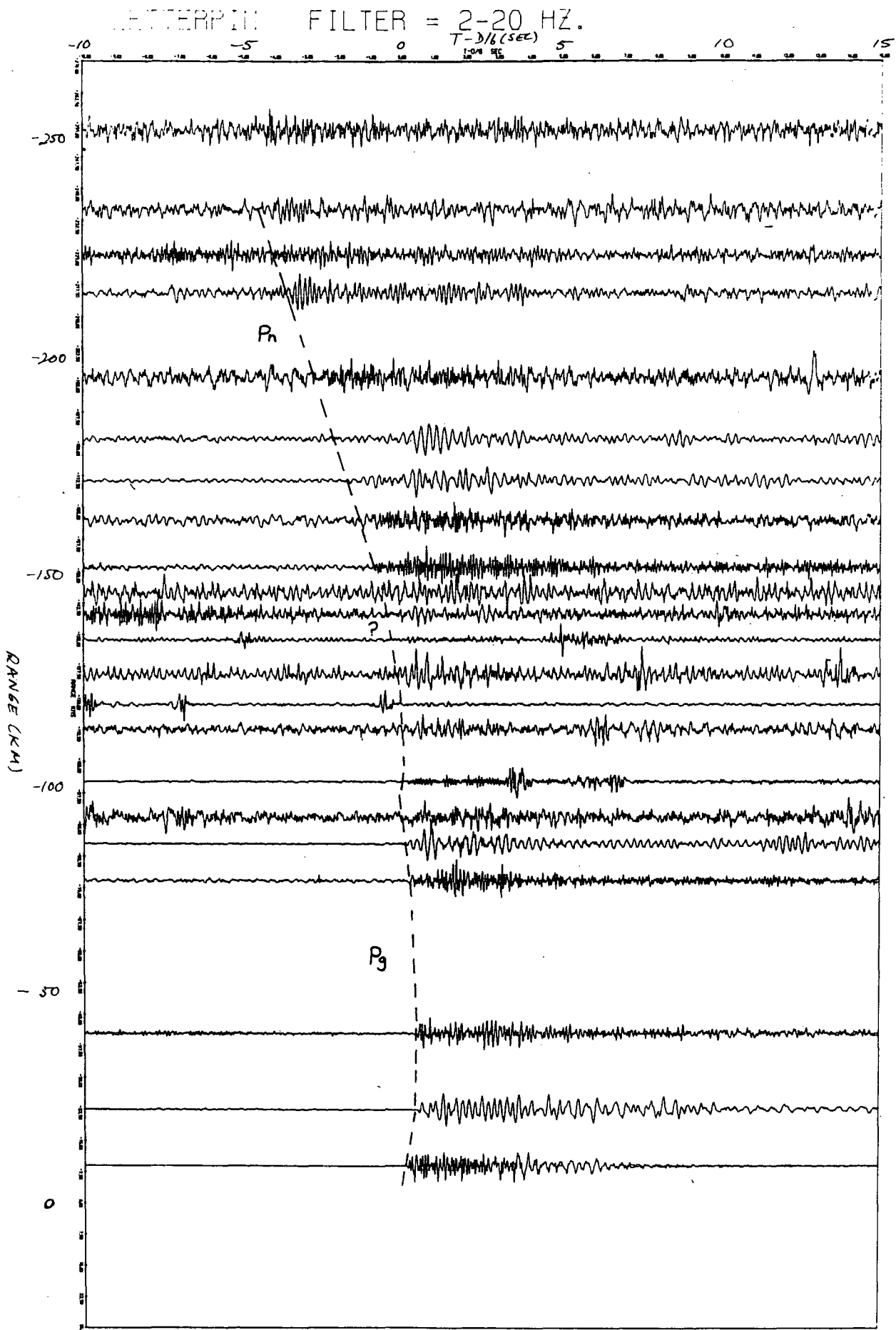
Fig.6.10:   Reduced   record   section   for   Letterpin   station   of   the
Girvan network.
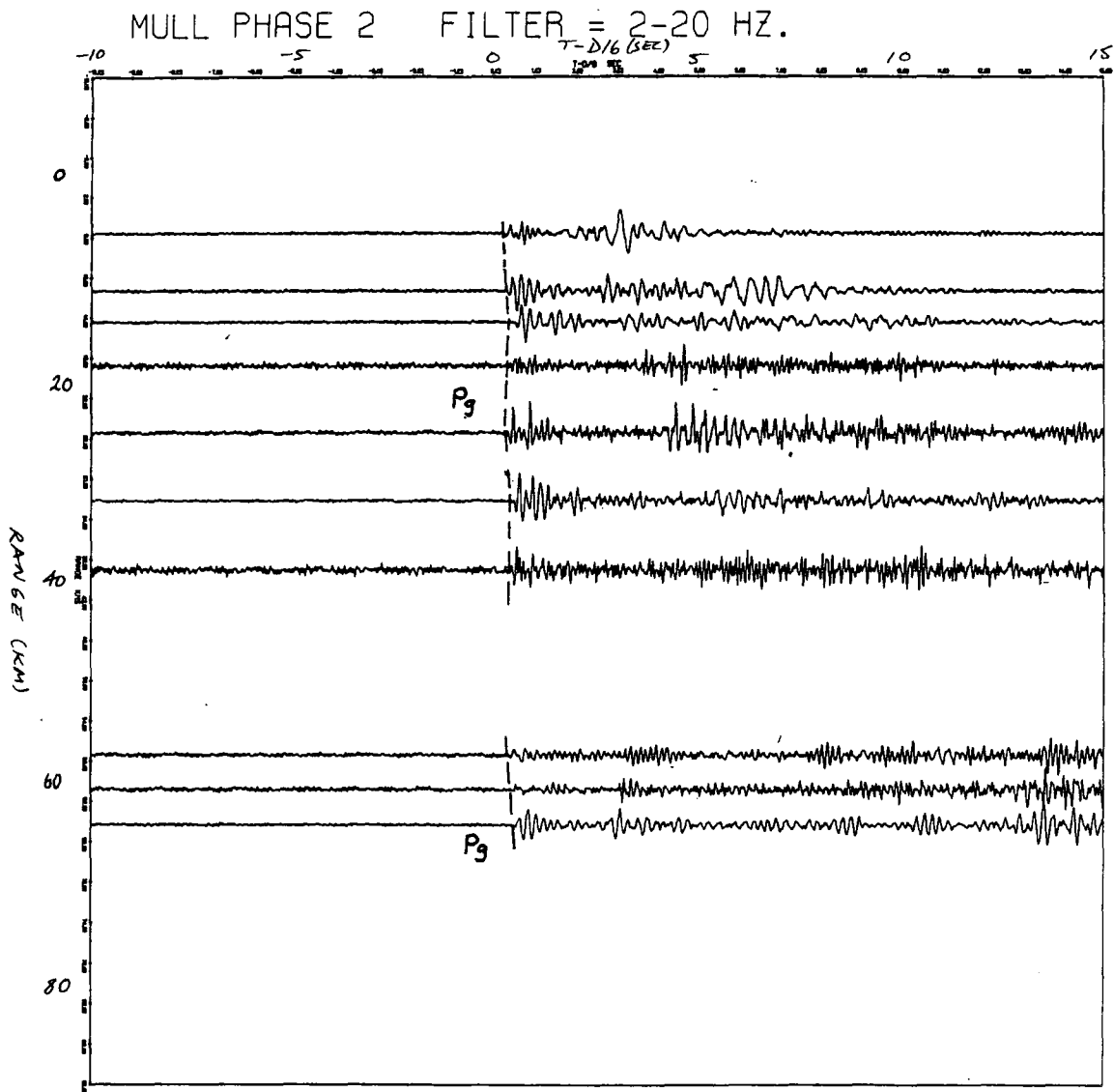
Fig.6.11:   Reduced record section for Mull station. Phase 2.

IONA PHASE 2 FILTER = 2-20 HZ.
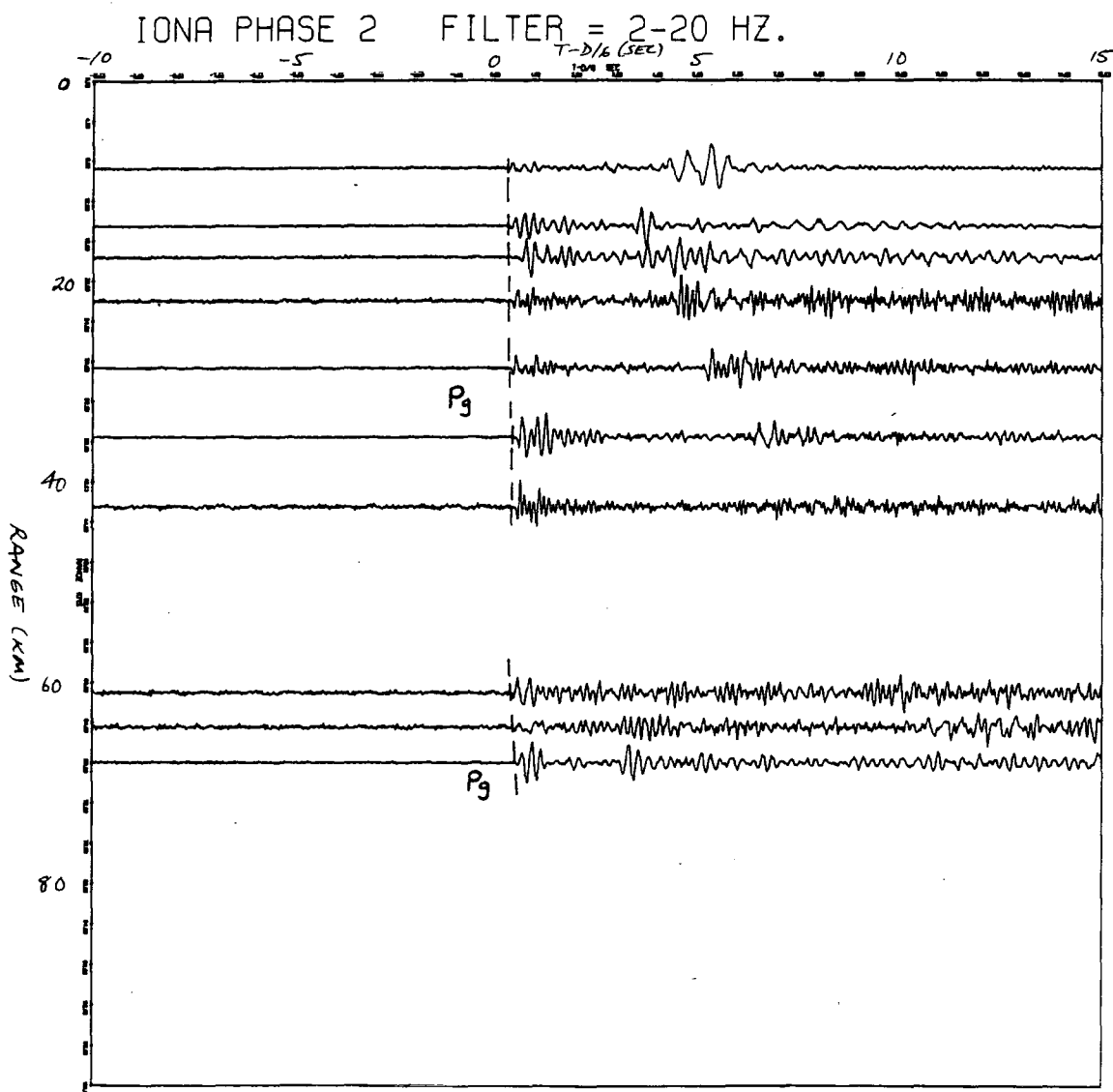
Fig.6.12:   Reduced record section for Iona station. Phase 2.
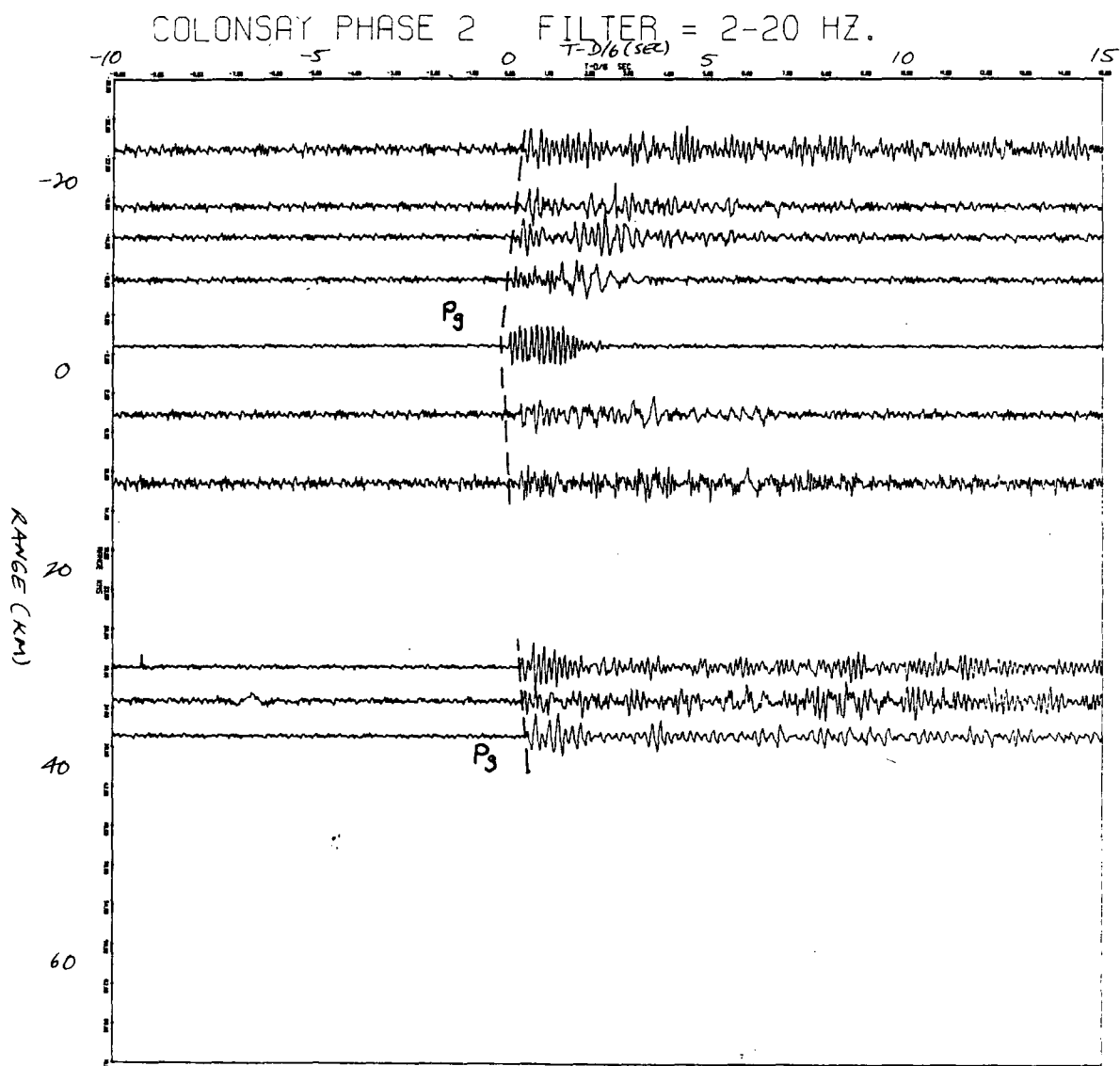
Fig.6.13:   Reduced record section for Colonsay station. Phase 2.
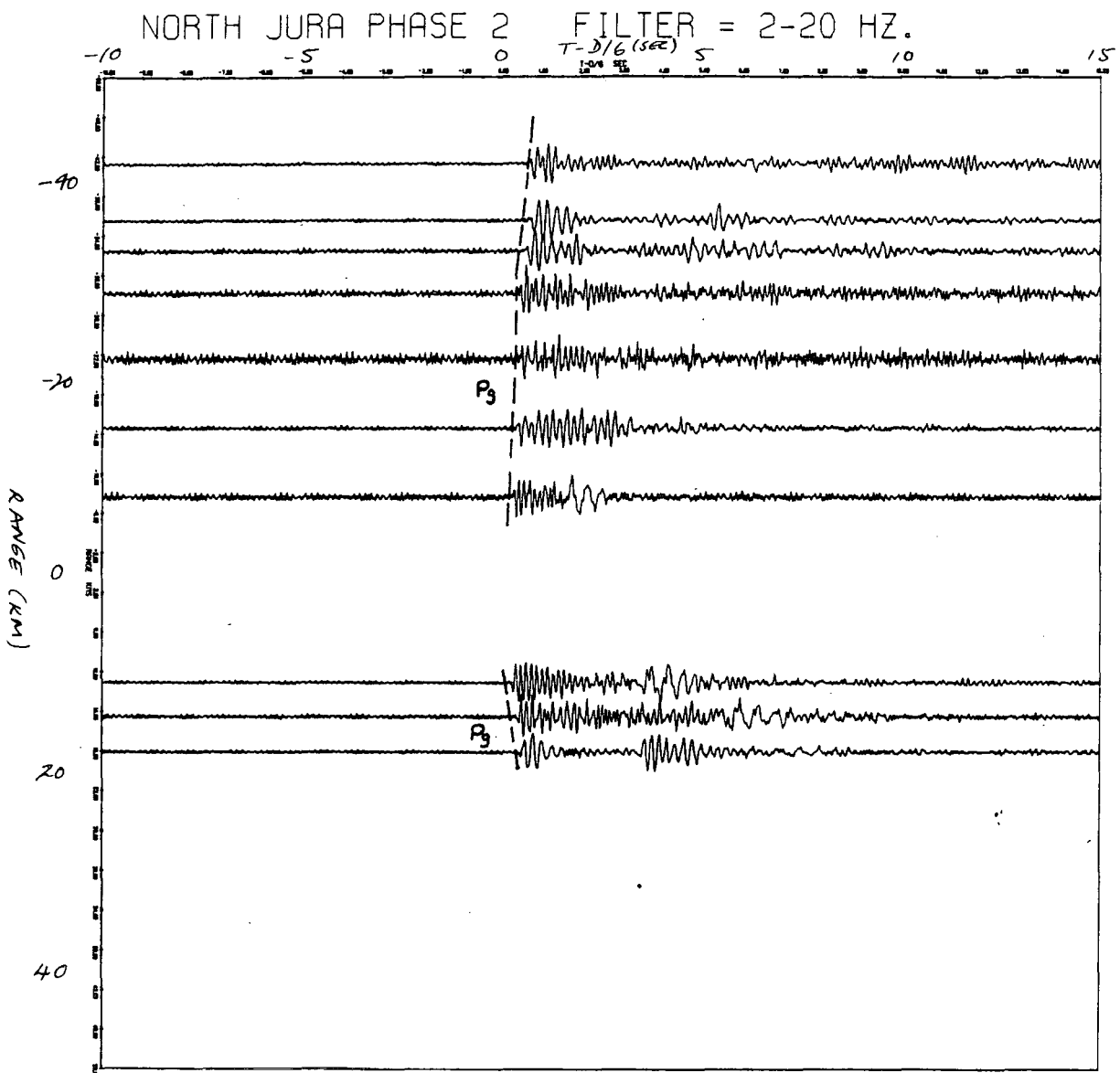
Fig.6.14:   Reduced record section for North Jura station. Phase 2

6.3.1 Prominent Arrivals on the Record Sections.

An examination of the records indicates two strong first arrivals. These have been identified as Pn and Pg phases. From the sections, the Pn Moho arrival shows a velocity of 7.98 +/- 0.05 km/sec and the Pg arrival, interpreted as a refraction from the basement, shows a velocity of 6.00 +/- 0.05 km/sec. The Pg phase is evident below ranges of 130 km and the Moho refraction is the first arrival beyond 150 km. The latter arrival is therefore restricted in number for the WISE profile. No intermediate crustal layer appears to be evident on the sections. An examination of the Barra section, which shows all arrivals along the line, should provide evidence of whether such an arrival was received. On this section (Fig. 6.5), the Pn phase can be traced at ranges greater than 153 km although it may crossover the Pg phase earlier than this, possibly as close as 137 km from the station. However, if a mid-crustal refractor were present, then it is between these ranges that it might be expected to be found. Unfortunately, the data quality along this part of the section is the poorest throughout the entire line and the first arrival cannot be adequately identified. The existence of a mid-crustal refractor is thus doubtful as subjective analyses could view the arrivals as being of the same velocity as those either side, or may be intermediate to the two. In addition, rather than the presence of a distinct interface, the possibility of a velocity gradient with depth cannot be ruled out.

More confidence might be made in proposing the existence of a mid crustal refractor after examination of the other sections. However, the station at the opposite end of the line, Letterpin, which provided the best data of the Girvan network, recorded very poor quality data in the section of the line of importance in discerning a mid-crustal refractor.

81

Bursts of energy can be seen at ranges greater than 110 km but confidence cannot be placed on the first arrivals in this area to make a decision on the possible structure. The Pn arrival can be traced through some of the traces of the section after 150 km with reasonable confidence though. The data at Tiree also provides little information only, in that confident identification can only be placed upon arrivals in the data within 60 km of the station. The data from the far shots both at this, the Ruaig station, and of the station at Vaul were very poor.

Examination of the Jura data shows a very well defined Pg arrival along the line but does not provide any clear evidence of a mid-crustal refractor. The data from these stations are of high quality and clearly show a significant relative decrease in travel time between shot 22 and shot 23 at a range of 152 km, thought to be the Moho arrival. No significant change is apparent between shot 20 and shot 22 where the range is such that a mid-crustal layer may become apparent. However, these shots were fired in the South Minch Basin and as such, have large sedimentary delays associated with them which may have the effect of masking another refracted phase, especially if its velocity is close to 6.0 km/sec.

The Pg arrivals are very uniform over all of the sections with delays where expected over the basins, due to the effect of the slower velocity sediments. Over most of the line this phase indicates a basement velocity close to 6.0 km/sec. On the records of the second phase of the experiment however, where shot separation was smaller, velocities less than 6.0 km/sec are evident near Colonsay, Jura and Kintyre. These can be interpreted in a number of different ways. They may either be refractions off an interface other than the basement close to the bottom of the basins, refractions off weathered basement, or they might reflect dip on the

82

basement itself. In the area where such arrivals are seen, high velocity Moine and Dalradian metasediments lie above the basement and these might give rise to such apparent velocities on the record sections. However, Hall (1978a) provides a measure of the velocity of the Lewisian and a value of apparent velocity between 5.5 and 5.8 km/sec lies within the bounds of Lewisian gneiss. To establish whether significant dip exists on the refractor, more detailed interpretation was required, the results of which are presented in the later sections.

Significantly absent from the records are wide angle reflections. Some of the data are very reverberant and this may obscure later phases that might be present but even where the later arrivals can be identified no consistent trend of wide angle reflections can be identified. This is unusual as other studies of the shelf area of north Scotland, such as HMSP, have shown the existence of these phases. Wide-angle reflections are usually identified by their high energy, so it is difficult to explain such an absence from the data as the energy would need to be dissipated. The ringing of the seismometers, as seen on the data recorded on Geostores, makes the identification of later phases such as wide-angle reflections, difficult. It is thought that it may be caused by two factors. Possibly, the seismometers, obtained from the I.G.S. equipment pool, were badly damped, or secondly, the reverberant effect may be a characteristic of the shot itself. Support for this argument may come from a comparison of the shots across records which show that the ringing is similar at different stations for any one particular shot.

The S-waves are also obscured by the ringing although they can be identified on some of the sections from the second phase. The sections are however, produced from the vertical or in-line horizontal

83

seismometer, whereas the seismometer perpendicular to the line is preferable in identifying the shear waves.

The frequency components of different shots are also very variable as can be seen from an examination of shots 17, 18, 21 and 22 in comparison with other shots. These show remarkably lower frequencies than most other shots and the similarity is once more shown across records sections. Again this may be a characteristic of a particular shot with the possibility that the energy is affected by the geology at the shot-point. These shots were fired over the sedimentary basin areas and the low frequency domination may be the result of attenuation of the high frequencies by the sediments.

6.4 Travel-Time Graphs.

For each station along the line, travel time graphs were constructed when producing record sections to provide a quantitative estimate of the change in velocity along the line rather than just relate the slope of the arrivals to the reducing velocity. No corrections for the sedimentary delays were made initially and therefore, the velocities obtained were not a true estimate of the velocity of the particular refractor. However, by assuming that the delays between shot points did not vary too rapidly over the range of the shots, these first estimates of refractor velocity were used to give indications of the basement velocity over different areas. After time-term analysis was carried out, the travel times were corrected for the sedimentary delays found and a second set of least square velocities calculated (Section 6.5).

Table 6.3 provides a list of velocities found for each section along the line. Where the shots used to determine the velocity have not been indicated, all the available shots recorded at the station for the

84

Table 6.3

VELOCITIES FROM TRAVEL TIME GRAPHS

NO CORRECTION FOR SEDIMENTARY DELAYS

Station (Shots Used)	Velocity (km/sec) North	South
Barra (Pg)		6.07
Barra (Pn)		8.12 - 8.26
Tiree	5.72	6.10
Tiree (21, 22, 23)	6.56	
Mull (W1 + W2)	6.06	5.91
Iona (W1 + W2)	6.09	5.92
Colonsay (W2 only)	5.50	5.63
Colonsay (3, 2, 1)		5.23
N. Jura (W2 only)	5.66	5.09
M. Jura	6.08	5.89
M. Jura (8, 6, 5)		5.35
M. Jura (9, 10, 11, 12, 13)	5.88	
S. Jura	6.12	5.88
S. Jura (8, 6, 5)		5.32
Letterpin (Pg)	6.09	
Letterpin (Pn)	7.05	

section of the line have been incorporated. The general pattern from this first set of travel time graphs indicate, within certain error bounds that almost all the Pg arrvals show a velocity close to 6.0 km/sec. However, along the shorter lines, lower velocities, identified on the reduced sections, are found to be as low as 5.50 km/sec and when the close range shots are taken alone, velocities approaching 5.2 km/sec are found. An example of such is found south of Colonsay. As previously stated, these might be due to metasediments or weathered Lewisian or dip on the refractor. A combination of all three might also exist.

In no areas along the line are velocities of Torridonian, Mesozoic or Tertiary rocks seen from the explosive shot records. This indicates that the range of shots compared with the thickness of sediment cover is generally large and the first arrivals received at the station are head waves from the basement refractor.

Further discussion of the basement velocities is presented in the later sections where the sedimentary delays have been accounted for.

6.5 Time-Term Analysis of the Explosive Shots.

After the identification of first arrival phases, the travel times were used in a time-term analysis to determine the sedimentary delays beneath stations and a velocity for the refractor. Due to the absence of Moho arrivals on many of the records, resulting from the shot-station ranges and poor data, the data set had to be supplemented by data from other sources. As stated in Chapter 2, the permanent Scottish networks were used along with shots in the North Sea. In addition, the time-term determined for a station common to WISE and HMSP, time-terms for LOWNET determined by NASP and LISPB and the time-term at Eskdalemuir were used to

85

constrain the solution for the analysis of Pn arrivals. The Pg arrivals were greater in number and were examined without external constraints being intoduced into the inversion process. The Malin station was to be incorporated for this purpose but as the records could only be picked to an accuracy of 0.1 sec and the Pg time terms were expected to be of the order of 0.1 to 0.5 sec, the use of such data would have introduced significant error into the solution.

In addition, the method of time-term analysis, or more exactly, the inversion of the matrix in the solution, requires that at least one shot and station position must be coincident in order to provide a link between all shots and stations within the network. This situation did not exist for WISE but the problem was overcome by assigning the same time-term to a shot and station along the line. This procedure was carried out in areas where shots and stations were particularly close and the geology, and hence the time-term, could be reasonably expected to be the same, such as shot 23 and Barra, shot 19 and Tiree and shot 8 and Jura.

6.5.1 Pg Time-Term Analysis.

The analysis of the Pg arrivals was carried out in several different ways. Firstly, all the data identified on the section as being arrivals from the basement were used to find a solution assuming that the time-term beneath each site was constant and not dependent on the direction of the shot relative to the station. However, in areas where the structure rapidly changes over short distances, as is the case for the WISE profile, this manner of solving the time-term equations is rather unrealistic. The rays do not meet or leave the refractor directly beneath the station and therefore, the time term of a ray travelling in one direction may be significantly different from that of an arrival from the opposite direction

for any particular station. To account for this, the data set was reorganised, assigning a different time-term to the northerly travelling rays, for each site, to that of the southerly travelling rays.

Another consideration is that although the first solution involved using all the data thought to originate from the same velocity refractor, it is possible, due to increase in velocity with depth or lateral changes in basement velocity, that the Pg arrivals may have been refracted at different velocities. The data set was therefore split up into subsets depending on range to determine changes in least square velocity. This could only be done to a large extent on the data assuming no difference in time-terms with direction as the solution for the anisotropic case, that is, where the time-terms to the north and south of a station, are different, often failed to converge due to lack of constraint.

Table 6.4 and Fig. 6.15 give the time-terms for the Pg data set assuming isotropy in time-term. The validity of the solution is shown by the zero or near zero time-terms at basement outcrop and the high time-terms over the sedimentary basins. The least square velocity obtained for the solution was 6.01 km/sec which is realistic for the Lewisian basement. It is also consistent with velocities for the younger Pre-Cambrian rocks that might be producing the 6.0 km/sec arrival south of Colonsay.

Table 6.5 and Fig. 6.16 show the solution obtained for the anisotropic case. The solid line indicates those time-terms for rays north of each station and the broken line, those to the south. It is evident that the isotropic case is an average of this solution. The least square velocity obtained for this solution was 5.95 km/sec. The distribution of the time-terms is interesting when considering the known geology of the area. The consistently low time-terms to the south in the Minch and the

Table 6.4

Pg TIME-TERMS (ISOTROPIC SOLUTION)

Site	Time-Term	B-W St. Err	N
WISE-1 Shots			
1	0.20	0.02	10
2	0.56	0.02	9
3	0.59	0.01	9
4	0.16	0.05	8
5	0.32	0.02	6
6	0.28	0.01	10
S.Jura/8	0.11	0.02	32
9	0.26	0.07	3
10	0.34	0.11	2
11	0.21	0.11	4
12	0.37	0.01	3
13	0.43	0.05	3
14	0.51	0.01	2
15	0.16	0.07	6
16	0.20	0.13	3
17	0.32	0.05	7
18	0.52	0.06	5
Vaul/19	0.07	0.02	6
20	0.18	0.05	5
21	0.42	0.08	5
22	0.41	0.08	7
Barra/23	-0.03	0.04	14
WISE-2 Shots			
10	0.26	0.07	4
9	0.31	0.06	6
8	0.35	0.06	6
7	0.19	0.05	6
6	0.29	0.03	5
5	0.31	0.04	5
4	0.32	0.06	6
3	0.19	0.06	6
2	0.26	0.04	6
1	0.32	0.06	6
Ruaig	0.13	0.03	5
Mull	0.11	0.02	17
Iona	0 5	0.02	17
Colonsay	0.06	0.04	15
N. Jura	0.13	0.04	10
M. Jura	0.10	0.03	21
Kintyre	0.25	0.03	10
Cundry Mains	0.05	0.02	7
Knockbain	0.03	0.02	5
Currarie	0.05	0.03	5
Breaker Hill	-0.04	0.02	6
Bargain Hill	-0.08	0.03	5
Lendal Foot	0.00	0.04	6
Letterpin	0.05	0.02	6

Table 6.5

Pg TIME TERMS (ANISOTROPIC SOLUTION)

Site	Time-Term	B-W St.Error	N
WISE-1 Shots			
1N	-0.07	0.06	3
1S	0.31	0.02	7
2N	0.32	0.03	2
2S	0.66	0.01	7
3N	0.49	0.02	2
3S	0.60	0.01	7
4N	0.19	0.01	3
4S	0.07	0.02	5
5N	0.28	0.02	5
5S	0.21	0.00	1
6N	0.13	0.06	3
6S	0.23	0.01	7
S. Jura/8N	-0.07	0.02	20
S. Jura/8S	0.07	0.02	12
9N	0.33	0.00	1
9S	0.39	0.02	2
10N	0.18	0.00	1
10S	0.64	0.00	1
11N	-0.04	0.08	2
11S	0.55	0.03	2
12N	0.30	0.00	1
12S	0.49	0.02	2
13N	0.44	0.00	1
13S	0.50	0.00	2
14S	0.62	0.04	2
15N	-0.01	0.01	4
15S	0.47	0.03	2
16N	-0.09	0.00	1
16S	0.32	0.02	2
17N	0.17	0.07	2
17S	0.39	0.07	5
18N	0.39	0.00	1
18S	0.57	0.08	4
Vaul/19S	0.06	0.03	6
20N	0.47	0.00	1
20S	0.07	0.02	4
21N	0.78	0.00	1
21S	0.27	0.03	4
22N	0.76	0.00	1
22S	0.26	0.07	6
Barra/23	-0.10	0.01	14
WISE-2 Shots			
10N	0.12	0.03	2
10S	0.44	0.07	2
9N	0.17	0.02	2
9S	0.44	0.08	4
8N	0.38	0.00	2
8S	0.40	0.07	4
7N	0.16	0.06	2
7S	0.28	0.07	4

Site	Time-Term	B-W St.Error	N
6N	0.17	0.01	2
6S	0.44	0.01	3
5N	0.30	0.01	2
5S	0.38	0.04	3
4N	0.24	0.05	3
4S	0.45	0.10	3
3N	0.10	0.05	5
3S	0.39	0.00	1
2N	0.18	0.02	5
2S	0.36	0.00	1
1N	0.26	0.03	5
1S	0.28	0.00	1
Ruaig	0.21	0.03	5
Mull - N.	0.02	0.04	6
Mull - S.	0.14	0.01	11
Iona - S.	0.14	0.02	17
Colonsay - N.	-0.08	0.09	6
Colonsay - S.	0.09	0.02	9
N. Jura - N.	-0.03	0.04	7
N. Jura - S.	0.15	0.02	3
M. Jura - N.	-0.13	0.02	14 .
M. Jura - S.	0.14	0.02	7
Kintyre	0.05	0.02	10
Cundry Mains	-0.07	0.01	7
Knockbain	-0.10	0.02	5
Currarie	-0.06	0.03	5
Breaker Hill	-0.10	0.01	6
Bargain Hill	-0.15	0.02	5
Lendal Foot	-0.10	0.02	6
Letterpin	-0.08	0.01	6

high time-terms for rays to the north might be indicative of the dip of the basement in that area, indicating a slope to the north. A discrepancy arises here however, in that the opposite occurs for the Inner Hebrides Basin whereas the same dip is expected. The significant differences in time-term either side of the stations near major fault zones are thought to reflect the differing rock types either side of the fault plane. The low time-term north of Mull is complemented by a high one south of the station. It is suggested that this reflects the higher velocity Lewisian to the north compared to the Moinian metasediments south of the station. The pattern of the time-terms betweem Mull and Jura and their significant variation over small distances are indicative of the complex structure of the different units in the region.

Unfortunately, the distribution and coverage of the line did not provide enough data for smaller sections of the line to be considered separately. As such, the least square velocity for all the arrivals is an estimate of the average crustal velocity over the region. Therefore, in areas where the true velocity may differ from the least square velocity, the time-terms at those particular stations might be higher or lower than shown. An example of this may be seen for shot 11. The time-term to the north for this shot is quite low relative to those of the surrounding stations. This may be due to the fact that only the Barra station was used to determine the time-term. Therefore, the rays probably travel lower in the crust with a velocity greater than 6.0 km/sec, which would subsequently increase the time-term and make it more agreeable with the surrounding values. Adjustment might also be necesary for time-terms determined using the data from the second phase whose rays, after examination of travel time graphs, have probably travelled at a velocity less than 6.0 km/sec and thus

should be lower than shown.

An estimate of this dependence of velocity on range was made by plotting the residuals from the isotropic solution against the ranges of the shots (Fig 6.17). This was then treated as a reduced travel time plot, positive slopes indicating a velocity below the least square velocity of 6.01 km/sec and negative slopes, a velocity greater than this velocity. It is evident therefore, that a lower velocity refractor exists at ranges less than 20 km and higher velocities at ranges greater than 110 km. These velocities were found to be 5.45 km/sec and 6.40 km/sec repectively. By treating the higher velocity as an interface an estimate of 9 km depth was determined. This is comparable to the velocity/depth model derived by Bamford et al. (1978) for the northern part of the LISPB line. The data set was reduced to include only those arrivals within this range limit and the time-term solution recalculated. There was not much alteration in the time-term values and the least squares velocity was increased to 6.08 km/sec. In addition, other solutions were determined for different ranges limits in an attempt to delineate further velocity variations. The results are shown in the velocity/range plots of Fig. 6.18 and 6.19.

From these relationships, it is noticed that a velocity dependence with range is introduced into the solution. When the upper range limit is extended at 10 km intervals from 70 to 100 km and the lower limit fixed at 10 km, the least squares velocity increases from 5.91 km/sec to 6.00 km/sec. The pattern is less well defined when the upper range is kept constant at 130 km and the lower one is varied. However a mean velocity of 6.15 +/- 0.05 km/sec is found for these ranges. When both upper and lower range limits are placed on the data the velocity is found to have an increasing trend when the lower limit is raised, as can be expected. The upper limits used were either 100 km or 110

89
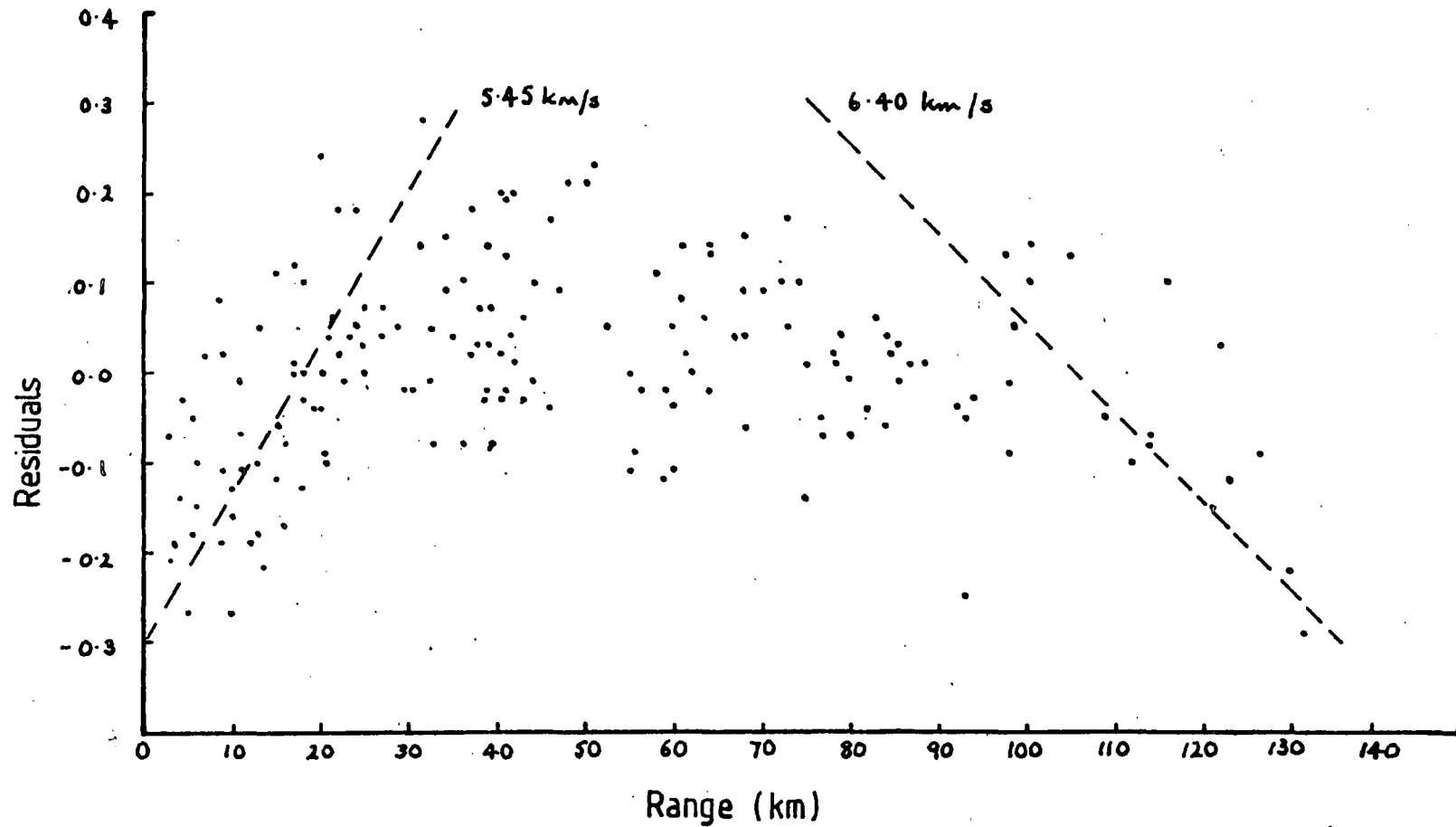
Fig.6.17:   Plot of the residuals of the time-term solution against range. Isotropic solution used.
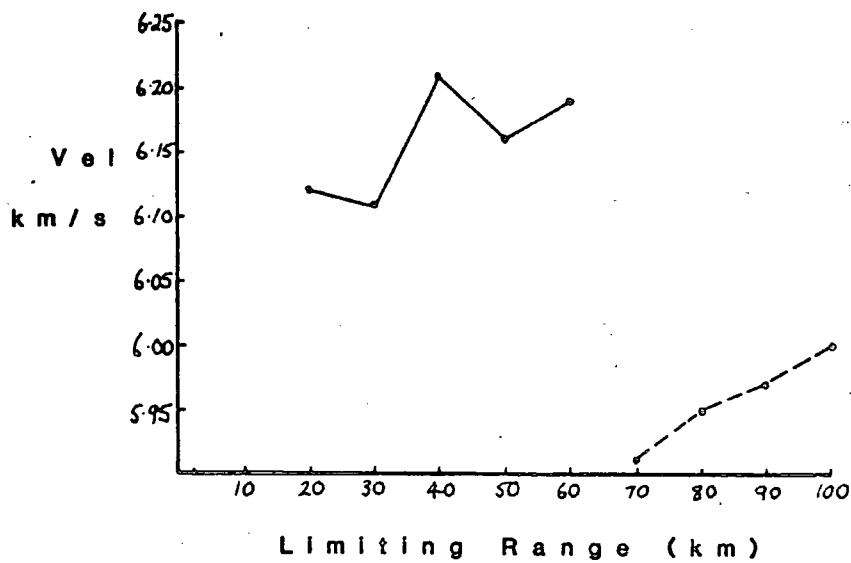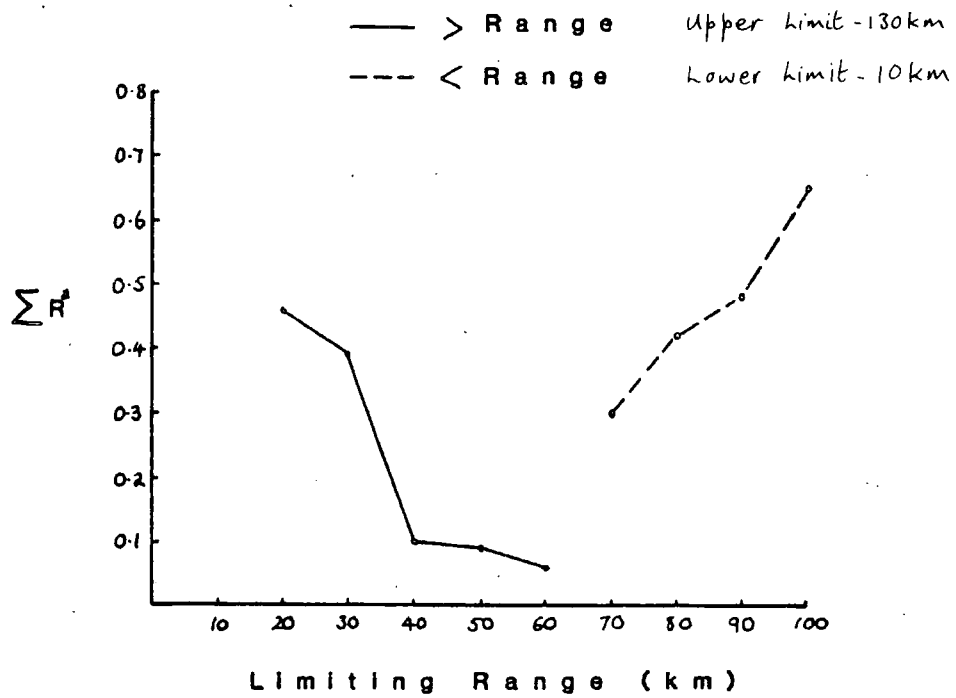
Fig.6.18:   Velocities   and   residuals   obtained   from   the   time-term
              solution when the uppermost range limit is decreased and the
              lowermost range limit is increased independently.
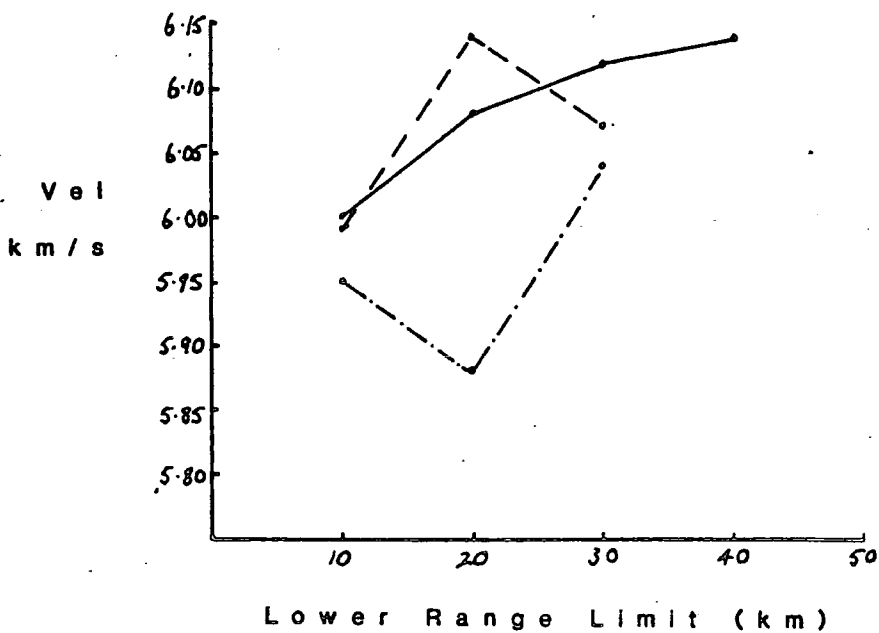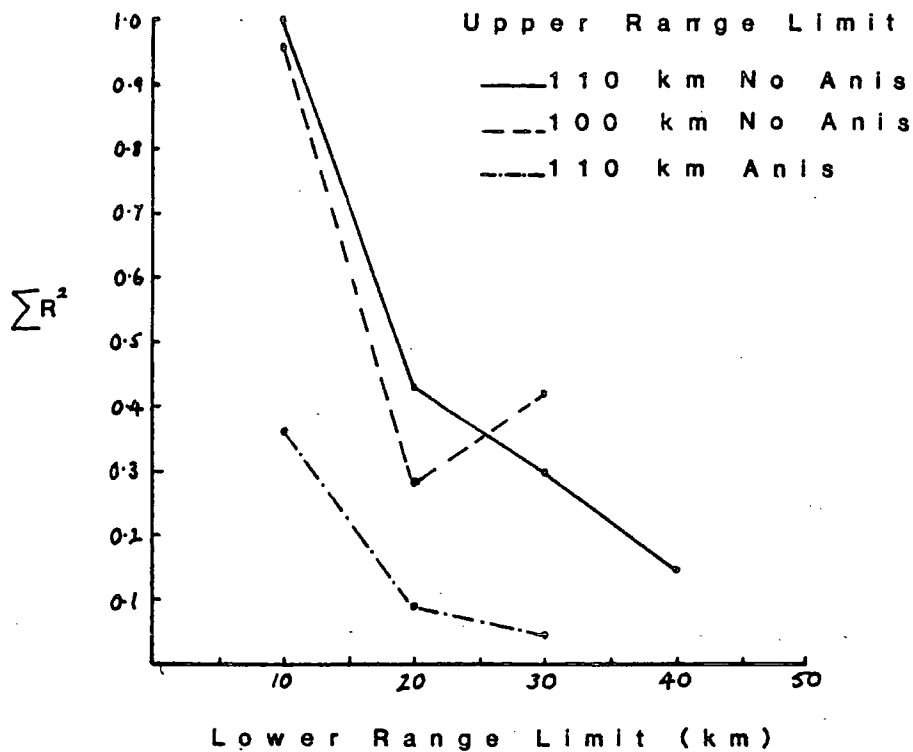
Fig.6.19: Velocities and residuals obtained from the time-term solution when the uppermost range limit is decreased and the lowermost range limit is increased simultaneously.

km. Further range limitations could not be placed upon the data as the solution failed to converge.

6.5.2 Pn Time-Term Analysis.

All the Pn arrivals that could be picked from the WISE stations and those of LOWNET and Eskdalmuir amounted to a data set of 47 travel times. Constraining this data set was carried out in different ways and comparison of results made. Smith (1974) determined time-terms for each of the LOWNET stations using the NASP data and using either all or only some of these as constraints, a solution was found. Also, the station near Fionnphort on Mull had been specifically reoccupied to tie in with the HMSP data, so the time term of 2.36 sec found by Armour (1977) was also used as a constraint on the solution. In addition, a detailed examination of Pn and Pg time-terms for the Eskdalemuir array has been carried out by Agger and Carpenter (1965) and the value of 3.10 sec they determined was used. Some estimate of the time-terms beneath the LOWNET stations is also provided by Bamford et al. (1978). Using combinations of these values, sensible constraints could be placed upon the data to ensure that a reliable solution was found.

It was found that the solution varied only slightly when different constraints were placed on the data set. The values of the Pn time-terms determined are given in Table 6.6 and are plotted beneath the their shot and station postitions in Fig. 6.20. The least square velocity obtained for the data was 7.98 km/sec. The solution is quite well constrained in that the time-term for Mull of 2.38 sec is close to that found by Armour (1977) and that the least square velocity is a good estimate of sub-Moho velocity. The analysis was also carried out using a

90

Table 6.6

MOHO TIME-TERMS

Site	Time-Term	B-W St. Err.	N
Shot 1	2.91	0.14	2
Shot 2	3.20	0.03	4
Shot 3	3.36	0.07	2
Shot 4	2.66	0.10	3
Shot 5	3.27	0.20	2
Shot 6	3.02	0.06	5
Shot 8	3.19	0.03	4
Shot 9	3.87	0.00	1
Shot 12	3.44	0.00	1
Shot 14	3.74	0.00	1
Shot 15	2.99	0.00	1
Shot 16	3.54	0.00	1
Shot 17	3.67	0.04	4
Shot 18	3.63	0.12	3
Shot 19	2.60	0.11	2
Shot 20	3.07	0.06	5
Shot 21	3.28	0.00	1
Shot 22	3.26	0.00	1
Barra/Shot 23	2.15	0.04	10
Ruaig	2.34	0.00	1
Mull	2.38	0.00	2
M. Jura	3.05	0.00	1
Letterpin	2.24	0.01	3

range of constrained velocities from 7.90 to 8.5 km/sec which changes the time terms accordingly.

The time-terms obtained from the WISE data reflect the known geology of the region when examined on a broad scale. High time-terms are found in the basin areas and low values in regions of high relief on the basement. These values however, have not been corrected for the delay time due to travel through the sedimentary layer and an accurate evaluation can only be obtained when used in conjunction with the analysis of the Pg time-terms.

6.5.3 Conversion to Depth.

The conversion of the time-terms to depth requires accurate measurement of the sedimentary velocities. As the airgun data did not provide much in the way of useful information on these velocities their results could only be used to a limited extent. The apparent velocities close to the stations were used in conjunction with velocities determined by Smythe et al. (1972), Hall (1978b) and Binns et al. (1975) for different parts of the area. Therefore, even though the individual sedimentary layers within the basins could not be determined, an average velocity could be estimated for each basin and the time-terms converted to depth. The depth section to the basement was calculated (Fig. 6.21) and then corrections were made to the Moho time-terms caused by the sedimentary delays and an estimate of crustal thickness determined (Fig. 6.21). This model was determined using constant velocities for each layer and as such is only a crude approximation to the true structure. A velocity ranging between 3.8 and 4.0 km/sec was used for the sediments except in the area between Colonsay and Kintyre where a higher velocity was used to account for the Dalradian metasediments. The basement velocity was taken as 6.00 km/sec

which does not make allowances for increase in velocity with depth. The depth section to the Moho must be treated with care as the time-terms are unlikely to have originated vertically beneath the station but may be offset by 60 or 70 km. Adjustments cannot be easily made in this two dimensional framework as most of the time-terms were derived from the arrivals offset from the line.

This interpretation indicates a crust of average thickness of just over 30 km. It is clearly evident though that as significant variations in delay time exist, if the velocity is constant, they indicate large lateral changes in depth to the Moho. However, if velocity variations exist within the crust, the low time-terms beneath Mull, Tiree and Barra might be more easily explained.

The proposal of significant velocity contrast within the crust, although not shown up on the reduced sections but indicated from the examination of the time-terms residuals with range and proposed from the examination of the variation in delay to the Moho, is supported by the gravity and magnetic studies of Shaw (1978). To model the positive anomalies over the area without including large undulations on the Moho, it was necessary to include an interface between amphibolite and granulite facies which had significant topography (Figs. 6.22 and 6.23). These two rock types are proposed to have contrasting physical properties (Smith and Bott, 1975; Hall, 1978a) including different velocites.[*] Therefore, high velocity gradients might be expected where the interface has been modelled as having large relief. These occur beneath Mull, Tiree and Barra. However, as no discrete interface is apparent from the record sections, it is possible that a gradational change occurs.

The interpretation of the depths to the Lewisian basement is

[*] Smith and Bott (1975) quote a value of 6.10 ± 0.15 km/s for amphibolite facies and 6.48 ± 0.06 km/s for granulites. Hall (1978a) quotes similar values in the velocity distribution determined by LUST of 6.0 – 6.10 km/s for amphibolite facies and 6.40 – 6.50 km/s for granulite facies.
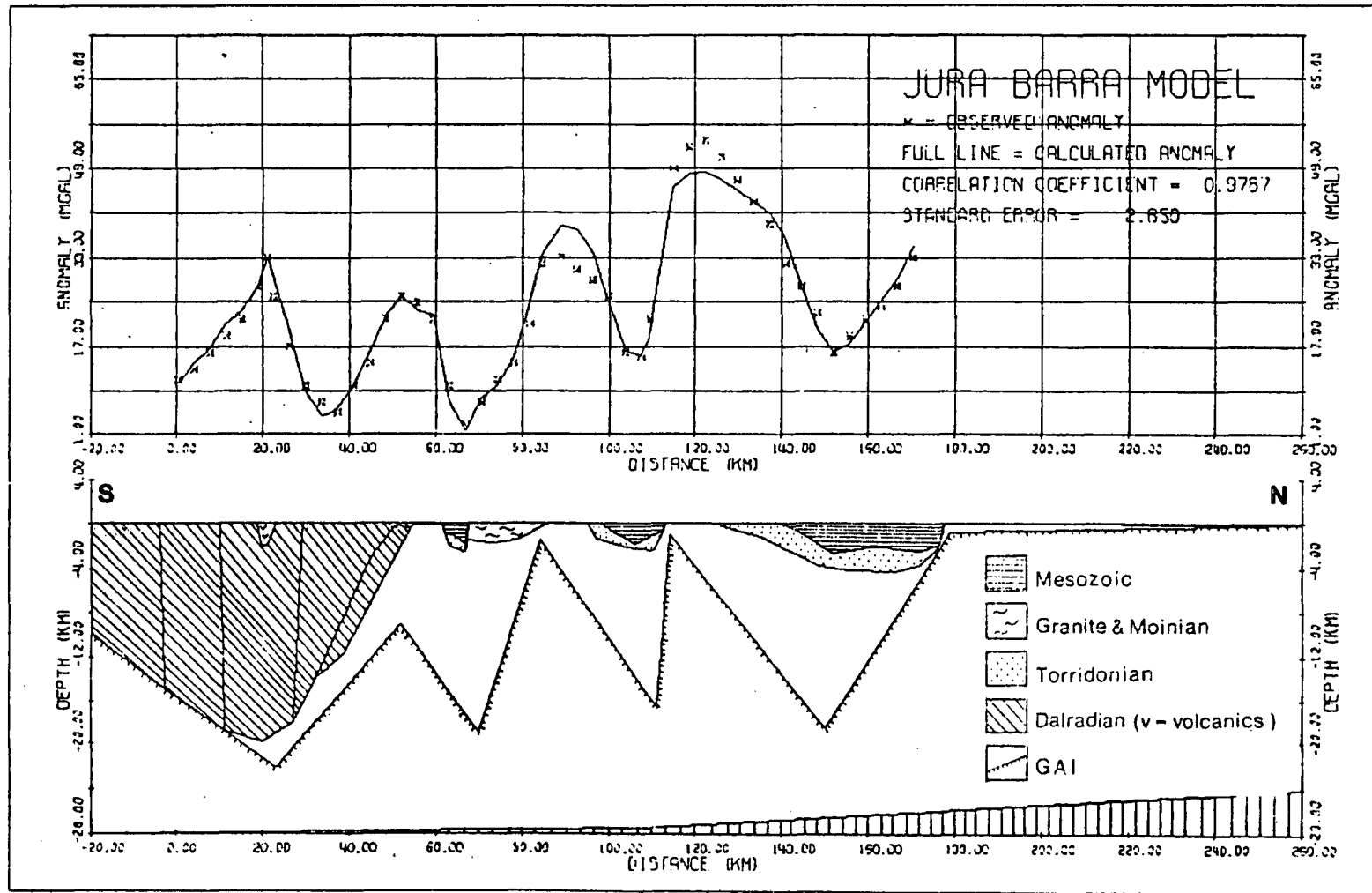
Fig.6.22:   Interpretation   of   gravity   anomalies   between   Jura   and
Barra as determined by Shaw (1978).
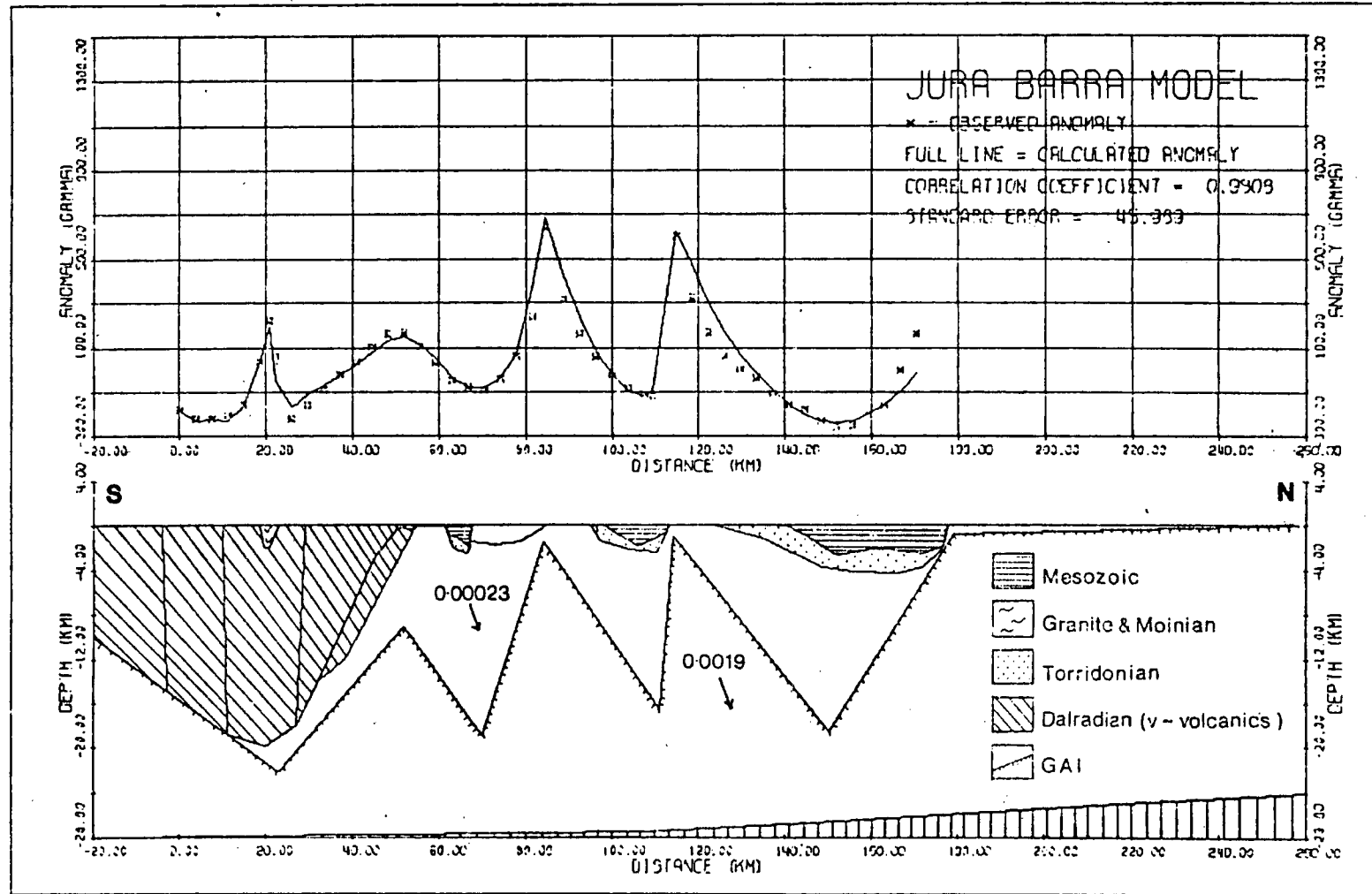
Fig.6.23: Interpretation of magnetic anomalies between Jura and Barra as determined by Shaw (1978).

also tenuous especially in the absence of accurate velocity information. Velocities from previously published work are generally broad estimates of the basins as a whole (Smythe & Kenolty, 1973; Binns et al., 1975). Those of the reflection lines shot in the area by I.G.S. are inadequate in that the stacking velocities have been determined from the multiples and not the primaries. Therefore, if the true velocities differ from those used, the topography of the basement will be changed. If the basins contain thicker sequences of Torridonian than accounted for, then their depths are going to be greater than shown and the opposite case is true for if the Mesozoic rocks are greater in thickness. From the section the Inner Hebrides Basin appears to comparable in thickness to the South Minch Basin, but if there were relative differences between thickness of rock type in the two basins shallowing of one might occur. In addition, the basins further south must be viewed with care in that the average velocities used are unlikely to truly reflect the rock type in these areas. The geology in the region is complex and without accurate knowledge of the extent of the metasediments compared to the younger sediments, the depth estimates may be incorrect.

An important consideration that must be placed on the depth section to the Lewisian basement is that it has been derived using the isotropic solution and as such is an average of the depth along the line. It is not necessarily satisfactory to plot the time-terms and resulting depths beneath the station and shot points as the rays would not have not originated from these points. However, in view of the lack of velocity information and accurate mapping of the sedimentary layers the origin of the ray paths are difficult to determine, especially in a region with large lateral variations over small distances due to major fault planes. In such a situation detailed mapping of the basement shape can only be carried out

93

with high quality, closely spaced data.

The travel time graphs that were originally constructed were only used to give first estimates of the velocities in different regions for identification of phases. Using the sedimentary delays determined from the time-term solution, the travel times were corrected and estimates of lateral variations in the basement along the line were made. The results of the changes in least square velocity made to the original data is presented in Table 6.7. The velocities show an increase in velocity in the basement from the south to the north of the line. This maybe a factor of the larger shot separation used for the first phase indicating higher velocities at depth. It may however, show that the refractor south of Colonsay is not Lewisian, but younger metasediments.

6.6 Minus-Time Analysis.

A summary of results obtained from using the method of Armour (1977) is presented in Table 6.8. All arrival times available between the quoted station pair were used and reducing velocities between 5.00 km/sec and 6.40 km/sec were applied in increments of 0.05 km/sec. The best reducing velocity is shown for each station pair along with the sum of residuals squared obtained with this velocity. Fig. 6.24 is a plot of the velocity and residuals against range. Apart from some exceptions, such as the Rualg/Iona pair and Barra/Colonsay, the pattern clearly indicates an increase in velocity with range suggesting such a situation with depth. The departures from this pattern might best be explained by inaccurate picking of the data, especially for the latter pair which shows large residuals between observed and calculated. The Rualg/Iona pair may reflect higher velocity basement in the region as compared with the velocities found for

94

Table 6.7

VELOCITIES FROM TRAVEL TIME GRAPHS

CORRECTED FOR SEDIMENTARY DELAYS

	(Velocity (km/sec))	
Station (Shots Used)	North	South.
Barra		6.12
Tiree	6.65	5.70
Mull (W1 + W2)	6.03	5.90
Iona (W1 + W2)	6.02	5.89
Colonsay (W2 only)	5.28	5.75
N. Jura (W2 only)	5.65	5.57
M. Jura	6.08	5.98
S. Jura (W1 + W2)	6.09	5.93
Kintyre (W2 only)	5.94	
Girvan Stns.		
Letterpin	5.90	
Cundry Mains	5.99	
Knockbain	6.03	
Currarie	6.03	
Breaker Hill	6.02	
Bargain Hill	6.05	
Lendal Foot	5.96	

Table 6.8

VELOCITIES OBTAINED FROM MINUS TIMES

No.	Station Pair	Range (km)	Velocity (km/s)	R^2
1	Barra/S.Jura	154.46	6.15	0.416
2	Barra/M.Jura	152.31	6.10	0.524
3	Barra/Colonsay	125.95	5.85	1.237
4	Barra/Mull	99.25	6.10	0.098
5	Barra/Iona	93.03	6.05	0.095
6	Barra/Tiree	63.92	5.85	0.013
7	Tiree/Iona	31.11	6.00	0.008
8	Iona/Kintyre	88.48	5.95	0.310
9	Iona/S.Jura	59.43	5.85	0.050
10	Iona/N.Jura	49.66	5.75	0.064
11	Iona/Colonsay	30.92	5.35	0.033
12	Mull/Kintyre	81.25	5.90	0.127
13	Mull/S.Jura	55.21	5.85	0.063
14	Mull/N.Jura	45.44	5.75	0.043
15	Mull/Colonsay	26.70	5.95	0.035
16	Colonsay/Kintyre	54.55	5.75	0.078
17	Colonsay/S.Jura	28.50	5.10	0.571
18	Colonsay/N.Jura	18.74	5.45	0.002
19	N.Jura/Kintyre	35.50	5.25	0.000
20	S.Jura/Kintyre	26.05	5.25	0.001
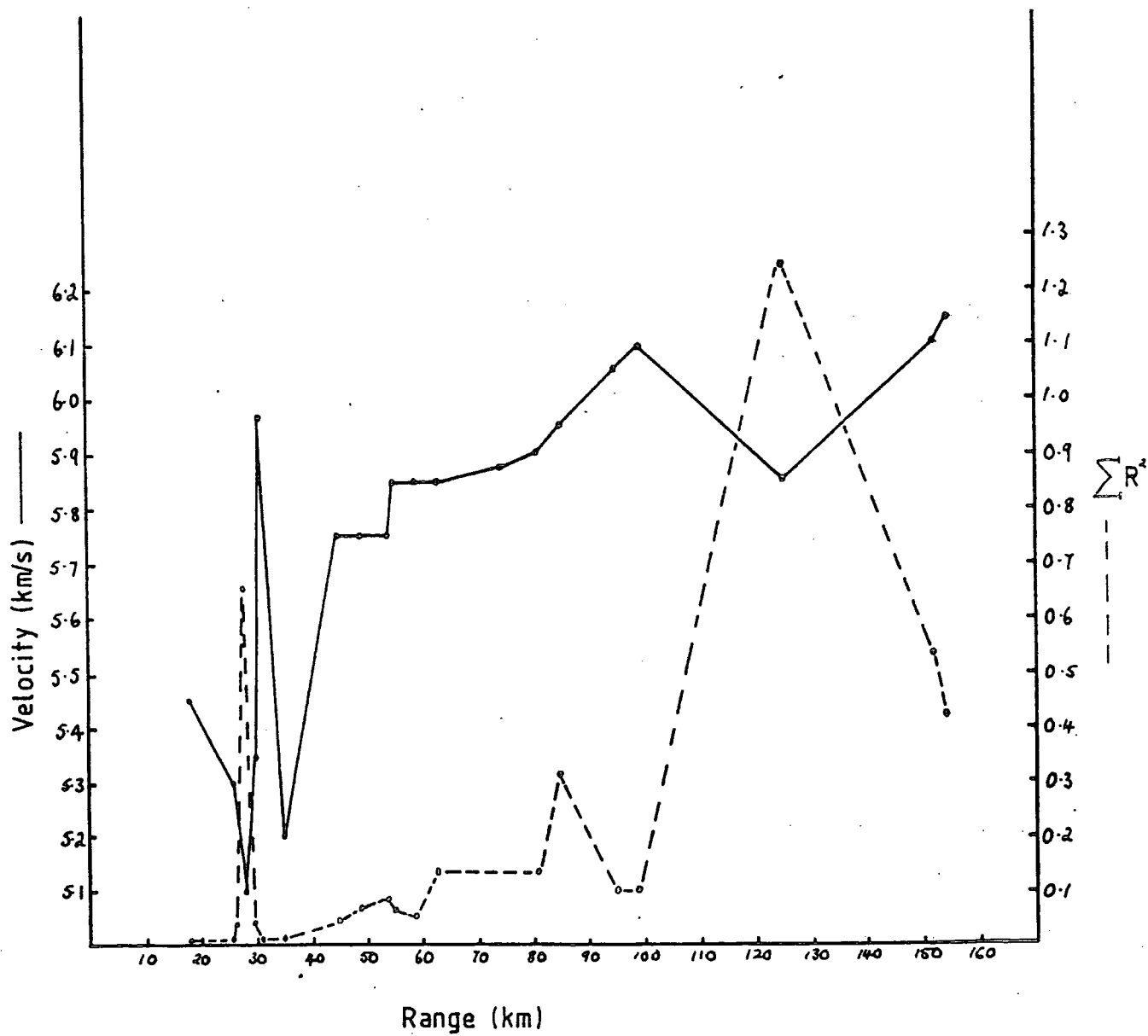
Fig.6.24:   Velocities   and   residuals   obtained   from   minus   time
analysis plotted against range. Method of Armour (1977).

the shorter ranges in the more southern areas. Fig. 6.25 shows the velocities found plotted at the mid points of the two stations concerned. They are coded according to the list in Table 6.8. This method of display gives a clearer indication of the lateral changes in velocity within the upper crust over the extent of the line.

The second method used for minus-time analysis was used in conjunction with the section shown in Fig. 6.25 to provide a more complete solution. For every station pair along the line, the velocity was found, using each pair of shots between the stations. The results of this are shown in Fig. 6.26 which is coded in the same manner as previously used. Allowing for some scatter of the points, which might be attributed to incorrect picking of arrivals, a trend can be identified. In the northern part of the line, high velocities are found, reaching 6.3 km/sec, this trend gradually falling off 10 km north of Colonsay where the velocity first has a scatter between 5.0 and 6.0 km/sec and then drops to 4.75 km/sec. Within 5 km of this point, the velocity once again is seen to increase sharply reaching an average of 6.5 km/sec. The underlying trend from this point to further south shows a gradual decline in velocity to an average of 5.5 km/sec in a region 15 km north of Kintyre. The velocity distribution shown in this analysis is a more detailed version of the trend shown in Fig. 6.25. The velocities determined between Mull and Colonsay are comparable with those of the airgun records, especially the low velocity region immediately south of the Great Glen Fault.

The velocities shown in Fig. 6.26, although having some scatter, do show increases with range from the station. Using selected shot pairs to define the velocity with range relationships along the line, velocity/distance curves were constructed, plotting the velocity against
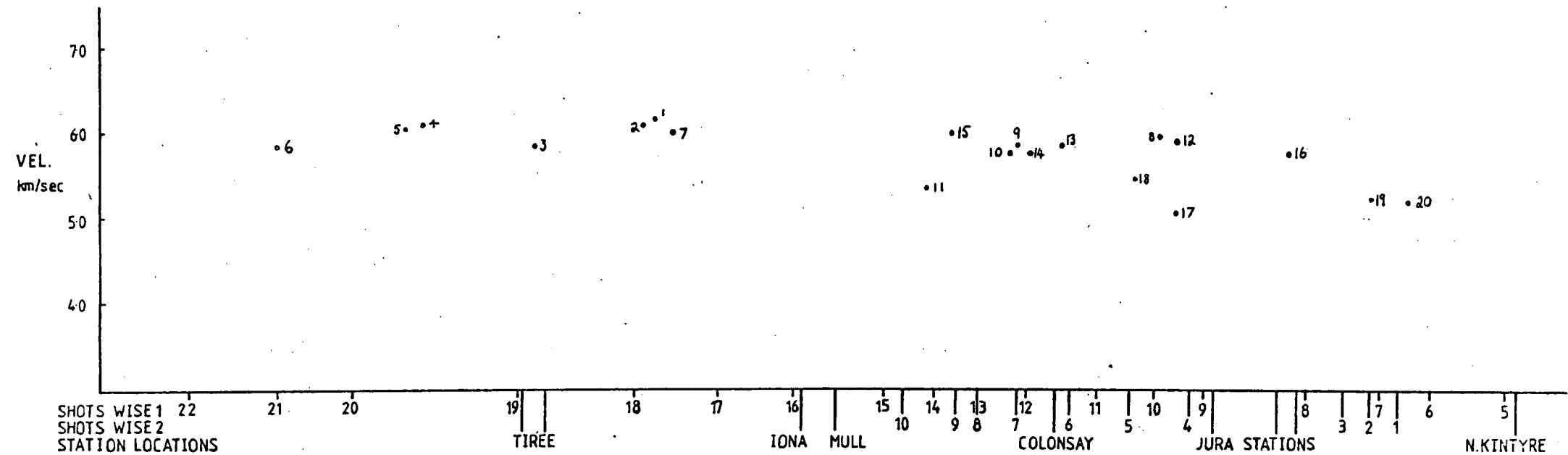
Fig.6.25:   Velocities   obtained   from   minus   time   analysis   plotted
at   the   mid-point   of   the   two   stations   concerned.
Method used described by Armour (1977).
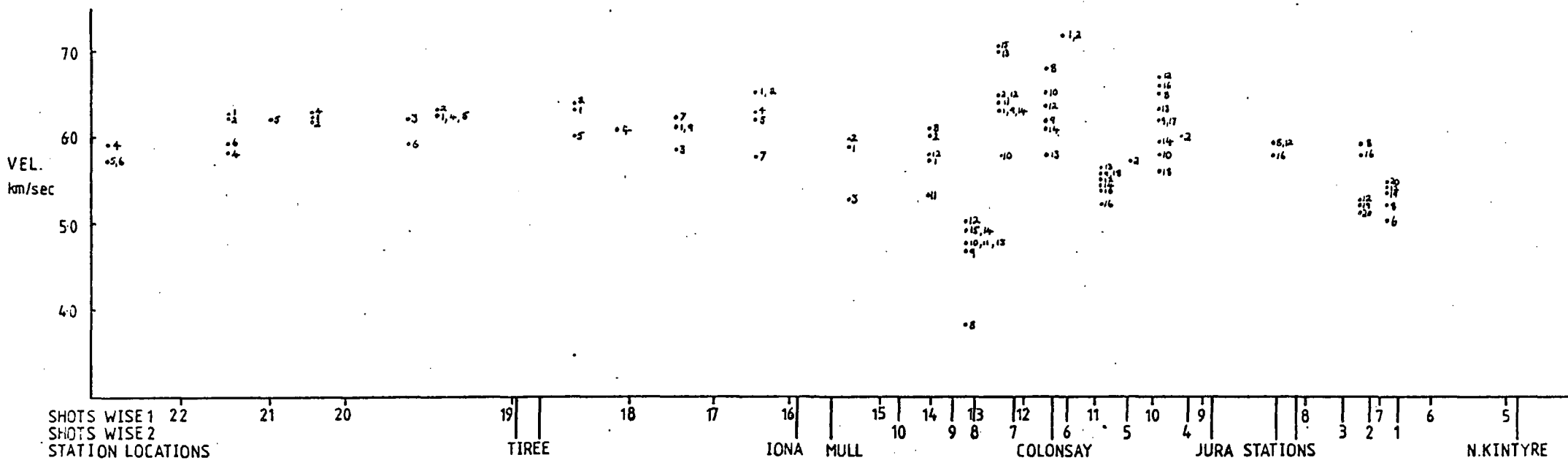
Fig.6.26: Velocities obtained from minus time analysis plotted at the mid-points of the two shots concerned. Station pairs coded as indicated in Table 6.8. Method used is described in Chapter 5.

the average of the ranges between the two shots to the two stations. Examples of these along the line are given in Figs. 6.27 and 6.28. The curves were then smoothed to give increasing velocities with range wherever thought valid. The resulting relationships were transformed into velocity/depth functions by applying Wiechert inversion.[*] The velocity/depth distributions found for different sections of the line from this process are shown in Figs. 6.29 and 6.30. As velocities at the surface had to be provided for inversion, three solutions were found for velocities of 3.0, 4.0 and 5.0 km/sec. The surface velocity of 5.0 km/sec is only likely between Colonsay and Kintyre where Pre-Cambrian metasediments are known to exist. As such, the velocity gradient for this region is likely to be at a shallower depth than indicated on the sections.

The resulting velocity variation within the crust displays interesting characteristics, especially when placed in the context of its effect of the time-term section to the Moho. Considering that the time-terms to the Moho are offset from the stations, possibly up to 50 km for a mean crustal velocity of 6.75 km/sec, the increase in velocity gradient beneath Mull and Jura might account for the low time-terms found beneath Tiree and Mull. The distribution shown however, must not be considered as a true picture of the velocities beneath the station positions. The velocity/distance curves had to be smoothed in order to obtain an increasing relationship with distance, thus introducing errors into the solution. In addition, to construct the model, averaging of the ranges had to be carried out, and therefore the resulting velocity distribution must be thought of as having a spatial property. This means that the high velocities found should be considered to lie over a region rather than vertically downward from the shot pair used. Features other than the high

96

* See Appendix 3, page 169 for note on Wiechert inversion.
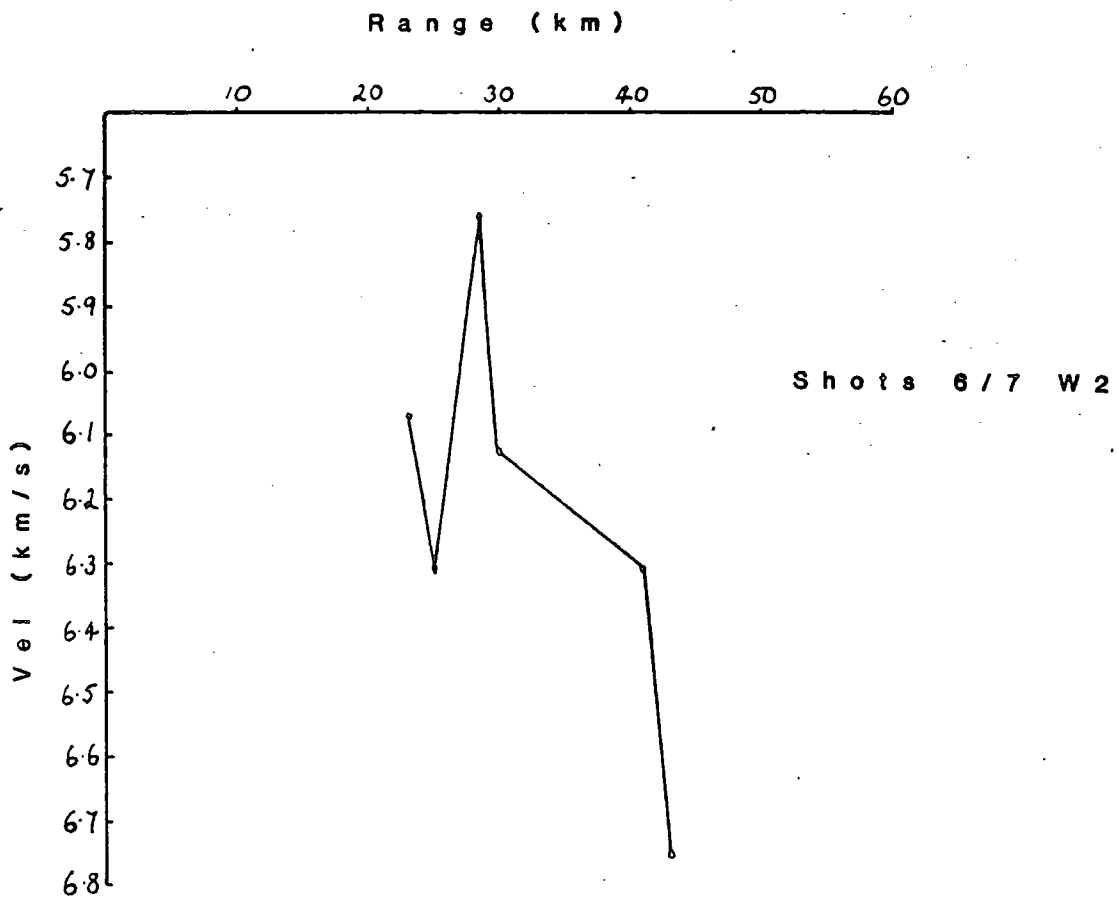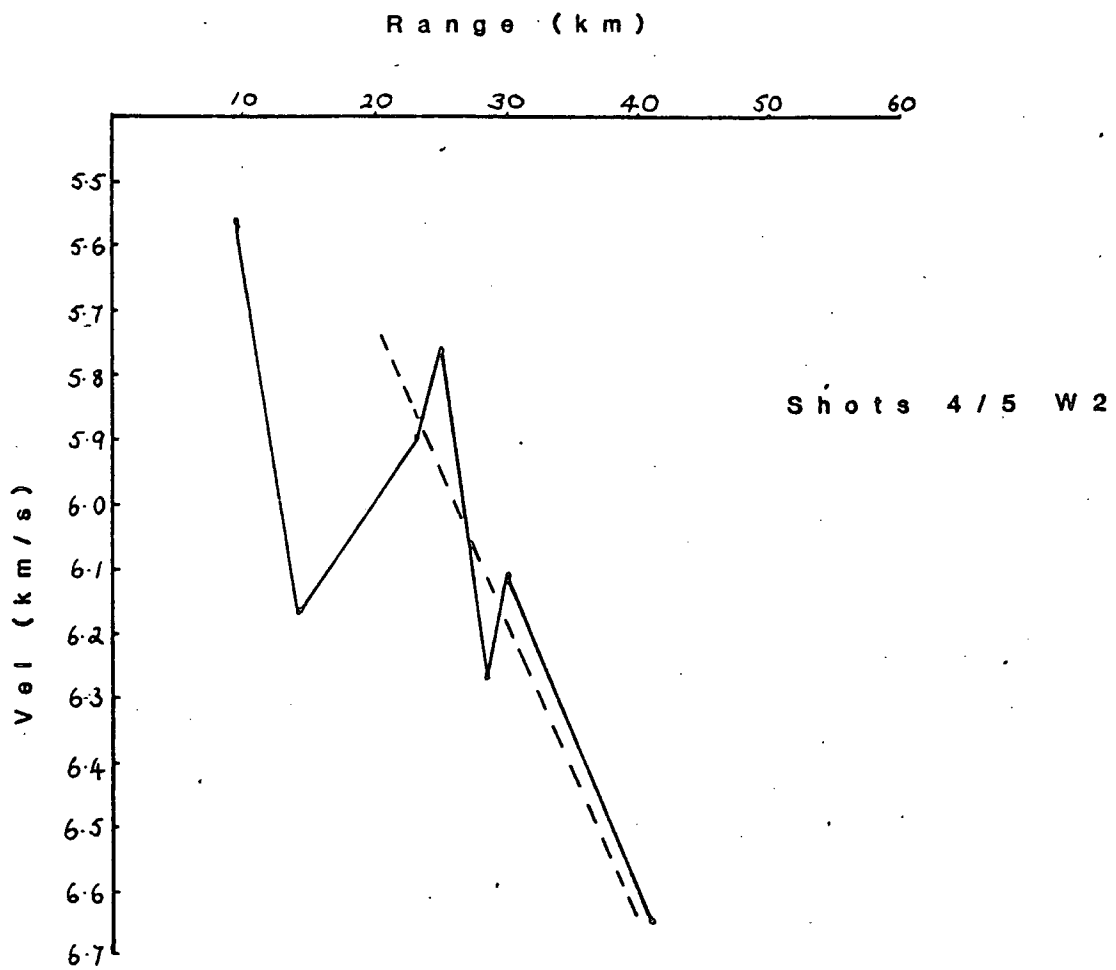
Fig.6.27: Velocity/distance relationships used in Wiechert Inversion. Shot pairs and velocities refer to those shown in Fig. 6.26.
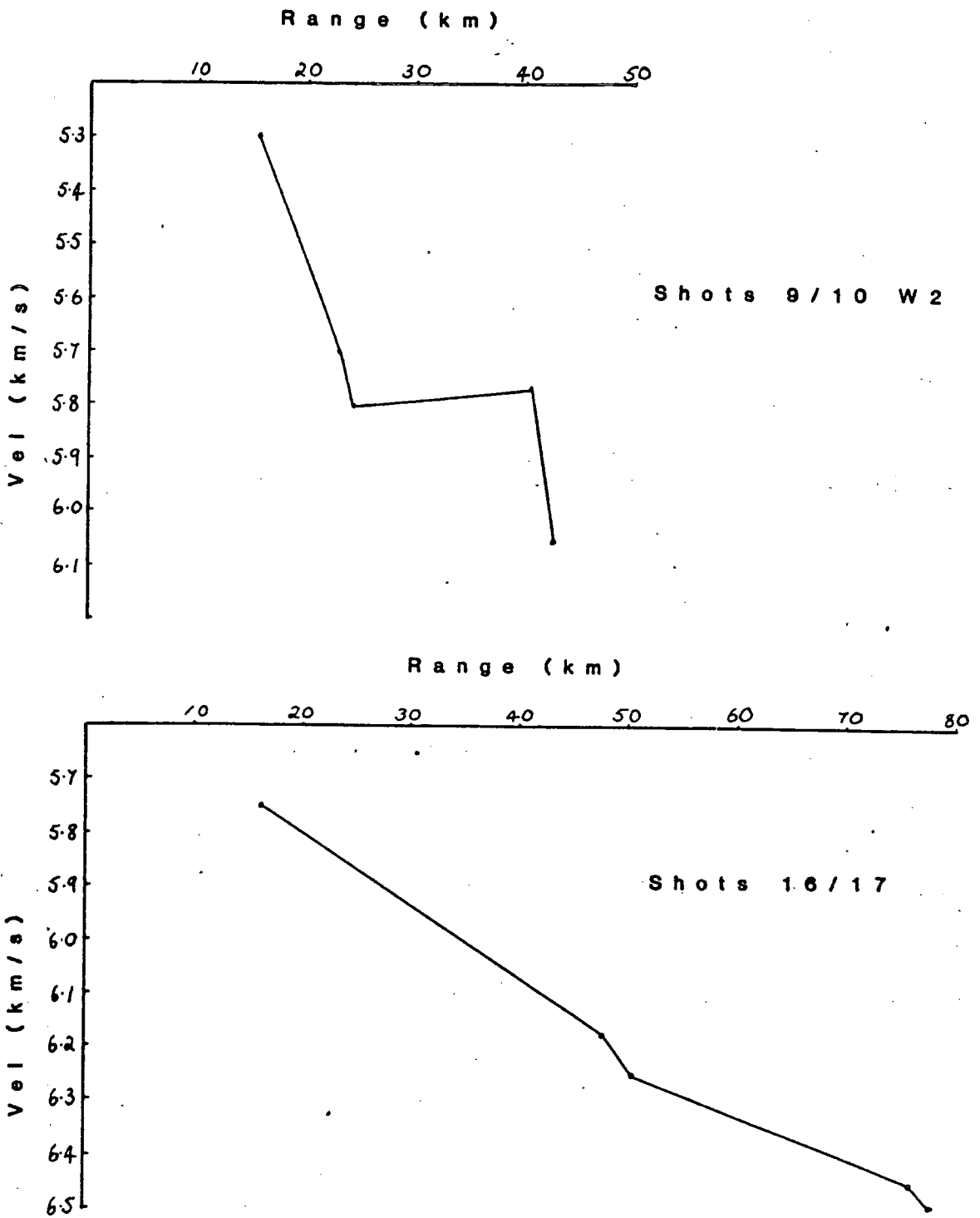
Fig.6.28: Velocity/distance relationships used in Wiechert inversion. Shot pairs and velocities refer to those shown in Fig. 6.26.
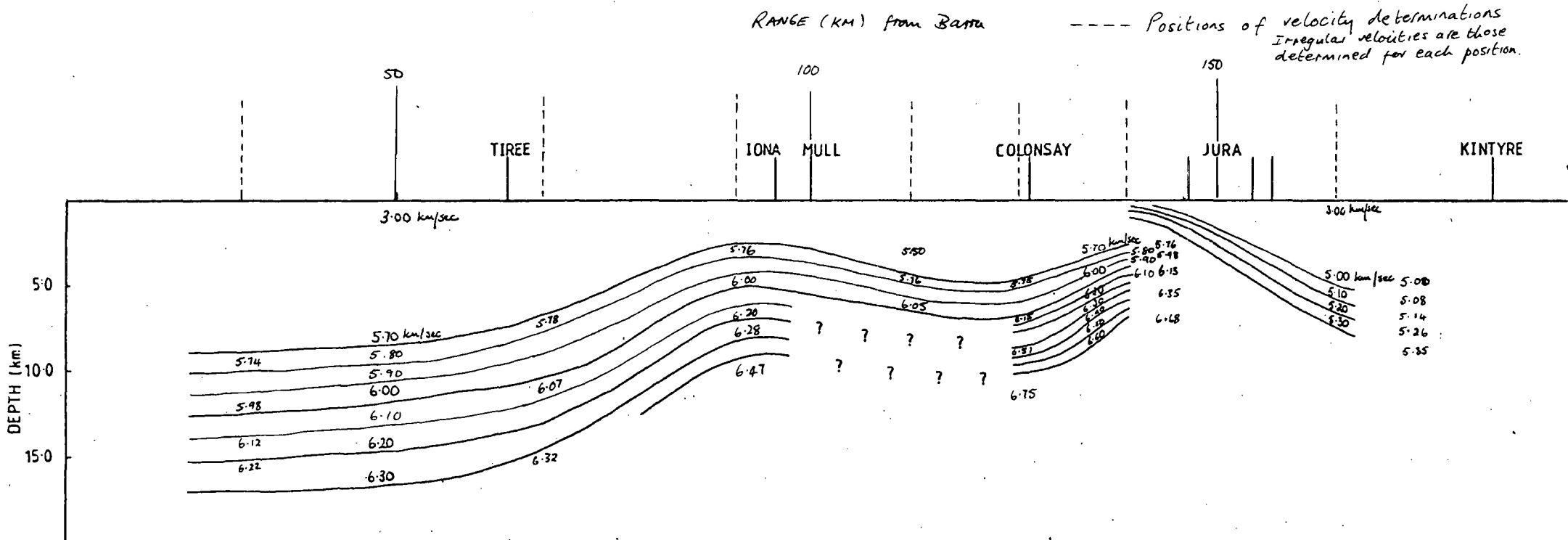
Fig.6.29: Velocity/depth relationships derived from Wiechert Inversion. Surface velocity used is 3.0 km/sec.
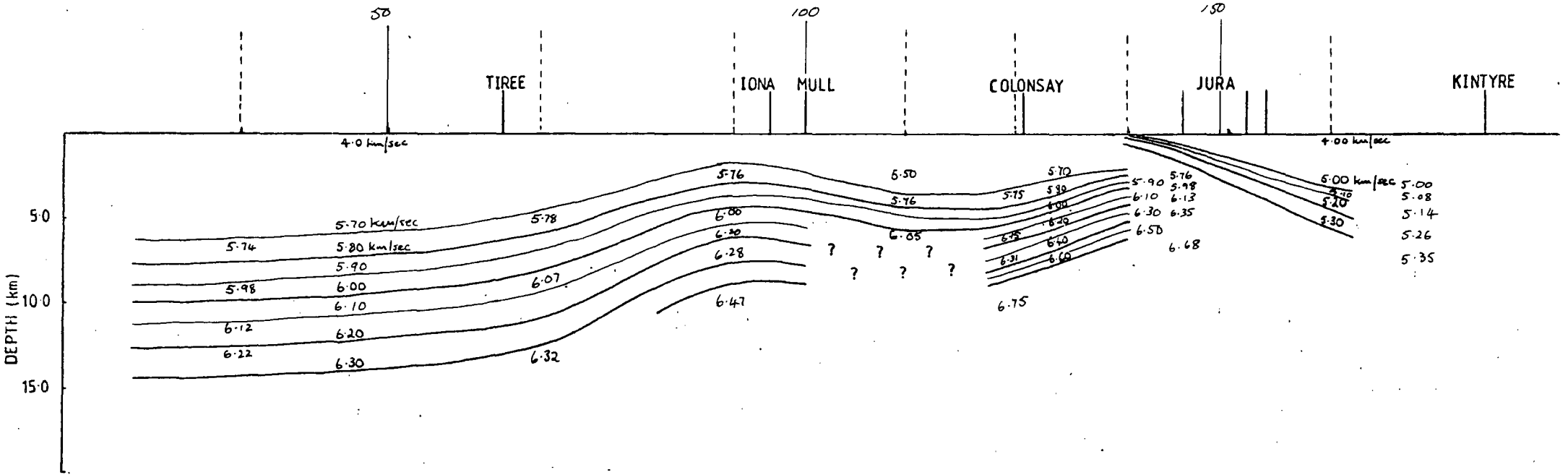
Fig.6.30: Velocity/depth relationships derived from Wiechert inversion. Surface velocity used is 4.0 km/sec.

velocities in the northern section can be seen however. In the region between Mull and Jura, a low velocity area quickly migrates into an area with a steep velocity gradient. This very possibly indicates the thick sediments close to the Great Glen Fault which are thought to exist over a very small region and then leads into the high relief on the basement as it once again outcrops on Colonsay. This also being shown by the airgun data. Further south the velocity once again decreases, possibly reflecting the Lewisian topography increasing in depth and the metasediments therefore extending deeper.

Significant in the model obtained from the inversion, is the lack of a velocity high beneath Tiree where significant undulation in the facies boundary has been modelled by Shaw (1978). This may or may not be real. The difficulty in determining this lies in the fact that the data for this region is sparse. It does show a steady trend of a velocity north of Mull of 6.00 to 6.30 km/sec though. Another explanation might be the wavelength of a velocity high if it does exist. The ranges of the shots from the stations and their separation. In this area are large compared to those further south. As such, it might not be possible to define a lateral increase in velocity within the upper crust.

Another feature to note on the velocity/depth model is the steep high between Colonsay and Jura, which if real, shows a significant change in the crust towards the orogenic belt. The shots used to define this high are generally at close range and have well defined arrival times. This appears to indicate that the high velocities are the true velocities within close range of the station. In addition, the velocity steeply increases for shots into stations in close range of Colonsay, such as Jura and Mull but the increase is not as marked for the larger range stations,

such as Barra. Therefore, even though the rays from Barra have travelled deeper in the crust, the overall velocity is not significantly greater than at closer range to the shot pair. This seems to point to a high in the region being real and lower velocity at depth further north. The rays from the close range data will not be offset from the inversion point to the extent of the large range and will therefore show the true velocity close to the surface in the region whereas at larger ranges, the rays would show the velocity of the deeper crust.

The interpretation of such a velocity distribution in an area of complex structure must be treated with caution as it oversimplifies the structural relationships. However, the velocity/depth relationships provided by the inversion can be explained to some extent the variation in the time-terms along the line. Moreover, the velocity/depth relationships, if accompanied as can be expected by changes in other properties of the basement such as density and magnetization, can possibly be mapped out as a gradual change in facies within the basement with a similar trend to the interface modelled by Shaw (1978). Using the velocity/depth distribution, the recalculated time-terms down to the Moho present a crustal model as shown by Fig. 6.31. The solid line represents the depth model using constant velocity crust and the dotted line, the depth to the Moho obtained using the velocity variation. This model must also be carefully treated due to the reasons presented previously concerning the derivation of the time-terms and the distribution of velocities.

6.7 Ray Tracing Interpretation.

The crustal model determined by time-term analysis and from the minus times was tested using the ray tracing technique. The results of its application to the upper crustal velocity model shown in Fig. 6.32 are

98

presented for different shots along the line in Figs. 6.33 to 6.37. Each model is accompanied by a reduced travel time graph showing the correlation between the observed travel times and the calculated. The model used correlates well with the observations at distances greater than 40 km, this being shown best in Figs. 6.33 and 6.34 for the south Jura station and ray tracing all shots. The method therefore enhances the proposal of significant lateral velocity variations within the crust. This solution fits better than a uniform increase in velocity within the crust or a distinct interface with velocity change across it.

The velocity/depth model derived from the Wiechert inversion can be seen to differ from that used in the ray-tracing and although the overall trend is the same for the broad structure, the fine detail which results in relative delays between travel times on the reduced travel time graphs has not been determined. This is because the model used is simplistic and only tests the large scale velocity variation. It is suggested that to further model the data, the oscillations in the velocity contours are underestimated and need to be increased. This might then result in a better fit between the observed travel times and those calcuated by ray-tracing.

Some large differences also exist between the observed and calculated travel times for shots at close range to the stations. These can be explained by the limitations placed by the program on velocity gradients over small ranges and the dip of the refractor which it cannot handle adequately. This results in gaps occuring between groups of arrivals close to the station. Some correction could be made with more accurate knowledge of the sedimentary velocities to obtain better estimates of the structure of the sediment/basement interface and carrying out full iterative

99

Key for Ray-Traced Models

B - Barra

T - Tiree

M - Mull

C - Colonsay

J - Jura

K - Kintyre

G - Girvan

☆ Observed Travel Times

▣ Calculated Travel Times

modelling. It was not possible however, to carry out more modelling within the time taken to complete this thesis. Furthermore, there are limitations to the extent that the process can be taken on such data. The velocities for the basins had to be taken as an average and depth calculated, because of the the lack of detail on the velocity provided by the airgun data and due to the way in which the interfaces have to be defined on input into the program. Any discrepancies therefore, between observed and calculated arrival times may be attributed to either incorrect sedimentary velocities and mapping of the basement depth or to an inaccurately defined velocity/depth relationship within the crust.

The velocities used for the conversion to depth were obtained from previous work, such as Smythe and Kenolty (1973) and Hall (1978a), and if these are realistic then the velocity at depth can be taken as being accurate where there is good correlation between observed and calculated arrivals. The velocities found differ from those determined using the previous methods but the trend of high and low gradients is the same. Also, as previously stated, care must be taken in the interpretation of the velocities from the Wiechert inversion of the velocity/distance curves as some inaccuracies are expected.

The arrivals in the Mull to Jura area are difficult to model due to the limitations caused by the dip on the interface mentioned previously. However, it appears that if the basin between Mull and Colonsay is made shallower than indicated by the time-term results, a closer correlation between observed and calculated arrivals can be obtained (Fig. 6.38). However, the region is very complex with varying rock types and sharp lateral variations caused by the major faults, thus making the modelling of the structure difficult without accurate constraint on the

data, which the airgun data did not provide. In addition, the program is primarily designed for use on plane layers and as such, fault planes cannot be modelled exactly. The velocity contrast used to represent such lateral discontinuities introduces some error into the solution.

A full crustal model showing the topography on the Moho and the rays traced through it is presented in Fig. 6.39. The depths determined are some 3 km less than those from the time-term method and minus time velocities. The discrepancy is thought to be due to the different velocity/depth relationships within the basement determined by both methods. Further ray tracing of the Moho arrivals was not undertaken due to the origin of the time-terms being considerably offset from the line and determined in the main from the permanent Scottish networks and therefore a two dimensional model is rather unrealistic. The study was also primarily on the upper crustal structure. It was thought therefore, that the example providing the estimated depth to the Moho was sufficient to show that the structure can provide the observed arrivals.

This method of interpretation has therefore provided some confirmation of the results from the previous interpretation stages. More work is necessary for the thorough development of the crustal model in this region. It is felt, however, that better control of the velocities and depths of the sedimentary basins is necessary before the deeper crustal structure within the basement can be determined with confidence.

101

CHAPTER 7

SUMMARY, GEOLOGICAL IMPLICATIONS AND DISCUSSION OF THE EXPERIMENT

7.1 Summary and Comparison with Adjacent Shelf Areas.

The results from the work of WISE and their interpretation in terms of velocity and depth structure presented in the previous chapter need to be viewed in a geological context and the implication on the development of the area considered. The interpretation has determined the following major features.

1. The sediment cover along the line is variable but cannot be fully examined without better information on its internal velocity structure. Basement outcrops at the islands along the line and reaches depths between 1 to 3 km in the basins. Velocities of Dalradian metasediments are found in the section of the line between Colonsay and Kintyre. These basins are shown by the variability of time-terms to be complex and it is difficult to model them satisfactorily.

2. The crust has a thickness varying between 30 and 35 km and has a varying velocity distribution. Steep velocity gradients are thought to exist beneath the Colonsay and Mull regions with more gentle gradients below the basin areas. The variation could not be fully examined further south but does not appear to be as complex. Large undulations on the Moho suggested by the time-terms might not necessarily be real as intra-basement velocity variation might explain the time-terms. The velocity contours follow the trend shown by the gravity and magnetic models of Shaw, where he models an interface between amphibolite and granulite facies except in the

102

region beneath Tiree. This however, might be due to lack of data in the area.

3. A basement velocity gradient is suggested as the presence of a distinct interface with a sharp velocity contrast across it cannot be determined from the records. There are only several arrivals on the records that show a velocity between 6.4 to 6.7 km/sec. Some lateral velocity variations in the refractor are noticed along the line with higher velocities to the north compared to the south This is thought to be due to the change in facies from the Lewisian to the younger metasediments.

4. The major faults of the area display themselves to a limited extent. Torridonian rocks are thought to have been downfaulted on the southern side of the Great Glen fault where it is at a lower structural level than the Moine. Velocities between 3.5 and 3.8 km/sec immediately south of the fault and extending 4 km towards Colonsay suggest the presence of thick Mesozoic sediments. Determination of rock type and structure near the Moine Thrust is more difficult. Time-terms indicate lower velocities south of the proposed line of the fault between Mull and Iona compared to the north. Relationships between faults south of Jura, and the Firth of Clyde in particular, were not investigated.

These results can be compared to those of other regions of the north Scottish shelf determined from previous experiments. It is noticed that significant similarities exist in the structure of this region and the area investigated in HMSP (Armour, 1977) and the northern part of

the LISPB profile (Bamford et al., 1978) but not with the NASP profile (Smith, 1974). No mid-crustal refractor was found in HMSP but an average crustal velocity of 6.6 km/sec and depth of 30 km was determined. An important observation is that the pattern of time-terms determined for the North Minch basin and surrounding land is very similar to that found by WISE for the South Minch basin and surrounding areas. In both cases the time-terms on the Moho show the same trend as those of the basement. Additionaly, Armour (1977) suggests that the large changes in Pn between the basin and basement highs do not necessarily indicate changes in the thickness of the crust but possibly velocity variations.

For the NASP line (Smith & Bott, 1975), a mid-crustal refractor of velocity, 6.48 km/sec, was positively identified, lying between 2 and 16 km beneath the surface in the foreland regions. The crustal depth in this area was uniform, being between 25 to 26 km which is significantly thinner than that of the western region studied by WISE. The mid-crustal refractor is not evident beneath the mobile belt however, but a thickening of the crust takes place. The findings of Bamford et al. (1978) identified a refractor equivalent to the 6.48 km/sec layer of NASP on the mainland of Scotland extending from the Caledonian foreland to the Midland Valley at a similar depth. However, recent work in ray tracing and the development of synthetic seismograms for the LISPB data by Cassell (1982) suggests that this is not the case and that the data can be more easily modelled by the existence of a gradational increase in velocity with depth rather than a distinct interface. This would again be in common with the results of WISE. Absent from all the areas on the north Scottish shelf off the mainland but evident on the LISPB profile is a layer with a velocity of 7.0 km/sec. Unlike the 6.48 km/sec interface, this can be more easily

modelled by synthetic seismograms and therefore its existence is supported.

No anisotropy is evident in the upper mantle velocities over the shelf region with a well defined sub-Moho velocity of 8.00 +/- 0.05 km/sec found for this and the other surveys.

7.2 Geological Implications.

The shallow structure along the line has been difficult to determine due to the lack of adequate reversed data over the line and as a result, the interpretation is limited. From a simplistic point of view, some control has been placed on the direction of the movement on the faults, but cannot be quantified. Therefore, further understanding of the present knowledge on the age and amount of movement of the major faults cannot be determined.

The deep structure determined for the WISE profile is interesting though, in that it has been shown to have similarities with other areas of the shelf and be in agreement in certain respects with the gravity and magnetic studies carried out in the area. However, after converting the time-terms to depth using the velocity information, although some of the topography can be accounted for, there still remain significant

undulations on the crust/mantle boundary. These might not exist at all, being ironed out by the velocity structure in the deeper crust. It must be noted that if the topography on the Moho is real, showing a similar trend to the basement surface, then the formation of the basins and their implication on the isostatic equilibrium in the region must be considered.

The formation of graben in western Europe has been described by Ziegler (1982) and related to rifting and megatectonic events throughout geological time. In his study, he includes details of the Great Glen fault and the fault systems of the Firth of Clyde where he proposes that the subsidence is governed by lithospheric thinning and sedimentary loading in response to regional tension. Bott (1982) suggests that the narrow graben bounded basins form as a result of stressing of the continental lithosphere, indicating horizontal deviatoric tension. Furthermore, Bott (1971) indicates that the formation of the Permo-Triassic basins of Britain may be related to early uplift on the formation of the rift. Differential loading as a result of isostatic readjustment occured at the margin with the lower ductile continental crust creeping toward the oceanic crust, resulting in subsidence in the upper brittle layer. The method was investigated using finite element analysis (Bott and Dean, 1972), and shown to be the primary cause of the faulting in the shelf areas as the brittle layer responded to the subsidence. The relation with depth however, is difficult to determine and that although thinning of the crust occurs as a result of the creep its trend in relation to the fault planes is not known.

It is now necessary to consider the depth to which the faults might extend to consider the effect on the deep structure. A study of the mechanism of the formation of graben, (Mithen, 1980), has led to

106

proposals of several modes depending on the rheology of the crust used in the model. The width of the graben and extent of the faulting depends on the depth to which the brittle layer extends and the way that the fault dies out with depth is dependent on the underlying material.

An examination of the depth section derived from the time-term analysis gives an indication of what is happening at depth between the lowermost crust and uppermost mantle in the area of WISE. It can be seen that unless the crystalline crust was originally much thicker beneath the present basin structures it does not neck across them. The best example of this is shown beneath the Minch. If it was thicker, then there would have been no compensation to achieve isostatic equilibrium within the crust itself as the area would have been a topographic high and as such, not likely to have formed a basin. To explain the crustal model derived from the time-terms, it was necessary to either consider an undulating Moho and constant crustal velocity or a flat Moho and a velocity gradient, but it does not leave an internal isostatic crustal balance between the basins and highs. If there is a balance between the two, it indicates that there must be lateral variations in the mantle.

Although it is not necessary to reach a perfect balance between the two with such small structural blocks, the way in which the crust has behaved in the area suggests that a balance can be expected. The nature of the movement along the major fault planes has been an alternation of thrusts and normal faulting, indicating compressional and extensional forces respectively. This was necessary to preserve the thick piles of Torridonian and Mesozoic sediments. This indicates movement in the mantle, a fact confirmed by the seismic reflection lines of MOIST which indicate very deep thrusts extending to 45 km (Matthews, pers. comm.) The evidence

therefore, indicates cold crust deformation without the readjustment suggested by Bott (1971) within the crust but including tectonic forces within the mantle.

7.3 Discussion of the Western Isles Seismic Experiment

The seismic refraction study of the western shelf region has determined, to some extent, estimates of the depth to the basement and variations in the upper crustal structure. In this respect, the experiment has achieved some of its initial aims. However, the results and interpretation are not as complete as had been desired, which can be attributed to a number of factors. Firstly the airgun data was, in general poor, and could not be interpreted to give good velocity and depth control to the basement. This has implications for the subsequent study of the structure within the basement itself. Without accurate knowledge of the upper layers, the interpretation of basement velocities and depth to the Moho are ambiguous. A second factor that must be considered is that the return of data from the explosive shots was not sufficient to give good coverage of the line, especially at important stations such as Tiree and Kintyre. For the first phase of the experiment, the shot ranges to these stations were such that they would define the structure of the middle crust. Absolute conclusions could therefore not be on the existence of a mid-crustal refractor and therefore, models using mid-crustal velocity gradients were constructed.

The interpretation of the area considering the overall data quality was therefore limited. Furthermore, seismic refraction data is difficult to interpret when the structure is laterally inhomogeneous and confidence cannot be placed on results obtained from poor data. Therefore,

for WISE, carried out in a region where the geology is complex, and where the line crossed the strike of the major structures, further difficulties were thus introduced and high data quality was needed to enhance the present knowledge of the area. It might be said that the same problems should have been encountered during LISPB. However, the station separation in that case was one third of that of WISE and the main strucͭural blocks could be mapped more accurately. The main problems and limitations therefore lie in the quality of the data, especially from the airguns, which meant that consͭraints could not be confidently placed on the upper sedimentary layers and basement depth, and hence obtain accurate estimates of the deeper structure.

On the positive aspects of the project, however, much has been determined and the framework of the northern Scottish shelf can be put in a better perspective by considering this and previous work. The results obtained on the deeper structure show significant comparison to those of other surveys over the North Scottish shelf, and provide interesting details of the velocity and mid-crustal structure over the region. The development of the sedimentary basins within the area has been investigated and ideas on the tectonic evolution of the area with relationships between the crust and mantle proposed. Future work in the area might further delineate the changes occuring within the basement by using later phases in the data which could not be examined in this thesis but should provide more evidence on facies variation and the nature of the crust/mantle boundary.

BIBLIOGRAPHY

AGGER, H.E., & CARPENTER, E.W. 1965. A crustal study in the vicinity of the Eskdalemuir seismological array station. Geophys. J. R. astr. Soc. 9, 63-83.

AHMAD, M.U., 1967. Some geophysical observations on the Gret Glen fault. Nature. Lond. 213, 275-277.

ANDERSON, J.G.C., 1947. The geology of the Highland border: Stonehaven to Arran. Trans. R. Soc. Edin. 61, 479-515.

ARMOUR, A.R., 1977. A seismic refraction study of the crustal structure of North-West Scotland and adjacent continental margin. Ph.D. Thesis. University of Durham.

ATTREE, M.C., 1982. Seismic refraction study between Colonsay and Mull. B.Sc. Thesis. University of Durham.

BACON, M., & CHESHER, A.J., 1974. Evidence against post-Hercynian movement on the Great Glen Fault. Scott. J. Geol. 11, 79-82.

BAILEY, E.B., 1916. The Islay anticline. Q. J. Geol. Soc. 72, 132-164.

BAILEY, E.B., & MAUFE, H.B., 1960. The geology of Ben Nevis and Glen Coe. Mem. geol. Surv. U.K. (Scotland).

BAMFORD, D., 1976. Mozaic time-term analysis. Geophys. J. R. astr. Soc. 44, 433-446.

BAMFORD, D., NUNN, K., PROEDEHL. C., & JACOB, B., 1978. LISPB-IV. Crustal structure of northern Britain. Geophys. J. R. astr. Soc. 54, 43-60.

BÅTH, M., 1976. An analysis of the time-term method in refraction seismology. Seism. Inst. Sweden. Report No. 10-76 23pp.

BARBER, P.L., DOBSON, M.R., & WHITTINGTON, R., 1979. The geology of the Firth of Lorne, as determined by seismic and dive sampling methods. Scott. J. Geol. 15, 217-230.

BERGLAND, G.D., 1969. A guided tour to the fast fourier transform. I.E.E.E. Spectrum 6, Jul. 41-52.

BERRY, M.J., & WEST, G.F., 1966. A time-term interpretation of the first arrival data of the 1963 Lake Superior experiment. In The Earth beneath the continents (Eds STEINHART, J.S, & SMITH, T.J.) 166-180, American Geophysical Union.

BINNS, P.E, McQUILLIN, R., & KENOLTY, N., 1973. The geology of the Sea of the Hebrides. Rep. Inst. geol. Sci. London. 73/14 43pp.

BINNS, P.E., McQUILLIN, R., FANNIN, N.G.T., KENOLTY, N., & ARDUS, D.A., 1975. Structure and stratigraphy of sedimentary basins in the Sea of the Hebrides and the Minches. In Petroleum and the continental shelf of North-West Europe (Ed WOODLAND, A.W.) 1, 93-102, Appl. Sci.

BIRTLES, R.G., 1980. Filtering techniques for the enhancement of refraction data from the Western Isles. M.Sc. Thesis, University of Durham.

BOTT, M.H.P., 1971. Evolution of young continental margins and formation of shelf basins. Tectonophysics, 11, 319-321.

BOTT, M.H.P., 1975. Structure and evolution of the North Scottish shelf, the Faroe Block and intervening region. In Petroleum and the continental shelf of North-West Europe (Ed WOODLAND, A.W.) 1, 105-116, Appl. Sci.

BOTT, M.H.P., 1982. Origin of the lithospheric tension causing basin formation. Philos. Trans. R. Soc. London. A 305, 319-324.

BOTT, M.H.P., & DEAN, D.S., 1972. Stress mechanisms at young continental margins. Nature (Phys. Sci.) Lond. 235, 23-25.

BOTT, M.H.P., & WATTS, A.B., 1970. Deep sedimentary basins proved in the Hebridean Shetland continental shelf and margin. Nature. Lond. 225, 265-268.

BOTT, M.H.P., HOLLAND, J.G., STORRY, P.G., & WATTS, A.B., 1972. Geophysical evidence cocerning the structure of the Lewisian of Sutherland, N.W. Scotland. J. geol. Soc., Lond. 128, 599-612.

BOWES, D.R., 1968. An orogenic interpretation of the Lewisian of Scotland. In Report of the 23rd session of the International Geological Congress, Czechoslovakia, Proceedings of Section 4, Geology of Pre-Cambrian, 225-236.

BRUCK, P.M., DEDMAN, R.E., & WILSON, R.C.L., 1967. The New Red Sandstone of Raasay and Scalpay, Inner Hebrides. Scott. J. Geol. 3, 168-180.

BULLARD, E., EVERETT, J.E., & SMITH, A.G., 1965. The fit of the continents around the Atlantic. Philos. Trans. R. Soc. A258, 41-51.

BURG, J.P., 1968. Maximum entropy spectral analysis. 37th Ann. Int. Meet., Soc. Explor. Geophys., Okla., Oct. 31, 1967.

CASSEL, B.R., 1982. Synthetic seismograms for the northern part of the laterally varying LISPB structure. Eur. Geophys. Soc. Meeting, Leeds, Aug. 27 (abstract).

111

CASSON, N., 1982. A seismic refraction investigation between the Hebridean Isles of Colonsay and Jura. B.Sc. Thesis, University of Durham.

ČERVENÝ, V., LANGER, J., & PŠENČIK, I., 1974. Computation of geometric spreading of seismic body waves in laterally inhomogeneous media with curved interfaces. Geophys. J. R. astr. Soc. 38, 9-20.

CLAERBOUT, J.F., 1976. Fundamentals of geophysical data processing. McGraw Hill 352 pp.

DEARNLEY, R., 1962. An outline of the Lewisian complex of the Outer Hebrides in relation to that of the Scottish mainland. Q. J. geol. Soc. Lond. 118, 143-176.

DEWEY, J.F., 1969. Evolution of the Appalachian/Caledonian orogen. Nature Lond. 222.124-129.

DEWEY, J.F., & PANKHURST, R.J., 1970. The evolution of the Scottish Caledonides in relation to their isotopic age pattern. Trans. R. Soc. Edinburgh, 68, 361-389.

DOBRIN, M.B., 1976. Introduction to geophysical prospecting, 3rd Edition. McGraw Hill, 630pp.

DOBSON, M.R., & EVANS, D., 1974. Geological structure of the Malin Sea. J. Geol. Soc. Lond. 130, 475-478.

DOBSON, M.R., EVANS, D., & WHITTINGTON, R., 1975. The offshore extension of the Loch Gruinart fault, Islay. Scott. J. Geol. 11, 23-35.

DRURY, S.A., 1972. The tectonic evolution of a Lewisian complex on Coll, Inner Hebrides. Scott. J. Geol. 8, 309-333.

DURRANCE, E.M., 1976. A gravity survey of Islay. Geol. Mag. 113, 251-261.

EVANS, C.R., 1965. Geochronology of the Lewisian basement near Lochinver, Sutherland. Nature. Lond. 207, 54-56.

EVANS, D., WILKINSON, G.C., & CRAIG, D.L., 1979. Tertiary sediments of the Canna Basin, Sea of the Hebrides. Scott. J. Geol. 15, 329-322.

FRANCIS, P.W., 1973. Scourian-Laxfordian relationships in the Barra Isles. J. geol. Soc. Lond. 129, 161-189.

FRIEND, P.F., & MacDONALD, R., 1968. Volcanic sediments, stratigraphy and tectonic backround of the Old Red Sandstone of Kintyre, West Scotland. Scott. J. Geol. 4, 265-282.

GARSON, M.S., & PLANT, J., 1972. Possible dextral movements on the Great Glen and Minch faults in Scotland. Nature. (Phys. Sci.) 240, 31-35.

GEORGE, T.N., 1966. Geomorphic evolution in Hebridean Scotland. Scott. J. Geol. 2, 1–34.

GUNN, W., 1903. The geology of north Arran, south Bute, and the Cumbraes. Mem. geol. Surv. U.K..

HAGEDOORN, J.G., 1959. The plus-minus method of interpreting seismic refraction sections. Geophys. Prospect. 7, 158–182.

HALL, J., 1978a. 'LUST'– a seismic refraction survey of the Lewisian basement complex in North-West Scotland. J. geol. Soc. Lond. 135, 555–563.

HALL, J., 1978b. Seismic refraction studies in the Firth of Clyde. In Solid geology of the Clyde Sheet 55N/6W. Rep. Inst. geol. Soc. Lond. 78/9.

HALL, J., & SMYTHE, D.K., 1973. Discussion of the relation of palaeogene ridge and basin structures of Britain to the North Atlantic. Earth. planet. Sci. Lett. 19, 54–60.

HALLAM, A., 1972. Relation of Palaeogene ridge and basin structures and vulcanicity in the Hebrides and Irish Sea regions of the British Isles to the opening of the North Atlantic. Earth. planet. Sci. Lett. 16, 171–177.

HOLGATE, N., 1963, Palaeozoic and Tertiary transcurrent movements on the Great Glen fault. Scott. J. Geol. 5, 97–139.

JACOB, A.W.B., 1976. Dispersed shots at optimum depth – an efficient seismic source for lithospheric studies. J. Geophys. 41, 63–70.

JEHU, T.J., & CRAIG, R.M., 1925. Geology of the Outer Hebrides, Part 1 – The Barra Isles. Trans. R. Soc. Edin. 53, 419–440.

JONES, E.J.W., 1981. Seismic refraction shooting on the continental margin west of the Outer Hebrides, North-West Scotland. J. geophys. Res. 86, 11553–11574.

KENNEDY, W.Q., 1946. The Great Glen Fault. Q. J. geol. Soc. Lond. 102, 41–72.

LEE, G.W., & BAILEY, E.B., 1925. The pre-Tertiary geology of Mull, Loch Aline and Oban. Mem. Geol. Surv. Scotland.

LONG, R.E., 1974. A compact portable seismic recorder. Geophys. J. R. astr. Soc. 37, 91–98.

LONG, R.E., 1975. Durham seismic recorder Mk.3 operating manual. 23pp.

MARSTON, R.J., 1967. Newer granites of Foyers and Strontian and the Great Glen Fault. Nature Lond. 214, 159–161.

113

McLEAN, A.C., & DEEGAN, C.E., 1978. A synthesis of the solid geology of the Firth of Clyde. In The solid geology of the Clyde Sheet 55N/6W. Rep. Inst. geol. Sci. Lond. 78/9.

McQUILLIN, R., & ARDUS, D.A., 1977. Exploring the geology of shelf seas. Graham and Trotman 234 pp.

McQUILLIN, R., & BINNS, P.E., 1973. Geological structure of the Sea of the Hebrides. Nature (Phys. Sci.) Lond. 241, 2-4.

McQUILLIN, R., & BINNS, P.E., 1975. Geological structure in the Minches, the Sea of the Hebrides and in the adjacent North-West British continental shelf. In Canada's continental margins and offshore petroleum exploration (Eds YORATH, C.J., PARKER, E.R., & GLASS, D.J.) 4, 283-293.

MITHEN, D.P., 1980. Numerical investigations into the mechanism of graben formation. Ph.D. Thesis, University of Durham.

MOORBATH, S., 1969. Evidence for the age of deposition of the Torridonian sediments of North-West Scotland. Scott. J. Geol. 5, 154-170.

NUNNS, A.G., 1980. Marine geophysical investigations in the Norwegian Greenland sea between latitudes 62N and 74N. Ph.D. Thesis, University of Durham.

PARK, R.G., 1970. Observations on Lewisian chronology. Scott. J. Geol. 6, 379-399.

PEACH, B.N., HORNE, J., GUNN, W., CLOUGH, C.T., HINXMAN, L.W. & TEALL, J.J.H., 1907. The geological structure of the north-west Highlands of Scotland. Mem. Geol. Surv. U.K.

PEACOCK, K.L., & TREITEL, 1969. Predictive deconvolution, theory and practice. Geophysics, 34, 155-169.

PITCHER, W.S., 1969. North-East trending faults in Scotland and Ireland. Mem. Am. Assoc. Petrol. Geol. 12, 723-733.

PITMAN, W.C., & TALWANI, M., 1972. Sea floor spreading in the North Atlantic. Bull. Geol. Soc. Am. 3, 301-314.

RACAL-THERMIONIC LTD., 1975. Geostore field recorder, technical handbook 41pp.

RAST, N., DIGGENS, J.N., & RAST, D.E., 1968. Triassic rocks of the Isle of Mull, their sedimentation, facies, structure and relationship to the Great Glen Fault and the Mull caldera. Proc. geol. Soc. Lond. 1645, 299-305.

RICHEY, J.E., ANDERSON, E.M., & MacGREGOR, A.G., 1930. The geology of North Ayrshire. Mem. geol. Surv. U.K.

RICHEY, J.E., MACGREGOR, A.G., & ANDERSON, F.W., 1961. The Tertiary Volcanic Districts. 3rd Ed. Brit. Reg. Geol.

ROBERTS, D.G., 1975. Marine geology of the Rockall Plateau. Philos. Trans. R. Soc. Lond. A278, 447-509.

ROBINSON, E.A., 1967. Statistical communication and detection with special reference to digital data processing of radar and seismic signals. Griffin 362 pp.

ROBINSON, E.A., & TREITEL, S., 1967. Principles of digital Wiener filtering. Geophys Prospect. 15, 311-333.

SAVAGE, J.E.G., 1979. A seismic investigation of the lithosphere of the Gregory Rift. Ph.D. Thesis, University of Durham.

SHAND, S.J., 1951. Mylonite, Slickensides, and the Great Glen Fault. Geol. Mag. 88, 423-428.

SHAW, B.H., 1978. The structure of the crust between Jura and Barra. M.Sc. Thesis, University of Durham.

SMITH, P.J., 1974. A seismic refraction study of crustal structure between the Faroe Isles and Scotland. Ph.D. Thesis, University of Durham.

SMITH, P.J., & BOTT, M.H.P., 1975. Structure of the crust beneath the Caledonian Foreland and Caledonian belt of the North Scottish shelf region. Geophys. J. R. astr. Soc. 40, 187-205.

SMITH, R.G., 1982. A study of airgun source signatures and signal processing techniques applied to airgun refraction data. M.Sc. Thesis.

SMYTHE, D.K., SOWERBUTTS, W.T.C., BACON, M., & MCQUILLIN, R., 1972. Deep sedimentary basin below Northern Skye and Little Minch. Nature (Phys. Sci.) Lond. 236, 87-89.

SMYTHE, D.K., & KENOLTY, N, 1975. Tertiary sediments in the Sea of the Hebrides. J. geol. Soc. Lond. 131, 227-233.

STEEL, R.J., 1971. New Red Sandstone movement on the Minch fault. Nature (Phys. Sci.) Lond. 234, 158-159.

STEEL, R.J., 1974. New Red Sandstone floodplain and alluvial fan sedimentation in the Hebridean province of Scotland. Jl. sedem. Petrol. 44, 336-357.

STEEL, R.J., & WILSON, A.C., 1975. Sedimentation and tectonism (? Permo-Triassic) on the margin of the North Minch basin, Lewis. J. geol. Soc. Lond. 131, 183-202.

STEPHENSON, D., 1972. Middle Old Red Sandstone alluvial fan and talus deposits at Foyers, Invernesshire. Scott. J. Geol. 8, 121-127.

STEWART, A.D., 1962. On the Torridonian sediments of Colonsay and their relationships to the main outcrop in North-West Scotland. Liverpool Manchester geol. J. 3, 121-156.

STEWART, A.D., 1966. An unconformity in the Torridonian. Geol.Mag. 103, 462-465.

STEWART, A.D., & IRVING, E., 1974. Palaeomagnetism of Precambrian sedimentary rocks from North-West Scotland and the apparent polar wandering path of Laurentia. Geophys. J. R. astr. Soc. 37, 51-72.

STOFFA, P.L., BUHL, P., DIEBOLD, J.B., & WENZEL, F., 1981. Direct mapping of seismic data to the domain of intercept time and ray parameter – A plane wave decomposition. Geophysics. 46, 255-267.

STORETVEDT, K.M., 1974. Possible large scale sinistral displacement along the Great Glen Fault. Geol. Mag. 111, 23-30.

SUTTON, J.W., & WATSON, J.V., 1951. The pre-Torridonian history of the Loch Torridonian and Scourie areas in the North-Western highlands and its bearing on the chronological classification of the Lewisian. Q. J. geol. Soc. Lond. 106, 241-307.

SWINBURN, P, 1975. The crustal structure of Northern England. Ph.D. Thesis, University of Durham.

TELFORD, W.M., GELDART, L.P., SHERRIFF, R.E., & KEYS, D.A., 1976. Applied geophysics. Cambridge University Press 860pp.

WARREN, R.D., 1981. Signal processing techniques applied to seismic refraction data. M.Sc. Thesis, University of Durham.

WATSON, J., 1975. The Lewisian Complex. In A correlation of the Precambrian rocks of the British Isles (Ed HARRIS, A.L.) Geol. Soc. Spec. Rep. 6, 15-29.

WATTS, A.B., 1971. Geophysical investigations on the continental shelf and slope north of Scotland. Scott. J. Geol. 7, 189-217.

WESTBROOK, G.K., 1972. Structure and metamorphism of the Lewisian of East Tiree. Scott. J. Geol. 8, 13-30.

WESTBROOK, G.K., 1973a. Crust and upper mantle structure in the region of Barbados and the Lesser Antilles. Ph.D. Thesis, University of Durham.

WESTBROOK, G.K., 1973b. Possible dextral movements on the Minch fault. Nature (Phys. Sci.) Lond. 241, 167.

WESTBROOK, G.K., & BORRADAILE, 1978. The geological significance of the magnetic anomalies in the region of Islay. Scott. J. Geol. 14, 213-224.

WHITBREAD, D.R., 1975. Geology and petroleum possibilities west of the United Kingdom. In Petroleum and the continental shelf of North-West Europe (Ed WOODLAND, A.W.) 1, 45-59, Appl. Sci.

WILLMORE, P.L., & BANCROFT, A.M. 1960. The time-term approach to refraction seismology. Geophys. J. R. astr. Soc. 3, 419-432.

WINCHESTER, J.A., 1973. Pattern of regional metamorphism suggests a sinistral displacement of 160 km along the Great Glen Fault. Nature (Phys. Sci.) Lond. 246, 81-84.

WRIGHT, A.B.N., 1979. A method of improving the resolution of band-limited seismic reflection data. M.Sc. Thesis, University of Durham.

ZIEGLER, P.A., 1982. Faulting and graben formation in western and central Europe. Philos. Trans. R. Soc. Lond. A305, 113-143.

ZIOLKOWSKI, A., 1980. Basic ideas behind the concept of deconvolution. Unpublished.

ZIOLKOWSKI, A., 1980. Least-squares prediction of stationary linear processes. Unpublished.

APPENDICES

APPENDIX 1 - Station locations.

Record of shots received at each station for the first phase of WISE.

Travel times and ranges for all shots picked.

APPENDIX 2 - Computer programs.

APPENDIX 1

119

LOCATION OF STATIONS IN WISE

Station	Latitude (North)	Longitude (West)
Barra (G + D)	56° 58.11'	7° 26.39'
Ruaig	56° 31.92'	6° 45.66'
Vaul	56° 32.35'	6° 48.48'
Mull (G)	56° 19.14'	6° 19.59'
Mull (D)	56° 17.50'	6° 15.51'
Mull (W2)	56° 19.19'	6° 19.66'
Iona (W1)	56° 20.02'	6° 24.13'
Iona (W2)	56° 20.08'	6° 23.79'
Colonsay (W1 + W2)	56° 04.92'	6° 10.09'
N. Jura (W1 + W2)	55° 57.01'	5° 58.92'
M. Jura (1)	55° 53.57'	5° 55.19'
M. Jura (2)	55° 53.49'	5° 54.83'
S. Jura (W1 + W2)	55° 52.53'	5° 53.87'
N. Kintyre (W1 + W2)	55° 41.95'	5° 37.43'
S. Kintyre (W1 + W2)	55° 34.77'	5° 27.84'
Arran	55° 30.49'	5° 21.19'
Girvan Stns.		
Letterpin	55° 11.41'	4° 50.28'
Lendalfoot	55° 10.55'	4° 55.67'
Cundry Mains	55° 10.68'	4° 54.15'
Knockbrain	55° 10.14'	4° 53.28'
Breaker Hill	55° 09.77'	4° 51.67'
Bargain Hill	55° 09.41'	4° 50.47'
Millenderdale	55° 10.70'	4° 51.70'
Currarie	55° 10.87'	4° 50.28'

G   Geostore Recorder

D   Durham Mk. 3 Recorder

W1   Phase 1

W2   Phase 2

STATION	SHOT NUMBER																						
	1	2	3	4	5	6	7	8	9	10	11	12	13	14	15	16	17	18	19	20	21	22	23
BARRA	a	a	a	a	b	b	f	b	b	b	b	b	b	a	b	a	a	a	a	a	a	a	a
RUAIG	c	b	c	d	d	d	f	c	c	c	b	b	b	b	a	a	a	a	d	a	a	a	
RUAIG	c	b	c	d	d	d	f	c	c	c	b	b	b	b	a	a	a	a	a	d	a	a	a
VAUL	c	b	c	b	c	a	f	c	c	c	c	b	b	c	c	c	b	a	a	c	e	e	e
MULL (6)	c	b	a	a	c	c	f	c	c	c	c	c	c	b	a	a	a	b	a	a	a	a	a
IONA	e	e	e	e	e	e	f	e	c	c	c	c	b	b	a	a	a	a	a	a	a	a	a
COLONSAY	a	d	d	a	d	d	f	b	a	a	a	d	b	b	d	d	a	b	d	d	d	a	d
N. JURA	d	d	d	d	d	d	f	c	d	d	d	d	d	d	d	d	d	d	d	d	d	d	d
M. JURA (1)	e	e	e	e	e	e	f	a	a	b	b	c	c	a	a	e	b	e	a	a	a	a	a
M. JURA (2)	a	a	a	a	a	a	f	a	a	a	a	a	a	a	a	a	a	a	a	a	a	a	a
S. JURA	a	a	a	a	a	a	f	a	c	c	a	a	a	a	a	a	a	a	a	a	a	a	a
LETTERPIN	a	a	a	a	a	a	f	a	c	c	c	c	c	c	b	b	c	c	c	b	c	c	c
CUNDRYMAINS	a	a	a	a	a	a	f	a	c	c	c	c	c	c	c	c	c	c	c	c	c	c	c
MILLENDERDALE	e	e	a	c	c	e	f	e	e	e	c	c	c	c	e	e	b	c	e	e	e	e	e
CURRARIE	a	a	a	a	b	b	f	b	e	e	e	e	e	e	e	e	e	e	e	e	e	e	e
BREAKER HILL	a	a	a	a	a	a	f	b	e	e	e	e	e	e	b	c	c	c	c	c	c	c	c
BARGAIN HILL	a	a	a	a	b	a	f	c	c	c	c	c	c	e	c	e	e	c	e	e	e	e	e
LENDALFOOT	a	a	a	a	a	a	f	b	c	c	c	c	c	c	c	c	c	c	c	c	c	c	c

a — Well recorded clear arrival

b — Recognisable but noisy arrival

c — Arrival obscured by noise

d — Dirty tape heads — not recorded

e — Equipment malfunction

f — Poor shot

Kintyre stations did not record MSF

TRAVEL TIMES AND RANGES FOR SHOTS RECEIVED - PHASE 1

Station	Shot	Travel Time (sec)	Range (km)
Barra	1	36.51	252.65
	2	34.52	234.52
	3	32.32	215.72
	4	30.05	198.62
	5	27.62	179.16
	6	26.67	170.43
	8	24.82	155.71
	9	23.71	143.28
	10	22.99	137.38
	11	21.64	130.33
	12	20.66	122.05
	13	19.79	116.03
	15	17.51	104.98
	16	15.65	93.89
	17	14.27	84.46
	18	12.76	74.63
	19	10.10	60.16
	20	7.07	40.37
	21	5.90	31.41
	22	4.10	20.88
	23	0.30	2.72
Ruaig	2	26.86	170.64
	15	7.11	41.08
	16	5.35	29.98
	17	3.77	20.53
	18	2.32	10.69
	19	0.51	4.15
	21	6.03	32.59
	22	7.78	43.12
	23	10.51	61.81
Vaul	6	18.42	108.96
	18	0.28	1.32
	19	3.02	13.27
Mull	2	22.93	135.74
	3	20.43	116.93
	4	16.92	99.81
	14	2.33	12.77
	15	1.20	6.48
	16	1.59	8.36
	17	3.04	15.86
	18	5.00	25.29
	19	6.84	39.82
	20	10.14	59.36
	21	11.83	68.30
	22	13.66	78.79
	23	16.20	97.44

CONTD..

Station	Shot	Travel Time (sec)	Range (km)
Iona	15	1.80	9.90
	16	0.95	3.98
	17	2.24	11.03
	18	3.93	20.65
	19	6.13	35.23
	20	9.46	54.88
	22	12.80	74.37
	23	15.55	93.04
Colonsay	1	21.23	126.69
	4	12.48	72.65
	9	3.32	17.31
	10	2.18	11.41
	11	0.86	4.39
	17	7.50	41.62
	18	9.36	51.43
	22	18.08	105.10
M. Jura	1	17.00	100.20
	2	14.26	82.06
	3	11.27	63.26
	4	8.10	46.17
	5	4.94	26.73
	6	3.34	17.99
	8	0.57	3.35
	9	1.78	9.19
	10	3.04	15.08
	11	4.17	22.13
	12	5.51	30.45
	13	6.51	36.48
	14	7.56	41.76
	15	8.45	47.98
	16	10.28	58.64
	17	11.83	68.10
	18	13.59	77.92
	19	15.48	92.31
	20	18.76	112.09
	21	20.50	121.05
	22	22.10	131.59
	23	23.95	150.27

Station	Shot	Travel Time (sec)	Range (km)
S. Jura	1	16.62	98.17
	2	13.90	80.03
	3	10.90	61.24
	4	7.72	44.15
	5	4.57	24.73
	6	2.97	15.99
	8	0.18	1.33
	11	4.52	24.16
	12	5.87	32.48
	13	6.92	38.52
	14	7.89	43.80
	15	8.80	50.02
	16	10.65	60.67
	17	12.18	70.13
	18	15.84	79.95
	19	13.91	94.33
	20	19.15	114.11
	21	20.87	123.07
	22	22.46	133.61
	23	24.31	152.29
Letterpin	1	1.77	9.01
	2	4.34	22.51
	3	7.35	40.56
	4	9.63	57.40
	5	13.06	76.76
	6	14.54	85.51
	8	16.93	100.30
	15	24.41	150.88
	16	26.11	161.91
	20	33.61	215.44
Cundry Mains	1	1.00	3.07
	2	3.99	19.16
	3	7.05	37.87
	4	9.40	54.95
	5	12.89	74.41
	6	14.32	83.13
	8	16.62	97.88
Knockbain	1	1.08	4.69
	2	4.21	20.13
	3	7.30	38.71
	5	13.03	75.20
	6	14.52	83.93
Currarie	1	1.36	6.11
	2	4.07	20.93
	3	7.11	39.37
	4	9.56	56.35
	6	14.40	84.52

CONTD..

Station	Shot	Travel Time (sec)	Range (km)
Breaker Hill	1	1.37	7.16
	2	4.42	23.21
	3	7.46	41.72
	4	9.78	58.73
	5	13.29	78.15
	6	14.70	86.89
Bargain Hill	1	1.61	8.50
	2	4.62	24.61
	3	7.46	43.07
	4	9.96	60.05
	6	14.88	88.21
Lendalfoot	1	0.64	3.07
	2	3.78	19.16
	3	6.92	37.87
	4	9.20	54.95
	6	14.16	83.13
	8	16.51	97.88
LOWNET STNS			
Achinoon	8	25.80	152.67
	14	29.86	180.29
	17	32.47	201.82
	18	33.67	210.00
	20	36.83	240.26
Aberfoyle	19	25.73	158.52
	20	28.36	174.70
	21	29.51	182.44
	22	30.63	191.57
	23	31.68	208.19
Black Hill	8	31.12	197.47
	9	26.99	158.38
	12	27.70	167.51
	17	30.50	188.84
	18	31.40	195.65
	20	33.78	220.22
Broadlaw	5	27.60	136.02
	6	27.74	168.58
	17	36.10	228.77
	20	40.04	267.02
Dundee	2	30.30	191.79
	4	29.03	187.07
	6	29.69	189.77

CONTD..

Station	Shot	Travel Time (sec)	Range (km)
Gala Law	1	26.44	160.99
	2	26.88	163.39
	3	27.71	168.03
	4	28.52	173.79
	6	29.69	187.82
	8	31.12	197.47
	15	34.61	226.78
	19	39.06	264.66
Eskdalemuir	6	27.24	169.78
	18	37.71	250.97
	20	41.53	283.32

TRAVEL TIMES AND RANGES FOR SHOTS RECEIVED - PHASE 2

Station	Shot	Travel Time (sec)	Range (km)
Mull	1	11.93	68.29
	2	11.29	64.79
	3	10.58	61.35
	4	7.64	43.03
	5	6.53	36.15
	6	5.27	29.41
	7	4.07	22.74
	8	3.62	18.40
	9	2.91	15.30
	10	1.84	9.59
Iona	1	12.53	71.96
	2	11.84	68.43
	3	11.28	64.98
	4	8.29	46.50
	5	7.11	39.55
	6	5.80	32.68
	7	4.73	25.96
	8	4.51	21.62
	9	3.41	18.50
	10	2.43	12.74
Colonsay	1	7.29	40.81
	2	6.54	37.24
	3	5.95	33.79
	4	2.77	15.16
	5	1.61	8.18
	7	0.99	5.55
	8	1.78	9.90
	9	2.35	13.02
	10	3.55	18.81
N. Jura	1	4.14	22.09
	2	3.48	18.53
	3	2.76	15.08
	4	0.83	3.60
	5	2.06	10.53
	6	3.34	17.51
	7	4.33	24.13
	8	5.25	28.40
	9	5.82	31.50
	10	6.76	37.23
S. Jura	1	2.30	12.41
	2	1.66	8.84
	3	0.92	5.41
	4	2.68	13.28
	5	3.78	20.25
	6	4.97	27.23
	7	6.08	33.87
	8	6.87	38.15
	9	7.47	41.25

Station	Shot	Travel Time (sec)	Range (km)
N. Kintyre	1	2.65	13.77
	2	3.33	17.34
	3	3.94	20.78
	4	7.27	39.42
	5	8.24	46.38
	6	9.48	53.36
	7	10.38	59.94
	8	11.26	64.17
	9	11.79	67.24
	10	12.70	72.91

APPENDIX 2

129

LIST OF COMPUTER PROGRAMS

TPTODSC.G

TPTODSC.D

CHPLOT.G

CHPLOT.D

CHDUMP.G

CHDUMP.D

TCPLOTS

TIMESAMP

FREQPLOT

GEOPLOT

DURHPLOT

GEOSECT.G

GEOSECT.T

DURHSECT.N

AGINTER

Those programs beginning with GEO and with the suffix .G are for use on data recorded on Geostore recorders and digitized at I.G.S. In Edinburgh. Those beginning with DUR and with the suffix .D are for use on data recorded on Durham Mk.3 recorders and digitized on the seismic processing equipment at Durham. They are same in structure and the only difference is that they call different subroutines. Therefore, only those for the Geostore data have been presented.

```
C
C***********************************************************************
C
C     NOTES ON PROGRAMS AND SUBROUTINES
C     ------------------------------------------
C
C
C     UNIT 1 IS USED FOR READING DATA
C     UNIT 7 IS USED FOR WRITING DATA TO A FILE
C     UNITS 5 & 6 ARE FOR INTERACTIVE USE
C
C     ALL PROGRAMS ARE WRITTEN FOR USE ON DATA WITH A
C     SAMPLING RATE OF 64 SAMPLES PER SECOND FOR
C     GEOSTORE RECORDINGS AND 5Ø SAMPLES PER SECOND
C     FOR MK.3 RECORDINGS.
C     IF THE SAMPLING RATE DIFFERS TO THIS THEN PARAMETERS
C     SUCH AS PULSE WIDTH IN THE DECODING ROUTINES WILL
C     NEED TO BE ALTERED AND CERTAIN OF THE HANDLING & PLOTTING
C     PARAMETERS. INSPECTION TO FIND MULTIPLES OF 64 AND
C     5Ø WILL INDICATE WHICH PARAMETERS NEED TO BE CHANGED.
C     THE PULSE WIDTH FOR DIFFERENT SAMPLING RATES CAN BE
C     FOUND USING PROGRAM TCPLOTS.
C
C
C     COMMON BLOCKS
C     -------------
C
C     SIX ARE USED:-
C
C     COMMON/A/ NSSAMP
C     COMMON/B/ LSAMP,ISEIS
C     COMMON/C/ ITCHAN,ISEIS1,ISEIS2,ISEIS3
C     COMMON/D/ NRANGE
C     COMMON/E/ IIHR,IIMIN,IISEC,FRAC
C     COMMON/F/ JCHAN
C
C     PARAMETERS:-
C
C     NSSAMP- NO. OF SAMPLES TO REQUESTED TIME
C     LSAMP - NO. OF SAMPLES AFTER NSSAMP TO PROCESS
C     ISEIS - NO. OF SEISMIC CHANNEL IN FILE, USED IN
C             PLOTTING REDUCED SECTION
C     ITCHAN- NO. OF TIME CHANNEL IN FILE
C     ISEIS1,ISEIS2,ISEIS3- TRACE NUMBERS OF THE THREE
C                           SEISMIC CHANNELS IN FILE
C     IIHR,IIMIN,IISEC,FRAC- TIME REQUIRED (SAMPLE NO. TO
C                           THIS TIME IS FOUND BY ROUTINES)
C     JCHAN - SEISMIC CHANNEL TO DUMP
C
C
C     OTHER PARAMETERS DEFINED BY CALLING PROGRAMS AND
C     SUBROUTINES THEMSELVES.
C
C
```

```
C*************************************************************************
C
C      PROGRAM TPTODSC.G
C      --------------------------
C
C  THIS PROGRAM TRANSFERS UP TO 8 DATA CHANNELS FROM
C  9-TRACK DIGITAL TAPE TO A PERMANENT DISK FILE.
C  BYTE-SWAPPING IS CARRIED OUT AS THE DATA WERE
C  WRITTEN TO TAPE USING A PDP 11/34.
C  DEMULTIPLEXING IS CARRIED OUT BEFORE WRITING TO A LINE
C  FILE AS ONE CHANNEL PER LINE UNFORMATTED.
C  EACH FILE ON TAPE CONTAINING DATA FOR ONE SHOT IS
C  GIVEN HEADER INFORMATION ON TRANSFER AND THE DISK FILE
C  CAN BE TREATED AS MANY SUB-FILES OF UP TO 8 CHANNELS.
C  OF A SINGLE SHOT SEPARATED BY THE HEADER.
C
C  DATA ARE READ FROM UNIT 1 AND WRITTEN TO UNIT 7
C  HEADER INFORMATION IS READ FROM UNIT 2
C
C  THE PROGRAM IS USED ON DATA DIGITIZED ON
C  THE SEISMIC PROCESSING SYSTEM AT I.G.S. EDINBURGH
C
C*************************************************************************
C
C  ISAM-ARRAY CONTAINING DEMULTIPLEXED DATA
C  IST-ELEMENT IN ARRAY WHERE FIRST SAMPLE OF EACH
C       TRACE IS STORED
C  ISTORE-LAST ELEMENT OF EACH TRACE
C  NOSAM-NO. OF SAMPLES IN EACH TRACE
C  BLK,SAMP-ARRAYS CONTAINING DATA READ FROM 1 BLOCK IN FILE
C  RBLK,RSAMP-ARRAYS CONTAINING ABOVE DATA AFTER BYTE SWAP
C  INFO-HEADER INFO. FOR EACH FILE READ
C  LEN,LNUM-REFER TO SUBROUTINE READ & WRITE (MTS MANUAL)
C
C
      DIMENSION IST(8),ISTOR(8),INFO(19)
      INTEGER LNUM
      INTEGER*2 RBLK(2048),BLK(2048),ISAM(400000),LEN
      LOGICAL*1 SAMP(4096),RSAMP(4096)
      EQUIVALENCE (BLK(1),SAMP(1)),(RBLK(1),RSAMP(1))
      DATA IST(1)/1/,IST(2)/40000/,IST(3)/80000/,IST(4)/120000/,
     %IST(5)/160000/,IST(6)/200000/,IST(7)/240000/,IST(8)/280000/
      NFILE=0
      WRITE(6,601)
C
C ENTER NO.OF FILES TO BE TRANSFERED AND NO. OF CHANNELS PER FILE
C
 601  FORMAT('ENTER NFILE1 & NCHAN'/'.....------')
      READ(5,202)NFILE1,NCHAN
 202  FORMAT(2I5)
  10  NFILE=NFILE+1
      IF(NFILE.GT.NFILE1) GO TO 20
      READ(2,201)INFO
 201  FORMAT(19A4)
      WRITE(7,201)INFO
      DO 15 I=1,8
  15  ISTOR(I)=IST(I)
      CALL READ(BLK,LEN,0,LNUM,1,&100)
      GO TO 30
  40  CALL READ(BLK,LEN,0,LNUM,1,&200)
  30  IBLK=LEN/2
      ICONT=LEN-1
```

/32

```
C
C 1 BLOCK OF DATA HAS NOW BEEN READ;PAIRS OF BYTES ARE NOW SWAPPED
C
      DO 25 I=1,ICONT,2
      CALL MOVEC(1,SAMP(I),RSAMP(I+1))
      CALL MOVEC(1,SAMP(I+1),RSAMP(I))
   25 CONTINUE
C
C DATA NOW IN FORMAT TO READ ON MTS;DEMULTIPLEX AND WRITE TO
C DISC FILE USING ROUTINE BELOW.
C
      JCH=0
      DO 35 I=1,NCHAN
      JCH=JCH+1
      NOSAM=ISTOR(I)
   .  DO 45 J=JCH,IBLK,NCHAN
      ISAM(NOSAM)=RBLK(J)
      NOSAM=NOSAM+1
   45 CONTINUE
      ISTOR(I)=NOSAM
   35 CONTINUE
      GO TO 40
  200 DO 55 J=1,NCHAN
      IBEG=IST(J)
      NOSAM=ISTOR(J)-IST(J)
      LEN=NOSAM*2
   55 CALL WRITE(ISAM(IBEG),LEN,0,LNUM,7)
      GO TO 10
  100 WRITE(6,500)
  600 FORMAT('***********WARNING EOF IN FIRST BLOCK***********')
   20 STOP
      END
```

```
C************************************************************************
C
C      PROGRAM TPTODSC.D
C      ---------------------
C
C  THIS PROGRAM TRANSFERS UP TO 6 DATA CHANNELS FROM
C  9-TRACK DIGITAL TAPE TO A PERMANENT DISK FILE.
C  DEMULTIPLEXING IS CARRIED OUT BEFORE WRITING TO A LINE
C  FILE AS ONE CHANNEL PER LINE UNFORMATTED.
C  EACH FILE ON TAPE CONTAINING DATA FOR ONE SHOT IS
C  GIVEN HEADER INFORMATION ON TRANSFER AND THE DISK FILE
C  CAN BE TREATED AS MANY SUB-FILES OF UP TO 6 CHANNELS
C  PER SHOT SEPARATED BY THE HEADER.
C
C  DATA ARE READ FROM UNIT 1 AND WRITTEN TO UNIT 7
C  HEADER INFORMATION IS READ FROM UNIT 2
C  THE MAXIMUM NUMBER OF BYTES THAT CAN BE
C  TRANSFERRED IS 32767
C
C  THE PROGRAM IS USED ON DATA DIGITIZED ON
C  THE SEISMIC PROCESSING SYSTEM AT DURHAM            .
C
C************************************************************************
C
C  ISAM-ARRAY CONTAINING DEMULTIPLEXED DATA
C  IST-ELEMENT IN ARRAY WHERE FIRST SAMPLE OF EACH
C       TRACE IS STORED
C  ISTORE-LAST ELEMENT OF EACH TRACE
C  NOSAM-NO. OF SAMPLES IN EACH TRACE
C  BLK-MULTIPLEXED DATA
C  RBLK- ARRAY CONTAINING DEMULIPLEXED DATA TO COPY TO ISAM
C  INFO-HEADER INFO. FOR EACH FILE READ
C  LEN,LNUM-REFER TO SUBROUTINE READ & WRITE (MTS MANUAL)
C
C
      DIMENSION IST(8),ISTOR(8),INFO(19)
      INTEGER LNUM
      INTEGER*2 RBLK(160000),BLK(256),ISAM(160000),LEN,LEN1,LEN2
      DATA IST(1)/1/,IST(2)/20000/,IST(3)/40000/,IST(4)/60000/,
     #IST(5)/80000/,IST(6)/100000/,IST(7)/120000/,IST(8)/140000/
      LEN1=5
      NFILE=0
      WRITE(6,601)
C
C  ENTER NO.OF FILES TO BE TRANSFERED AND NO. OF CHANNELS PER FILE
C  & NO. OF BLOCKS TO TRANSFER
C
 601  FORMAT('ENTER NFILE1 & NCHAN & JBLK1'/'.....-----.....')
      READ(5,202)NFILE1,NCHAN,JBLK1
 202  FORMAT(3I5)
  10  NFILE=NFILE+1
      IF(NFILE.GT.NFILE1) GO TO 20
      JBLK=0
      READ(2,201)INFO
 201  FORMAT(19A4)
      WRITE(7,201)INFO
      DO 15 I=1,8
  15  ISTOR(I)=IST(I)
      JBEG=0
      CALL CNTRL('FSR 1',LEN1,1,RET,&300,&300,&300)
      CALL READ(BLK,LEN,0,LNUM,1,&100)
      GO TO 30
  50  CALL READ(BLK,LEN,0,LNUM,1,&200)
```

```
C
C   READ REQUIRED NO. OF BLOCKS INTO LARGE ARRAY
C
   30 DO 40 I=1,256
      RBLK(JBEG+I)=BLK(I)
   40 CONTINUE
      JBEG=JBEG+256
      JBLK=JBLK+1
      IF (JBLK.LT.JBLK1) GOTO 50
      CALL CNTRL('FSF 1',LEN1,1,RET,&300,&300,&300)
  200 JCH=0
      DO 35 I=1,NCHAN
      JCH=JCH+1
      NOSAM=ISTOR(I)
C
C   DEMULTIPLEX LARGE ARRAY AND WRITE EACH TRACE TO DISK
C   ONE LINE PER TRACE
C
      DO 45 J=JCH,JBEG,NCHAN
      ISAM(NOSAM)=RBLK(J)
      NOSAM=NOSAM+1
   45 CONTINUE
      ISTOR(I)=NOSAM
   35 CONTINUE
      DO 55 J=1,NCHAN
      IBEG=IST(J)
      NOSAM=ISTOR(J)-IST(J)
      LEN=NOSAM*2
   55 CALL WRITE(ISAM(IBEG),LEN,0,LNUM,7)
      CALL CNTRL('FSF 2',LEN1,1,RET,&100,&100,&100)
      GO TO 10
  100 WRITE(6,600)
  600 FORMAT('***********WARNING EOF IN FIRST BLOCK************')
  300 WRITE(6,602)
  602 FORMAT('*********ERROR IN MOVING TO EOF**********')
   20 STOP
      END
```

```
C***********************************************************************
C
C      PROGRAM CHPLOT.G
C      ------------------------
C
C      THIS PROGRAM TAKES UNFORMATTED DATA FROM A FILE ON DISK
C      AND PLOTS THEM. UP TO 8 CHANNELS CAN BE PLOTTED.
C      THE FILE MUST HAVE A HEADING ('A' FORMAT) AND BE FOLLOWED
C      BY THE APPROPRIATE NUMBER OF TRACES FOR THE EVENT.
C      FOR 'WISE' THIS PROGRAM WAS USED FOR GEOSTORE RECORDS
C
C      DATA ARE READ FROM UNIT 1
C
C
C***********************************************************************
C
C
       DIMENSION INFO(20),XCOORD(40000),IST(8),COORD(8000)
       INTEGER LNUM
       REAL ASAMP(40000)
       INTEGER*2 ISAM(320000),LEN
       DATA IST(1)/1/,IST(2)/40000/,IST(3)/80000/,IST(4)/120000/,
      %IST(5)/160000/,IST(6)/200000/,IST(7)/240000/,IST(8)/280000/
       WRITE(6,601)
C
C ENTER NO. OF CHANNELS TO BE PLOTTED
C AND READ IN DATA
C
  601 FORMAT('ENTER NCHAN'/'...')
       READ(5,501)NCHAN
  501 FORMAT(I3)
       READ(1,101)INFO
  101 FORMAT(20A4)
       DO 15 J=1,NCHAN
       IBEG=IST(J)
       CALL READ(ISAM(IBEG),LEN,0,LNUM,1,10)
   15 CONTINUE
       ICONT=LEN/2
   10 X=FLOAT(ICONT)/500.0
C
C GENERATE AXES & BORDER
C
       CALL PAXIS(1.0,1.0,INFO,76,-10.5,90.0,0.0,1.0,1.0)
       CALL PAXIS(1.0,1.0,'NO. OF SAMPLES',-14,X,0.0,0.0,500.0,1.0)
       CALL PGRID(1.0,1.0,X,10.5,1,1)
       Z=0.0
       DO 25 I=1,ICONT
       Z=Z+1.0
       XCOORD(I)=Z
   25 CONTINUE
       WRITE(7,701)XCOORD(ICONT)
  701 FORMAT(4F12.0)
C
C GENERATE PLOT OF ALL CHANNELS
C
       Y=9.5
       CALL PLTOFS(0.0,500.0,0.0,1.0,1.0,1.0)
       DO 35 J=1,NCHAN
       JST=IST(J)-1
       IF (J.LE.2) GO TO 100
       DO 45 I=1,ICONT
       ASAMP(I)=(ISAM(JST+I)*0.0025)+Y
   45 CONTINUE
       GO TO 200
  100 DO 55 I=1,ICONT
       ASAMP(I)=(ISAM(JST+I)*0.00025)+Y
   55 CONTINUE
  200 CALL PENUP(1.0,Y)
       CALL PLINE(XCOORD,ASAMP,ICONT,1,0,0,1)
       Y=Y-1.25
   35 CONTINUE
       CALL PLTEND
       STOP
       END
```

```
C*************************************************************************
C
C      PROGRAM CHDUMP.G
C      -------------------
C
C
C      THIS PROGRAM DECODES THE TIME CODE RECORDED ON A
C      GEOSTORE RECORDER AND DUMPS THE TIME TRACK AND
C      A REQUESTED SEISMIC TRACK TO ANOTHER FILE FROM
C      THE TIME REQUIRED.
C
C      DATA ARE READ FROM UNIT 1
C      DATA ARE WRITTEN TO UNIT 7
C
C*************************************************************************
C
C
       DIMENSION IST(8),INFO(20)
       INTEGER*2 ISAM(160000),LEN
       INTEGER LNUM
       COMMON /A/NSSAMP
       COMMON /C/ITCHAN,ISEIS1,ISEIS2,ISEIS3
       COMMON /F/JCHAN
       COMMON /E/IIHR,IIMIN,IISEC,FRAC
       DATA IST(1)/1/,IST(2)/20000/,IST(3)/40000/,IST(4)/60000/,
      #IST(5)/80000/,IST(6)/100000/,IST(7)/120000/,IST(8)/140000/
       NFILE1=0
C
C  ENTER NUMBER OF FILES, CHANNELS AND SHOTS IN EACH FILE
C  AND SECONDS TO DECODE
C
       WRITE(6,601)
 601   FORMAT('ENTER NFILE,NCHAN,NSHOT & NO. OF SECS TO DECODE'/
      #'.....-----.....-----')
       READ(5,501)NFILE,NCHAN,NSHOT,MSEC
 501   FORMAT(4I5)
C
C  ENTER TIME CHANNEL AND SEISMIC CHANNEL
C
       WRITE(6,602)
 602   FORMAT('ENTER TCHANNEL & SEISMIC CHANNEL REQD.'/'...---')
       READ(5,502)ITCHAN,JCHAN
 502   FORMAT(2I3)
   1   IF (NFILE1 .EQ.NFILE) GO TO 100
       NFILE1=NFILE1+1
       READ(1,101)INFO
 101   FORMAT(20A4)
       DO 20 J=1,NCHAN
       IBEG=IST(J)
       CALL READ(ISAM(IBEG),LEN,0,LNUM,1,&100)
  20   CONTINUE
       DO 10 KK=1,NSHOT
C
C  ENTER TIME TO DUMP FROM
C
       WRITE(6,605)
 605   FORMAT('ENTER HOUR,MINUTE,SECOND,FRACTION OF SECOND'/
      #'.....-----.....-----')
       READ(5,505)IIHR,IIMIN,IISEC,FRAC
 505   FORMAT(3I5,F5.0)
       CALL GDCODE(ISAM,MSEC,LEN,IST)
   3   CALL DUMP(ISAM,IST,LEN,INFO)
  10   CONTINUE
       GO TO 1
 100   STOP
       END
```

```
C************************************************************
C
C      PROGRAM TCPLOTS
C      ------------------
C
C
C    THIS PROGRAM PLOTS A SMALL SECTION OF THE INTERNAL
C    TIME CODE AND MSF. THE DIFFERENCE IN SAMPLES BETWEEN
C    THE TWO CAN THEN BE USED FOR THE TIMING CORRECTIONS
C    IN THE LATER PROCESSING STAGES.
C
C************************************************************
C
C
       DIMENSION XCOORD(1000),INFO(19),IST(8)
       INTEGER*2 ISAM(320000),LEN
       REAL ASAM(1000)
       INTEGER LNUM
       DATA IST(1)/1/,IST(2)/40000/,IST(3)/80000/,IST(4)/120000/,
      #IST(5)/160000/,IST(6)/200000/,IST(7)/240000/,IST(8)/280000/
C
C    ENTER NUMBER OF CHANNELS IN FILE AND THE
C    TWO TIME CHANNELS
C    READ IN THE DATA
C
       WRITE(6,601)
  601 FORMAT('ENTER NCHAN,TIME CHANNELS- 3I2')
       READ(5,501)NCHAN,IT1,IT2
  501 FORMAT(3I2)
    1 READ(1,101)INFO
  101 FORMAT(19A4)
       DO 10 I=1,NCHAN
       IBEG=IST(I)
       CALL READ(ISAM(IBEG),LEN,0,LNUM,1,&700)
   10 CONTINUE
       Z=0.0
       DO 20 J=1,500
       Z=Z+1.0
       XCOORD(J)=Z
   20 CONTINUE
C
C   GENERATE PLOT OF TIME CODES
C
       CALL PAXIS(1.0,1.0,INFO,76,-9.0,90.0,0.0,1.0,1.0)
       CALL PAXIS(1.0,1.0,'SAMPLES',-7,20.0,0.0,0.0,25.0,1.0)
       CALL PGRID(1.0,1.0,20.0,9.0,1,1)
       Y=7.0
       CALL PLTOFS(0.0,25.0,0.0,1.0,1.0,1.0)
       FACTOR=0.001
       JBEG=IST(IT1)+1000
       DO 40 II=1,500
       ASAM(II)=(ISAM(JBEG+II)*FACTOR)+Y
   40 CONTINUE
       CALL PENUP(1.0,Y)
       CALL PLINE(XCOORD,ASAM,500,1,1,13,1)
       Y=Y-4.0
       IBEG=IST(IT2)+1000
       DO 30 JJ=1,500
       ASAM(JJ)=(ISAM(JJ+IBEG)*FACTOR)+Y
   30 CONTINUE
       CALL PENUP(1.0,Y)
       CALL PLINE(XCOORD,ASAM,500,1,1,13,1)
       CALL PLTEND
  700 STOP
       END
```

```
C***************************************************************
C
C     PROGRAM TIMESAMP
C     ------------------
C
C     THIS PROGRAM FINDS THE NUMBER OF SAMPLES IN EACH SECOND
C     FOR A SECTION OF THE TIME CODE RECORDED ON THE MK.3
C     RECORDER. IT IS USED TO DETERMINE THE AVERAGE SAMPLING RATE
C     AND FOR TIMING OF SHOTS WHEN FULL FLUTTER COMPENSATION
C     IS NOT ACHIEVED
C
C***************************************************************
C
C
      INTEGER*2 ISAM(320000),LEN
      DIMENSION IST(8),INFO(20)
      DATA IST(1)/1/,IST(2)/40000/,IST(3)/80000/,IST(4)/120000/,
     #IST(5)/160000/,IST(6)/200000/,IST(7)/240000/,IST(8)/280000/
C
C  ENTER NO. OF SHOTS IN A FILE, NO. OF CHANNELS,
C  TIME CHANNEL AND NO. OF SECONDS TO DECODE.
C
      WRITE(6,601)
  601 FORMAT('ENTER NO. SHOTS,CHANNELS,TIME CHANNEL & NO. SECS'/
     #'.....-----.....-----')
      READ(5,501)NSHOT,NCHAN,ITCHAN,MSEC
  501 FORMAT(4I5)
      DO 10 I=1,NSHOT
      READ(1,101)INFO
  101 FORMAT(20A4)
      DO 20 J=1,NCHAN
      IBEG=IST(J)
      CALL READ(ISAM(IBEG),LEN,0,LNUM,1,&100)
   20 CONTINUE
      WRITE(7,101)INFO
C
C***************************************************************
C
      SUBROUTINE TIMESC(ISAM,IST,LEN,ITCHAN,MSEC)
C
C     THIS IS AN EDITED VERSION OF SUBROUTINE MDCODE AND IS
C     USED TO LOCATE SECOND MARKERS
C
C     ISAM = DATA ARRAY
C     IST = STARTING ELEMENT OF EACH TRACE IN ARRAY
C     LEN = NUMBER OF BYTES IN TRACE
C     ITCHAN = TIME CHANNEL
C     MSEC = NUMBER OF SECONDS TO DECODE
C
      INTEGER*2 LEN,ISAM(320000),JSAMP(100000),ID(6),
     #NSEC(300),JSEC(300)
      DIMENSION IST(8)
      INTEGER LNUM
C
C  READ IN TIME REQD. IIHR,IIMIN,IISEC,FRAC,MCHAN
C  MSEC =NO. OF SECS TO DECODE.
C
      WRITE(7,701)
  701 FORMAT('NO. OF SAMPLES TO SECOND          AVERAGE NO. OF SAMPLES
     #IN SECOND')
      IMAX=0
      IMIN=100
      NY=1
      LSEC=1
      DO 50 I=1,100000
      JSAMP(I)=0
   50 CONTINUE
      IBEG=IST(ITCHAN)-1
      ICONT=LEN/2
      DO 60 I=1,ICONT
      IF (ISAM(I+IBEG) .GT. IMAX ) IMAX=ISAM(I+IBEG)
      IF (ISAM(I+IBEG) .LT. IMIN) IMIN=ISAM(I+IBEG)
   60 CONTINUE
      JMIN=2*(IMAX+IMIN)/3
      DO 70 J=1,ICONT
      IF (ISAM(J+IBEG+1) .GT.JMIN) JSAMP(J)=1
      IF (ISAM(J+IBEG+1) .LE.JMIN) JSAMP(J)=0
   70 CONTINUE
```

```
      JJ=2
    1 IF(JSAMP(JJ-1).EQ.1) GO TO 2
      JJ=JJ+1
      GO TO 1
    2 LSAM=JJ-1
      DO 10 II=JJ,100
      IF(JSAMP(II).EQ.0 .AND. JSAMP(II-1).EQ.1 .AND.
     #JSAMP(II+1).EQ.0) GO TO 3
      LSAM=LSAM+1
   10 CONTINUE
C
C     RISING PULSE-IST SEC.
C
    3 NSEC(1)=LSAM
      WRITE(7,709)LSAM
  709 FORMAT('NO. OF SAMPLES TO 1ST SECOND=',I3)
      DO 20 J=2,MSEC
      LSEC=LSEC+1
      NY=NY+1
      NOSAM=LSAM+1
      IF (NY.EQ.MSEC) GO TO 100
      NX=0
      DO 30 I=NOSAM,ICONT
      LSAM=LSAM+1
      IF(JSAMP(I).EQ.0) NX=NX+1
      NCONT1=JSAMP(I-1)+JSAMP(I)+JSAMP(I+1)
      IF (NCONT1.EQ.1) JSAMP(I)=0
      IF (NCONT1.EQ.1) NX=NX+1
      IF (JSAMP(I-1).EQ.1 .AND. JSAMP(I) .EQ. 1
     #.AND. JSAMP(I+1) .EQ. 0) GO TO 4
   30 CONTINUE
    4 NSEC(J)=LSAM
      LSAMAV=(NSEC(J)-NSEC(1))/(NY-1)
      WRITE(7,705)LSAM,LSAMAV
  705 FORMAT(8X,I5,30X,I5)
      IF (NX .LT. 50) JSEC(J)=2
      IF (NX .LT. 25) JSEC(J)=1
      IF (NX .LT. 15) JSEC(J)=0
      IF (JSEC(J) .NE. 2) GO TO 20
C
C     MINUTE MARKER
C
    5 WRITE(6,601)
  601 FORMAT('MINUTE PULSE DETECTED')
   20 CONTINUE
  100 RETURN
      END
```

```
C***********************************************************************
C
C      PROGRAM FREQPLOT
C      -------------------
C
C    THIS PROGRAM TRANSFORMS A TIME SERIES INTO
C    THE FREQUENCY DOMAIN AND PLOTS THE AMPLITUDE
C    SPECTRUM
C
C    *GHOST ROUTINES ARE USED
C***********************************************************************
C
C
      INTEGER*2 ISAM(5000),LEN
      REAL*8 X(4096),Y(4096),S(4096)
      REAL*4 TITLE(20),A(4096),XCOORD(4096)
C
C   ENTER TITLE, NO. OF SAMPLES, SAMPLING RATE
C   AND READ IN DATA
C
      WRITE(6,601)
 601  FORMAT('ENTER TITLE')
      READ(5,501)TITLE
 501  FORMAT(20A4)
      WRITE(6,602)
 602  FORMAT('ENTER NO. SAMPLES,SAMP. RATE'/'.....----- I5,F5.0')
      READ(5,502)LX,SAMPR
 502  FORMAT(I5,F5.0)
      CALL READ(ISAM,LEN,0,LNUM,1,&100)
      DO 10 I=1,LX
      X(I)=ISAM(I)
      S(I)=0.0
      Y(I)=0.0
 10   CONTINUE
C
C   TRANSFORM DATA, FORM AMPLITUDE SPECTRUM,
C   NORMALISE TO THE MAXIMUM AMPLITUDE AND PLOT
C
      CALL SINTAB(LX,S)
      SIGNI=-1.0
      CALL FFTA(LX,X,Y,SIGNI,S)
      LSAMP=LX/2
      FFREQ=SAMPR/LX
      XMAX=0.0
      DO 20 I=1,LSAMP
      X(I)=DSQRT(X(I)**2+Y(I)**2)
      XCOORD(I)=FFREQ*FLOAT(I)
      IF (X(I) .GT. XMAX) XMAX=X(I)
 20   CONTINUE
      FACT=1.0/XMAX
      DO 30 J=1,LSAMP
      A(J)=X(J)*FACT
 30   CONTINUE
      CALL PAPER(1)
      CALL PSPACE(0.05,0.80,0.05,0.55)
      CALL MAP(0.0,25.0,0.0,1.0)
      CALL AXES
      CALL CTRMAG(15)
      CALL PLOTCS(5.0,1.1,TITLE,80)
      CALL PTPLOT(XCOORD,A,1,LSAMP,-2)
      CALL GREND
 100  STOP
      END
```

```
C***********************************************************
C
C       PROGRAM GEOPLOT
C       -----------------
C
C
C       THIS PROGRAM TAKES 3 SEISMIC TRACES FROM A FILE
C       BANDPASSES THEM IF REQUIRED & PLOTS THEM WITH THE
C       TIME CODE BOTH SIDES IN ORDER TO PICK EVENTS
C       THE PROGRAM OPERATES ON GEOSTORE RECORDS
C
C       INPUT/OUTPUT DEVICES
C       UNIT 1=DATAFILE
C       UNIT 5=RUNNING PARAMETERS -TIMES, NO. OF SAMPLES ETC.
C       UNIT 6=INFO FOR ABOVE- FORMATS ETC.
C       UNIT 9=PLOTFILE
C
C
C***********************************************************
C
C
      DIMENSION TITLE(20),IST(8),JSTRT(3),INFO(20),OPTION(2)
      INTEGER*2 ISAM(160000),LEN
      INTEGER LNUM
      REAL*8 ASAM(15000),XSAM(5000),F1,F2,F3,F4,X(4096)
      COMMON/A/NSSAMP
      COMMON/B/LSAMP,ISEIS
      COMMON/C/ITCHAN,ISEIS1,ISEIS2,ISEIS3
      COMMON /E/IIHR,IIMIN,IISEC,FRAC
      DATA IST(1)/1/,IST(2)/20000/,IST(3)/40000/,IST(4)/60000/,
     #IST(5)/80000/,IST(6)/100000/,IST(7)/120000/,IST(8)/140000/,
     #JSTRT(1)/1/,JSTRT(2)/5000/,JSTRT(3)/10000/
      DATA OPTION(1)/'Y'/,OPTION(2)/'N'/
C
C   ENTER TITLE, NUMBER OF SECONDS, CHANNELS AND LENGTH
C   OF PLOT IN SAMPLES
C
      WRITE(6,601)
  601 FORMAT('ENTER TITLE')
      READ(5,501)TITLE
  501 FORMAT(20A4)
      WRITE(6,602)
  602 FORMAT('ENTER NO. OF SECS TO DECODE & NO. OF CHANNELS'/
     #'.....-----')
      READ(5,502)MSEC,NCHAN
  502 FORMAT(2I5)
      WRITE(6,603)
  603 FORMAT('ENTER NO. OF SAMPLES FOR PLOT, 1920=30SECS,960=15SECS'/
     #'.....    F5.0')
      READ(5,503)ZSAM
  503 FORMAT(F5.0)
C
C   ENTER TIME CHANNEL, SEISMIC CHANNELS AND
C   BANDPASSING PARAMETERS
C
      WRITE(6,604)
  604 FORMAT('ENTER TIME CHANNEL,SEISMIC1,SEISMIC2,SEISMIC3'/
     #'...---...---')
      READ(5,504)ITCHAN,ISEIS1,ISEIS2,ISEIS3
  504 FORMAT(4I3)
      WRITE(6,605)
  605 FORMAT('ENTER SAMPLING RATE'/'..... F5.0')
      READ(5,505)SAMPR
  505 FORMAT(F5.0)
      WRITE(6,606)
  606 FORMAT('IS BANDPASSING REQD.- ENTER Y OR N')
      READ(5,506)BOPT
  506 FORMAT(A1)
      LSAMP=ZSAM
      IF (BOPT .EQ. OPTION(2)) GO TO 3
```

```
      WRITE(6,607)
 607 FORMAT('ENTER NO. OF SAMPLES,HANNING WINDOW RANGE'/
    #'......------.....------......  I6,4F6.0')
      READ(5,507)LSAMP,F1,F2,F3,F4
 507 FORMAT(I6,4F6.0)
   3 ISEIS=1
      LX=LSAMP*2
      READ(1,101)INFO
 101 FORMAT(20A4)
      DO 10 I=1,NCHAN
      IBEG=IST(I)
C
C   READ IN DATA AND ENTER TIME TO START PLOT
C
      CALL READ(ISAM(IBEG),LEN,0,LNUM,1,&700)
  10 CONTINUE
      WRITE(6,608)
 608 FORMAT('ENTER HOUR,MINUTE,SECOND,FRACTION OF SECOND'/
    #'.....-----.....-----')
      READ(5,508)IIHR,IIMIN,IISEC,FRAC
 508 FORMAT(3I5,F5.0)
      CALL GDCODE(ISAM,MSEC,LEN,IST)
   6 CALL PLACE(ISAM,XSAM,ASAM,JSTRT,IST)
   1 CALL MEAN2(ASAM,XSAM,JSTRT)
      IF (BOPT .EQ. OPTION(2)) GO TO 2
      CALL PAD2(ASAM,JSTRT,LX,X)
      CALL BPASS2(ASAM,LX,F1,F2,F3,F4,JSTRT,X,SAMPR)
   2 CALL NORM1(XSAM,ASAM,LEN,KCONT,JSTRT,ZSAM)
      ISEIS=ISEIS+1
      IF (ISEIS .LE. 3) GO TO 1
      CALL PLOT1(ASAM,XSAM,TITLE,KCONT,JSTRT,ZSAM)
 700 STOP
      END
```

```
C*****************************************************************************
C
C      PROGRAM GEOSECT.N
C      --------------------
C
C
C
C      THIS PROGRAM TAKES DATA FROM A PERMANENT DISK FILE AND
C      ADJUSTS IT TO A FORM TO BE PLOTTED ON A REDUCED SEISMIC
C      SECTION,REDUCING IT BY ANY VELOCITY REQUIRED.
C      UP TO TWENTY-FIVE EVENTS CAN BE PLOTTED AND ANY OF THE
C      SEISMIC CHANNELS CAN BE SPECIFIED BY NAMING IT'S LINE NO.
C      IN THE FILE.
C      THE PROGRAM WAS WRITTEN FOR USE ON GEOSTORE RECORDS
C
C      DATA IS READ IN AS FOLLOWS:-
C
C         UNIT 1- SEISMIC DATA, UP TO 8 CHANNELS.
C         UNIT 2- RANGE OF EACH SHOT & DIFFERENCE IN SAMPLES
C                  BETWEEN TIMECODE & MSF.
C                  FORMAT - F10.0,I5
C         UNIT 5- NO. OF CHANNELS, NO. OF SEISMIC CHANNEL &
C                  NO. OF SECS. TO BE READ
C         UNIT 6- COMMANDS TO INDICATE FORMAT OF PARAMETERS
C         UNIT 8- TIMES OF EVENTS. HR,MIN,SEC,FRACTION OF SEC
C                  FORMAT - 4I5,F5.0
C         UNIT 9- PLOTFILE.
C         UNITS 5 & 6 ENABLE PARAMETERS TO BE ENTERED INTERACTVELY
C
C
C         BANDPASSING IS CARRIED OUT IF REQUIRED
C         EACH TRACE IS NORMALISED BEFORE PLOTTING
C
C*****************************************************************************
C
C      D =RANGE,MDIFF=DIFF. BETWEEN T.CODE & MSF IN SAMPLES
C      IST=STARTING ELEMENT OF TRACE IN ARRAY ISAM
C      ISTORE=STARTING ELEMENT OF TRACE IN ARRAY XSAM ( FOR PLOT)
C      INFO=HEADER INFORMATION FOR EACH SHOT
C      NSSAMP=NO. OF SAMPLES TO (T-D/V)=0 FOR SHOT
C
C
C
       DIMENSION IST(8),ISTRT(25),D(25),INFO(20),MDIFF(25),TITLE(10)
      #,OPTION(2)
       INTEGER*2 ISAM(160000),LEN,NOSAM
       REAL*8 F1,F2,F3,F4,X(4096),XSAM(75000)
       INTEGER LNUM
       DATA IST(1)/1/,IST(2)/20000/,IST(3)/40000/,IST(4)/60000/,
      #IST(5)/80000/,IST(6)/100000/,IST(7)/120000/,IST(8)/140000/,
      #ISTRT(1)/1/,ISTRT(2)/3000/,ISTRT(4)/9000/,
      #ISTRT(5)/12000/,ISTRT(6)/15000/,ISTRT(7)/18000/,
      #ISTRT(8)/21000/,ISTRT(9)/24000/,ISTRT(10)/27000/,
      #ISTRT(11)/30000/,ISTRT(12)/33000/,ISTRT(13)/36000/,
      #ISTRT(14)/39000/,ISTRT(15)/42000/,ISTRT(16)/45000/,
      #ISTRT(17)/48000/,ISTRT(18)/51000/,ISTRT(19)/54000/,
      #ISTRT(20)/57000/,ISTRT(21)/60000/,ISTRT(22)/63000/,
      #ISTRT(23)/66000/,ISTRT(24)/69000/,ISTRT(25)/72000/
       DATA OPTION(1)/'Y'/,OPTION(2)/'N'/
       COMMON /A/NSSAMP
       COMMON /B/LSAMP,ISEIS
       COMMON /C/ITCHAN,ISEIS1,ISEIS2,ISEIS3
       COMMON /D/NRANGE
       COMMON /E/IIHR,IIMIN,IISEC,FRAC
       NRANGE=0
       LSAMP=1600
C
C   ENTER TITLE, NO. OF SHOTS, CHANNELS IN FILE,
C   REDUCING VELOCITY AND SECONDS TO DECODE
C
       WRITE(6,601)
  601 FORMAT('ENTER TITLE')
       READ(5,501)TITLE
  501 FORMAT(10A4)
```

```
      WRITE(6,602)
  602 FORMAT('ENTER NO.OF SHOTS & NO. OF CHANNELS '
     #/'.....------')
      READ(5,502)NSHOT,NCHAN
  502 FORMAT(2I5)
      WRITE(6,603)
  603 FORMAT('ENTER REDUCING,VELOCITY'/' .....(F5.0)')
      READ(5,503)VEL
  503 FORMAT(F5.0)
      WRITE(6,604)
  604 FORMAT('ENTER NO. OF  SECONDS'/'.....')
      READ(5,504)MSEC
  504 FORMAT(I5)
C
C  ENTER SAMPLING RATE AND BANDPASSING PARAMETERS
C
      WRITE(6,605)
  605 FORMAT('ENTER SAMPLING RATE..... F5.0')
      READ(5,505)SAMPR
  505 FORMAT(F5.0)
      WRITE(6,606)
  606 FORMAT('IS BANDPASSING REQD.- ENTER Y OR N')
      READ(5,506)BOPT
  506 FORMAT(A1)
      IF (BOPT .EQ. OPTION(2)) GO TO 1
      WRITE(6,607)
  607 FORMAT('ENTER NO. OF  SAMPLES,HANNING WINDOW RANGE'/
     #'......------.....------...... I6,4F6.0')
      READ(5,507)LSAMP,F1,F2,F3,F4
  507 FORMAT(I6,4F6.0)
C
C  ENTER RANGES & DIFFERENCE IN SAMPLES BETWEEN TIME CODES
C
    1 DO 30 J=1,NSHOT
      READ(2,201)D(J),MDIFF(J)
  201 FORMAT(F10.0,I5,10X)
   30 CONTINUE
C
C  GO INTO LOOP, READ DATA FROM FILE AND ENTER
C  TIME REQUIRED. THEN SELECT SEISMIC CHANNEL
C  FROM THE NCHAN DATA CHANNELS FOR EACH SHOT
C  AND PROCESS IT BEFORE PLOTTING
C  THIS IS DONE NSHOT TIMES
C
      DO 20 K=1,NSHOT
      NRANGE=NRANGE+1
      READ(1,101)INFO
  101 FORMAT(20A4)
      DO 10 I=1,NCHAN
      IBEG=IST(I)
      CALL READ(ISAM(IBEG),LEN,0,LNUM,1,&700)
   10 CONTINUE
      LX=2*LSAMP
      READ(8,801)IIDAY,IIHR,IIMIN,IISEC,FRAC
  801 FORMAT(4I5,F5.0)
      ASEC=IISEC+FRAC+(ABS(D(NRANGE)))/VEL
      IISEC=ASEC
      FRAC=ASEC-IISEC
      IF(IISEC.LT.60) GOTO 7
      IISEC=IISEC-60
      IIMIN=IIMIN+1
    7 CALL GDCODE(ISAM,MSEC,LEN,IST)
   12 CALL ADJUST(IST,ISTRT,ISAM,MDIFF,XSAM,SAMPR)
      CALL MEAN1(ISTRT,XSAM)
      IF (BOPT .EQ. OPTION(2)) G TO 2
      CALL PAD1(XSAM,ISTRT,LX,X)
      CALL BPASS1(XSAM,LX,F1,F2,F3,F4,ISTRT,X,SAMPR)
    2 CALL NORM(NSHOT,ISTRT,XSAM,SAMPR)
   20 CONTINUE
      CALL PLOTG(ISTRT,D,NSHOT,TITLE,XSAM)
  700 STOP
      END
```

```
C******************************************************************
C
C         PROGRAM AGINTER
C         ----------------
C
C     THIS PROGRAM IS USED TO INTERPRET CLOSELY SPACED
C     REFRACTION DATA. THE DATA MUST CONSIST OF A REVERSED
C     LINE AND APPARENT VELOCITIES OF ARRIVALS AT STATIONS
C     AT EACH END. AN ITERATIVE PROCEDURE IS THEN USED
C     TO HOME IN ON THE TRUE REFRACTOR VELOCITY AND DEPTHS
C     BENEATH SHOT POINTS.
C
C     REFER TO TEXT FOR THE THEORY OF THE METHOD.
C
C     PARAMETERS:-
C
C     INPUT
C     -----
C
C     RANGA,RANGB - RANGES OF SHOTS FROM BOTH STATIONS
C     TTA,TTB - TRAVEL TIMES OF SHOTS FROM BOTH STATIONS
C     APVA,APVB - APPARENT VELOCITY OF SHOTS FROM STATIONS
C
C     READ IN THESE SHOT DATA CONSECUTIVELY FROM ONE END OF LINE
C     TO THE OTHER.
C
C     CALCULATED VALUES
C     -----------------
C
C     X1,X2 - DISTANCES ALONG REFRACTOR FROM SHOT WHERE RAY IS
C             FIRST REFRACTED
C     Z1,Z2 - DEPTH AT POINT WHERE RAY FROM SHOT IS REFRACTED
C     XX1,XX2 - DISTANCES ALONG REFRACTOR FROM STATION TO
C               POSITION WHERE RAY IS FIRST REFRACTED.
C     VELRA,VELRB - TRUE VELOCITY OF REFRACTOR FOUND BY
C                   INTERPOLATION. TWO SHOULD CONVERGE EVENTUALLY
C
C
C******************************************************************
C
C
      IMPLICIT REAL*8 (A-H,O-Z)
      DIMENSION X1(500),X2(500),Z1(500),Z2(500),XX1(500),XX2(500)
     #,VELRA(500),VELRB(500),TTA(500),TTB(500),RANGA(500),RANGB(500)
     #,APVA(500),APVB(500)
      COMMON /A/X1,X2,Z1,Z2,XX1,XX2
      COMMON /B/TTA,TTB,RANGA,RANGB,APVA,APVB
      COMMON /C/VELRA,VELRB
C
C     ENTER NUMBER OF ITERATIONS REQUIRED, NUMBER OF SHOTS
C     REFRACTOR AND OVERBURDEN VELOCITIES, STATION DELAYS
C     AND DISTANCE BETWEEN THE TWO STATIONS.
C     REFRACTOR VELOCITY IS FIRST ESTIMATE
C
      WRITE(6,601)
  601 FORMAT('ENTER NO. OF ITERATIONS , NO. OF SHOTS'/'...---')
      READ(5,501)ITER1,NSHOT
  501 FORMAT(2I3)
      DO 10 I=1,NSHOT
   10 READ(1,101)TTA(I),RANGA(I),APVA(I),TTB(I),RANGB(I),APVB(I)
  101 FORMAT(6F10.0)
      WRITE(6,602)
  602 FORMAT('ENTER REFRACTOR VEL. AND UPPER VEL.'/'.....-----')
      READ(5,502)VREF,V1
  502 FORMAT(2F5.0)
      WRITE(6,603)
  603 FORMAT('ENTER DELAY STNA.,DELAY STNB.,DISTAB'/'.....-----.....')
      READ(5,503)DA,DB,DISTAB
  503 FORMAT(3F5.0)
      VEL1=V1**2
      DO 20 I=1,NSHOT
      VELRA(I)=VREF
      VELRB(I)=VREF
   20 CONTINUE
```

```fortran
C
C     CALCULATE FIRST SOLUTION, WRITE OUT RESULTS
C
      CALL CALC(NSHOT,DA,DB,V1,VEL1)
      WRITE(7,701)
 701  FORMAT(///,3X,'RANGA',5X,'TTA',6X,'X1',5X,'XX1',6X,'Z1',4X,'APVA',
     #3X,'VELRA',3X,'RANGB',5X,'TTB',6X,'X2',5X,'XX2',6X,'Z2',4X,'APVB',
     #3X,'VERRB')
      DO 30 I=1,NSHOT
      WRITE(7,702)RANGA(I),TTA(I),X1(I),XX1(I),Z1(I),APVA(I),VELRA(I),
     #RANGB(I),TTB(I),X2(I),XX2(I),Z2(I),APVB(I),VELRB(I)
 702  FORMAT(14F8.3)
  30  CONTINUE
      ITER=0
C
C     INTERPOLATE NEW REFRACTOR VELOCITY FROM PREVIOUS
C     SOLUTION AND RECALCULATE.
C     REPEAT UNTIL HAVE A GOOD ESTIMATE OF REFRACTOR
C     TOPOGRAPHY AND LATERAL VELOCITY
C
    1 CALL INTERP(NSHOT,DISTAB)
      ITER=ITER+1
      CALL CALC(NSHOT,DA,DB,V1,VEL1)
      WRITE(7,701)
      DO 40 I=1,NSHOT
  40  WRITE(7,702)RANGA(I),TTA(I),X1(I),XX1(I),Z1(I),APVA(I),VELRA(I),
     #RANGB(I),TTB(I),X2(I),XX2(I),Z2(I),APVB(I),VELRB(I)
      IF (ITER .LT. ITER1) GO TO 1
      STOP
      END
C
C
C
      SUBROUTINE CALC(NSHOT,DA,DB,V1,VEL1)
C
C    CALCULATES XA,XB,ZA,ZB FOR EACH SHOT
C    USING EQUATIONS GIVEN IN TEXT
C
      IMPLICIT REAL*8 (A-H,O-Z)
      DIMENSION X1(500),X2(500),Z1(500),Z2(500),XX1(500),XX2(500),
     #VELRA(500),VELRB(500),TTA(500),TTB(500),RANGA(500),RANGB(500),
     #APVA(500),APVB(500)
      COMMON /A/X1,X2,Z1,Z2,XX1,XX2
      COMMON /B/TTA,TTB,RANGA,RANGB,APVA,APVB
      COMMON /C/VELRA,VELRB
      DO 10 I=1,NSHOT
      X1(I)=VEL1*(VELRA(I)*(TTA(I)-DA)-RANGA(I))
     #/((VELRA(I)*APVA(I))-VEL1)
      XX1(I)=RANGA(I)-X1(I)
      X2(I)=VEL1*(VELRB(I)*(TTB(I)-DB)-RANGB(I))
     #/((VELRB(I)*APVB(I))-VEL1)
      XX2(I)=RANGB(I)-X2(I)
      Z1(I)=X1(I)*(DSQRT(APVA(I)**2-VEL1))/V1
      Z2(I)=X2(I)*(DSQRT(APVB(I)**2-VEL1))/V1
  10  CONTINUE
      RETURN
      END
```

```
C
C
      SUBROUTINE INTERP(NSHOT,DISTAB)
C
C
C     INTERPOLATES BETWEEN APPARENT VELOCITIES TO OBTAIN VALUES
C     AT CONSTANT INTERVALS & OBTAINS ESTIMATE OF TRUE REFRACTOR
C     VELOCITY.
C
C
C     ALL OTHER ARRAYS THAN THOSE GIVEN IN CALLING PROGRAM
C     ARE USED AS WORKSPACE IN THIS SUBROUTINE. REQUIRED IN
C     EXTENSION OF ARRAYS TO FULL LENGTH OF LINE AND
C     INTERPOLATING NEW VELOCITY OF REFRACTOR.
C
      IMPLICIT REAL*8 (A-H,O-Z)
      DIMENSION VELR(500),VELA(500),VELB(500),XY1(500),XY2(500),
     #XZ1(500),XZ2(500),VELA1(500),VELB1(500),VTEMP(500),
     #TREFA(500),TREFB(500),TTRA(500),TTRB(500),X1(500),X2(500),
     #XX1(500),XX2(500),TTA(500),TTB(500),RANGA(500),RANGB(500),
     #APVA(500),APVB(500),VELRA(500),VELRB(500),Z1(500),Z2(500),
     #VREFA(500),VREFB(500)
      COMMON /A/X1,X2,Z1,Z2,XX1,XX2
      COMMON /B/TTA,TTB,RANGA,RANGB,APVA,APVB
      COMMON /C/VELRA,VELRB
C
C     INTERPOLATE TO GIVE VELOCITIES AT KM. INTERVALS
C     SCAN THROUGH TO FIND LIMITING VALUES ABOUT POINT
C     OF INTEREST. FIND GRADIENT AND USE TO GET VELOCITY.
C
      IMIN=XX1(1)+1
      AMIN=IMIN
      KSHOT=NSHOT-1
      DO 10 J=1,KSHOT
      IPT1=0
      IPT2=0
      DO 20 I=1,NSHOT
      IF (XX1(I) .LT. AMIN) IPT1=I
      IF (XX1(NSHOT-I+1) .GT. AMIN) IPT2=NSHOT-I+1
   20 CONTINUE
      VGRAD=(APVA(IPT2)-APVA(IPT1))
      AGRAD=(XX1(IPT2)-XX1(IPT1))
      AVGRAD=VGRAD/AGRAD
      XY1(J)=AMIN
      VELA(J)=APVA(IPT1)+((AMIN-XX1(IPT1))*AVGRAD)
      AMIN=AMIN+1
   10 CONTINUE
C
C     SAME ROUTINE IN OPPOSITE DIRECTION
C
      JMIN=XX2(1)
      BMIN=JMIN
      DO 30 J=1,KSHOT
      IPT1=0
      IPT2=0
      DO 40 I=1,NSHOT
      IF (XX2(I) .GT. BMIN) IPT1=I
      IF (XX2(NSHOT-I+1) .LT. BMIN) IPT2=NSHOT-I+1
   40 CONTINUE
      VGRAD=(APVB(IPT1)-APVB(IPT2))
      BGRAD=(XX2(IPT1)-XX2(IPT2))
      BVGRAD=VGRAD/BGRAD
      XY2(J)=BMIN
      VELB(J)=APVB(IPT2)+((AMIN-XX2(IPT2))*BVGRAD)
      BMIN=BMIN-1
   30 CONTINUE
C
C
C  HAVE VELOCITIES DEFINED AT KM. INTERVALS BUT AT
C  DIFFERENT ORIGIN. EXTEND ARRAYS TO HAVE VELOCITIES
C  DEFINED FROM 0 TO DISTAB.
C
C
C
      IF1=XY1(1)+1
      IL1=XY1(KSHOT)+1
      IF2=XY2(KSHOT)
      IL2=XY2(1)
      MSHOT=DISTAB
      LSHOT=MSHOT+1
      IF3=MSHOT-IL2+1
      IL3=MSHOT-IF2+1
```

```
      XZ1(1)=0.0D0
      VELA1(1)=VELA(1)
      DO 50 I=2,IF1
      XZ1(I)=FLOAT(I-1)
      VELA1(I)=VELA(1)
   50 CONTINUE
      DO 60 I=1,IF2
      XZ2(I)=MSHOT-I+1
      VELB1(I)=VELB(1)
   60 CONTINUE
      DO 70 I=IF1,IL1
      XZ1(I)=XY1(I-IF1+1)
      VELA1(I)=VELA(I-IF1+1)
   70 CONTINUE
      DO 80 I=IF3,IL3
      XZ2(I)=XY2(I-IF3+1)
      VELB1(I)=VELB(I-IF3+1)
   80 CONTINUE
      DO 90 I =IL1,LSHOT
      XZ1(I)=FLOAT(I-1)
      VELA1(I)=VELA(IL1-2)
   90 CONTINUE
      DO 100  I=IL3,MSHOT
      XZ2(I)=MSHOT-I+1
      VELB1(I)=VELB(IL2-1)
  100 CONTINUE
      XZ2(LSHOT)=0.0D0
      VELB1(LSHOT)=VELB(IL2-1)
      DO 110 I=1,LSHOT
  110 VTEMP(I)=(VELA1(I)+VELB1(I))/2
C
C   INTEGRATE TIME TRAVELLED UP TO EACH KILOMETRE
C   BY USING VELOCITY FUNCTION
C
      VREFA(1)=VTEMP(1)
      TREFA(1)=0.0D0
      DO 120 I=2,LSHOT
      VREFA(I)=(VTEMP(I)+VTEMP(I-1))/2
      TREFA(I)=TREFA(I-1)+(1/VREFA(I))
  120 CONTINUE
C
C  INTEGRATE REFRACTOR VELOCITY IN OPPOSITE DIRECTION
C
      VREFB(LSHOT)=VTEMP(LSHOT)
      TREFB(LSHOT)=0.0D0
      DO 130 I=2,LSHOT
      VREFB(LSHOT-I+1)=(VTEMP(LSHOT-I+2)+VTEMP(LSHOT-I+1))/2
      TREFB(LSHOT-I+1)=TREFB(LSHOT-I+2)+(1/VREFB(LSHOT-I+1))
  130 CONTINUE
C
C   HAVE TIME TRAVELLED ALONG REFRACTOR AT KM INTERVALS
C   INTERPOLATE TO FIND TIME TRAVELLED TO POINT RANGA-X1
C   INVERT TO FIND VELOCITY UP TO THAT POINT
C
      DO 140 J=1,NSHOT
      NPT1=0
      NPT2=0
      DO 150 I=1,LSHOT
      IF (XZ1(I) .LT. XX1(J)) NPT1=I
      IF (XZ1(LSHOT-I+1) .GT. XX1(J)) NPT2=LSHOT-I+1
  150 CONTINUE
      TDIFF=TREFA(NPT2)-TREFA(NPT1)
      XD1=XX1(J)-XZ1(NPT1)
      TDIFF=XD1*TDIFF
      TTRA(J)=TREFA(NPT1)+TDIFF
      VELRA(J)=XX1(J)/TTRA(J)
  140 CONTINUE
C
C   DO SAME IN OPPOSITE DIRECTION TO GET VELOCITY UP TO RANGB-X2
C
      DO 160 J=1,NSHOT
      NPT1=0
      NPT2=0
      DO 170 I=1,LSHOT
      IF (XZ2(I) .GT. XX2(J)) NPT2=I
      IF (XZ2(LSHOT-I+1) .LT. XX2(J)) NPT1=LSHOT-I+1
  170 CONTINUE
      TDIFF=TREFB(NPT2)-TREFB(NPT1)
      XD2=XX2(J)-XZ2(NPT1)
      TDIFF=XD2*TDIFF
      TTRB(J)=TREFB(NPT1)+TDIFF
      VELRB(J)=XX2(J)/TTRB(J)
  160 CONTINUE
      RETURN
      END
```

149

SUBROUTINE LIST

GDCODE

DDCODE

MDCODE

ADJUST

MEAN1(2)

PAD1(2)

BPASS1(2)

FFTA

HANN

SINTAB

NORM

PLACE

NORM1(2)

AMPSET

DUMP

PLOTG

PLOTW1(2)

PLOT1(2)

The subroutines with (2) following them are second versions of the same subroutine for use with different calling parameters. Only one version is presented. The complete set of subroutines are available in the file SUBLIB.U.

```
C
C*******************************************************************
C
C      SUBROUTINE GDCODE
C      -------------------
C
C    THIS SUBROUTINE DECODES THE TIMECODE AND RETURNS
C    THE NO. OF SAMPLES TO THE SECOND REQUIRED.
C    THE MINUTE PULSE IS RECOGNISED AND SUBEQUENTLY DECODED
C    BY TAKING ACCOUNT OF WHETHER EACH SECOND PULSE IS WIDE
C    OR NARROW FROM THE NO. OF SAMPLES.THE NO. OF SAMPLES TO
C    EACH SECOND IS STORED IN JSEC. THE NO. OF SAMPLES IN EACH
C    PULSE IS STORED IN N.
C    THE DECODING TAKES ACCOUNT OF THE FACT THAT THE NO. OF
C    SAMPLES BETWEEN RISING PULSES IS CONSTANT AT 64.
C
C    JSAM = DATA ARRAY
C    NSEC = NUMBER OF SECONDS TO DECODE
C    LLEN = NUMBER OF BYTES IN EACH TRACE
C    IST  = STARTING ELEMENT FOR EACH TRACE IN JSAM
C
C*******************************************************************
C
       SUBROUTINE GDCODE(JSAM,NSEC,LLEN,IST)
       DIMENSION N(300),ID(6),JSEC(300),IST(8)
       INTEGER*2 JSAM(160000),LLEN
       COMMON /A/NSSAMP
       COMMON /B/LSAMP,ISEIS
       COMMON /D/NRANGE
       COMMON /E/IIHR,IIMIN,IISEC,FRAC
       NX=0
       NY=0
       IZ=1
       KSAM=0
       LSAM=1
       NOSAM=1
       JMIN=0
       JJ=1
     7 IF(JSAM(JJ).LT.0) GO TO 8
       JJ=JJ+1
       GO TO 7
     8 LSAM=JJ
       DO 10 II=JJ,70
       IF (JSAM(II) .GT.0) GO TO 11
       LSAM=LSAM+1
    10 CONTINUE
C
C   FIRST SECOND PULSE FOUND
C
    11 WRITE(6,601)LSAM
   601 FORMAT(/,'NO. OF SAMPLES TO 1ST COMPLETE SECOND=',I3)
       JSEC(1)=LSAM
     3 K=1
     2 NZ=IZ
       DO 20 J=NZ,NSEC
       ID1=0
       ID2=0
       ID3=0
       ID4=0
       ID5=0
       ID6=0
       ID7=0
       ID8=0
       IZ=IZ+1
       NY=NY+1
       IF (NY.EQ.NSEC) GO TO 700
     1 NOSAM=LSAM
       ICONT=LLEN/2
       DO 30 I=LSAM,ICONT
       KSAM=KSAM+1
       NOSAM=NOSAM+1
       IF(JSAM(I).GT.0) NX=NX+1
       IF(KSAM.EQ.64) GO TO 13
    30 CONTINUE
```

```
   13 LSAM=NOSAM
      JSEC(J+1)=NOSAM
      N(J)=NX
      KSAM=Ø
      NX=Ø
      IF (NY.LT.1Ø) GO TO 2Ø
      IF (N(J).GT.45) GO TO 14
      GO TO 2Ø
   14 IF (N(J-1).GT.45)GO TO 15
C
C  WIDE PULSE FOUND.
C  IF TEN SECOND MARKER DECODE PREVIOUS BLOCK (1ØS)
C  CHECK ON WHETHER IT IS FINAL BLOCK
C  IF YES RETURN VALUE OF MINUTE AND CHECK IF
C  IT IS TIME REQUIRED. IF SO, RETURN NUMBER
C  OF SAMPLES TO CALLING PROGRAM AND EXIT.
C  IF TWO PULSES START OF NEXT MINUTE SO RETURN TO
C  DECODING ROUTINE
C
      M=Ø
      L=J-1Ø
   18 M=M+1
      L=L+1
      IF(N(L).GT.25) GO TO 16
      IF(M.EQ.9) GO TO 17
      GO TO 18
   16 IF (M.EQ.1) ID1=8Ø.Ø
      IF (M.EQ.2) ID2=4Ø.Ø
      IF (M.EQ.3) ID3=2Ø.Ø
      IF (M.EQ.4) ID4=1Ø.Ø
      IF (M.EQ.5) ID5=8.Ø
      IF (M.EQ.6) ID6=4.Ø
      IF (M.EQ.7) ID7=2.Ø
      IF (M.EQ.8) ID8=1.Ø
      IF(M.LT.9) GO TO 18
   17 ID(K)=ID1+ID2+ID3+ID4+ID5+ID6+ID7+ID8
      IF (K.EQ.6) GO TO 21
      K=K+1
   2Ø CONTINUE
   15 WRITE(6,6Ø2)
  6Ø2 FORMAT(/,'MINUTE PULSE DETECTED')
      JMIN=JMIN+1
      IF(JMIN.GT.1) GO TO 3
      NMSAMP=JSEC(J-2)
      GO TO 3
   21 WRITE(6,6Ø3)ID(2),ID(3),ID(4)
  6Ø3 FORMAT(/,I3,' DAYS:',I3,' HOURS:',I3,' MINUTES:')
      IF (ID(4).EQ.IIMIN) GO TO 22
      GO TO 3
   22 JL=J-59
      NSSAMP=JSEC(JL+IISEC)
      SSAMP=(FRAC*64.Ø)+Ø.5
      NNSAMP=SSAMP
      NSSAMP=NSSAMP+NNSAMP
      WRITE(6,6Ø4)NSSAMP
  6Ø4 FORMAT(/'NO. OF SAMPLES TO REQD. SECOND =',I1Ø)
  7ØØ RETURN
      END
```

```
C************************************************************
C
C       SUBROUTINE DDCODE
C       -----------------
C
C
C       DECODES TIME CODE OF DURHAM SEISMIC RECORDER
C       AND RETURNS NO. OF SAMPLES TO A SPECIFIED TIME.
C
C       ISAM = ARRAY  INTO WHICH TIME CODE IS READ
C       JSAMP = ARRAY USED FOR COSMETIC TIME CODE
C       JSEC = ARRAY CONTAINING BINARY CODE, Ø
C              FOR NARROW PULSE,1 FOR WIDE, 2 FOR MINUTE
C       NSEC = ARRAY WITH NO. OF SAMPLES TO EACH SECOND
C       ID = ARRAY CONTAINING DECODED MINUTE
C       IST = STARTING ELEMENT FOR EACH TRACE IN ISAM
C       MSEC = NUMBER OF SECONDS TO DECODE
C       LEN = NUMBER OF BYTES IN EACH TRACE
C
C       PROGRAM WORKS BY SCANNING WIDTH OF PULSES &
C       PUTTING BINARY DIGITS IN AN ARRAY. WHEN MINUTE MARK
C       IS FOUND THE PREVIOUS 6Ø ELEMENTS ARE DECODED.
C
C************************************************************
C
        SUBROUTINE DDCODE(ISAM,IST,MSEC,LEN)
        INTEGER*2 LEN,ISAM(16ØØØØ),JSAMP(5ØØØØ),ID(6),
       #NSEC(3ØØ),JSEC(3ØØ)
        DIMENSION IST(8),DD(25)
        INTEGER LNUM
        COMMON/A/NSSAMP
        COMMON/B/LSAMP,ISEIS
        COMMON /C/ITCHAN,ISEIS1,ISEIS2,ISEIS3
        COMMON/D/NRANGE
        COMMON /E/IIHR,IIMIN,IISEC,FRAC
      7 IMAX=Ø
        IMIN=1ØØ
        NY=1
        LSEC=1
        DO 1Ø I=1,5ØØØØ
        JSAMP(I)=Ø
     1Ø CONTINUE
        IBEG=IST(ITCHAN)-1
        ICONT=LEN/2
C
C  SCAN THROUGH TIME CODE FOR MAXIMUM AND MINIMUM AND SET LEVEL.
C  ALTER TIME CODE TO BE Ø OR 1 DEPENDING ON WHETHER VALUES
C  ARE ABOVE OR BELOW THE THRESHOLD.
C  TIME CODE CAN THEN BE DECODED WITHOUT CORRUPTION.
C
        DO 2Ø I=5ØØ,ICONT
        IF (ISAM(I+IBEG) .GT. IMAX ) IMAX=ISAM(I+IBEG)
        IF (ISAM(I+IBEG) .LT. IMIN) IMIN=ISAM(I+IBEG)
     2Ø CONTINUE
        JMIN=2*(IMAX+IMIN)/3
        DO 3Ø J=1,ICONT
        IF (ISAM(J+IBEG+5ØØ) .GT.JMIN) JSAMP(J)=1
        IF (ISAM(J+IBEG+5ØØ) .LE.JMIN) JSAMP(J)=Ø
     3Ø CONTINUE
        JJ=2
      1 IF(JSAMP(JJ-1).EQ.1) GO TO 2
        JJ=JJ+1
        GO TO 1
      2 LSAM=JJ-1
        DO 4Ø II=JJ,1ØØ
        IF(JSAMP(II).EQ.Ø .AND. JSAMP(II-1).EQ.1 .AND.
       #JSAMP(II+1).EQ.Ø) GO TO 3
        LSAM=LSAM+1
     4Ø CONTINUE
```

/53

```
C
C      RISING PULSE-IST SEC.
C
    3 NSEC(1)=LSAM
      DO 50 J=2,MSEC
      LSEC=LSEC+1
      NY=NY+1
      NOSAM=LSAM+1
      IF (NY.EQ.MSEC) GO TO 100
      NX=0
      DO 60 I=NOSAM,ICONT
      LSAM=LSAM+1
      IF(JSAMP(I).EQ.0) NX=NX+1
      NCONT1=JSAMP(I-1)+JSAMP(I)+JSAMP(I+1)
      IF (NCONT1.EQ.1) JSAMP(I)=0
      IF (NCONT1.EQ.1) NX=NX+1
      IF (JSAMP(I-1).EQ.1 .AND. JSAMP(I) .EQ. 1
     *.AND. JSAMP(I+1) .EQ. 0) GO TO 4
   60 CONTINUE
    4 NSEC(J)=LSAM
      IF (NX .LT. 50) JSEC(J)=2
      IF (NX .LT. 30) JSEC(J)=1
      IF (NX .LT. 10) JSEC(J)=0
      IF (JSEC(J) .NE. 2) GO TO 50
C
C      MINUTE MARKER
C
C      DECODE THE PREVIOUS MINUTE AND IF FIND TIME REQUIRED
C      RETURN THE NO. OF SAMPLES TO CALLING PROGRAM.
C      IF NOT FIND NEXT MINUTE MARKER AND DECODE..
C
C
    5 WRITE(6,601)
  601 FORMAT('MINUTE PULSE DETECTED')
      IF (LSEC .LE. 60) GO TO 50
      JL=LSEC-60
      DO 70 KK=1,6
      ID1=JSEC(JL+1)*80
      ID2=JSEC(JL+2)*40
      ID3=JSEC(JL+3)*20
      ID4=JSEC(JL+4)*10
      ID5=JSEC(JL+5)*8
      ID6=JSEC(JL+6)*4
      ID7=JSEC(JL+7)*2
      ID8=JSEC(JL+8)*1
      ID(KK)=ID1+ID2+ID3+ID4+ID5+ID6+ID7+ID8
      JL=JL+10
   70 CONTINUE
      WRITE(6,602)(ID(K),K=1,3)
  602 FORMAT('MIN.=',I3,' HR.=',I3,' DAY=',I3)
      IF(ID(1).EQ.IIMIN .AND. ID(2).EQ.IIHR) GO TO 6
   50 CONTINUE
    6 JL=JL-61
      NSAMP=NSEC(JL+IISEC)
      MSAMP=(NSEC(JL+IISEC+1)-NSEC(JL+IISEC))*FRAC
      NSSAMP=MSAMP+NSAMP+500
      WRITE(6,603)NSSAMP
  603 FORMAT('NO. OF SAMPLES TO TIME REQD.=',I8)
  100 RETURN
      END
```

154

```
C
C********************************************************************
C
C       SUBROUTINE MDCODE
C       ----------------
C
C       USES SAME PROCEDURE AS DDCODE AND SAME ARRAY NAMES
C       ONLY DECODING ROUTINE IS DIFFERENT.
C       PARAMETER LIST IS THE SAME AS IN DDCODE
C
C********************************************************************
C
        SUBROUTINE MDCODE(ISAM,IST,MSEC,LEN)
        INTEGER*2 LEN,ISAM(160000),JSAMP(50000),ID(6),
       #NSEC(300),JSEC(300)
        DIMENSION IST(8),DD(25)
        INTEGER LNUM
        COMMON /A/NSSAMP
        COMMON /B/LSAMP,ISEIS
        COMMON /C/ITCHAN,ISEIS1,ISEIS2,ISEIS3
        COMMON /D/NRANGE
        COMMON /E/IIHR,IIMIN,IISEC,FRAC
      7 IMAX=0
        IMIN=100
        NY=1
        LSEC=1
        DO 10 I=1,50000
        JSAMP(I)=0
     10 CONTINUE
        IBEG=IST(ITCHAN)-1
        ICONT=LEN/2
        DO 20 I=500,ICONT
        IF (ISAM(I+IBEG) .GT. IMAX ) IMAX=ISAM(I+IBEG)
        IF (ISAM(I+IBEG) .LT. IMIN) IMIN=ISAM(I+IBEG)
     20 CONTINUE
        JMIN=2*(IMAX+IMIN)/3
        DO 30 J=1,ICONT
        IF (ISAM(J+IBEG+500) .GT.JMIN) JSAMP(J)=1
        IF (ISAM(J+IBEG+500) .LE.JMIN) JSAMP(J)=0
     30 CONTINUE
        JJ=2
      1 IF(JSAMP(JJ-1).EQ.1) GO TO 2
        JJ=JJ+1
        GO TO 1
      2 LSAM=JJ-1
        DO 40 II=JJ,100
        IF(JSAMP(II).EQ.0 .AND. JSAMP(II-1).EQ.1 .AND.
       #JSAMP(II+1).EQ.0) GO TO 3
        LSAM=LSAM+1
     40 CONTINUE
C
C       RISING PULSE-IST SEC.
C
      3 NSEC(1)=LSAM
        DO 50 J=2,MSEC
        LSEC=LSEC+1
        NY=NY+1
        NOSAM=LSAM+1
        IF (NY.EQ.MSEC) GO TO 100
        NX=0
        DO 60 I=NOSAM,ICONT
        LSAM=LSAM+1
        IF(JSAMP(I).EQ.0) NX=NX+1
        NCONT1=JSAMP(I-1)+JSAMP(I)+JSAMP(I+1)
        IF (NCONT1.EQ.1) JSAMP(I)=0
        IF (NCONT1.EQ.1) NX=NX+1
        IF (JSAMP(I-1).EQ.1 .AND. JSAMP(I) .EQ. 1
       #.AND. JSAMP(I+1) .EQ. 0) GO TO 4
     60 CONTINUE
```

```
    4 NSEC(J)=LSAM
      IF (NX .LT. 50) JSEC(J)=2
      IF (NX .LT. 25) JSEC(J)=1
      IF (NX .LT. 15) JSEC(J)=0
      IF (JSEC(J) .NE. 2) GO TO 50
C
C     MINUTE MARKER,ENTER DECODE ROUTINE
C     IF CORRECT MINUTE EXIT FROM SUBROUTINE
C
    5 WRITE(6,601)
  601 FORMAT('MINUTE PULSE DETECTED')
      IF (LSEC .LE. 60) GO TO 50
      JL=LSEC-30
      ID1=JSEC(JL)*20
      ID2=JSEC(JL+1)*10
      ID3=JSEC(JL+2)*8
      ID4=JSEC(JL+3)*4
      ID5=JSEC(JL+4)*2
      ID6=JSEC(JL+5)*1
      ID7=JSEC(JL+6)*4
      ID8=JSEC(JL+7)*2
      ID9=JSEC(JL+8)*1
      ID10=JSEC(JL+9)*20
      ID11=JSEC(JL+10)*10
      ID12=JSEC(JL+11)*8
      ID13=JSEC(JL+12)*4
      ID14=JSEC(JL+13)*2
      ID15=JSEC(JL+14)*1
      ID16=JSEC(JL+15)*40
      ID17=JSEC(JL+16)*20
      ID18=JSEC(JL+17)*10
      ID19=JSEC(JL+18)*8
      ID20=JSEC(JL+19)*4
      ID21=JSEC(JL+20)*2
      ID22=JSEC(JL+21)*1
      ID(1)=ID1+ID2+ID3+ID4+ID5+ID6
      ID(2)=ID7+ID8+ID9
      ID(3)=ID10+ID11+ID12+ID13+ID14+ID15
      ID(4)=ID16+ID17+ID18+ID19+ID20+ID21+ID22-1
      WRITE(6,602)(ID(K),K=1,4)
  602 FORMAT('DATE=',I3,' DAY=',I3,' HR=',I3,' MIN=',I3)
      IF(ID(4).EQ.IIMIN .AND. ID(3).EQ.IIHR) GO TO 6
   50 CONTINUE
    6 JL=JL-31
      NSAMP=NSEC(JL+IISEC)
      MSAMP=(NSEC(JL+IISEC+1)-NSEC(JL+IISEC))*FRAC
      NSSAMP=MSAMP+NSAMP+500
      WRITE(6,603)NSSAMP
  603 FORMAT('NO. OF SAMPLES TO REQD. TIME=',I8)
  100 RETURN
      END
```

```
C
C*******************************************************************
C     SUBROUTINE ADJUST
C     ---------------------
C
C     THIS SUBROUTINE USES THE VALUE RETURNED BY
C     THE DECODING ROUTINE AND THE DIFFERENCE IN SAMPLES
C     BETWEEN THE TWO CLOCKS TO OBTAIN THE CORRECT NUMBER
C     OF SAMPLES TO THE SECOND REQUIRED.
C     NO. OF SAMPLES TO  THE TIME REQUIRED.
C     SAMPLES IN THE RANGE -10SEC TO 15SEC ARE
C     THEN WRITTEN IN ARRAY ASAM TO BE  PLOTTED.
C     ENTER NUMBER OF SEISMIC CHANNEL IN FILE
C     ON UNIT 8. FORMAT - I5
C
C     JSAM = DATA ARRAY
C     JST  = STARTING ELEMENT FOR EACH TRACE IN JSAM
C     ASAM = ARRAY WHERE PLACE REQUIRED TRACE FROM JSAM
C     JSTRT = STARTING ELEMENT OF EACH TRACE IN ASAM
C     NDIFF = DIFFERENCE IN SAMPLES BETWEEN TIME CODE AND MSF
C     SAMPR = SAMPLING RATE
C
C*******************************************************************
C
      SUBROUTINE ADJUST(JST,JSTRT,JSAM,NDIFF,ASAM,SAMPR)
      DIMENSION NDIFF(25),JSTRT(25),JST(8)
      INTEGER*2 JSAM(160000)
      REAL*8 ASAM(75000)
      COMMON /A/NSSAMP
      COMMON /B/LSAMP,ISEIS
      COMMON /D/NRANGE
      ISUB=(SAMPR*10)-2
      MMSAMP=NDIFF(NRANGE)+NSSAMP-ISUB
      READ(8,801)JNUM
 801  FORMAT(I5)
      IBEG=JST(JNUM)
      JBEG=JSTRT(NRANGE)
      DO 10 I=1,LSAMP
      ASAM(JBEG+I-1)=JSAM(IBEG+I+MMSAMP)
  10  CONTINUE
      RETURN
      END
```

157

```
C
C************************************************************************
C      SUBROUTINE MEAN1
C      ------------------
C
C      THIS SECTION FINDS THE MEAN VALUE OF THE
C      SAMPLES IN ASAM AND SUBTRACTS THIS FROM
C      EACH VALUE TO REMOVE ANY D.C. LEVEL.
C      THE ROUTINE IS USED WITH PROGRAMS GEOSECT AND DURHSECT
C
C      ASAM = DATA ARRAY (SEISMIC TRACES)
C      JSTRT = STARTING ELEMENT OF EACH TRACE
C
C************************************************************************
C
       SUBROUTINE MEAN1(JSTRT,ASAM)
       DIMENSION JSTRT(25)
       REAL*8 ASAM(75000)
       COMMON /B/LSAMP,ISEIS
       COMMON /D/NRANGE
       AAV=0.0
       JBEG=JSTRT(NRANGE)
       DO 10 I=1,LSAMP
       AAV=AAV+ASAM(JBEG+I-1)
   10  CONTINUE
       AAV=AAV/LSAMP
       DO 20  I=1,LSAMP
       ASAM(JBEG+I-1)=ASAM(JBEG+I-1)-AAV
   20  CONTINUE
       RETURN
       END
C
C************************************************************************
C      SUBROUTINE PAD1
C      ------------------
C
C
C      THIS ROUTINE INCREASES EACH TRACE TO DOUBLE ITS
C      LENGTH BY FILLING THAT PARTICULAR PART OF ARRAY
C      X AFTER THE TRACE WITH ZEROS.
C
C      ASAM = INPUT TRACE
C      JSTRT = STARTING ELEMENT FOR EACH TRACE
C      X = PADDED ARRAY
C      LX = SIZE OF ARRAY X
C      IT IS USED WITH GEOSECT.N(T) AND DURHSECT.N
C
C************************************************************************
C
       SUBROUTINE PAD1(ASAM,JSTRT,LX,X)
       DIMENSION JSTRT(25)
       REAL*8 ASAM(75000)
       REAL*8 X(LX)
       COMMON /B/LSAMP,ISEIS
       COMMON /D/NRANGE
       JBEG=JSTRT(NRANGE)-1
       DO 20 J=1,LSAMP
       X(J)=ASAM(JBEG+J)
   20  CONTINUE
       L1=LSAMP+1
       DO 10 I=L1,LX
       X(I)=0.0
   10  CONTINUE
       RETURN
       END
```

158

```
C
C******************************************************************
C      SUBROUTINE BPASS1
C      ---------------------
C
C
C    AN EDITED VERSION OF BRIAN RUSSELL'S SUBROUTINE TO
C    PERFORM BANDPASS FILTERING ON EACH SEISMIC TRACE.
C    SUBROUTINES FFTA SINTAB & HANN ARE CALLED.
C
C    X = INPUT ARRAY (OUTPUT FROM PAD1)
C.   LX = LENGTH OF X
C    ASAM = BANDPASSED TRACE
C    JSTRT = STARTING ELEMENT FOR EACH TRACE IN ASAM
C    SAMPR = SAMPLING RATE
C    F1,F2,F3,F4 = DEFINES FREQUENCY RANGE FOR HANNING WINDOW
C
C    F1 MUST BE GREATER THAN THE FUNDAMENTAL FREQUENCY
C    F4 MUST BE LESS THAN THE NYQUIST FREQUENCY
C
C    USED WITH GEOSECT.N(T) AND DURHSECT.N
C
C******************************************************************
C
      SUBROUTINE BPASS1(ASAM,LX,F1,F2,F3,F4,JSTRT,X,SAMPR)
      IMPLICIT REAL*8 (A-H,O-Z)
      DIMENSION X(LX),Y(4096),S(4096),F(4096),JSTRT(25),ASAM(75000)
      COMMON /B/LSAMP,ISEIS
      COMMON /D/NRANGE
      L1=LX/2+1
      L2=L1+1
      DO 10 I=1,LX
      S(I)=0.0
      Y(I)=0.0
   10 CONTINUE
C
C   TRANSFORM THE TIME SERIES
C
      CALL SINTAB(LX,S)
      SIGNI=-1.0
      CALL FFTA(LX,X,Y,SIGNI,S)
      DF=SAMPR/DFLOAT(LX)
      DO 20 I=1,L1
      F(I)=DF*DFLOAT(I)
   20 CONTINUE
C
C   SET UP SAMPLE NUMBERS FOR HANNING WINDOW LIMITS
C
      DO 30 I=2,L1
      IF(F1.GE.F(I-1).AND.F1.LE.F(I)) JJ=I-1
      IF(F2.GE.F(I-1).AND.F2.LE.F(I)) J=I-1
      IF(F3.GE.F(I-1).AND.F3.LE.F(I)) K=I-1
      IF(F4.GE.F(I-1).AND.F4.LE.F(I)) KK=I-1
   30 CONTINUE
      CALL HANN(X,L1,JJ,KK,J,K)
      CALL HANN(Y,L1,JJ,KK,J,K)
      DO 40 I=L2,LX
      X(I)=X(LX-I+2)
      Y(I)=-Y(LX-I+2)
   40 CONTINUE
      SIGNI=1.0
      CALL FFTA(LX,X,Y,SIGNI,S)
      JBEG=JSTRT(NRANGE)-1
      DO 50 J=1,LSAMP
      ASAM(JBEG+J)=X(J)
   50 CONTINUE
      RETURN
      END
```

```
C
C***********************************************************************
C
C     SUBROUTINE FFTA
C     ---------------
C
C
C     DESCRIPTION - THIS SUBROUTINE COMPUTES THE FAST FOURIER
C                   TRANSFORM BY THE COOLEY-TUKEY ALGORITHM.
C     PARAMETERS - LX=NUMBER OF DATA POINTS
C                  X=ARRAY CONTAINING REAL PART OF TRANSFORM
C                  Y=ARRAY CONTAINING IMAGINARY PART OF TRANSFORM
C                  SIGNI=+1. FOR FORWARD TRANSFORM
C                       =-1. FOR REVERSE TRANSFORM
C                  S=ARRAY OF SINE VALUES GENERATED BY SUBROUTINE
C                    SINTAB CALLED BY FFTA
C
C     SOURCE - CLAERBOUT, MODIFIED BY ALAN NUNNS
C***********************************************************************
C
      SUBROUTINE FFTA(LX,X,Y,SIGNI,S)
      IMPLICIT REAL*8(A-H,O-Z)
      DIMENSION X(LX),Y(LX),S(LX)
      SC=1.0
      IF(SIGNI.LT.0.0) SC=1.0/LX
      NN=LX/2
      N=LX/4
      J=1
      DO 30 I=1,LX
      IF(I.GT.J) GO TO 10
      TEMPX=X(J)*SC
      TEMPY=Y(J)*SC
      X(J)=X(I)*SC
      Y(J)=Y(I)*SC
      X(I)=TEMPX
      Y(I)=TEMPY
 10   M=NN
 20   IF(J.LE.M) GO TO 30
      J=J-M
      M=M/2
      IF(M.GE.1) GO TO 20
 30   J=J+M
      L=1
      NL=NN
 40   ISTEP=2*L
      IND=1
      DO 55 M=1,L
      INDN=IND-N-1
      IF(INDN) 41,42,43
 41   WX=S(1-INDN)
      WY=S(IND)*SIGNI
      GO TO 45
 42   WX=0.
      WY=SIGNI
      GO TO 45
 43   WX=-S(INDN+1)
      WY=S(N+1-INDN)*SIGNI
 45   DO 50 I=M,LX,ISTEP
      TEMPX=WX*X(I+L)-WY*Y(I+L)
      TEMPY=WX*Y(I+L)+WY*X(I+L)
      X(I+L)=X(I)-TEMPX
      Y(I+L)=Y(I)-TEMPY
      X(I)=X(I)+TEMPX
 50   Y(I)=Y(I)+TEMPY
 55   IND=IND+NL
      L=ISTEP
      NL=NL/2
      IF(L.LT.LX) GO TO 40
      RETURN
      END
```

```
C
C************************************************************************
C
C      SUBROUTINE SINTAB
C      ---------------------
C
C   DESCRIPTION - THIS SUBROUTINE RETURNS VALUES
C   S(I)=SIN(2*PI*(I-1/)/LX)  I=1,2,.....,LX/4+1
C   WHERE LX=2**INTEGER IS THE NUMBER OF POINTS IN THE
C   TIME SERIES IN MAIN
C
C   WRITTEN BY ALAN NUNNS.
C************************************************************************
C
       SUBROUTINE SINTAB(LX,S)
       IMPLICIT REAL*8(A-H,O-Z)
       DIMENSION S(LX)
       DOUBLE PRECISION ARG,DELARG
       N1=LX/4+1
       ARG=0.0
       DELARG=0.62831853071795860D01/LX
       DO 10 I=1,N1
       S(I)=DSIN(ARG)
       ARG=ARG+DELARG
   10 CONTINUE
       RETURN
       END
C
C************************************************************************
C
C      SUBROUTINE HANN
C      ------------------
C   AN EDITED VERSION OF A SUBROUTINE BY BRIAN RUSSELL
C   IT APPLIES A HANNING WINDOW TO THE TRANSFORMED DATA
C   BETWEEN THE FREQUENCIES SET UP IN BPASS
C
C   X  = SPECTRUM OF DATA
C   N  = SIZE OF ARRAY
C   JJ = ELEMENT OF ARRAY STARTING WINDOW
C   KK = ELEMENT OF ARRAY ENDING THE WINDOW
C   J  = ELEMENT OF ARRAY ENDING RISING TAPER
C   K  = ELEMENT OF ARRAY STARTING DECREASING TAPER
C
C   VALUE OF WINDOW BETWEEN J & K = 1
C   WINDOW = 0 AT JJ & KK
C
C************************************************************************
C
       SUBROUTINE HANN(X,N,JJ,KK,J,K)
       IMPLICIT REAL*8(A-H,O-Z)
       DIMENSION X(N)
       NN=N-1
       PI2=0.62831853071796D+01
       IF(JJ.EQ.1)GO TO 15
       DO 5 I=2,JJ
    5 X(I-1)=X(I-1)*0.0D0
   15 IF(J.EQ.JJ) GO TO 25
       CON1=PI2/DFLOAT(2*(J-JJ))
       DO 10 I=JJ,J
       ARG=DFLOAT(I-JJ)*CON1
   10 X(I)=X(I)*0.5D0*(.1D+01-DCOS(ARG))
   25 IF(K.EQ.KK)GO TO 30
       CON2=PI2/DFLOAT(2*(KK-K))
       DO 20 I=K,KK
       ARG=DFLOAT(KK-I)*CON2
   20 X(I)=X(I)*0.5D0*(.1D+01-DCOS(ARG))
   30 IF(KK.EQ.N) GOTO 40
       DO 50 I=KK,NN
   50 X(I+1)=X(I+1)*0.0D0
   40 RETURN
       END
```

```
C
C*******************************************************************
C
C      SUBROUTINE NORM
C      -------------------
C
C      THIS SUBROUTINE SCANS THE DATA FOR THE MAXIMUM SAMPLE
C      VALUE, SCALES IT AND NORMALIZES THE TRACE TO IT.
C
C      ASAM = DATA ARRAY
C      JSTRT = ELEMENT IN ARRAY WHERE TRACE BEGINS
C      MSHOT = NUMBER OF SHOTS
C      SAMPR = SAMPLING RATE
C
C*******************************************************************
C
       SUBROUTINE NORM(MSHOT,JSTRT,ASAM,SAMPR)
       DIMENSION JSTRT(25)
       REAL*8 ASAM(75000)
       COMMON /B/LSAMP,ISEIS
       COMMON /D/NRANGE
       JBEG=JSTRT(NRANGE)-1
       AMAX=ASAM(JBEG+1)
       KSAMP=IFIX(SAMPR*25)
       DO 10 I=2,KSAMP
       IF (ASAM(JBEG+I).GT.AMAX)AMAX=ASAM(JBEG+I)
   10 CONTINUE
       FACTOR=4.0/AMAX
       DO 20 J=1,KSAMP
       ASAM(JBEG+J)=ASAM(JBEG+J)*FACTOR
   20 CONTINUE
       RETURN
       END
C
C*******************************************************************
C
C      SUBROUTINE PLACE
C      -------------------
C
C
C      THIS SUBROUTINE PLACES THE SEISMIC AND TIME CHANNELS
C      FROM THE REQUESTED SAMPLE INTO ARRAYS READY FOR
C      BANDPASSING AND PLOTTING.
C
C      ISAM = ARRAY CONTAINING ALL DATA
C      XSAM = ARRAY CONTAINING TIME CODE ONLY
C      ASAM = ARRAY CONTAINING SEISMIC CHANNELS
C      IST = STARTING ELEMENT FOR EACH TRACE IN ISAM
C      JSTRT = STARTING ELEMENT FOR EACH TRACE IN ASAM
C
C      USED WITH DURHPLOT AND GEOPLOT
C
C*******************************************************************
C
       SUBROUTINE PLACE(ISAM,XSAM,ASAM,JSTRT,IST)
       DIMENSION JSTRT(3),IST(8)
       INTEGER*2 ISAM(160000)
       REAL*8 ASAM(15000),XSAM(5000)
       COMMON /A/NSSAMP
       COMMON /B/LSAMP,ISEIS
       COMMON /C/ITCHAN,ISEIS1,ISEIS2,ISEIS3
       IBEG=IST(ISEIS1)-2
       JBEG=JSTRT(1)-1
       DO 10 I=1,LSAMP
   10 ASAM(I+JBEG)=ISAM(I+IBEG+NSSAMP)
       IBEG=IST(ISEIS2)-2
       JBEG=JSTRT(2)-1
       DO 20 I=1,LSAMP
   20 ASAM(I+JBEG)=ISAM(I+IBEG+NSSAMP)
       IBEG=IST(ISEIS3)-2
       JBEG=JSTRT(3)-1
       DO 30 I=1,LSAMP
   30 ASAM(I+JBEG)=ISAM(I+IBEG+NSSAMP)
       IBEG=IST(ITCHAN)-2
       DO 40 I=1,LSAMP
   40 XSAM(I)=ISAM(I+IBEG+NSSAMP)
       RETURN
       END
```

```
C
C*********************************************************************
C
C      SUBROUTINE NORM1 ·
C      -------------------
C
C      THIS SUBROUTINE NORMALIZES THE TRACES TO THE MAXIMUM
C      AMPLITUDE AND SCALES DOWN PRIOR TO PLOTTING
C      IT IS USED WITH GEOPLOT AND DURHPLOT.
C
C      XSAM  = TIME CODE
C      ASAM  = SEISMIC CHANNELS
C      LEN   = NUMBER OF BYTES IN EACH TRACE
C      JSTRT = STARTING ELEMENT OF SEISMIC TRACES IN ASAM
C      ZSAM  = NUMBER OF SAMPLES TO PLOT
C      KCONT = RECALCULATED NUMBER OF SAMPLES,
C              USED AS CHECK FOR END OF TRACE
C
C
C*********************************************************************
C
       SUBROUTINE NORM1(XSAM,ASAM,LEN,KCONT,JSTRT,ZSAM)
       INTEGER*2 LEN
       REAL*8 ASAM(15000),XSAM(5000),AMAX,AMIN,XMAX,XMIN,FACT
       DIMENSION JSTRT(3)
       COMMON /A/NSSAMP
       COMMON /B/LSAMP,ISEIS
       ICONT=NSSAMP+ZSAM
       JCONT=LEN/2
       IF (ICONT .GT. JCONT) ICONT=JCONT
       KCONT=ICONT-NSSAMP
       IBEG=JSTRT(ISEIS)-1
       AMAX=0.0
       AMIN=0.0
       DO 10 J=1,KCONT
       IF ((ASAM(IBEG+J)) .GT. AMAX) AMAX=(ASAM(IBEG+J))
       IF (ASAM(IBEG+J) .LT. AMIN) AMIN=ASAM(IBEG+J)
   10  CONTINUE
       AMIN=DABS(AMIN)
       AMAX=DABS(AMAX)
       IF (AMAX .LT. AMIN) AMAX=AMIN
       FACT=1.0/AMAX
       DO 20 J=1,KCONT
   20  ASAM(IBEG+J)=(ASAM(IBEG+J))*FACT
       IF (ISEIS .GT. 1) GO TO 5
       XMAX=0.0
       XMIN=0.0
       DO 30 I=1,KCONT
       IF (XSAM(I) .GT. XMAX) XMAX=XSAM(I)
       IF (XSAM(I) .LT. XMIN) XMIN=XSAM(I)
   30  CONTINUE
       XMIN=DABS(XMIN)
       XMAX=DABS(XMAX)
       IF (XMAX .LT. XMIN) XMAX=XMIN
       FACTX=1.0/XMAX
       DO 40 I=1,KCONT
   40  XSAM(I)=(XSAM(I))*FACTX
    5  RETURN
       END
```

```
C
C*********************************************************************
C      SUBROUTINE AMPSET
C      ---------------------
C
C
C      THIS SUBROUTINE ADJUSTS THE AMPLITUDE OF EACH
C      TRACE BY TAKING ACCOUNT OF THE SEISMOMETER
C      AND DIGITIZER GAIN FOR EACH SHOT.
C      IN ADDITION EACH TRACE IS MULTIPLIED BY THE
C      RANGE TO TAKE ACCOUNT FOR FALL IN AMPLITUDE.
C
C      ASAM = DATA ARRAY
C      JSTRT = STARTING ELEMENT FOR EACH TRACE
C      DD = RANGE OF SHOT
C      ISGAIN = SEISMOMETER GAIN
C      IDGAIN = DIGITIZER GAIN
C
C*********************************************************************
.C
       SUBROUTINE AMPSET(ASAM,JSTRT,DD,ISGAIN,IDGAIN)
       DIMENSION JSTRT(25),DD(25),ISGAIN(25),IDGAIN(25)
       REAL ASAM(75000)
       COMMON /A/NSSAMP
       COMMON /D/NRANGE
       JBEG=JSTRT(NRANGE)-1
       F1=1.0
       F2=1.0
       IF(ISGAIN(NRANGE).EQ.1) F1=250.0
       IF(ISGAIN(NRANGE).EQ.2) F1=100.0
       IF(ISGAIN(NRANGE).EQ.3) F1=50.0
       IF(ISGAIN(NRANGE).EQ.4) F1=25.0
       IF(ISGAIN(NRANGE).EQ.5) F1=10.0
       IF(ISGAIN(NRANGE).EQ.6) F1=5.0
       IF(ISGAIN(NRANGE).EQ.7) F1=2.5
       IF(ISGAIN(NRANGE).EQ.8) F1=1.0
       IF(ISGAIN(NRANGE).EQ.9) F1=0.5
       IF(ISGAIN(NRANGE).EQ.10) F1=0.25
       IF(IDGAIN(NRANGE).EQ.0) F2=4.0
       IF(IDGAIN(NRANGE).EQ.1) F2=2.0
       IF(IDGAIN(NRANGE).EQ.2) F2=1.0
       IF(IDGAIN(NRANGE).EQ.3) F2=0.5
       DO 10 J=1,1600
       ASAM(JBEG+J)=(ASAM(JBEG+J)*F1*F2*(ABS(DD(NRANGE))))/10000.0
  10   CONTINUE
       RETURN
       END
```

```
C
C*************************************************************************
C
C      SUBROUTINE DUMP
C      -------------------
C
C      THIS SUBROUTINE DUMPS 700 SAMPLES OF THE TIME CODE
C      & SEISMIC CHANNEL FROM THE SAMPLE NO. FOUND BY
C      TIME DECODING ROUTINE.
C
C      ISAM = DATA ARRAY
C      IST = STARTING ELEMENT OF EACH TRACE IN ARRAY
C      LEN = NUMBER OF BYTES IN EACH TRACE
C      INFO = HEADER INFORMATION FOR EACH SHOT
C
C*************************************************************************
C
       SUBROUTINE DUMP(ISAM,IST,LEN,INFO)
       DIMENSION IST(8),INFO(20),TITLE(20)
       INTEGER*2 ISAM(160000),LEN,LEN1
       INTEGER LNUM
       COMMON /A/NSSAMP
       COMMON /C/ITCHAN,ISEIS1,ISEIS2,ISEIS3
       COMMON /F/JCHAN
       WRITE(6,601)
 601   FORMAT('ENTER TITLE')
       READ(5,501)TITLE
 501   FORMAT(20A4)
       IBEG=IST(JCHAN)+NSSAMP-1
       JBEG=IST(ITCHAN)+NSSAMP-1
       LEN1=1400
       JCONT=LEN-(NSSAMP*2)
       IF (JCONT.LT.1400) LEN1=JCONT
       WRITE(7,701)TITLE
 701   FORMAT(20A4)
       CALL WRITE(ISAM(JBEG),LEN1,0,LNUM,7,&200)
       CALL WRITE(ISAM(IBEG),LEN1,0,LNUM,7,&200)
 200   RETURN
       END
```

```
C
C*********************************************************************
C       SUBROUTINE PLOTG
C       ------------------
C
C       THIS SUBROUTINE PLOTS EACH EVENT TO PROVIDE A
C       REDUCED SECTION (T-X/V). ASAM CONTAINS ALL EVENTS
C       *PLOTSYS ROUTINES ARE USED.
C       IT IS USED WITH PROGRAM GEOPLOT
C
C       ASAM = DATA ARRAY
C       JSTRT = STARTING ELEMENT FOR EACH TRACE IN ASAM
C       DD = RANGES OF SHOTS
C       MSHOT = NUMBER OF SHOTS
C       PTITLE = TILTLE OF PLOT
C
C*********************************************************************
C
        SUBROUTINE PLOTG(JSTRT,DD,MSHOT,PTITLE,ASAM)
        DIMENSION DD(25),JSTRT(25),PTITLE(10)
        REAL*8 ASAM(75000),TCOORD(1600)
        COMMON /A/NSSAMP
        COMMON /B/LSAMP,ISEIS
        COMMON /D/NRANGE
        DMIN=DD(1)
        DO 30 K=2,MSHOT
        IF (DD(K) .LT.DMIN )DMIN=DD(K)
  30    CONTINUE
        IMIN=IFIX((DMIN-20)/10)
        DMIN=FLOAT(IMIN*10)
        CALL PLTXMX(45.0)
        CALL PAXIS(2.0,1.0,'T-D/6   SEC',10,25.0,90.0,-10.0,1.0,1.0)
        CALL PAXIS(2.0,1.0,'RANGE   KMS',-10,40.0,0.0,DMIN,7.5,1.0)
        CALL PGRID(2.0,1.0,40.0,25.0,1,1)
        CALL PSYMB(1.0,2.0,0.6,PTITLE,90.0,40)
        CALL PLTOFS(DMIN,7.5,-10.0,1.0,2.0,1.0)
        DO 10 J=1,MSHOT
        JBEG=JSTRT(J)
        Z=0.0
        DO 20 I=1,1600
        TCOORD(I)=(Z-640.0)/64.0
        ASAM(JBEG+I-1)=ASAM(JBEG+I-1)+DD(J)
        Z=Z+1.0
  20    CONTINUE
        CALL PENUP(DD(J),-10.0)
        CALL PLINE(ASAM(JBEG),TCOORD,1600,2,0,0,1)
  10    CONTINUE
        CALL PLTEND
        RETURN
        END
```

```
C
C*********************************************************************
C     SUBROUTINE PLOTW1
C     ---------------------
C
C     THIS SUBROUTINE PLOTS EACH EVENT TO PROVIDE A
C     REDUCED SECTION (T-X/V). ASAM CONTAINS ALL EVENTS
C     *PLOTSYS ROUTINES ARE USED.
C     IT HAS THE SAME PARAMETERS AS PLOT.G BUT IS USED
C     ON DATA RECORDED ON THE MK.3 RECORDERS DURING
C     THE FIRST PHASE OF WISE.
C
C*********************************************************************
C
      SUBROUTINE PLOTW1(JSTRT,DD,MSHOT,PTITLE,ASAM)
      DIMENSION DD(25),JSTRT(25),PTITLE(10)
      REAL*8 ASAM(75000),TCOORD(1250)
      DMIN=DD(1)
      DO 30 K=2,MSHOT
      IF (DD(K).LT.DMIN) DMIN=DD(K)
   30 CONTINUE
      IMIN=IFIX((DMIN-20.0)/10)
      DMIN=FLOAT(IMIN*10)
      CALL PLTXMX(45.0)
      CALL PAXIS(2.0,1.0,'T-D/6   SEC',10,25.0,90.0,-10.0,1.0,1.0)
      CALL PAXIS(2.0,1.0,'RANGE   KMS',-10,40.0,0.0,DMIN,7.5,1.0)
      CALL PGRID(2.0,1.0,40.0,25.0,1,1)
      CALL PSYMB(1.0,2.0,0.6,PTITLE,90.0,40)
      CALL PLTOFS(DMIN,7.5,-10.0,1.0,1.0,1.0)
      DO 10 J=1,MSHOT
      JBEG=JSTRT(J)
      Z=0.0
      DO 20 I=1,1250
      TCOORD(I)=(Z-500.0)/50.0
      ASAM(JBEG+I-1)=ASAM(JBEG+I-1)+DD(J)
      Z=Z+1.0
   20 CONTINUE
      CALL PENUP(DD(J),-10.0)
      CALL PLINE(ASAM(JBEG),TCOORD,1250,2,0,0,1)
   10 CONTINUE
      CALL PLTEND
      RETURN
      END
```

/67

```
C
C***********************************************************************
C
C       SUBROUTINE PLOT1
C       ----------------
C
C     THIS SUBROUTINE PLOTS THREE SEISMIC TRACKS STRADDLED
C     BY A TIME CODE.
C     THE SCALE IS EITHER 1 OR 0.5 SECONDS PER INCH.
C     IT IS USED WITH PROGRAM GEOPLOT.
C
C     ASAM = SEISMIC TRACES
C     XSAM = TIME CODE
C     JSTRT = STARTING ELEMENT OF EACH TRACE IN ASAM
C     ZSAM = NUMBER OF SAMPLES IN PLOT
C     KCONT = RECALCULATED NUMBER OF SAMPLES (FROM NORM1)
C
C     *PLOTSYS ROUTINES ARE USED
C
C***********************************************************************
C
      SUBROUTINE PLOT1(ASAM,XSAM,TITLE,KCONT,JSTRT,ZSAM)
      REAL*8 ASAM(15000),XCOORD(3000),XSAM(5000)
      DIMENSION TITLE(20),JSTRT(3)
      COMMON /A/NSSAMP
      COMMON /C/ITCHAN,ISEIS1,ISEIS2,ISEIS3
      X=0.0
      DO 10 I=1,KCONT
      X=X+1.0
      XCOORD(I)=X
   10 CONTINUE
      ZSAM=ZSAM/30.0
      XLEN=KCONT/ZSAM
      CALL PLTXMX(40.0)
      CALL PAXIS(2.0,0.5,'A',0,-10.0,90.0,0.0,1.0,1.0)
      CALL PAXIS(2.0,0.5,'B',0,-XLEN,0.0,0.0,ZSAM,1.0)
      CALL PGRID(2.0,0.5,XLEN,10.0,1,1)
      CALL PSYMB(1.5,1.0,0.3,TITLE,90.0,80,0)
      CALL PLTOFS(0.0,ZSAM,0.0,1.0,2.0,0.5)
      Y=1.00
      CALL PENUP(0.0,Y)
      DO 20 I=1,KCONT
   20 XSAM(I)=XSAM(I)+Y
      CALL PLINE(XCOORD,XSAM,KCONT,2.,0,0,1)
      Y=Y+1.75
      CALL PENUP(0.0,Y)
      IBEG=JSTRT(1)
      JBEG=IBEG+KCONT-1
      DO 30 I=IBEG,JBEG
   30 ASAM(I)=ASAM(I)+Y
      CALL PLINE(XCOORD,ASAM(IBEG),KCONT,2.,0,0,1)
      Z=Y+0.2
      CALL PSYMB(ZSAM,Z,0.25,'SEISMIC 1',0.0,9,1)
      Y=Y+2.0
      CALL PENUP(0.0,Y)
      IBEG=JSTRT(2)
      JBEG=IBEG+KCONT-1
      DO 40 I=IBEG,JBEG
   40 ASAM(I)=ASAM(I)+Y
      CALL PLINE(XCOORD,ASAM(IBEG),KCONT,2.,0,0,1)
      Z=Y+0.2
      CALL PSYMB(ZSAM,Z,0.25,'SEISMIC 2',0.0,9,1)
      Y=Y+2.0
      CALL PENUP(0.0,Y)
      IBEG=JSTRT(3)
      JBEG=IBEG+KCONT-1
      DO 50 I=IBEG,JBEG
   50 ASAM(I)=ASAM(I)+Y
      CALL PLINE(XCOORD,ASAM(IBEG),KCONT,2.,0,0,1)
      Z=Y+0.2
      CALL PSYMB(ZSAM,Z,0.25,'SEISMIC 3',0.0,9,1)
      Y=Y+0.75
      CALL PENUP(0.0,Y)
      DO 60 I=1,KCONT
   60 XSAM(I)=XSAM(I)+Y
      CALL PLINE(XCOORD,XSAM,KCONT,2.,0,0,1)
      CALL PLTEND
      RETURN
      END
```

168

APPENDIX 3

NOTE ON THE APPLICATION OF WIECHERT INVERSION TO THE DATA

The method of deriving a velocity/depth distribution from velocity/distance data by Wiechert Inversion assumes a spherically symmetrical earth and therefore, no lateral inhomogeneities. For the region investigated by WISE such a situation does not exist and care had to be taken in the determination of the velocity/depth functions and their interpretation.

The minus time analysis of the upper crustal data provided the variation of velocity with range for pairs of shots between Barra and Kintyre. The raypaths from shots 4 and 5 of the second phase of WISE into the Mull, Colonsay and Jura stations is as follows.

Fig. A1
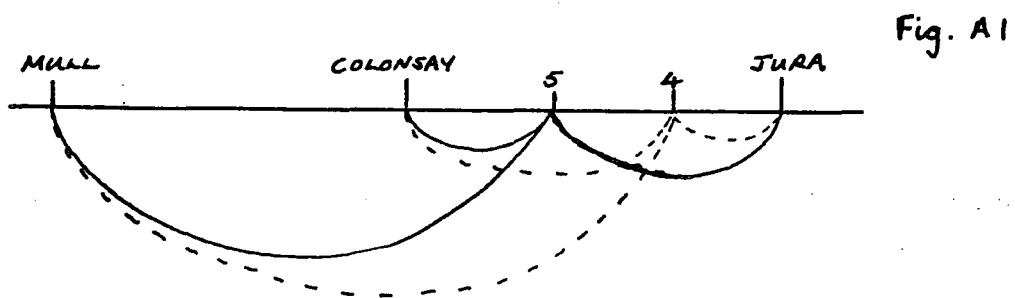
Similar raypaths exist for every other shot pair.

To apply the inversion, it had to be assumed that the velocity structure was homogeneous between the two end stations. The furthest station from the shots that this could be considered true was used and where the rays were thought to cross major structural boundaries, such station/shot pairs were excluded.

The velocity / distance data were then used in a program written by Swinburn (1975) to perform the inversion. This program uses the integral to transform the data described by Bullen (1976).[*] The data need not be entered with equal intervals of distance but are converted to such a format internally in the program to carry out the integration. The program outputs the corresponding depth for those velocities specified on input.

The velocity / depth distribution obtained must be treated with care. Although Figs. 6.29 and 6.30 were derived from plotting the velocities beneath each inversion point, that is, the mid-point of the two shots concerned, this is not the true case. Reference to Fig. A.1 shows that, due to the geometry of shots and stations, the velocities are those of different parts of the basement and not beneath one point on the surface. The velocity / depth distribution obtained should be considered as the average function for the crust beneath the full station range of the shot pair considered.

[*] BULLEN, K.E.   An Introduction to the Theory of Seismology
          C. U. P. 381 pp.